

UNCLASSIFIED
AD 406 872

DEFENSE DOCUMENTATION CENTER
FOR
SCIENTIFIC AND TECHNICAL INFORMATION
CAMERON STATION, ALEXANDRIA, VIRGINIA



UNCLASSIFIED

NOTICE: When government or other drawings, specifications or other data are used for any purpose other than in connection with a definitely related government procurement operation, the U. S. Government thereby incurs no responsibility, nor any obligation whatsoever; and the fact that the Government may have formulated, furnished, or in any way supplied the said drawings, specifications, or other data is not to be regarded by implication or otherwise as in any manner licensing the holder or any other person or corporation, or conveying any rights or permission to manufacture, use or sell any patented invention that may in any way be related thereto.

NOTICES

When Government drawings, specifications, or other data are used for any purpose other than in connection with a definitely related Government procurement operation, the United States Government thereby incurs no responsibility nor any obligation whatsoever; and the fact that the Government may have formulated, furnished, or in any way supplied the said drawings, specifications, or other data, is not to be regarded by implication or otherwise as in any manner licensing the holder or any other person or corporation, or conveying any rights or permission to manufacture, use, or sell any patented invention that may in any way be related thereto.

Qualified requesters may obtain copies of this report from the Armed Services Technical Information Agency, (ASTIA), Arlington Hall Station, Arlington 12, Virginia.

This report has been released to the Office of Technical Services, U.S. Department of Commerce, Washington 25, D. C., in stock quantities for sale to the general public.

Copies of this report should not be returned to the Aeronautical Systems Division unless return is required by security considerations, contractual obligations, or notice on a specific document.

FOREWORD

This report was prepared by Nuclear Metals, Inc. under USAF Contract No. AF 33(616)-7065. This contract was initiated under Project No. 7351, "Metallic Materials," Task No. 735104, "Beryllium and Beryllium Alloys". The work was administered under the direction of the Directorate of Materials and Processes, Deputy for Technology, Aeronautical Systems Division with Lt. S. S. Christopher, succeeded by Capt. L. F. Bubba, acting as project engineer.

This report covers work conducted from 1 April 1960 to 30 September 1961.

ABSTRACT

The report summarizes the work conducted on the Beryllium Research and Development Program for the period April 1, 1960 through September 30, 1961. The aim of this program is to make beryllium more useful as an Air Force structural material.

The program was divided into eleven major efforts, eight of which were sub-contracted and three carried out at the site of the prime contractor, Nuclear Metals, Inc. Detailed abstracts of each program are presented in their respective sections. In addition, work contemplated for a future program is described in a separate section.

Two programs deal with the purification and evaluation of purified beryllium: (1) "The Preparation of Pure Beryllium Metal by the Iodide Decomposition Method" (Nuclear Metals and Equipment Corporation), (2) "Purification of Beryllium by Distillation" (Nuclear Metals, Inc.). In this effort it was found that high purity beryllium could be produced by a vacuum distillation process. Preparation of pure metal by decomposition of the iodide did not appear to be feasible.

Four programs deal with the joining of beryllium: (1) "Brazing of Beryllium" (The Brush Beryllium Company), (2) "The Forge Welding of Beryllium" (The Brush Beryllium Company), (3) "Investigation of the Ultrasonic Weldability of Beryllium Metal Sheet", (Aeroprojects Inc.), (4) "Resistance Welding of Beryllium Sheet" (Rensselaer Polytechnic Institute). The feasibility of joining beryllium by ultrasonic welding was shown. The resistance spot welding program led to definition of the welding parameters, and to methods of altering the weld nugget structure and of eliminating cracking and porosity. The application of warm working in the form of roll-planishing improved to some extent the mechanical behavior of welds made by the Tungsten-arc Inert Gas (TIG) process. In the brazing effort, the optimum time and temperature for brazing beryllium with silver was defined and the effects of post-braze heat treatment on the room temperature and elevated temperature mechanical properties were determined.

The remaining programs, dealing with the flow and fracture characteristics of beryllium and the effect of impurities and alloying additions are: (1) "The Role of Oxides and Voids in Beryllium" (Manufacturing Laboratories, Inc.), (2) "A Study of the Brittle Behavior of Beryllium by Means of Transmission Electron Microscopy" (The Franklin Institute), (3) "Surface Damage in Beryllium" (Lockheed Missiles and Space Company), (4) "Aging and Strain Aging in Beryllium" (Nuclear Metals, Inc.), (5) "Raising the Yield Strength of Beryllium" (Nuclear Metals, Inc.).

In this group of programs, heat-treatment of commercially pure Brush QMV beryllium was found to alter the mechanical properties. These changes were shown to be due to the precipitation of a fcc compound having a lattice parameter $a_0 = 6.07 \text{ \AA}$. This appears to be associated with a precipitation reaction involving Fe and possibly Si and Al. The occurrence of a yield point in beryllium was shown to be consistent with the locking of dislocations by impurities.

Techniques for determining the distribution of beryllium oxides and voids in beryllium by replication electron metallography have been improved and the morphology of oxide layers artificially introduced between pressure-bonded beryllium discs under different conditions were studied.

Many very fine precipitate particles were found, by transmission electron microscopy, to be present in commercially pure beryllium. These particles appeared to affect the movement of dislocations. Dislocation structures associated with "bend plane" formation were also found.

Twinning was found to be one of the major factors contributing to surface damage in beryllium. Cracks were found to be a relatively minor factor. Inclusions were found to play a role in the initiation of cracks.

A low reduction rolling process was developed that produced sheet having three-dimensional ductility superior to high reduction rolled sheet and equivalent tensile properties. A Be-1 ^{w/o} Cu alloy showed uniaxial properties superior to unalloyed Be but somewhat lower three-dimensional properties.

This technical documentary report has been reviewed and is approved.



I. Perlmutter
Chief, Physical Metallurgy Branch
Metals and Ceramics Laboratory
Directorate of Materials and Processes

TABLE OF CONTENTS

Page No.

VOLUME II

SECTION 7 - THE BRAZING OF BERYLLIUM - B. M. Macpherson, R. B. Magalski and R. G. O'Rourke, The Brush Beryllium Company, Cleveland, Ohio.	1
ABSTRACT.	1
INTRODUCTION.	2
7-2 Experimental Work and Results	2
7-3 Discussion of Results	17
7-4 Conclusions	19
REFERENCES.	21
SECTION 8 - FORGE WELDING OF BERYLLIUM - B.M. MacPherson and W. W. Beaver, The Brush Beryllium Company, Cleveland, Ohio	22
ABSTRACT.	22
8-1 Introduction.	23
8-2 Experimental Work and Results	23
8-3 Discussion of Results	44
8-4 Conclusions	45
REFERENCES.	46
SECTION 9 - RESISTANCE WELDING OF BERYLLIUM SHEET - E. F. Nippes. W. F. Savage, F. A. Wassell and D. A. Karlyn, Rensselaer Polytechnic Institute, Troy, New York.	47
ABSTRACT.	47
9-1 Introduction.	49
9-2 Material.	49
9-3 Equipment	49
9-4 Procedure	55
9-5 Discussion.	57
9-6 Conclusions	89
REFERENCES.	94

TABLE OF CONTENTS (Continued)

	<u>Page No.</u>
Appendix 9-A - RESISTANCE BRAZING OF BERYLLIUM.	95
9A-1 Introduction.	95
9A-2 Object.	95
9A-3 Material.	95
9A-4 Equipment	95
9A-5 Procedure	97
9A-6 Discussion.	97
9A-7 Summary and Conclusions	103
9A-8 Literature Cited.	103
SECTION 10 - THE PURIFICATION OF BERYLLIUM BY DISTILLATION - J. F. Fensler, S. H. Gelles, E. D. Levine and A. R. Kaufmann, Nuclear Metals, Inc., Concord, Massachusetts.	104
ABSTRACT	104
10-1 Introduction.	105
10-2 Theory.	105
10-3 Previous Distillation Results	106
10-4 Experimental Work	107
10-5 Chemical Evaluation of Distilled Beryllium.	111
10-6 Mechanical Evaluation of Distilled Beryllium	116
10-7 Summary	125
ACKNOWLEDGEMENT	126
REFERENCES	127

TABLE OF CONTENTS (Continued)

	<u>Page No.</u>
SECTION 11 - AGING AND STRAIN AGING IN BERYLLIUM - A. K. Wolff, L. R. Aronin, and S. H. Gelles Nuclear Metals, Inc., Concord, Massachusetts. . .	128
ABSTRACT.	128
11-1 Introduction	129
11-2 Experimental Procedure and Results	130
11-3 Conclusions.	156
REFERENCES.	158
Appendix 11A - COMPLETE QUENCH-AGING TENSILE DATA.	159
Appendix 11B - RESULTS OF CHEMICAL AND SPECTROGRAPHIC ANALYSES .	166
SECTION 12 - RAISING THE YIELD STRENGTH OF BERYLLIUM - E. D. Levine and L. R. Aronin, Nuclear Metals, Inc., Concord, Massachusetts.	167
ABSTRACT.	167
12-1 Introduction	168
12-2 Experimental Procedure	168
12-3 Results.	175
12-4 Discussion	198
REFERENCES.	204
SECTION 13 - FUTURE PROGRAM.	205
SECTION 14 - REPORTS AND PUBLICATIONS GENERATED ON THIS CONTRACT.	207

LIST OF ILLUSTRATIONS

<u>Figure</u>		<u>Page No.</u>
1	Beryllium rods brazed together with pure silver, showing one specimen as brazed and one after machining to a buttonhead tensile specimen.	3
2	Beryllium joint brazed with silver at 900°C for 1 minute.	7
3	Beryllium joint brazed with silver at 975°C for 1 minute.	7
4	Phase diagram, silver-beryllium.	9
5	Beryllium blocks brazed together with silver, showing a section ready for heat treatment and a tensile specimen machined after heat treatment.	10
6	Silver-brazed beryllium joint in the as-brazed condition . .	13
7	Silver-brazed beryllium joint after heating at 600°C for 6 hours.	14
8	Silver-brazed beryllium joint after heating at 600°C for 1 week	14
9	Silver-brazed beryllium joint after heating at 800°C for 6 hours.	15
10	Silver-brazed beryllium joint after heating at 800°C for 1 week	15
11	Cross-sections of the heat-affected zone of fusion weld in 0.062-inch thick sheet. The weld reinforcement has been rolled flush to the sheet surface in the welding direction .	25
12	Cross-sections of fusion welds that have had the weld reinforcement hot rolled flush with the sheet surfaces along the welding direction (roll planishing).	27
13	Cross-sections of fusion welds that show the distortion of grain structure produced by various mechanical working techniques	28
14	Cross-sections of fusion welds that have been hot rolled to 10% reduction in sheet thickness in the welding direction.	29
15	Cross-sections of fusion welds that have been hot rolled to 10% reduction in thickness, transverse to the weld. . . .	30

LIST OF ILLUSTRATIONS (continued)

<u>Figure</u>		<u>Page No.</u>
16	Average increase in temperature at a position along a line 2-1/2 inches from beginning of weld vs. electrode position.	33
17	This special welding fixture with plastic enclosure for the inert gas welding atmosphere was built for resistance butt welding 5/8-inch diameter beryllium specimens. A 5/8-inch diameter, centerless ground, resistance butt welded beryllium specimen (with arrow marking the weld) is shown with the alumina retaining tube.	36
18	Resistance butt welded specimens.	38
19	Photomicrograph of resistance butt weld made with five impulses, 51% phase shift (no alumina retainer)	40
20	Resistance butt welded specimens welded with aluminum oxide retaining tubes at five impulses and 56% phase shift.	41
21	Photomicrograph of resistance butt welds made with an alumina retainer and five impulses. "a" shows a partially diffused joint and "b" shows a joint that is relatively indistinct.	42
22	Atmosphere Box.	51
23	200 K.V.A. Dual Force-Type spot welder.	53
24	Two-leaf spring used for high electrode forces.	54
25	Comparison of pickling techniques used for surface cleaning of beryllium sheet preparatory to resistance welding. (Tests conducted at room temperature.)	56
26	Typical examples of external cracks in beryllium resistance spot welds.	59
27	Approximate welding current range as a function of welding time for 0.020-inch beryllium sheet. Electrode material: RWMA Class 2, 4-inch radius dome, 0.140-inch restricted diameter. Electrode force: 250 lbs.	63
28	Approximate welding current range as a function of welding time for 0.020-inch beryllium sheet. Electrode material: RWMA Class 2, 4-inch radius dome, 0.140-inch restricted diameter. Electrode force: 400 lbs.	64
29	Approximate welding current range as a function of welding time for 0.040-inch beryllium sheet. Electrode material: RWMA Class 2, 6-inch radius dome, 0.156-inch restricted diameter. Electrode force: 300 lbs.	65

LIST OF ILLUSTRATIONS (Continued)

<u>Figure</u>		<u>Page No.</u>
30	Approximate welding current range as a function of welding time for 0.040-inch beryllium sheet. Electrode material: RWMA Class 2, 6-inch radius dome, 0.156-inch restricted diameter. Electrode force: 550 lbs.	67
31	Approximate welding current range as a function of welding time for 0.060-inch beryllium sheet. Electrode material: RWMA Class 2, 6-inch radius dome, 0.219-inch restricted diameter. Electrode force: 500 lbs.	68
32	Approximate welding current range as a function of welding time for 0.060-inch beryllium sheet. Electrode material: RWMA Class 2, 6-inch radius dome, 0.219-inch restricted diameter. Electrode force: 700 lbs.	69
33	Weld diameter vs. welding current, 0.020-inch beryllium sheet. Electrodes: RWMA Class 2, 4-inch radius dome, 0.140-inch restricted diameter. Electrode force: 150 lbs. Weld time: 1, 5 and 10 cycles.	70
34	Weld diameter vs. welding current, 0.020-inch beryllium sheet. Electrodes: RWMA Class 2, 4-inch radius dome, 0.140-inch restricted diameter. Electrode force: 325 lbs. Weld time: 1, 5 and 10 cycles.	71
35	Weld diameter vs. welding current, 0.020-inch beryllium sheet. Electrodes: RWMA Class 2, 4-inch radius dome, 0.140-inch restricted diameter. Electrode force: 400 lbs. Weld time: 1, 5 and 10 cycles.	72
36	Weld diameter vs. welding current, 0.040-inch beryllium sheet. Electrodes: RWMA Class 2, 6-inch radius dome, 0.156-inch restricted diameter. Electrode force: 300 lbs. Weld time: 1, 6 and 15 cycles.	74
37	Weld diameter vs. welding current, 0.040-inch beryllium sheet. Electrodes: RWMA Class 2, 6-inch radius dome, 0.156-inch restricted diameter. Electrode force: 450 lbs. Weld time: 1 and 15 cycles	75
38	Weld diameter vs. welding current, 0.040-inch beryllium sheet. Electrodes: RWMA Class 2, 6-inch radius dome, 0.156-inch restricted diameter. Electrode force: 550 lbs. Weld time: 1, 6 and 15 cycles.	76
39	Weld diameter vs. welding current, 0.060-inch beryllium sheet. Electrodes: RWMA Class 2, 6-inch radius dome, 0.219-inch restricted diameter. Electrode force: 500 lbs. Weld time: 3, 8 and 15 cycles.	77

LIST OF ILLUSTRATIONS (Continued)

<u>Figure</u>		<u>Page No.</u>
40	Weld diameter vs. welding current, 0.060-inch beryllium sheet. Electrodes: RWMA Class 2, 6-inch radius dome, 0.219-inch restricted diameter. Electrode force: 700 lbs. Weld time: 3, 8 and 15 cycles.	77
41	Typical examples of tensile-shear specimen failures	79
42	Tensile shear strength vs. welding current for 0.040-inch beryllium sheet. Electrodes: RWMA Class 2, 6-inch radius dome, 0.156-inch restricted diameter. Initial force: 450 lbs. No forging force. No preheat. Postheat: 5 cycles at 50% of weld current. Welding time: 11 cycles	80
43	Tensile shear strength vs. welding current for 0.040-inch beryllium sheet. Electrodes: RWMA Class 2, 6-inch radius dome, 0.156-inch restricted diameter. Initial force: 450 lbs. Forging force: 1000 lbs. No preheat. Postheat: 5 cycles at 50% of weld current. Welding time: 11 cycles. Forging delay: 0.5 cycle after weld.	81
44	Tensile shear strength vs. welding current for 0.040-inch beryllium sheet. Electrodes: RWMA Class 2, 6-inch radius dome, 0.156-inch restricted diameter. Initial force: 450 lbs. No forging force. No preheat. Post heat: 125 cycles at 95% of weld current. Welding time: 11 cycles. . .	82
45	Tensile shear strength vs. welding current for 0.040-inch beryllium sheet. Electrodes: RWMA Class 2, 6-inch radius dome, 0.156-inch restricted diameter. Initial force: 450 lbs. Forging force: 1000 lbs. No preheat. Postheat: 125 cycles at 95% of weld current. Welding time: 11 cycles. Forging delay: 0.5 cycle after weld.	83
46	Tensile shear strength vs. welding current for 0.040-inch beryllium sheet. Electrodes: RWMA Class 2, 6-inch continuous radius dome. Initial force: 550 lbs. Forging force: 1350 lbs. Preheat: 200 cycles at 80% of weld current. Postheat: 120 cycles at 95% of weld current. Welding time: 11 cycles. Forging delay: 77 cycles.	84
47	Tensile shear strength vs. welding current for 0.040-inch beryllium sheet. Electrodes: RWMA Class 2, 6-inch radius dome, 0.156-inch restricted diameter. Initial force: 450 lbs. Forging force: 1225 lbs. Preheat: 200 cycles at 80% of weld current. Postheat: 120 cycles at 95% of weld current. Welding time: 11 cycles. Forging delay: 77 cycles.	85

LIST OF ILLUSTRATIONS (Continued)

<u>Figure</u>		<u>Page No.</u>
48	Section through beryllium resistance spot weld with horizontal void.	87
49	Beryllium resistance spot weld with internal crack and fractures at edge of weld.	88
50	Beryllium resistance spot weld exhibiting porosity and some recrystallization at the edges of the nugget	90
51	Completely recrystallized beryllium resistance spot weld . . .	91
52	30 kva resistance welder used for resistance brazing experiments.	96
53	Tensile shear strength as a function of resistance brazing current, 0.020-inch beryllium sheet. 0.625-inch diameter RWMA Class 10-faced electrodes. Electrode force: 350 lbs. Brazing time: 20 cycles. 0.075-inch diameter button of 0.003-inch BrBt alloy.	99
54	Tensile shear strength as a function of resistance brazing current, 0.020-inch beryllium sheet. 0.625-inch diameter RWMA Class 10-faced electrodes. Electrode force: 450 lbs. Brazing time: 20 cycles. Two 0.075-inch diameter buttons of 0.003-inch BrBt alloy located 0.090-inch on centers transverse to axis of loading.	101
55	Resistance braze in beryllium sheet.	102
56	Diagram of distillation apparatus.	106
57	Cone of distilled beryllium.	110
58	Longitudinal section of distillate No. 5 after rolling at 760°C through a 2.5:1 reduction.	118
59	Longitudinal section of distillate No. 5 after rolling at 760°C through a 2.5:1 reduction and subsequently annealing for 2 hours at 750°C	120
60	Precipitate particles on fracture surface of distillate No. 16	123
61	Precipitate particles on fracture surface of vacuum melted and extruded distillate.	124
62	Effect of solution treatment at 1100°C for 1 hour on grain size of hot-extruded beryllium (all photos transverse to extrusion direction)..	132

LIST OF ILLUSTRATIONS (Continued)

<u>Figure</u>		<u>Page No.</u>
63	Design of cylindrical sample employed in tensile testing of beryllium rod. (As machined)	134
64	Effect of various cooling rates from the solutionizing temperature on ultimate tensile strength of polycrystalline beryllium rod. (Solution treatment: 1100°C; 1 hr).	135
65	Effect of various cooling rates from the solutionizing temperature on the percent elongation of polycrystalline beryllium rod. (Solution treatment: 1100°C; 1 hr)	136
66	Typical fractures of aged beryllium rod showing characteristic angle of fracture propagation ($\sim 70^\circ$ to tensile direction).	138
67	Ultimate tensile strength vs. aging time for solution-treated beryllium rod aged at various temperatures.	141
68	Ultimate tensile strength vs. percent elongation for solution treated beryllium rod after various aging treatments	143
69	Ultimate tensile strength vs. aging time for solution-treated beryllium rod aged at 800°C, with vertical lines showing the scatter in the data	144
70	Typical tensile curve shapes obtained after aging of solution treated and quenched beryllium rod.	146
71	Variation in grain size among three beryllium rods extruded at 1050°C and 30:1 reduction and subsequently aged at 400°C for 7 hours. (All photos transverse to extrusion direction).	147
72	Recovery of the yield point in beryllium by strain aging. . .	151
73	Effect of aging time and temperature on yield point recovery in strained beryllium	154
74	Geometry of tensile specimens	171
75	Variation in 0.2% offset yield strength with reduction in thickness of unalloyed beryllium sheet bi-directionally rolled at various temperatures.	178
76	Variation in ultimate tensile strength with reduction in thickness of unalloyed beryllium sheet bi-directionally rolled at various temperatures.	179

LIST OF ILLUSTRATIONS (Continued)

<u>Figure</u>		<u>Page No.</u>
77	Variation in tensile elongation with reduction in thickness of unalloyed beryllium sheet bi-directionally rolled at various temperatures.	180
78	Effect of a 10% finish pass on 0.2% offset yield strength of unalloyed beryllium sheet after various prior rolling procedures.	182
79	Effect of a 10% finish pass on ultimate tensile strength of unalloyed beryllium sheet after various prior rolling procedures.	183
80	Effect of a 10% finish pass on tensile elongation of unalloyed beryllium sheet after various prior rolling procedures.	184
81	Effect of finish rolling at various temperatures on the 0.2% offset yield strength of unalloyed beryllium sheet after prior reduction at 1950°F	186
82	Effect of finish rolling on the ultimate tensile strength of unalloyed beryllium sheet after prior reduction at 1950°F.	187
83	Effect of finish rolling on the tensile elongation of unalloyed beryllium sheet after prior reduction at 1950°F.	188
84	Variation in 0.2% offset yield strength with reduction in thickness of beryllium - 1 ^W /o copper alloys bi-directionally rolled at various temperatures.	190
85	Variation in ultimate tensile strength with reduction in thickness of beryllium - 1 ^W /o copper alloys bi-directionally rolled at various temperatures.	191
86	Variation in tensile elongation with reduction in thickness of beryllium - 1 ^W /o copper alloys bi-directionally rolled at various temperatures	192
87	Effect of finish rolling at 1400°F on the tensile properties of beryllium - 1 ^W /o copper alloys after prior rolling at 1950°F.	194
88	Transverse ductility of beryllium and beryllium - 1 ^W /o copper alloy sheet bi-directionally rolled to reductions of 6:1. . . .	197
89	Comparison of 0.2% offset yield strengths of sheet produced by various techniques	199

LIST OF ILLUSTRATIONS (Continued)

<u>Figure</u>		<u>Page No.</u>
90	Comparison of ultimate tensile strengths of sheet produced by various techniques.	200
91	Comparison of tensile elongations of sheet produced by various techniques	202
92	Comparison of transverse ductility of sheet produced by various techniques	203

LIST OF TABLES

	Page No.
1 Tensile Strength of Specimens Butt-Brazed with Silver at 10 PSI.	5
2 Tensile Strength of Specimens Butt-Brazed with Silver Under Various Conditions	6
3 Summary of Tensile Test Data, for Specimens Brazed with Silver and Then Heat Treated	11
4 X-Ray Analysis of Powder Attritioned From the Fractured Surfaces of Silver-Brazed Tensile Specimens.	16
5 Tensile Strength of Specimens Butt-Brazed with Silver-Base Alloys	18
6 Mechanical Properties of Mechanically Worked Fusion Welds. . .	26
7 Grain Size From Cross Section of Mechanically Worked Fusion Welds	31
8 Grain Size From Cross Section of Fusion Weld Mechanically Worked Immediately Following the Welding Arc	35
9 Room Temperature Mechanical Properties of Resistance Butt Welded Specimens	39
10 Mechanical Properties of Resistance-Butt Welded Specimens. . .	43
11 Summary of Mechanical Properties of Beryllium Sheet Used in This Investigation	50
12 Description of Distillation Experiments.	109
13 Chemical Analyses of Beryllium Starting Material	113
14 Chemical Analyses of Beryllium Produced by Vacuum Distillation	114
15 Chemical Analyses of Distillation Residues	115
16 Analysis of Brush Beryllium Company -200 Mesh QMV Beryllium Powder	131
17 Room Temperature Tensile Properties as a Function of Aging Treatment for Beryllium Rod Extruded From Brush QMV Powder . .	139
18 Position and Orientation Relation of Observed Peaks Occurring During Aging	149
19 Summary of Strain Aging Data	152
20 Elevated Temperature Tensile Properties of Beryllium	155

LIST OF TABLES (Continued)

		<u>Page No.</u>
21	Chemical Analyses of Brush QMV -200 Mesh Powder Starting Material.	169
22	Effect of H_2SO_4 Content on Deposition of Copper on Beryllium From $Cu(NO_3)_2$ Solution	173
23	Uniformity of Copper Content in Beryllium Powder Processed to Obtain Copper Contents of 1 and 6 Weight Percents.	174
24	Tensile Properties of Unalloyed Beryllium Sheet Bi-Directionally Rolled at Temperatures Between 1400 and 1800°F to Reductions Between 1.5:1 and 6:1.	177
25	Effect of a 10% Finish Pass at 1000°F on the Tensile Properties of Unalloyed Beryllium Sheet Bi-Directionally Rolled at Temperatures Between 1400 and 1800°F to Reductions of 1.5:1 and 3:1	181
26	Effect of Low-Temperature Finish Passes on the Tensile Properties of Unalloyed Beryllium Sheet Bi-Directionally Rolled 3:1 at 1950°F	185
27	Tensile Properties of Beryllium - 1 ^W /o Copper Alloy Sheet Bi-Directionally Rolled at Temperatures Between 1400 and 1800°F to Reductions Between 1.5:1 and 6:1	189
28	Effect of Finish Passes at 1400°F on the Tensile Properties of Beryllium - 1 ^W /o Copper Alloy Sheet Initially Rolled Bi-Directionally 3:1 at 1950°F.	193
29	Bend Properties of Bi-Directionally Rolled Beryllium Sheet. . .	195
30	Bend Properties of Bi-Directionally Rolled Beryllium - 1 ^W /o Copper Alloy Sheet.	196

SECTION 7

THE BRAZING OF BERYLLIUM

B. M. MacPherson, R. B. Magalski and R. G. O'Rourke
(The Brush Beryllium Company, Cleveland, Ohio)

ABSTRACT

Optimum conditions for the brazing of beryllium with silver were defined on the basis of tensile tests and metallographic and X-ray examination. The effect of heat treatment at temperatures of 600 and 800°C for periods of 6 hours and 1 week on the room temperature and elevated temperature properties of the brass joints was determined and correlated with metallographic and X-ray diffraction observations. Silver base alloys with additives of zinc, germanium, tin, silicon, indium, cadmium, aluminum and phosphorus were studied as brazing alloys and compared to the currently used silver-lithium brass alloy.

**Manuscript released by authors September 1962 for publication as an ASD
Technical Documentary Report.**

7-1 INTRODUCTION

The objective of this program was to develop further the technology for silver brazing of beryllium. Phase I of the program dealt with the determination of the optimum conditions for brazing beryllium made from -200 mesh QMV powder to itself with silver. Phase II was a study of the effects of heat treatment on joints that were brazed under the best conditions established in Phase I. The effects of heat-treatment were investigated because beryllium joined by brazing might find ultimate use in elevated-temperature structural applications. In Phase III various silver-base alloys were evaluated as brazing materials for beryllium to determine whether they might prove superior to the presently accepted silver-lithium alloy. The alloys investigated in Phase III were silver with binary additions of tin, zinc, germanium, silicon, indium, cadmium, aluminum and phosphorus.

7-2 EXPERIMENTAL WORK AND RESULTS

7-2.1 Equipment and General Techniques. Because of the great affinity of beryllium for oxygen and the lack of a suitable flux or reducing atmosphere, beryllium should be brazed in vacuum or inert gas. Vacuum furnace brazing was chosen for use in this study. Vacua of the order of 10^{-4} to 10^{-6} mm of mercury were employed.

The brazing operations in Phases I and III of this program were carried out in a glass bell jar of 9-1/2 in. ID by 15 in. long. A graphite-sleeve susceptor heated by induction was used as a radiating surface to heat the assembly to be brazed. The induction power source consisted of a 10 kc/sec, 30 kw unit. A heating cycle of 20 min was usually used.

In the Phase II brazing operation, a steel-shell furnace equipped with a hydraulic pressing ram and resistance-wire heating elements was used. Heating cycles of 2-1/2 hr. were normally used with this unit.

In preparation for brazing in Phases I and II, silver was plated to a pre-determined thickness on the beryllium surfaces to be brazed. Only a light abrasive action with steel wool, followed by toluene cleaning, was required in order to remove all traces of dirt and oil from the beryllium. For Phase III (brazing alloy development), the beryllium was not plated; instead, alloy discs were placed between the beryllium rods. The beryllium required a light pickle in a mixture of nitric and hydrofluoric acids followed by toluene cleaning. The braze alloys were lightly abraded, then cleaned with toluene.

7-2.2 Brazing with Pure Silver (Phase I). Since an ideal braze joint has the least possible thickness of braze metal between the two mating surfaces, a brazing technique that would yield a thin silver braze layer was chosen. In the method used, silver was first plated on the flat ends of beryllium rods, and the plated surfaces were held in intimate contact at a temperature either (1) above the melting point of silver, or (2) above the Be-Ag eutectic temperature but below the melting point of silver. The thickness of the silver plate and the length of time at temperature were varied. The brazed rods were machined into 1/4-inch button head test specimens (shown in Figure 1), which were tensile tested at room temperature.

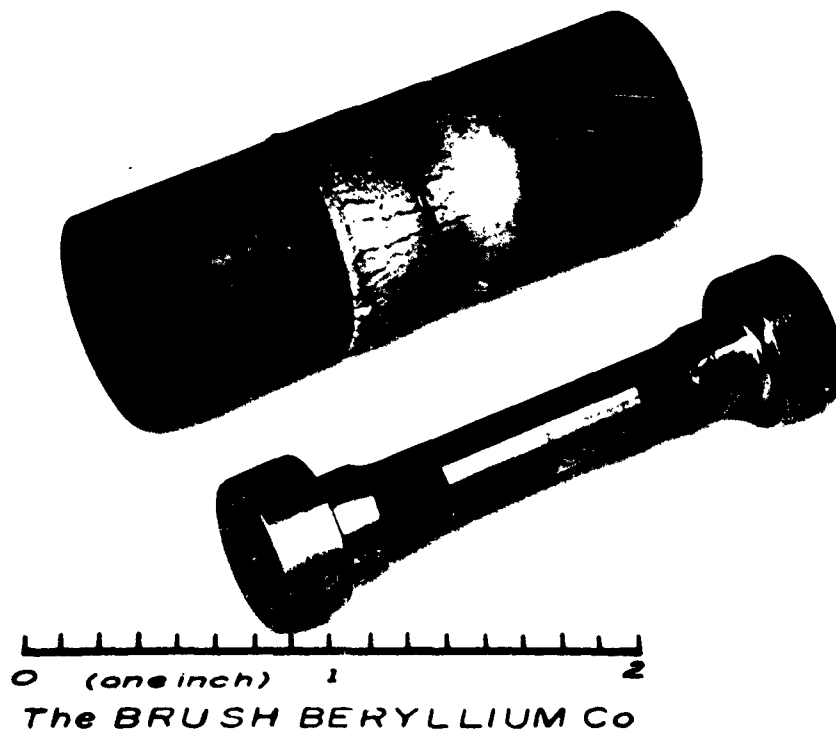


Figure 1 - Beryllium rods brazed together with pure silver, showing one specimen as brazed and one after machining to a button-head tensile specimen.

The beryllium specimens were 1 in. lengths cut from a 3/4-in.-diameter hot-extruded beryllium rod. The specimens were plated on one of their machined ends with silver to a thickness of either approximately 0.0005 or 0.002 in. The blanks were then matched for plating thickness and placed in the brazing fixture, which was composed of graphite plates and steel weights and was designed to allow brazing of the specimens under a constant, predetermined joint pressure. The following heating conditions were used for brazing:

- (1) 975°C for 1 min
- (2) 975°C for 5 min
- (3) 900°C for 1 min
- (4) 900°C for 5 min

Tensile tests were conducted on a Riehle Universal Testing machine at a strain rate of 0.005 min⁻¹. The tensile data reported in Table 1 are for brazed joints made at 10 psi dead load. Since there was such a large spread in the data, no positive conclusions can be made about the effect of heating conditions and silver thickness on the bond strength for samples brazed under these conditions. The strengths were not as high as anticipated, and unbonded areas were found in an examination of the tested specimens. To obtain more intimate contact of the plated surfaces, a higher pressure (40 psi) was applied by using the same load as previously while reducing the cross section of the joint by a factor of four. Problems were encountered in this system due to a shifting of the mating surfaces. This resulted in rejection of most of the samples brazed in this manner. To achieve higher joint pressure consistently, a third setup was inaugurated in which pressure was applied by the differential thermal expansion of steel bolts and the beryllium pieces being brazed. In addition, a dead load equivalent to 10 psi on the joint was introduced. Alignment of the sample components could be closely controlled in this fixture. Although the pressure could not be measured in this arrangement, stronger and more consistent braze joints were produced, as is evidenced in Table 2. The data indicate that the following conditions are the best of those investigated for joining beryllium with silver braze:

- (1) 900°C brazing temperature
- (2) Either 1 or 5 min time at temperature
- (3) A probable minimum of 40 psi joint pressure
- (4) Approximately 0.001 in. total initial silver thickness

Metallographic examination of the joints brazed at the higher pressures has indicated that the joint is composed of two discernible phases, as shown in Figures 2 and 3. The bright center phase shown in those figures is most likely the silver-rich phase. The other discernible phase, located between the parent metal and the silver-rich phase, appears to be a beryllium-rich material which is more prevalent in some areas than in others. The growth characteristics of this phase seem to be related to the beryllium metal grains. The phase may grow into the parent metal as well as into the silver-rich phase, although most of the growth appears to be into the silver-rich phase.

Powder samples were prepared from material at the fractured surfaces of silver-brazed tensiles, and these were studied by X-ray diffraction techniques.* It was

* The diffraction patterns were obtained with a Norelco 114.59 mm powder camera with filtered CuK α radiation. Powder samples were packed in 0.2 mm glass capillaries.

**Table 1. TENSILE STRENGTH OF SPECIMENS BUTT-BRAZED
WITH SILVER AT 10 PSI**

Brazing Conditions		Total Initial Thickness of Silver in Joint (in. x 10 ⁻³)	Ultimate Tensile Strength* (psi)
Temp. (°C)	Time (min)		
900	1	3.1	8,000
900	1	3.0	13,800
900	1	2.3	Broke during machining
900	5	2.8	11,500
900	5	4.0	12,300
900	5	4.2	9,300
900	5	2.5	Broke during machining
975	1	2.0	16,040
975	1	2.0	8,900
975	1	2.8	12,300
975	5	2.2	7,400
975	5	2.2	13,600
975	5	1.3	Broke during machining

* All failures occurred at brase joint.

**Table 2. TENSILE STRENGTH OF SPECIMENS BUTT-BRAZED
WITH SILVER UNDER VARIOUS CONDITIONS**

Brazing Conditions		Joint Pressure (psi)	Total Initial Thickness of Silver in Joint (in. x 10 ⁻³)	Ultimate Tensile Strength** (psi)
Temp. (°C)	Time (min)			
900	1	*	2.5	23,100
900	1	*	1.1	33,700
900	1	*	1.2	38,400
900	1	*	3.8	23,000
900	5	*	3.6	25,400
900	5	*	1.0	28,200
900	5	*	1.0	38,400
900	5	*	0.9	25,100
975	1	40 ⁺	2.5	17,800
975	1	40 ⁺	2.6	20,500
975	1	40 ⁺	0.7	23,700
975	5	40 ⁺	3.2	20,500
975	5	*	3.1	Broke during machining
975	5	*	4.6	800
975	5	*	0.6	3,000

* Bolted fixture; pressure not determined.

** All failures occurred at braze joint.

+ Dead load.

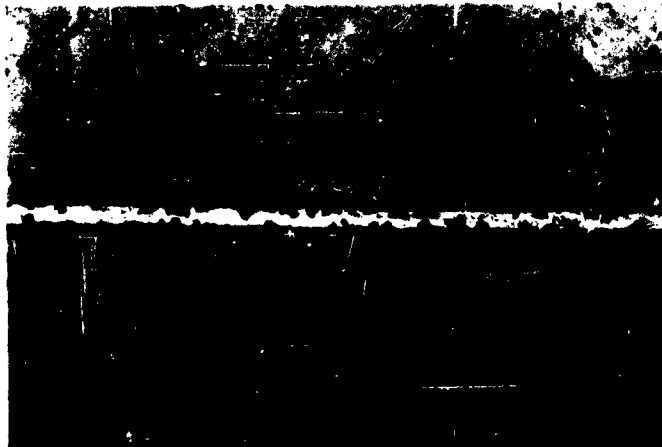


Fig. 2 - Beryllium joint brazed with silver at 900°C for 1 minute (HF etch; bright light; 250X).



Fig. 3 - Beryllium joint brazed with silver at 975°C for 1 minute (HF etch; bright light; 250X).

necessary to attrition powder from several brazed tensiles to obtain sufficient powder for each diffraction specimen. In addition to silver and beryllium, the presence of the Be-Ag delta phase⁽¹⁾ (Figure 4) was indicated for joints brazed at both 900° and 975°C. The delta phase lines in this powder diffraction study were not strong enough for quantitative analysis of the phases present in the brazed joints. The fractured surfaces of one set of tensile specimens brazed at 900°C were attritioned so that powder samples from three different positions in the brazed joints were obtained. The first powder specimen taken from the center of the braze contained primarily silver and a small quantity of delta phase. The next two samples contained various amounts of silver and beryllium according to the position of the sample relative to the parent beryllium, as well as a small quantity of delta phase. There was an indication of quartz being present in two powder samples; this was probably introduced inadvertently during or after the attritioning operation. In this study there was also a diffraction line which could not be identified with the published data for silver, beryllium, or the beryllides.

7-2.3 Effects of Heat Treatment on the Silver Brazed Joints (Phase II). Using the optimum brazing conditions developed in Phase I of this study, pairs of beryllium blocks 2-7/8 x 2 x 1-1/8 in. were silver plated on the surfaces to be joined to a thickness approximating 0.0005 inch. They were then vacuum brazed at 900°C and cut into samples (Figure 5) for heat treatment. The specimens were heat treated and then machined into 1/4 in. buttonhead tensile specimens. Testing was conducted in air on a Riehle Universal Testing machine at a strain rate of 0.005 min.⁻¹ at room temperature, 600° and 800°C after heat treatment at 600° and 800°C. For the elevated temperature tests thermocouples were positioned at the sample. The sample was allowed to remain at temperature for 0.5 hour, tested and removed from the furnace immediately after testing.

Although radiographs indicated a sound braze the first pair of blocks, which had been brazed with the joint pressure applied by a bolted fixture, showed evidence from joint strengths that there had been a higher pressure at the edge than at the center. In an effort to apply uniform pressure over the entire brazing area, all subsequent blocks were brazed in a vacuum furnace equipped with a hydraulic pressing ram. The pressures applied to the joints during brazing were either 100 or 200 psi. The room-temperature tensile strength of these blocks was between 27,000 and 41,000 psi, with results for any one block being fairly uniform throughout the block.

Each set of brazed blocks used (No. 2 brazed at 100 psi, No. 6 brazed at 200 psi, and No. 7 brazed at 200 psi) provided a minimum of 12 tensile specimens. The specimens for heat treatment were placed in a gas-tight stainless steel container which was filled with helium to prevent atmospheric corrosion during heating. To prevent contact reaction with the steel container, separator plates of beryllium were used between the steel and the test specimens. After air cooling to room temperature, the test specimens were removed from their protective container and machined into 1/4-inch buttonhead tensiles.

Table 3 lists the conditions of heat treatment and summarizes the tensile test data for the heat-treated specimens. Room temperature tensile strengths for samples in the as-brazed condition taken from positions adjacent to the heat-treated samples are supplied for comparison purposes. The data indicate that room temperature tensile strength increases when the specimens are heat treated at 600°C. Room temperature tests of the specimens heat treated at 800°C for 6 hr show a

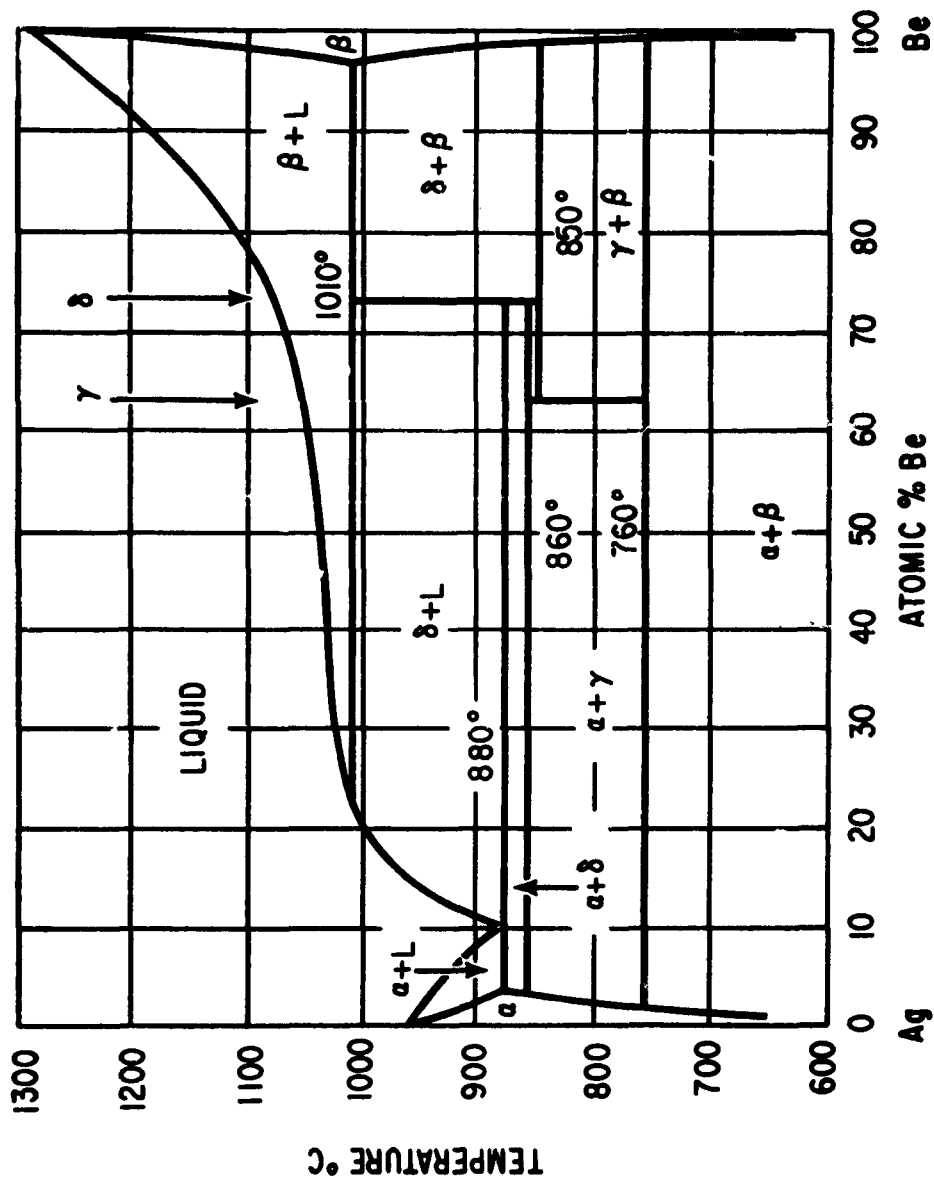


Figure 4 - Phase diagram, silver-beryllium.
Taken from Winkler(1).

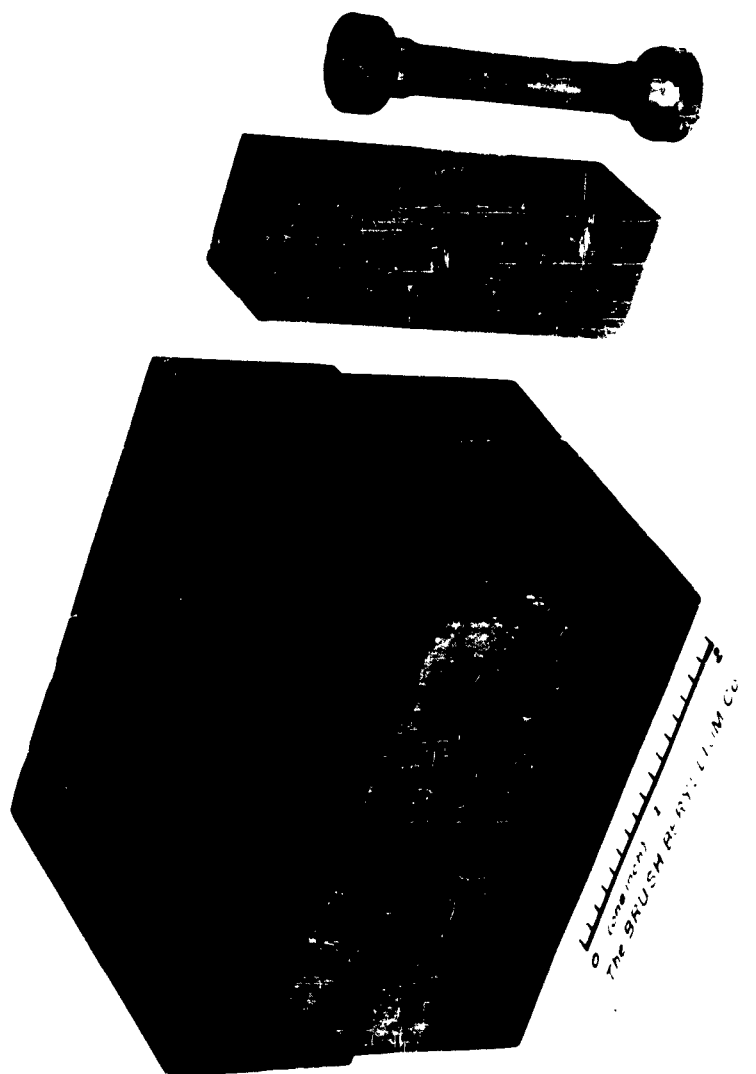


Fig. 5 - Beryllium blocks brazed together with silver, showing a section ready for heat treatment and a tensile specimen machined after heat treatment.

**Table 3 SUMMARY OF TENSILE TEST DATA FOR SPECIMENS
BRAZED WITH SILVER AND THEN HEAT TREATED**

Heat Treatment Conditions		Testing Temperature (°C)	Ultimate* Strength (x 10 ³ psi) As-Brazed	Ultimate Strength (x 10 ³ psi)	Yield Strength (x 10 ³ psi)
Temperature (°C)	Time at Temperature				
600	6 hr.	R.T.	35.0 31.0 <u>36.0</u> Av. 34.0	41.6 41.3 <u>40.8</u> 41.2	33.5 33.6 <u>34.2</u> 33.8
600	1 wk.	R.T.	34.0 33.0 <u>35.0</u> Av. 34.0	39.8 40.6 <u>39.8</u> 40.1	32.4 32.8 <u>32.7</u> 32.6
800	6 hr.	R.T.	29.7 29.5 <u>29.7</u> Av. 29.7	18.9 15.0 <u>21.8</u> 18.6	- - -
800	1 wk.	R.T.	29.6 29.7 29.5 <u>29.7</u> Av. 29.6	36.8 22.5 29.4 <u>41.4</u> 32.5	33.0 - - <u>33.1</u> 33.1
None	None	600	- - - Av.	15.9 15.8 <u>15.7</u> 15.8	15.3 15.7 - 15.5
600	6 hr.	600	- - - Av.	15.3 14.5 <u>13.6</u> 14.5	- - -
600	1 wk.	600	- - - Av.	12.5 13.4 <u>15.6</u> 13.8	- - -
None	None	800	- - - Av.	6.3 7.0 <u>3.1</u> 5.5	- - -
800	6 hr.	800	- - - Av.	4.8 5.5 6.1 <u>5.1</u> 5.4	- - -
800	1 wk.	800	All samples broke in testing fixture.		

* Samples taken from positions adjacent to the heat-treated samples.

drastic lowering of the tensile strength, while heat treatment of the specimens at 800°C for 1 wk resulted in a slight increase in tensile strength over non-heat-treated specimens. In the elevated temperature tests of the brazed specimens, the tensile strengths did not seem to be appreciably affected by the heat treatments studied, with the exception of the specimens heat treated at 800°C for 1 wk; the latter specimens could not support the weight of the testing fixture at 800°C. Elongation increased with increasing tensile strength but was too erratic to measure accurately.

Photomicrographs of the brazed joints before and after the various heat treatments are shown in Figures 6 through 10. In all conditions, the brazed joints appear to be much thinner than those studied in Phase I. No change in microstructure appears to take place as a result of heat treating the specimens at 600°C for either 6 hr or 1 wk, as can be noted in Figures 7 and 8. After heating at 800°C for 6 hr, the joint consists of a new single phase which polarizes. After heating at 800°C for 1 wk, the well-defined joint has disappeared, presumably due to the diffusion of the silver. The silver seems to be present as spherical particles in some areas.

The brazed surfaces of the fractured tensile specimens from this phase of the work were attritioned into powder for X-ray diffraction studies. The results are reported in Table 4. From these studies it appears that long time aging at 600°C eliminates the beryllide from the silver-brazed joints, which could account for the observed increase in strength (Table 3.). The decrease in room temperature strength for the specimens heat treated at 800°C for 6 hr is explained by the finding that the major phase is the gamma silver-beryllium intermetallic compound reported by Winkler⁽¹⁾. In the specimens heat treated at 800°C for 6 hr and tested at that temperature, the major phase present was silver, which could account for the excellent strengths obtained. A sample for metallographic observation was not available for the specimens that were heated at 800°C for 1 wk and tested at room temperature, but specimens with this history showed relatively high tensile strength and only silver and beryllium at the braze joint. For some unexplained reason, the joints in the specimens heat-treated at 800°C for 1 wk and tested at that temperature oxidized heavily, leaving beryllium oxide and very minor amounts of metallic silver and beryllium in the joint. This accounts for the premature breaking of the specimens.

7-2.4 Development of Improved Braze Alloys (Phase III). The emphasis of this study was on alloys containing binary additions to the silver. The additions that appeared to have merit for improving the brazing characteristics of silver were:

- | | |
|-------------|----------------|
| (1) tin | (5) germanium |
| (2) zinc | (6) phosphorus |
| (3) silicon | (7) indium |
| (4) cadmium | (8) aluminum |

The relatively volatile elements, zinc, cadmium and phosphorus, were chosen because of the expected improvement in the wettability of the braze metal. The remaining elements were investigated for possible improvements in strength. The additions were evaluated on the basis of their effect upon wettability, flow, diffusion characteristics, and tensile strength. Fifty-gram buttons of most of the alloys were prepared in an argon atmosphere by melting commercially pure components in an induction-heated clay-graphite crucible. For cadmium and phosphorus alloys, arc melting in argon was used to minimize loss of additive by vaporization.



Figure 6 - Silver-brazed beryllium joint in the as-brazed condition (HF etch; bright light; 250X).



Fig. 7 - Silver-brazed beryllium joint after heating at 600°C for 6 hrs. (HF etch; bright light; 250X).



Fig. 8 - Silver-brazed beryllium joint after heating at 600°C for 1 week (HF etch; bright light; 250X).

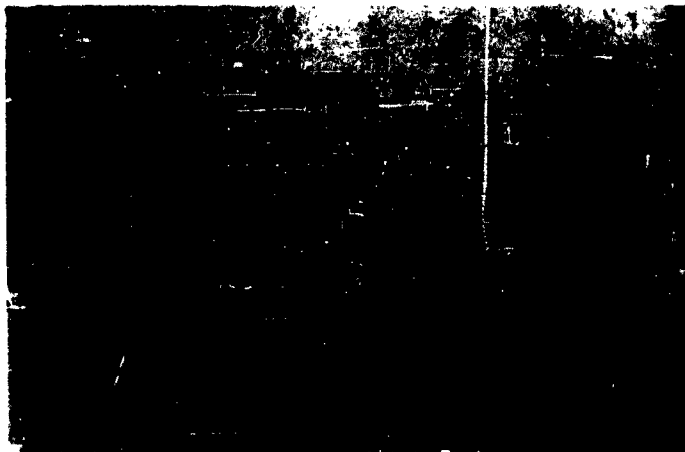


Fig. 9 . Silver-brazed beryllium joint after heating at 800°C for 6 hrs. (HF etch; bright light; 250X).

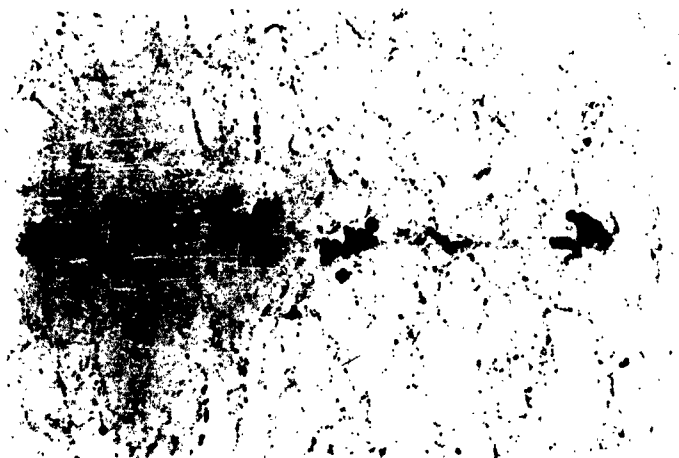


Fig. 10 - Silver-brazed beryllium joint after heating at 800°C for 1 week (HF etch; bright light; 250X).

Table 4. X-RAY ANALYSIS OF POWDER ATTRITIONED FROM THE FRACTURED SURFACES OF SILVER-BRAZED TENSILE SPECIMENS

Heat Treatment		Testing Temperature (°C)	Major Phase Present	Minor Phases Present
Temperature (°C)	Time at Temperature			
None	--	R.T.	Silver	Beryllium; delta phase*
None	--	600	Silver	Beryllium; delta phase
600	6 hr	R.T.	Silver	Beryllium; delta phase unidentified line
600	6 hr	600	Silver	Beryllium; delta phase
600	1 wk	R.T.	Silver	Beryllium only
600	1 wk	R.T.	Silver	Beryllium only
None	--	800	Silver	Beryllium; delta phase gamma phase*
800	6 hr	R.T.	Gamma Phase	Silver; beryllium; delta phase; un- identified phase
800	6 hr	800	Silver	Delta phase; gamma phase
800	1 wk	R.T.	Silver	Beryllium only
800	1 wk	800	BeO	Silver; beryllium; unidentified phase

* Corresponds to one of the Ag-Be intermetallic phases reported by Winkler⁽¹⁾.

After melting, the ingots were cleaned and rolled to approximately 0.005-in.-thick foil. The foil was placed between the beryllium specimens to be joined, and the braze was made in a vacuum furnace at 900°C for 3 min. using the bolted fixture of Phase I.

Table 5 gives the tensile strength of the specimens butt-brazed with the silver-base alloys. Data from other specimens brazed under the same conditions are also included with Ag-Li alloy for comparison.

A study was made of the flow and wetting action of the alloys on beryllium. Small strips of each alloy were melted in a vacuum chamber in small beryllium cups. None of the alloys appeared to wet the beryllium appreciably, with the exception of the Ag-Li alloy. All of the alloys did, however, bond to the beryllium where contact was maintained.

7-3 DISCUSSION OF RESULTS

7-3.1 Brazing Conditions and the Effects of Post-Brazing Heat Treatments.
In the brazing studies of Phases I and II, the joints produced were less than 0.001 inch thick; silver beryllides in these joints were detectable by X-ray diffraction of powder attritioned from the fractured joints.

The X-ray diffraction data obtained in Phase II generally follow the silver-beryllium phase diagram determined by Winkler⁽¹⁾. Cooling rates and soaking conditions may be the cause for the variation in the presence of intermetallics in the silver-brazed joint in that soaking the brazed specimens at temperatures below 760°C will apparently yield no intermetallics but excellent physical properties. At temperatures from 760°C to 860°C, the gamma phase (which apparently is very unstable below 760°C) is formed. In the temperature range from 850°C to 1010°C, the more common delta phase is encountered. When brazing at 900° to 1000°C, the delta phase is undoubtedly formed during cooling as one of the eutectic phases, and some of this phase is retained to room temperature.

The presence of intermetallic compounds in the braze joint appears to be deleterious to the mechanical properties of the joint. Maintaining the sample at elevated temperatures below 760°C will remove the intermetallics and strengthen the braze joint. This indicates that the rate at which the specimens are cooled to room temperature after brazing with silver has a critical effect on the properties of the joints. Maintaining the braze joint for short times at 760 - 860°C leads to room temperature embrittlement of the joint presumably due to the formation of the γ -phase. Extended holding times in this temperature range appear to eliminate the γ -phase and improve the room temperature mechanical properties. A temperature of 760°C, however, appears to be the maximum temperature for extended application of beryllium if intermetallics are to be completely avoided.

Because of the tendency of most braze alloys to consolidate rather than flow on the surface of beryllium, the application of external pressure to the joint is necessary. Selection of the proper pressure is partially dependent upon the geometric configuration of the pieces to be brazed, since deformation occurs readily at these brazing temperatures. For this study, a joint pressure was sought that would produce a sound brazed joint but minimum deformation. A

Table 5. TENSILE STRENGTH OF SPECIMENS BUTT-BRAZED WITH SILVER-BASE ALLOYS

Binary Addition	w/o Addition	Average Ultimate Tensile Strength (psi)
Lithium	0.5	41,200 30,300 <u>32,000</u> Av. 34,500
Zinc	2.3	13,400 22,400 <u>27,600</u> Av. 21,100
Phosphorus	0.16	20,100 23,800 <u>18,700</u> Av. 20,900
Indium	0.20	20,300 14,400 <u>22,800</u> Av. 19,200
Tin	2.1	16,600 <u>16,700</u> Av. 16,700
Cadmium	0.30	26,500 14,700 <u>9,400</u> Av. 16,900
Germanium	6.0	10,900 18,800 15,400 <u>14,200</u> Av. 14,800
Silicon	1.0	15,700 8,200 <u>16,800</u> Av. 13,600
Aluminum	5.6	4,400 <u>3,300</u> Av. 3,900

preliminary trial of various joint pressures indicated that a minimum pressure of 40 psi should be used to produce a sound joint with pure silver, although pressures up to 200 psi have been used without appreciable deformation. Pressures of less than 40 psi may yield small unbrazed areas in the joint.

Plating of silver on beryllium surfaces is not without difficulties. Variations in thickness of the silver plate should be minimized, as this might affect strength. Two conditions are opposed to obtaining a uniform thickness: (1) silver is deposited more slowly near the center than near the extremities of the surface being plated, so a slight gradient in thickness is obtained on each surface being plated; (2) beryllium prepared by powder metallurgy unavoidably contains some porosity. Pores at the surface are penetrated by silver during plating, thereby causing some areas of the joint to contain more silver than others. The first condition might be rectified by the use of more pressure on the joint to spread the silver to a more uniform thickness during brazing.

7-3.2 Developmental Braze Alloys. Of the developmental silver-base alloys studied, generally those containing highly volatile additives (e.g., zinc, phosphorus, and lithium) displayed the highest tensile strength, while those with relatively non-volatile additives (aluminum, silicon, tin and germanium) yielded relatively poor tensile results. The presence of a volatile additive to silver appears to be beneficial for the wetting and brazing of beryllium.

Only the silver alloys containing lithium showed any ability to flow on beryllium. Perhaps, in any further studies of additives to silver braze alloys, a ternary addition to the silver-lithium alloy would produce an alloy having superior braze properties.

Indium and phosphorus, in spite of their low concentration (0.2 %w/o) in their respective braze alloys, gave brazes of strength comparable to the silver-zinc alloy and better strengths than the tin, cadmium, germanium and silicon alloys. Further studies appear advisable on the use of indium and phosphorus in larger concentrations as additives to silver-base alloys for brazing beryllium.

7-4 CONCLUSIONS

(1) Brazed joints of improved quality can be made in structural beryllium by brazing with pure silver at a temperature of 900°C, using a brazing time of 1-5 min and a pressure in excess of 40 psi.

(2) Quality and reliability of the braze can be increased by starting with a very thin layer of silver and maintaining close control over brazing conditions.

(3) Quality of the silver-brazed joint can be improved by heating after brazing at 600°C for long periods of time.

(4) The presence of silver-beryllium intermetallics in a brazed joint appears to be detrimental to the tensile strength of the joints.

(5) The silver-lithium braze alloy, which is presently being used as a braze alloy for elevated-temperature applications, gives stronger joints than the other silver binary alloys tested in this program.

(6) Volatile additives (in small quantities) to silver produce braze alloys which result in stronger joints than those containing non-volatile additives.

REFERENCES

1. O. Winkler, Zeitschrift für Metallkunde, 30:162 (1938).

SECTION 8

FORGE WELDING OF BERYLLIUM

B. M. MacPherson and W. W. Beaver

(The Brush Beryllium Company, Cleveland, Ohio)

ABSTRACT

An investigation was carried out to determine the effect of hot working welds produced in beryllium by the tungsten-arc-inert gas method. The intention was to alter the cast structure of the weld zone and thereby produce welds having improved mechanical properties. Changes in the structure of the weld zone accompanied by strengthening of the weld were noted. However, little difference in weld ductility was observed. In a cursory investigation of resistance butt-welding of beryllium rods it was noted that high strength joints having a structure indistinguishable from that of the parent metal could be produced by this technique.

8-1 INTRODUCTION

Several years ago when the existing processes for joining structural beryllium shapes were aluminum-silicon braze welding and furnace brazing with silver-copper eutectic, The Brush Beryllium Company initiated a program to develop other processes for joining beryllium. Successful butt-type tungsten inert gas (TIG) fusion welding, the development of silver-lithium as a braze alloy for beryllium and silver braze welding were reported to Lockheed⁽¹⁾ in April, 1958. Since then, both silver brazing and fusion welding with beryllium filler wire have been used in fabricating experimental and production type components. In the WADD program "Fusion Welding of Beryllium" (Contract AF 33(616)-6413),⁽²⁾ which was recently completed, TIG fusion welding studies were continued. In 1958, a Brush program was started to study the joining of heavy sections by techniques similar to flash welding. This developed into a study of the resistance butt welding of beryllium.

The objective of the present program was to refine the grain structure in beryllium weldments by mechanical working and thereby improve the mechanical properties of such beryllium structures. Pronounced refinement of the grain structure of the cast metal was not necessarily expected with limited amounts of mechanical hot working of the beryllium fusion weld, but it was hoped that it would change the cast microstructure of the weld metal sufficiently so that failure in tension would occur in the parent metal.

The objectives of the resistance butt welding study were, to obtain the maximum strength of butt joint (in excess of 45,000 psi) without a cast structure in the weld joint, without excessive upsetting of the joint, and without appreciably changing the parent metal structure in the heat-affected zone.

8-2 EXPERIMENTAL WORK AND RESULTS

8-2.1 Mechanical Working of Fusion Welds. It has been shown with other metals that mechanical working of fusion welds by techniques such as roll planishing or peening produces stronger welds. With this as a basis, beryllium fusion welds have been hot worked either immediately behind the welding electrode or in a secondary working operation. For the latter operation, the fusion welds were made by the TIG welding process on 0.062- and 0.125-inch thick S-100 cross-rolled beryllium sheet, using 0.062-inch diameter drawn S-100 beryllium wire as described in Reference (2). All fusion welds were made transverse to the last direction of rolling of the sheet. These fusion welds were stress relieved at 825°C (1515°F) for 30 minutes prior to the secondary mechanical working operations.

(1) Hot Rolling of Welds as a Secondary Working Operation. The welds, prepared as described above, were mechanically deformed bare at 760°C (1400°F) or 825°C by one of the following techniques:

- (a) Hot rolling the weld reinforcement in the direction of welding, by techniques similar to roll planishing.
- (b) Hot rolling the weld and parent metal perpendicular to the weld, by techniques similar to ring rolling.

(c) Hot rolling the weld and parent metal in the welding direction.

For the first technique (roll planishing), the fusion welds were hot rolled flush to the sheet surfaces immediately following the stress-relieving operation. On all other hot rolling work, the reinforcements were removed by machining prior to hot rolling.

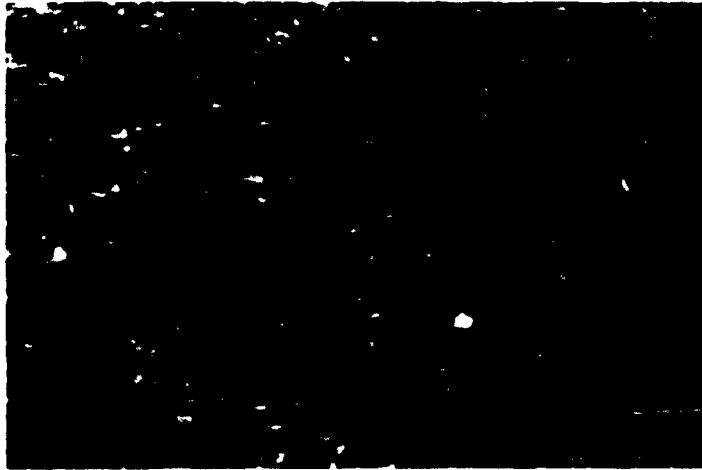
Metallographic examination of the fusion welds made for the hot rolling studies showed a heat-affected zone in the parent metal adjacent to the cast weld metal, as noted in Figure 11. This zone is not usually observed in similarly prepared beryllium fusion welds. The grains in this zone are slightly larger (about 30 to 50 percent) and do not have the elongated appearance of the grains in the parent metal (hot rolled S-100 sheet). Data for the unworked welds given in Table 1 show the mechanical properties to be low compared to the ultimate strengths of previous welds of this type (31,300 psi for 0.125-inch thick sheet), while the average grain size of this weld metal is about the same as previously encountered. Failure was usually along the center-line of the weld.

Fusion welds were either roll-planished or hot rolled to 10, 20, 35 or 50 percent reduction in thickness in both the welding direction and transverse to it. Some of these specimens had cracks which appeared to have started from edge tears in the parent metal and weld. The rolling temperature initially chosen was 760°C but because of the occurrence of cracks in some of the specimens, 825°C was also evaluated as a rolling temperature. Although some of the specimens still cracked during rolling at 825°C, rolling was continued to the scheduled thicknesses so that the mechanical deformation of the welds could still be studied metallographically.

Metallographic examination of weld cross-sections indicates a definitely deformed structure of the weld region in those welds (Figures 12 and 13) for which the reinforcement was rolled flush with the beryllium sheet (similar to roll planishing). The cast structure appears to be bent and distorted everywhere although some grains appear to have deformed considerably more than others. The welds which were hot rolled to 10 percent reduction in sheet thickness (Figures 13b, 14, and 15) have a slightly deformed structure, and the cast structure in the center of the weld shows indications of glide bending and deformation. Additional hot working to 35 percent reduction in thickness does not seem to have significantly changed the structure from that obtained with the 10 percent reduction in thickness.

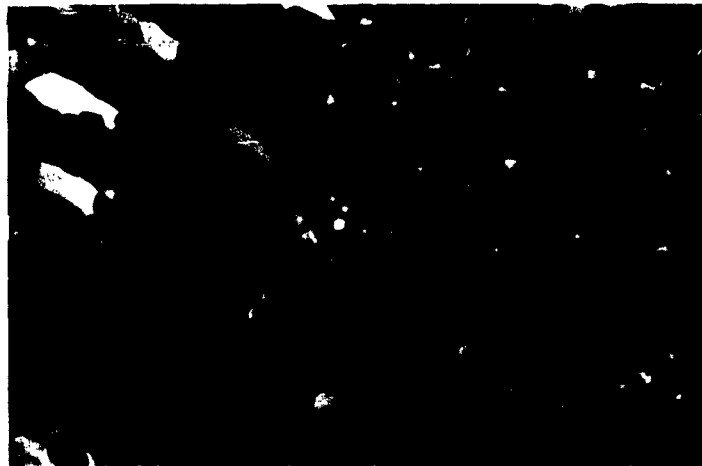
Table 7 gives the average grain size (measured on a cross-section perpendicular to the welding direction) for the hot rolled welds in 0.062- and 0.125-inch thick beryllium sheet. Although some refinement in grain size appears to result from mechanical hot working of beryllium fusion welds, there seems to be no significant reduction in grain size except for the 0.062-inch welded sheet which underwent a 35 percent reduction transverse to the direction of welding. On cross-sections of welds rolled in the welding direction, the apparent grain refinement might be due to elongation of the grains in a direction perpendicular to the metallographic section. Thus, the apparently smaller grain size in specimens rolled in the welding direction is not necessarily indicative of grain refinement.

Comparison of the mechanical properties of the mechanically deformed welds (Table 6) indicates that roll-planishing of welds in 0.062-inch sheet will yield relatively high ultimate strengths (45,300 psi). None of the fractures in this



(a) parent metal

weld heat affected zone parent metal



(b) heat-affected zone

Figure 11 - Cross sections of the heat-affected zone of fusion weld in 0.062-inch thick sheet. The weld reinforcement has been rolled flush to the sheet surface in the welding direction. 100X Pd. Lt.

Table 6. MECHANICAL PROPERTIES OF MECHANICALLY WORKED FUSION WELDS

Mechanical Working	Direction Of Working	Temp. of Working (°C)	Original Thickness (in.)	Ultimate Strength (psi x 10 ³)	Average Ultimate Strength (psi x 10 ³)	Location of Fracture with Reference to the Weld
None	--	--	0.062	35.4	28.8	center line
None	--	--	0.125	28.0		a
				30.7		center line
				27.4		center line
Roll planishing	Long.	760	0.062	44.5	45.3	edge
				41.7		edge
				49.4		parent metal
				46.5		edge
				44.5	43.4	edge
10%	Long.	760	0.062	43.8		center line
				46.7		center line
				39.6		center line
10%	Trans.	825	0.062	40.0	41.2	edge
				44.9		center line
				38.7		center line
10%	Long.	825	0.125	36.4	33.9	center line
				35.2		center line
				30.1		center line
10%	Trans.	825	0.125	40.1	40.2	center line
				40.3		center line
20%	Long.	760	0.062	47.1	49.9	center line
				52.2		center line
				50.5		center line
20%	Trans.	760	0.062	48.6	36.7	center line
35%	Trans.	825	0.062	27.0		a
				41.3		center line
				41.7		center line
50%	Long.	825	0.125	25.1	27.4	a
				28.6		a
				28.4		a

a - Weld and parent metal had surface defects - failures occurred at these defects.



(a) parent metal
0.062-inch thick sheet



(b) center of weld
0.062-inch thick sheet

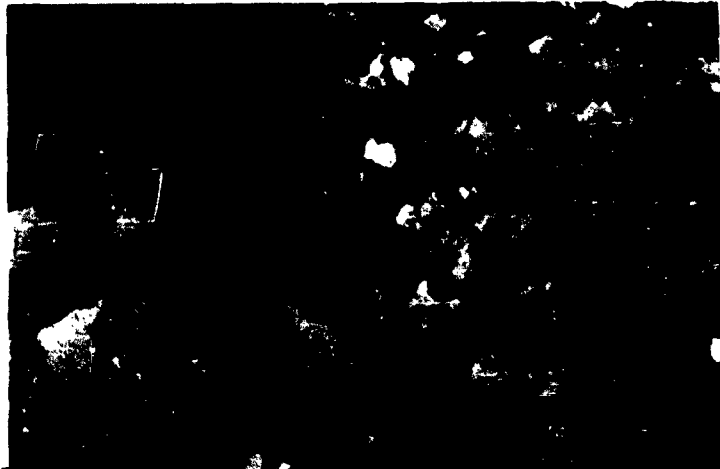


(c) parent metal
0.125-inch thick sheet



(d) center of weld
0.125-inch thick sheet

Figure 12 - Cross-sections of fusion welds that have had the weld reinforcement hot rolled flush with the sheet surfaces along the welding direction (roll planishing). 100X Pd. Lt.



(a) Edge of weld and parent metal which has had the weld reinforcement hot rolled flush with sheet surface (roll planishing).



(b) Edge of weld and parent metal which have been hot rolled in the welding direction to 10% reduction in thickness.

Figure 13 - Cross-sections of fusion welds that show the distortion of grain structure produced by various mechanical working techniques. 100X Pd. Lt.



(a) parent metal
0.062-inch thick sheet



(b) center of weld
0.062-inch thick sheet



(c) parent metal
0.125-inch thick sheet



(d) center of weld
0.125-inch thick sheet

Figure 14 - Cross sections of fusion welds that have been hot rolled to 10% reduction in sheet thickness in the welding direction.
100X Pd. Lt.



(a) parent metal
0.062-inch thick sheet



(b) center of weld
0.062-inch thick sheet



(c) parent metal
0.125-inch thick sheet



(d) center of weld
0.125-inch thick sheet

Figure 15 - Cross sections of fusion welds that have been hot rolled to 10% reduction in thickness, transverse to the weld.
100X Pd. Lt.

**Table 7. GRAIN SIZE FROM CROSS SECTION OF MECHANICALLY
WORKED FUSION WELDS**

Amount of Deformation	Temp. of Working Operation (°C)	Rolling Direction	Grain Size of Parent Metal (μ)	Grain Size of Weld Metal (μ)
0.062-Inch Thick Beryllium Sheets				
None	None	None	19	71
Roll Planishing	760	Long.	21	57
10%	760	Long.	17	53
10%	825	Trans.	25	64
20%	760	Long.	20	64
20%	760	Trans.	21	80
35%	760	Long.	21	53
35%	825	Trans.	28	43
0.125-Inch Thick Beryllium Sheets				
None	None	None	20	80
Roll Planishing	760	Long.	20	71
10%	825	Long.	19	64
10%	825	Trans.	19	80
20%	825	Long.	16	71
20%	760	Trans.	--	--
50%	825	Long.	16	49
50%	825	Trans.	18	64

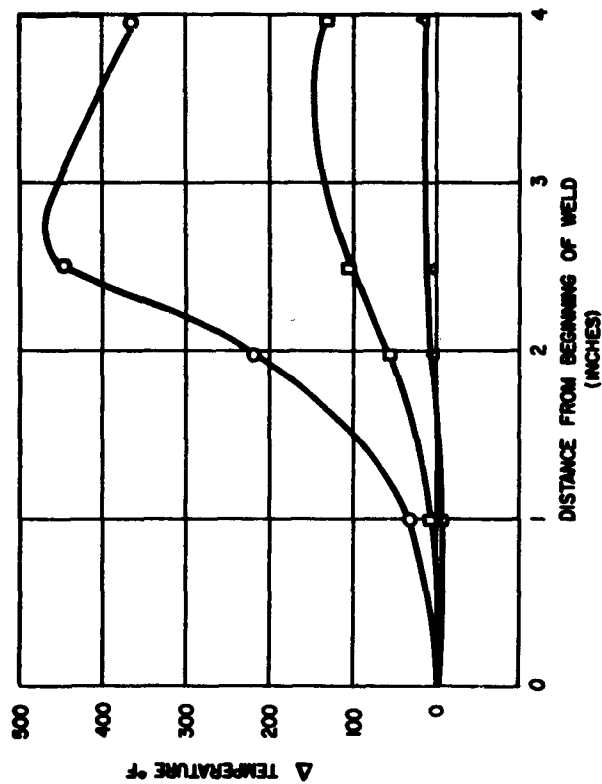
group occurred in the center line of the weld as would be normal for beryllium fusion welds, but rather at the edge of the weld metal or (in the case of the specimen that fractured at 49,400 psi) in the parent metal. Tensile samples of rolled-planished welds made in 0.125-inch thick sheet could not be obtained due to cracking of the welds during the planishing operation. Relatively high strengths could be produced in welds made in 0.062-inch thick sheet rolled 20 percent at 760°C in the welding direction. Failure, however still occurred along the weld center line. From the mechanical test data in Table 6, it appears that prolonged rolling at 825°C is detrimental to the mechanical properties and surface conditions.

(2) Mechanical Working of Welds Immediately Following the Arc. Beryllium fusion welds in 0.062-inch thick sheet were mechanically deformed immediately following the welding arc to determine how this affects the structure of the weld area.

It was determined from past studies (2) that it would be necessary to preheat the weld in order to maintain a sufficiently high temperature in the region just behind the arc. In order to define the preheat condition for these beryllium welds, fusion welds (without mechanical working) were made under various preheating conditions - at room temperature, 100°, 200°, 300°, 400°, 500°, and 600°F. This study was made on 0.062-inch thick sheet using the automatic TIG welding process with 1/16-inch diameter beryllium welding wire. Thermocouples were placed on a line perpendicular to the weld and 2-1/2 inches from the beginning of the weld. The temperatures at positions along this line (1/2, 1-1/2 and 2-1/2 inches from the center line of the weld) were recorded. At each preheat temperature welding conditions were altered to compensate for the change in thermal conditions. Therefore, the curves of temperature vs. torch position obtained at the various preheat temperatures were basically similar. Each of the curves in Figure 16 is the average of the seven curves showing the increase in temperature from the starting preheat temperature. Because of the sharp temperature gradient behind the arc, even at the slow welding speed of 4 inches/minute, a preheat temperature of 600°F was chosen so that the fusion welds would be in the warm working range. A peening operation took place about 2 inches behind the welding arc.

The beryllium fusion welds were made by automatic TIG welding using a ceramic-coated metal backup for the mechanical working apparatus, and a 600°F preheat temperature. The A.C. automatic TIG welding conditions for this operation were: travel speed, 4 inches/minute; wire feed, 2 to 3 inches/minute; and 50-50 argon-helium arc atmosphere of 40 cfh.

In an effort to determine the proper peening conditions for this operation, beryllium fusion welds which had previously been prepared were mechanically deformed with a blunt tool at 800° - 850°F under conditions simulating those scheduled for the operation of mechanical working immediately following the arc. The welds were given various amounts of deformation. Although the worked welds generally were not cracked on top where the impact was made, the weld bottoms were cracked. Therefore, it was determined that the fusion welds could not be peened flush with the sheet in this temperature range but a deformation of only about 0.025 to 0.040 inch on the weld reinforcement could be accomplished without cracking the weld on the bottom.



Average Increase in Temperature

○ .5 in. from center line of weld
 □ 1.5 in. from center line of weld
 ▲ 2.5 in. from center line of weld.

Figure 16 Average increase in temperature at a position along a line 2-1/2 inches from beginning of weld vs. electrode position.

An 8-inch long fusion weld, that was made in 0.062-inch thick sheet by the automatic TIG welding process, was manually peened (Super Slugger Model 500 manufactured by Noble and Stanton, Inc., Bedford, Ohio) immediately following the welding arc. There were four basic conditions or sections in the weld: (1) weld metal that was mechanically worked, (2) weld metal that was mechanically worked and was vibrated during solidification by the mechanical working operations, (3) weld metal that was vibrated during solidification by the mechanical working operations, but was not mechanically worked, and (4) weld metal not subjected to mechanical working or vibration.

Although, once the peening operation started, the arc was difficult to maintain, microsections were nevertheless obtained on all four types of weld metal. There is an indication that grain size is finer in the mechanically worked welds than in those which were not mechanically worked, as shown in Table 8. Section (1) and (2) metal shows a deformed grain structure in the cast weld metal. However, vibration at this level is apparently not sufficient to produce grain refinement in the cast structure, since there appears to be no significant difference in grain size between the metal of Section (3) and that of Section (4).

(c) Forging of Welds as a Secondary Working Operation. Fusion welds made in 0.125-inch thick beryllium with 1/16-inch diameter beryllium wire were upset under warm working conditions. These welds, which were made by the manual TIG welding process, had their reinforcements forged to various degrees. The forging press used had flat dies preheated to 800° - 825°F. The beryllium welds to be forged were heated to temperatures of 1050°, 1200°, and 1500°F in either a salt pot or a furnace. The best forging results were obtained after heating to a temperature of 1500°F in the salt pot. Although ram speeds of 20 to 30 inches per minute were used, the welds apparently were well below 1500°F when the forging operation took place, and cracking occurred. Welds forged flush with the sheet under these warm working conditions exhibited cracking in the welds and in the parent metal. However, smaller reductions on the weld reinforcement could be accomplished without cracking. From previous experience it is expected that, with slower upsetting speeds, stock temperatures in the range of 1350° to 1500°F, and die temperatures in the same range, successful upsetting of welds employing single or multiple upsetting operations would be possible. This would then approach the conditions encountered in the hot-working of welds by multiple hot rolling operations.

8-2.2 Resistance Butt Welding of Beryllium. The initial resistance butt welding studies were performed on a 600 KVA Sciaky machine, using both a specially built weld fixture for clamping the 5/8-inch diameter beryllium specimens and an argon filled plastic enclosure as shown in Figure 17. Specimens made from 5/8-inch diameter S-100 hot extruded beryllium, having 2-1/2 inch radius spherical domes on the butting ends, were prepared for welding by pickling (after machining) in a 40 percent nitric - 2 percent hydrofluoric acid bath. The initial machine settings were similar to those used for aluminum butt welding using a weld pressure range of 6,000 to 8,000 psi with a single impulse.* A variation of less than

- - - - -

* Four cycles where one cycle = 1/60 sec.

**Table 8. GRAIN SIZE FROM CROSS SECTION OF FUSION WELD
MECHANICALLY WORKED IMMEDIATELY FOLLOWING
THE WELDING ARC**

Metal Condition	Grain Size (μ)	
	Weld Metal	Parent Metal
1 - Mechanically worked	58	20
2 - Mechanically worked and vibrated	64	24
3 - Vibrated only	80	23
4 - As welded	80	24

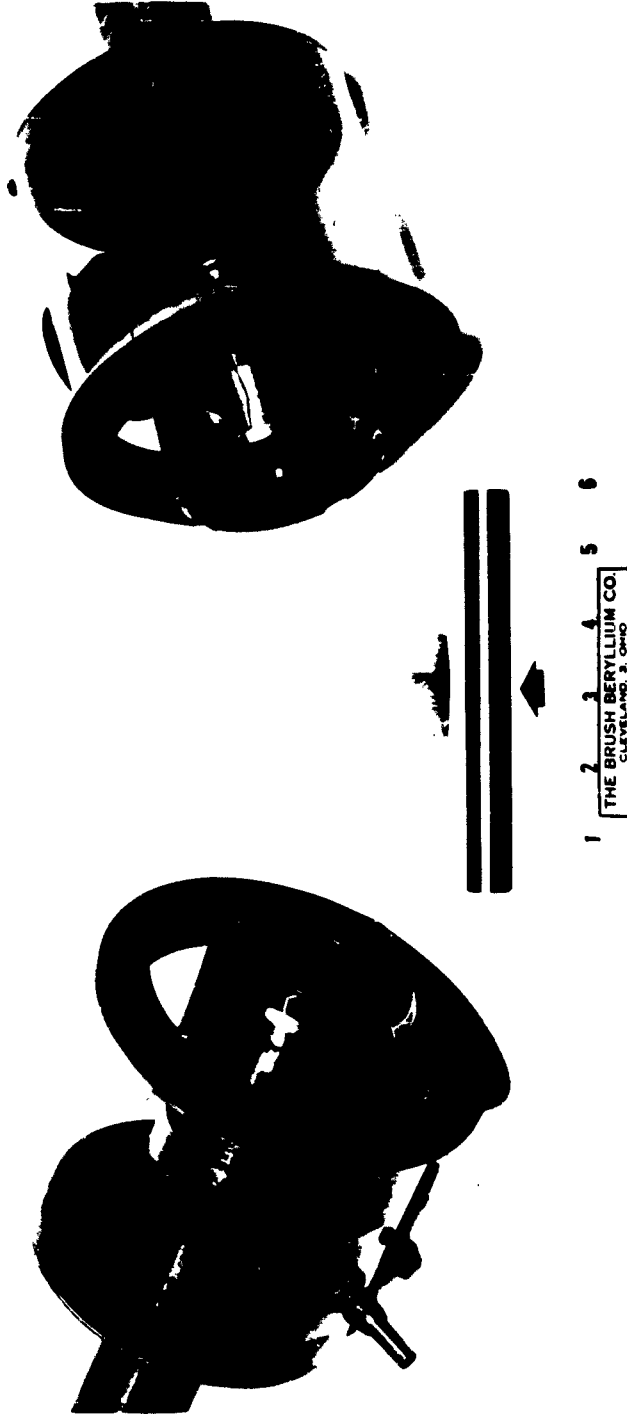


Figure 17 - This special welding fixture with plastic enclosure for the inert gas welding atmosphere was built for resistance butt welding 5/8-inch diameter beryllium specimens. A 5/8-inch diameter, centerless ground, resistance butt welded beryllium specimen (with arrow marking the weld) is shown with the alumina retaining tube.

8 percent on the weld phase shift setting was sufficient to go from no weld to expulsion of liquid beryllium metal from the joint. In the specimens that were joined, there was a thick area of cast metal in the center, whereas the outside area had not reached joining temperatures. As expected, this cast weld metal broke quite easily. The temperature variation across the joint may have been caused by the proximity of the clamps to the weld joint or by the sample geometry. The spherical radius of 2-1/2 inches on the beryllium butting surfaces seems to have been excessive for proper forging action in the resistance butt welding and poor results were obtained.

Additional resistance butt welding studies were made with five impulses,** and the welding operation was performed on a 400-KVA machine. The 5/8-inch diameter beryllium specimens were gripped 3/4 inch from the flat butting surfaces, and an 8,000 psi weld pressure was applied to the joint. Although considerable improvement in the results was obtained with multiple impulses and the changed sample geometry, the operating range of current was not as wide as desired. Figure 39 shows the appearance of typical resistance butt welds made with multiple impulses; the room temperature mechanical properties of the welds (Specimens 3 and 5) are given in Table 9. Because of the narrow operating range of current, these welds may have a cast metal structure (Figure 19).

In order to obtain more consistent welding results, 5/8-inch-ID aluminum oxide tubes were placed so as to encompass the weld joint completely. By use of these retainers and five impulses, a much wider welding range was realized and upsetting of the beryllium in the joint area was minimized (Figure 20). In addition, the use of an alumina retaining tube prevents expulsion of liquid metal should a hot spot occur.

When alumina tubes are used, butt welds can be made with the weld interface indistinct (as in Figure 21b) except for the outside surface. The mechanical properties of these welds (Specimens 14 and 16) are given in Table 9.

In the light of these encouraging results, further studies were made on the same 400 KVA press head resistance welder with 5/8-inch diameter beryllium specimens using alumina retainers under the best conditions developed in the previous tests. The microstructure of the weld made with five impulses (for which mechanical data are reported in Table 10) is entirely different than was obtained in the previous welds made at five impulses (Table 9) in that a heavy cast structure was noted in the center while no weld was made on the outside.

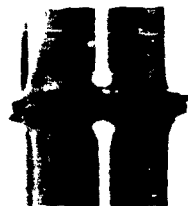
Since the ability to bond improved when the number of impulses increased from one to five, (Table 9), it seemed advisable to try longer times at diffusion temperatures by increasing the number of impulses to ten. Tensile and metallographic specimens were prepared under the best conditions developed at ten impulses and the results are also reported in Table 10.^b The microstructure for the ten-impulse weld, 41% phase shift, was similar to that shown in Figure 21b with the exception of slightly enlarged grains in the joint area.

- - - - -

** 1-1/2 cycles between impulses.



(a) Specimen No. 3, five impulses,
52% phase shift (125,000 amperes)



(b) Specimen No. 5, five impulses,
51% phase shift (123,000 amperes)

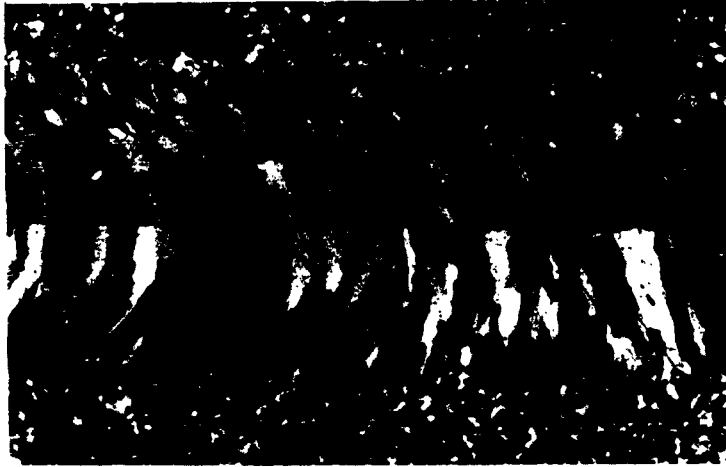
Figure 18 - Resistance butt welded specimens.

Table 9. ROOM TEMPERATURE MECHANICAL PROPERTIES OF RESISTANCE
BUTT WELDED SPECIMENS

(All welds made with five impulses at 8000 psi pressure.)

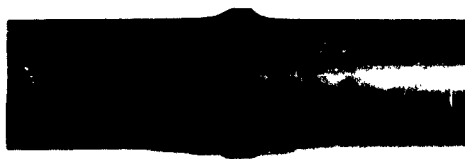
Specimen Number	Welding Conditions		Al ₂ O ₃ Retainer	Modulus of Elasticity (psi x 10 ⁶)	Ultimate Strength (psi x 10 ³)	0.2 Percent Offset Yield Strength (psi x 10 ³)	Elongation in 2 inches (%)	Location of Fracture
	Phase Shift (%)	Current, (amps x 10 ³)						
3	52	125	No	--	47.4	41.3	0.6	Button Head
5	51	123	No	47.5	49.9	46.5	0.4	Weld Zone
14	56	133	Yes	47.8	52.5	45.7	0.6	Button Head
16	56	133	Yes	47.5	45.3	--	0.2	Weld ^(a)

(a) Unbonded area in weld.



100X Pd. Lt.

Figure 19 - Photomicrograph of resistance butt weld made with five impulses, 51% phase shift (no alumina retainer).



Specimen 14

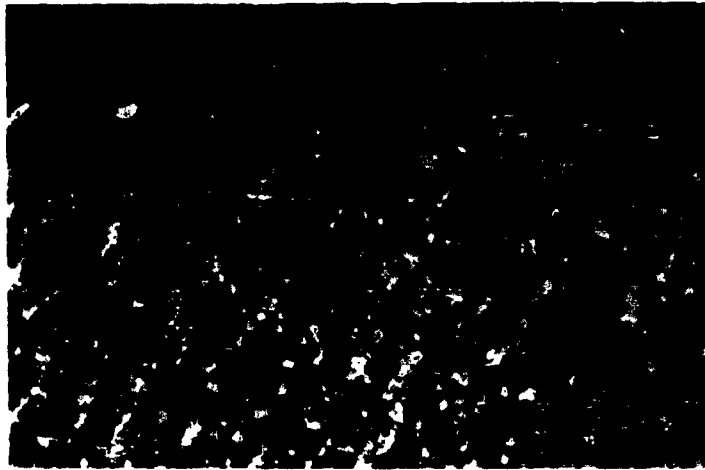


Specimen 15

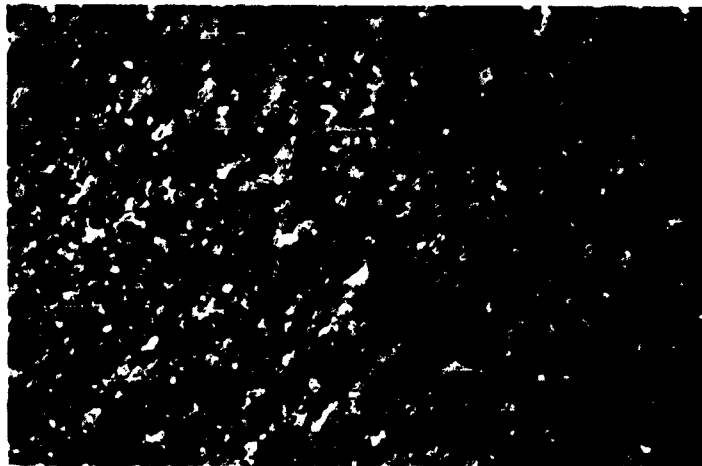


Specimen 16

Figure 20 - Resistance butt welded specimens welded with aluminum oxide retaining tubes at five impulses and 56% phase shift. (133,000 amperes)



(a) Made with 52% phase shift, 125,000 amperes.



(b) Made with 56% phase shift, 133,000 amperes.

Figure 21 - Photomicrograph of resistance butt welds made with an alumina retainer and five impulses. "a" shows a partially diffused joint and "b" shows a joint that is relatively indistinct. 250X Pd. Lt.

Table 10. MECHANICAL PROPERTIES OF RESISTANCE-BUTT WELDED SPECIMENS
(Pressure 8,000 psi)

Number of Impulses	Phase Shift Setting (%)	Modulus (psi x 10 ⁶)	Ultimate Strength (psi x 10 ³)	Average Ult. Str ⁴ (psi x 10 ³)	0.2 Percent Offset Yield Strength (psi x 10 ³)	Elongation 1 Inch (%)	Location of Fracture
5	56	47.6	29.8		--	0.16	Weld Zone
5	56	43.4	50.7		44.4	0.79	Weld Zone
5	56	--	27.5	36.3	--	0.41	Weld Zone
5	57	--	34.7		--	0.39	Weld Zone
5	57	45.4	31.2		--	0.18	Weld Zone
5	57	--	30.2	32.0	--	0.24	Weld Zone
10	41	43.4	54.0		44.8	1.39	Gauge Mark
10	41	44.1	48.3		43.5	0.86	Weld Zone
10	41	41.9	58.3	53.5	43.2	1.55	Weld Zone
10	42	45.4	41.6		--	0.61	Weld Zone
10	40	--	47.9		43.1	0.93	Weld Zone
10	40	--	45.3	44.9	43.3	0.47	Weld Zone

8-3 DISCUSSION OF RESULTS

8-3.1 Mechanical Working of Fusion Welds. There are three major factors affecting the properties of the cast metal in beryllium fusion welds: (1) grain size, (2) grain shape, and (3) crystallographic texture. The past programs have endeavored to refine the weld grain structure by means of closer control of the welding parameters, nucleating agents, etc., but there has been no concerted effort to refine the grain structure by mechanical working of the weld.

In cross rolled beryllium sheet, the basal planes are preferentially oriented parallel to the plane of the sheet. This yields good mechanical properties in the rolling and transverse directions. Fusion welds made in such beryllium sheets have preferentially oriented (determined by metallographic examination in polarized light) elongated grains lying parallel to the weld at the weld center line. This leads to a plane of weakness normal to the usual direction of tensile testing. This unfavorable grain structure has been altered by mechanical working of the weld to the extent that it may be possible to have failure occur in the parent metal rather than in the weld metal.

Rolling of the weld reinforcements (roll planishing) seems to have a greater effect on the weld properties than does reduction by hot rolling of welds from which the reinforcement has been removed. The weld metal must be hot worked carefully in the initial working operations prior to heavier reductions. For this reason, roll planishing seems to be easier than other forms of mechanical working and seems to be less likely to cause cracking in the weld and parent metal.

It also appears from this work that weld reinforcements can be hot-worked (but not warm-worked) flush with the parent metal without extreme difficulties. Higher hot working temperatures lead to greater ease of working, but temperatures above 800°C apparently cause detrimental grain growth. Welds rolled at 760°C, at which temperature detrimental grain growth does not seem to be encountered, show mechanical properties improving with the degree of working. Ultimate tensile strengths in excess of 50,000 psi could be obtained with a 20% reduction at 760°C.

The elongated columnar grains usually present in the weld zone have been shown to be undesirable; it is advantageous to refine this structure. It may be possible to obtain a refined grain structure in the as-welded condition by use of ultrasonic or sonic vibration of the molten pool during the welding operation. Low-frequency vibrations such as are caused by peening the sheet during the welding operation do not seem to have a significant effect upon the weld structure, but perhaps higher frequency vibrations will have beneficial effects.

8-3.2 Resistance Butt Welding. Although good mechanical properties may be obtained with a minimum of cast structure at the interface of a resistance butt welded joint, joints produced completely in the solid state should yield superior properties. It appears that such a joint (in which the joint interface is indistinct) can be made by resistance butt welding and that such joints are as strong or stronger than the parent beryllium metal being joined. The best welding conditions for consistently making this resistance welded joint have not been definitely determined, but the effects of various welding parameters have been determined: (a) longer time at diffusion temperatures seems to promote a stronger

and more reproducible bond (as determined metallographically and by tensile testing), (b) excessive upsetting of the weld zone is thought to be detrimental because of the unfavorable basal plane texture caused by the deformation (basal planes oriented perpendicular to the direction of tension), (c) the beryllium metal to be joined should not be gripped too close to the joint, because of the high thermal conductivity of the beryllium metal, and (d) the mating surfaces to be joined should be flat and clean.

A contributing factor to the attaining of high strength joints in this operation may be the thermal cycling between the α and β phase fields of beryllium.

8-4 CONCLUSIONS

- (1) Properties are definitely improved by mechanically deforming the beryllium fusion weld by hot rolling under controlled conditions.
- (2) The greater the degree of mechanical deformation of the cast weld metal (reduction in thickness by hot rolling) the greater is the improvement in mechanical properties under controlled mechanical working conditions.
- (3) The best weld microstructure was obtained by mechanically hot working the fusion weld reinforcement flush with the parent metal by roll planishing techniques.
- (4) Hot working of the fusion weld reinforcement flush with the welded sheet is preferred over warm working.
- (5) Resistance butt welds can be made in beryllium to give a weld joint that is indistinct from the parent metal and with ultimate strengths in excess of 45,000 psi.
- (6) For resistance butt welding of beryllium, longer time at diffusion temperatures in the solid state diffusion range seem to promote more reliable joints.

REFERENCES

1. B. M. MacPherson, Brush Beryllium Company, private communication to Lockheed Aircraft Corporation, April, 1958.
2. B. M. MacPherson and W. W. Beaver, Fusion Welding of Beryllium, WADD TR 60-917, January, 1961.

SECTION 9

RESISTANCE WELDING OF BERYLLIUM SHEET

E. F. Nippes, W. F. Savage, F. A. Wassell and D. A. Karlyn

(Rensselaer Polytechnic Institute, Troy, New York)

ABSTRACT

This report summarizes the results of studies of the effect of the following variables on the spot welding of 0.020-, 0.040-, and 0.060-inch AMC beryllium sheet:

- (1) Welding current magnitude
- (2) Welding time
- (3) Electrode force
- (4) Electrode geometry
- (5) Forging force
- (6) Forging delay time
- (7) Preheat current magnitude
- (8) Preheat current time
- (9) Post-heat current magnitude
- (10) Post-heat current time

Weld diameter measurements were employed, together with sheet separation and indentation measurements, to study the influence of welding variables on the welding process. Tensile-shear test results were found to be erratic, and the strength of welds with no apparent defects was disappointingly low.

The useful range of the important welding variables is summarized in graphical form for each of the three thicknesses studied. Cracking was observed in almost every case with single impulse welds. The application of preheat and postheat currents and the utilization of a forging force, applied after an appropriate forging delay time following the weld interval, were found to eliminate cracking and porosity in the weld. Although metallographic evidence is presented that the application of a forging force after the weld interval may cause recrystallization of the columnar dendritic weld metal, the timing of the instant of application of the forging force is too critical to be reproducible with existing welding controls.

A novel spring-loaded electrode assembly is described which provides the rapid electrode follow-up essential in the resistance welding of beryllium. The design of the spring-loaded electrode assembly also permits the use of dual-pressure cycles in order to provide forging action during cooling of the weld.

A brief exploratory investigation of the feasibility of resistance brazing of beryllium is contained in the Appendix to this report.

9-1 INTRODUCTION

The object of this investigation was to develop techniques for the resistance spot welding of beryllium sheet in three thickness combinations, 0.020 to 0.020 inch, 0.040 to 0.040 inch, and 0.060 to 0.060 inch. In addition, resistance brazing utilizing a silver-copper eutectic as an intermediate material between the beryllium sheets was to be investigated.

9-2 MATERIAL

9-2.1 Source. The three thicknesses of beryllium sheet used in this investigation were supplied by Nuclear Metals, Inc. The material was produced as part of the AMC beryllium sheet rolling program conducted by the Brush Beryllium Company, Cleveland, Ohio, from November 1957 to March 1960. Table 11 summarizes the important mechanical properties of this material.⁽¹⁾

9-2.2 Surface Appearance and Defects. All three sheets were poor in surface appearance. The rough surface finishes suggest that the sheets were ground or abrasive finished sometime during their processing. Evidence of some sub-surface damage has been observed⁽²⁾ in some of the microscopic studies conducted. Micro-cracks and the rough surface finish of the sheet are believed to cause significant reductions in the weld strengths as a result of the high notch sensitivity of the material, but no practical means of insuring the absence of surface defects was available.

The sheets varied in thickness by as much as 20 percent. This is greater than normal for sheets of these dimensions in other commercial materials. The greatest variation was noted at the edges, which were always thicker than the rest of the sheet. These variations in thickness made it difficult to control the thickness of the sheet after the etching operations used to produce a satisfactory surface for welding. In addition, numerous surface blemishes made some sections of the sheets unusable.

The thinner sheets were so severely warped that even the 1 x 3-inch weld coupons were not flat. The fact that the specimens were not flat initially undoubtedly caused variations in the amount of residual stress present in the completed welds and contributed to the observed scatter in weld strength data.

9-3 EQUIPMENT

9-3.1 Atmosphere Box and Exhaust System. An 8 x 8 x 8-inch clear plastic atmosphere box was constructed around the resistance welding electrodes to contain any expulsion of toxic products during welding without sacrifice in visibility of the welding operation (see Figure 22). The top of the box consisted of a 7-inch diameter rubber diaphragm which permitted the top electrode to move approximately 1 inch vertically. The front of the box was removable to provide access for changing electrodes and inserting the work between the electrodes for welding. A soft rubber gasket was provided as a seal for the access door.

Table 11. SUMMARY OF MECHANICAL PROPERTIES OF BERYLLIUM SHEET USED IN THIS INVESTIGATION (1)

Sheet No.	Gauge (inches)	Test Direction	Ultimate Tensile Strength (psi)	Yield Strength	Elong. (%)	Red. in Area (%)	Grain Size (microns)	Degree of Basal Plane Orient.	BeO Content
14B	0.020	Long.	69,800	47,000	5.8	5.5	13	5.9	1.51
		Trans.	--	--	--	--			
38A	0.040	Long.	65,400	44,200	6.0	4.8	13	6.9	1.30
		Trans.	--	--	--	--			
15	0.060	Long.	77,200	43,100	11.0	9.4	20	3.4	1.30
		Trans.	--	--	--	--			
		Long.	65,600	41,500	11.5	9.0			
		Trans.	--	--	--	--			

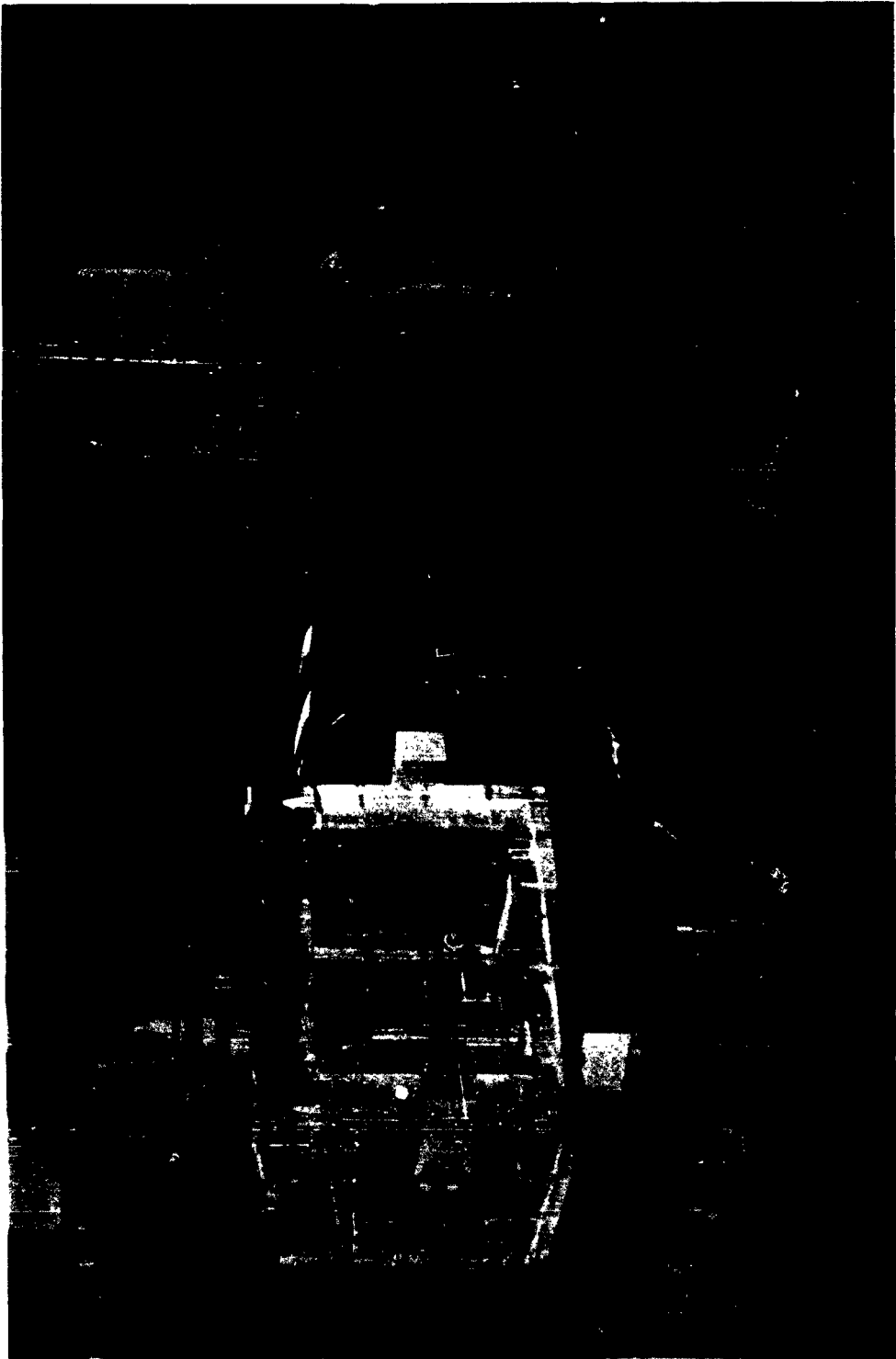


Figure 22 - Atmosphere Box.

Helium gas was permitted to flow through the box for approximately 30 sec. before welding, and a positive pressure of helium was maintained within the atmosphere box during welding operations. The helium out-flow was bubbled through a water bath located outside of the laboratory and exhausted to the atmosphere. A high-velocity exhaust fan provided atmosphere ventilation for the area in the front of the box, and was connected to an exhaust duct terminating outside the building.

9-3.2 Resistance Welding Equipment. A 200 K.V.A. dual force type spot welder, shown in Figure 23 was used for all welding conducted during this investigation. This welder provides a forging mechanism which can be initiated at any instant during the weld cycle.

During the early stages of the investigation a conventional spring-loaded electrode assembly was utilized to provide rapid follow-up of the electrodes during welding. Since the maximum capacity of this device was 550 pounds, a new electrode loading system was devised for use during experiments in which forging operations were performed after completion of the weld. This system, shown in Figure 24, functions as follows:

- (1) The top electrode is mounted at the lower end of the water-cooled electrode holder. This electrode holder is free to slide up and down through a bushing clamped in the upper arm of the welding machine. The top end of the electrode holder is restrained from moving upward by contact with the mid-point of the lower member of the two-leaf spring assembly visible in Figure 23 and 24.
- (2) The initial welding force is controlled by the initial deflection produced in the two-leaf spring by the action of the air cylinder visible at the top of Figure 23. An adjustable stop on the piston assembly permits the selection of any desired initial deflection and thus controls the initial welding force. The elastic deflection of the two-leaf spring provides the desired rapid follow-up of the electrode holder during welding.
- (3) After an adjustable, predetermined forging delay, the adjustable stop is freed by actuation of a solenoid-operated latch; an additional deflection of the two-leaf spring was introduced to provide the desired forging force. The design of the two-leaf spring results in a force increment of 4.2 pounds per 0.001-inch deflection at midspan. Thus, for example, a forging force of 1000 pounds requires a deflection of 0.238 inch. The amount of deflection during the forging interval is controlled by a second adjustable stop to arrest the downward motion of the loading piston at the appropriate point. Since the amount of indentation of the welded specimens rarely exceeds 0.006 inch, the total decrease in the forging force caused by indentation of the work does not exceed 26 pounds during the entire welding operation.

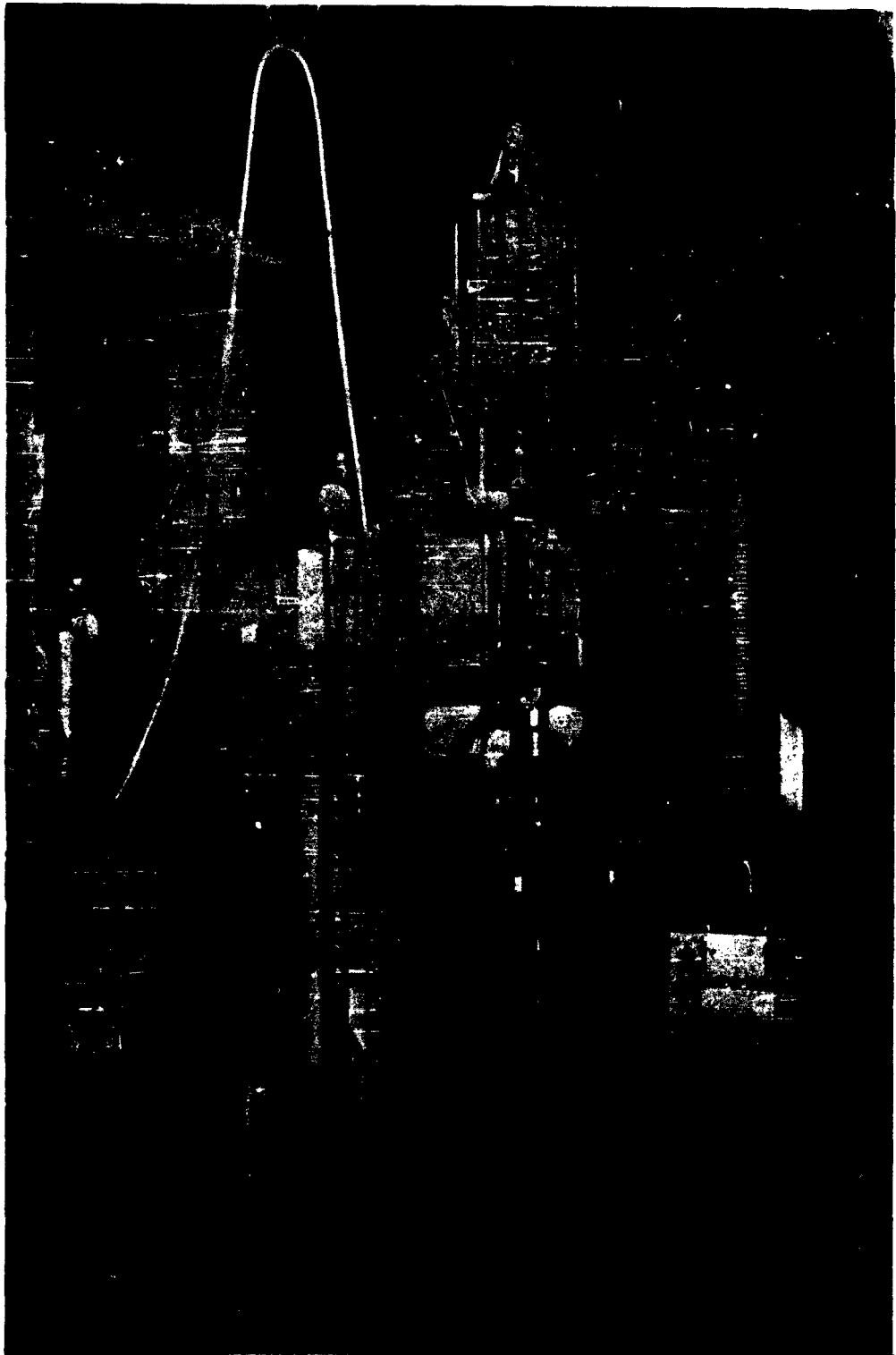


Figure 23 - 200 K.V.A. Dual Force-Type Spot Welder.

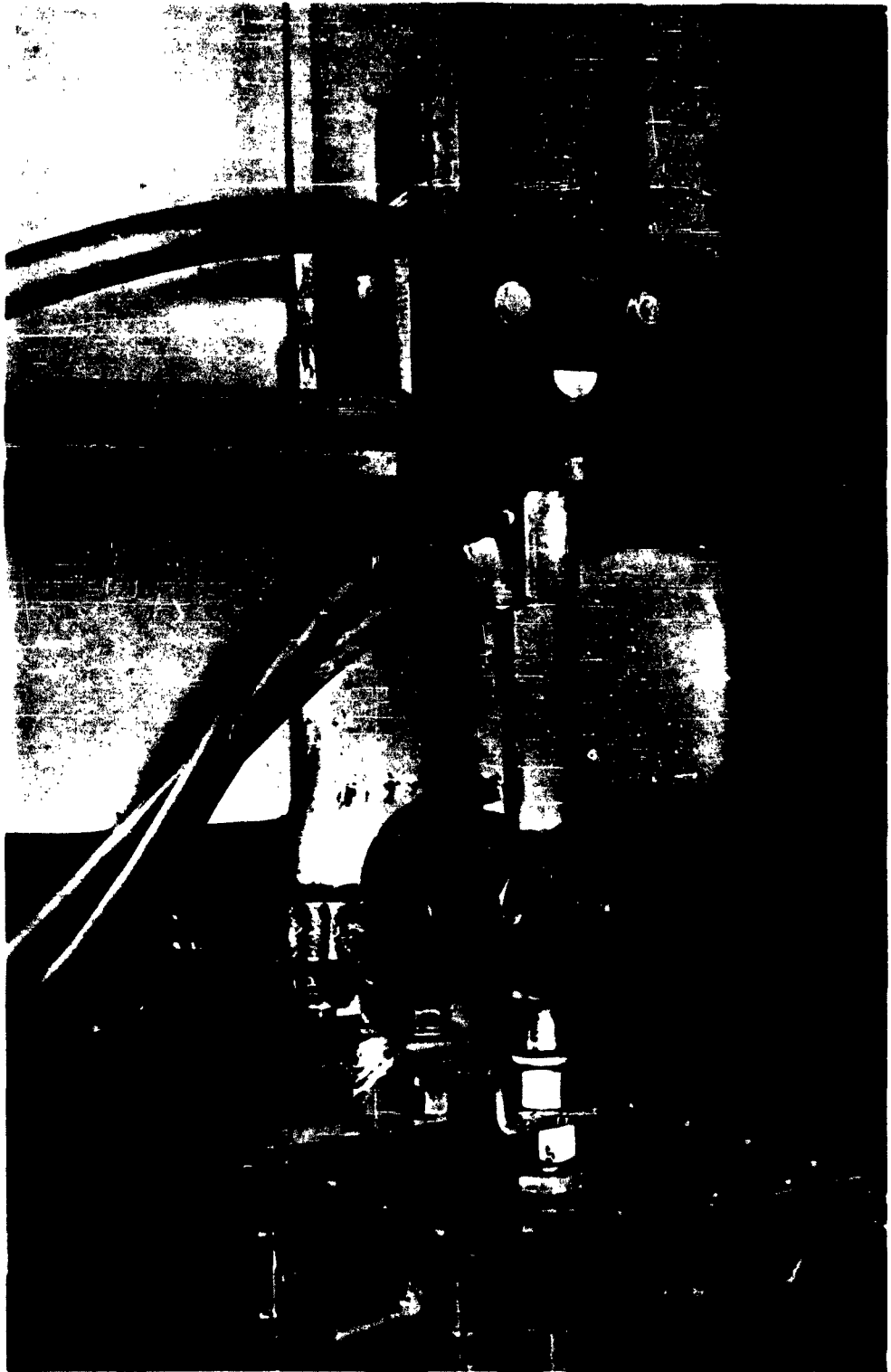


Figure 24 - Two-leaf spring used for high electrode forces.

The welding controls include a modified NEMA Type 5B synchronous timer and an experimental program controller. The former provides synchronous timing of both a weld and a postheat cycle with independent electronic control of the weld and postheat current magnitude. The program controller provides up to ten consecutive, independently controlled time intervals, each incorporating independent electronic control of the current magnitude. Provision is also made for incorporating up-and-down slope control during two intervals, and a separate timer allows application of a forging force after an adjustable forging delay interval.

Electrodes used are RWMA Class 2. The bottom electrode is inserted in a suitable water-cooled electrode holder while the top electrode is mounted as described above.

Surface contact resistance measurements, used to evaluate surface condition, were made using a modified Kelvin double bridge designed and constructed in the R.P.I. Welding Research Laboratory⁽³⁾. A pair of RWMA Class 2 electrodes machined with a 4-inch continuous radius dome was used with an electrode force of 500 pounds for all contact resistance measurements.

Welding current values were measured using a commercially available portable secondary welding current meter with an accuracy of $\pm 3\%$. All welding currents are reported as true RMS secondary current.

A commercially available deflection-type force gage was employed to measure static electrode force.

9-4 PROCEDURE

9-4.1 Material Preparation. The 24 x 60-inch sheets were acid machined into 1 x 3-inch coupons by painting both sides and the edges of each sheet with several coats of lacquer and scribing through the lacquer at the locations where cutting was to take place. The sheet was then immersed in a 10% to 30% sulphuric acid solution until individual specimens were separated by the etching action at the scribe marks.

After rinsing the coupons with water, the lacquer was removed by either dissolving in acetone or by boiling in water for about 30 min. and peeling the lacquer off. The latter method was found to be the fastest and easiest method to use. After the lacquer was peeled off, the coupons were rinsed in acetone to remove any residual traces of lacquer.

All material was etched prior to welding in order to obtain a uniformly low surface contact resistance. Attempts at abrasive cleaning with both steel wool or a fine wool and fine emery paper proved unsatisfactory since a high, variable contact resistance was found to result with either method.

Etching in 2% sulphuric acid at room temperature for three minutes was found to produce a satisfactory, clean surface with a minimum loss of thickness. Longer periods of etching resulted in a gradual increase in surface contact resistance, as shown by the dashed curve in Figure 25. The increase in contact resistance is probably due to a film or residue which is formed on the surface. The minimum contact resistance obtainable with this solution was about 6 micro-ohms, as shown. The 2% sulfuric acid solution provided a clean surface which appeared clean and not materially different from that of the as-received stock.

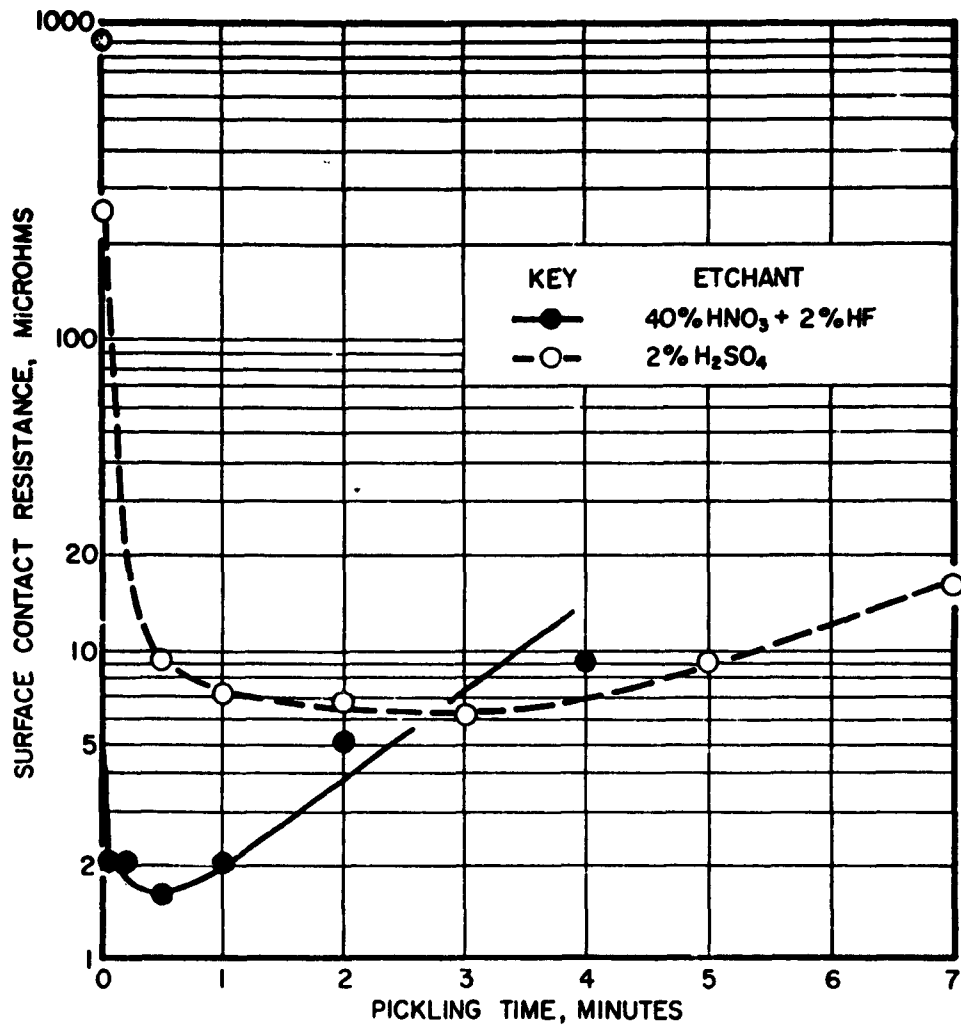


Figure 25 - Comparison of pickling techniques used for surface cleaning of beryllium sheet preparatory to resistance welding. (Tests conducted at room temperature.)

A 40% nitric acid-2% hydrofluoric acid etch was found⁽⁴⁾ to provide a brighter, cleaner surface than the sulphuric acid etch. In addition, the pickling time was reduced and a slightly lower contact resistance was obtained (Figure 25). However, the high activity of this etchant results in rapid heating of the solution, necessitating cooling of the bath in order to control the rate of attack. A four-minute etching time was found to produce a consistent surface contact resistance of approximately 10 micro-ohms with a bath temperature between 60 and 80°F. Although shorter times produced lower surface contact resistance, the four-minute etch was helpful in removing the superficial layer of damaged material at the surface of the sheet.

It is desirable to weld within a few hours after etching, but storage in a clean, dry atmosphere for not more than two days was found to be permissible. Longer periods of storage resulted in an excessive increase in the surface contact resistance. A desiccator was used for storage of etched material in this investigation.

9-4.2 Resistance Welding. All welding was performed inside the atmosphere box, primarily to localize any expelled metal and prevent contamination of the laboratory. The helium gas served to reduce the oxidation of the expelled molten particles and to carry off any air-borne dust.

The 1 x 3-inch coupons of beryllium were placed between the electrodes in the box, using a 1-inch overlap. The weld nugget was located as nearly as possible in the center of the 1-inch overlap. The electrodes were brought in contact with the weld coupons and the initial force applied through the spring-loaded electrode holder as described previously. The atmosphere box was then sealed and purged with helium for approximately 30 sec. prior to initiation of the welding sequence. After completion of the welding sequence, the box was purged with helium for an additional 30 to 60 sec. before opening the box for removal of the weld specimen. Precautions were taken to provide adequate ventilation of the immediate vicinity whenever a weld specimen was being removed from the atmosphere box.

A direct-inking oscillograph was employed to obtain a record of each weld sequence. Welding current was measured with the secondary current meter.

Electrodes were cleaned with fine emery paper whenever the weld specimens had a tendency to stick to the electrodes. The electrodes were re-machined whenever arcing, pitting, or excessive change in the electrode geometry was observed.

9-5 DISCUSSION

9-5.1 Exploratory Work on Weld Cracking. Initial work on determining welding variables for 0.040-inch beryllium indicated that a serious weld cracking problem existed. Welds made using the normal range of welding times (6 to 15 cycles) exhibited cracks on both surfaces of the welded specimen. Generally, three cracks occurred on each surface extending from the center of the welded area into the parent metal at approximately 120° intervals. Both sides of the weld exhibited the same 120° separation of cracks, indicating that the cracks probably extended through both sheets. Occasionally, a single crack alone was observed, across the

center of the weld area, which branched out at the weld-base metal interface to exhibit the characteristic 120° separation in the parent metal. Typical examples of the types of cracking observed are shown in Figure 26. The welds shown in Figure 26 were lightly etched to render the cracks more readily visible.

Metallographic examination of the welds indicated that the cracks followed an intergranular path along the columnar grain boundaries within the weld nugget. Porosity was also found to exist in many instances.

The tendency towards cracking appeared to be independent of the size of the fusion zone. Cracking occurred with fusion zone diameters ranging from 0.040 to 0.180 inch.

Since beryllium exhibits improved ductility between 400°C and 800°C , it was reasoned that if the effect of thermal shock could be reduced by more gradual heating to 800°C the cracking condition might be eliminated. Gradual up-and-down slope of the welding current was therefore tried. The first up-and-down slope tests were limited by the control used to a maximum total weld time of 30 cycles (60 cycles = 1 sec.). A typical welding cycle provided up-slope in 10 cycles from 40 percent of welding current to the full welding current magnitude. Following a 6-cycle weld period, a 14-cycle down-slope to 40 percent of the welding current was introduced. However, cracking was still present in welds made under these conditions.

9-5.2 Long-Cycle Welding. The electronic program controller described above was next used in conjunction with the normal resistance welding controls to permit the application of a wide variety of preheating and postheating currents and times, using welding cycles ranging up to 330 cycles. For convenience, welding cycles in excess of 60 cycles are hereafter termed "long-cycle" welds, as contrasted to welding cycles of 30 cycles or less which are termed "short-cycle welds". A typical weld cycle which reduced the incidence of cracking is given below for 0.040-inch beryllium sheet:

	<u>Time</u>	<u>Current Magnitude</u>
Preheat	90 cycles	7500 amp.
Main Welding Heat	8 cycles	9000 amp.
Postheat	90 cycles	8100 amp.

Electrodes: RWMA Class 2, 6-inch
continuous radius dome

Electrode Force: 450 lbs.

Several welds without externally visible cracks were made using the above weld sequence. However, it was subsequently found to be difficult to duplicate the crack-free welds under identical conditions. To reduce the effects of surface roughness on cracking, the surfaces of the unwelded specimens were polished with 1/0 emery paper. Cracking still occurred however, despite the improved appearance of the specimen surface prior to welding.

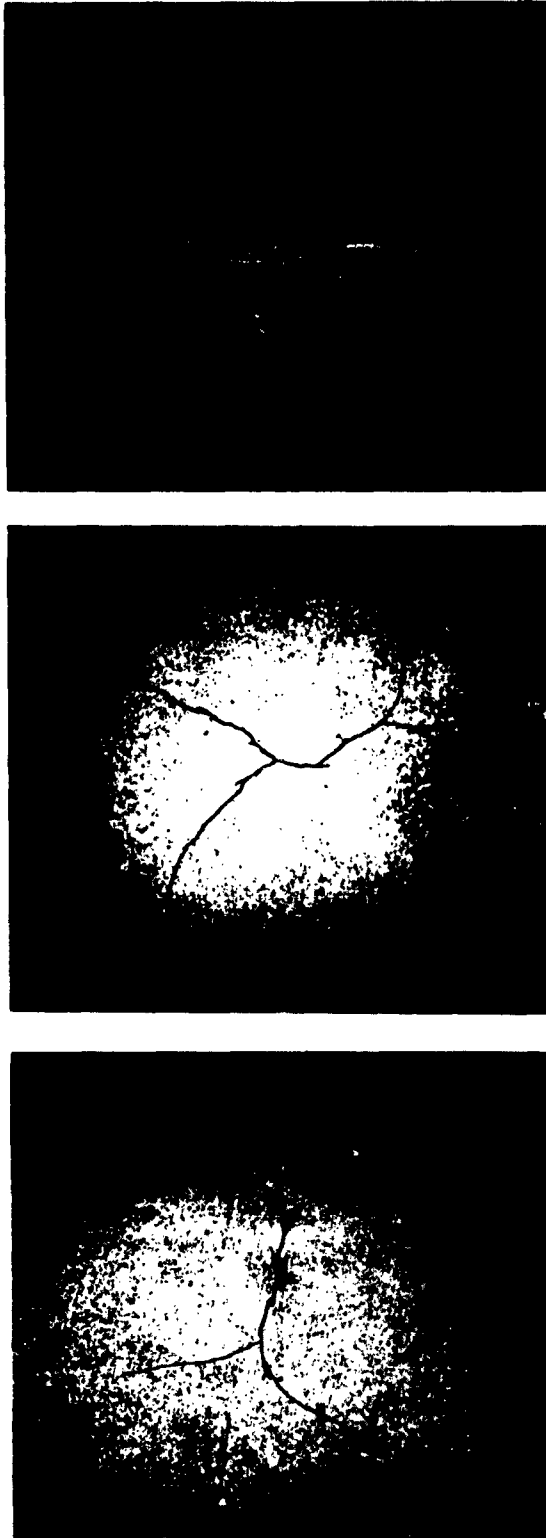


Figure 26 - Typical examples of external cracks in beryllium resistance spot welds.

Several welds without external cracks were sectioned and examined metallographically for cracks, voids and porosity. Some welds were defect-free in the section observed, but others exhibited internal cracks and porosity. Since only one plane of the weld could be observed in a given metallographic section, it was possible that porosity or small internal cracks existed at other locations even in welds apparently free of defects. Therefore, a micro-radiographic technique which permitted positive identification of defects as thin as 0.005 inch in a total thickness of 0.090 inch was developed. The technique involved the use of a copper target X-ray diffraction tube with the following conditions: 20 KV potential, 50-ma.-minute exposure at a distance of 2.5 inches with Kodak Orthographic Plate (Type No. 5480). All exposures were made with the X-ray beam normal to the surface of the spot weld, and the sheet surface in contact with the film. Fortunately, all cracks previously detected using the metallographic technique were normal to the surface of the weld along the columnar grain boundaries, and thus appeared to be favorably oriented for detection by the micro-radiographic technique. This method was found to provide a faster, more reliable method of determining weld quality than the metallographic technique.

To determine in which portion of the weld sequence cracking was occurring, temperature measurements were made in the weld zone. Chromel-alumel thermocouples (0.010-inch diameter) were percussion welded to one sheet at a location corresponding to the edge of the fusion zone of the completed weld. Temperatures were recorded during the weld sequence using an electromagnetic recording oscillograph. The welding conditions used for these measurements were identical to those for the long-cycle weld listed above. The results of these measurements were as follows for 0.040-inch beryllium sheet:

- (1) The temperature at the edge of the fusion zone approached a steady state value of 600°C with a preheat current of 7600 amperes in slightly less than 90 cycles.
- (2) The time to cool from 1283°C, the melting point, to 800°C was 0.06 sec. (providing an average cooling rate of approximately 8,000°C per sec.) without postheat current.
- (3) The time to cool from 1283°C to 400°C was 0.25 sec. Therefore, cooling from 800°C to 400°C required 0.19 sec. without postheat current. Thus, an average cooling rate of 2,100°C per sec. over the range 800-400°C was found to be characteristic of this weld geometry.
- (4) A post-heat current of 8100 amperes maintained the weld area at 600°C as a steady state value, and decreased the average cooling rate to approximately 600°C/sec. from 1283°C to 600°C.

The above data indicated that the heating and cooling rates and the temperature in the weld zone could be controlled by appropriate choice of preheat and postheat current. It also indicated that the most critical portion of the cycle appeared to occur immediately following the termination of the main welding current. At this point, the cooling rates without the application of postheat

current were found to be high enough to cause cracking induced by thermal shock. Steps taken to reduce these cooling rates included increasing the initial postheat current to 95 percent of the main welding current, and providing down-slope of the postheat current to 45 percent of the welding current after various intervals of down-slope delay. The down-slope of the postheat current was accomplished by motorized operation of the postheat control rheostat on the program control. External cracking of the weld was almost completely eliminated using this approach, internal cracks occurred, however, in all but a few welds, indicating that thermal shock was not the only factor causing cracking.

9-5.3 Dual-Pressure Cycle Welding. Metals subject to brittle fracture or hot shortness have often been successfully resistance welded without cracking by the application of a forging force at some instant during or after solidification of the weld metal. It is believed that the effect of the forging force either causes recrystallization of the columnar-dendritic grain structure in the weld nugget or counteracts the effect of shrinkage stresses attending solidification. By utilizing a forging force during a long postheat cycle, it was possible to eliminate internal cracking of 0.040-inch thick beryllium almost completely.

Metallographic examination of welds made with this technique showed no evidence of recrystallization of the large columnar grains in the weld nugget. The effect produced by the forging force in the case of beryllium is therefore probably related to the reduction in shrinkage stresses during cooling.

The forging technique consisted of increasing the electrode force at some predetermined instant during the welding cycle. The application of this large force had to be synchronized with the welding cycle in order to prevent excessive deformation. An initial electrode force of 450 lbs was employed on 0.040-inch sheet, followed by forging forces ranging from 1000 lbs to 1500 lbs. The forging force was applied after a forging force delay ranging from 1/2 cycle to as much as 77 cycles after the end of the main welding current interval.

Using the 1500-lb forging force and the welding conditions listed below, defect-free resistance spot welds were made repeatedly in 0.040-inch thick beryllium sheet.

	<u>Time</u>	<u>Current Magnitude</u>
Preheat	200 cycles	6700 amp.
Main Welding Heat	8 cycles	9000 amp.
Postheat	110 cycles	8500 amp.

Electrodes: RWMA Class 2, 6-inch continuous radius dome

Initial Force: 450 lbs.

Forging Force: 1500 lbs.

Forging Delay: 77 cycles

No slope control of the welding current during preheat and postheat was used. Occasional cracking, observed with a forging force of 1000 lbs., was completely eliminated by increasing the forging force to 1500 lbs.

9-5.4 Determination of Welding Parameters. Welding parameters for the three thicknesses of beryllium sheet used in this investigation were determined by choosing a set of conditions for weld time, electrode force, and electrode geometry and varying the weld current over a range from that which caused slight fusion to that which caused expulsion of weld metal. Welding-current times ranged from 1 cycle to 15 cycles; electrode force varied from 150 to 700 lbs. Electrode geometry was varied from a 4-inch radius, 5/32-inch restricted diameter to a 6-inch radius, 7/32-inch restricted diameter. A 6-inch continuous radius dome electrode geometry was also employed. The presence of external cracks in most of the welds was ignored in this portion of the investigation since it was desired only to evaluate the effect of welding variables on nugget dimensions.

(1) Welding Time. Figures 27 and 28 summarize the effect of welding time on the magnitude of welding current required to cause measurable strength and that required to cause expulsion in 0.020-inch beryllium sheet. Figure 27 was prepared using an electrode force of 250 lbs., while Figure 28 was obtained using an electrode force of 400 lbs. As may be seen by inspection of Figure 27 a welding current of approximately 8000 amperes is required to cause sticking with a 1-cycle weld time. The current required to cause sticking decreased with increase in weld time to about 6100 amperes with 6 cycles and to about 5400 amperes with 15 cycles. Expulsion currents ranged from 10,200 amperes with 1 cycle to about 8000 amperes with a 15-cycle weld time when an electrode force of 250 lbs. was utilized. Thus, Figure 27 summarizes welding current requirements for weld times for 1 to 15 cycles and an electrode force of 250 lbs., and Figure 28 summarizes the welding current requirements for weld times from 1 to 15 cycles, utilizing an electrode force of 400 lbs. for 0.020-inch sheet.

Figures 29 and 30 summarize the welding current requirements for 0.040-inch beryllium using electrode forces of 300 lbs. and 550 lbs., respectively.

Figures 31 and 32 present similar data for 0.060-inch sheet with electrode forces of 500 lbs. and 700 lbs., respectively.

In all cases, the current limits for both sticking and expulsion decrease with increase in weld time. It should be noted that only a small decrease in the welding current limits is produced by increasing the time beyond 6 to 8 cycles. This indicates that, for all three thicknesses, times in the range 6 to 10 cycles would be considered satisfactory, since minor changes in weld time exert little influence on the current requirements.

(2) Weld Diameter. Figures 33, 34, and 35 summarize the effects of the welding current and welding time on the weld diameter of 0.020-inch thick beryllium sheet. The data of Figure 33 were obtained using a force of 150 lbs., while Figures 34 and 35 were obtained with forces of 325 and 400 lbs., respectively. As may be clearly seen by inspection of Figure 35 the welding current required to obtain a weld diameter of 0.120 inch utilizing a 10-cycle weld time is 6800 amperes. To obtain the same weld diameter with a 5-cycle weld time

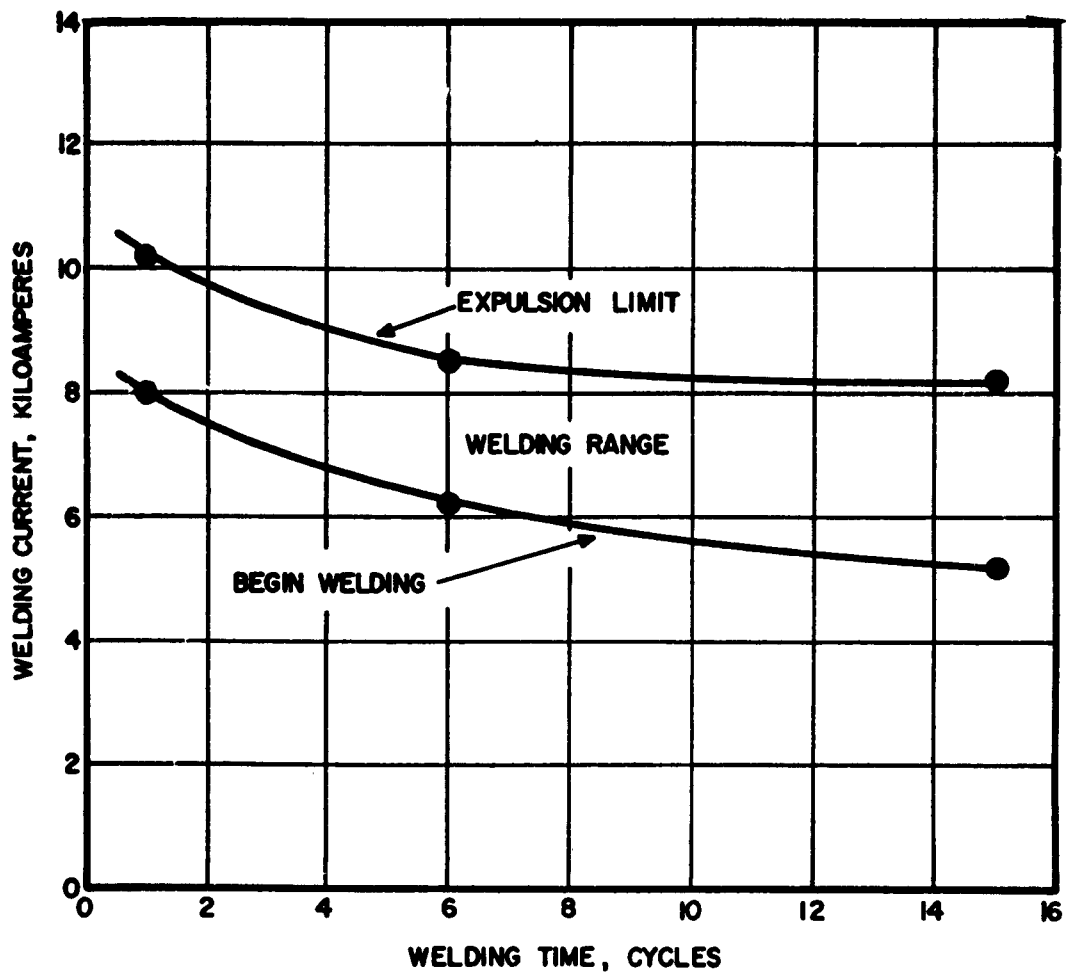


Figure 27 - Approximate welding current range as a function of welding time for 0.020-inch beryllium sheet. Electrode material: RIMA Class 2, 4-inch radius dome, 0.140-inch restricted diameter. Electrode force: 250 lbs.

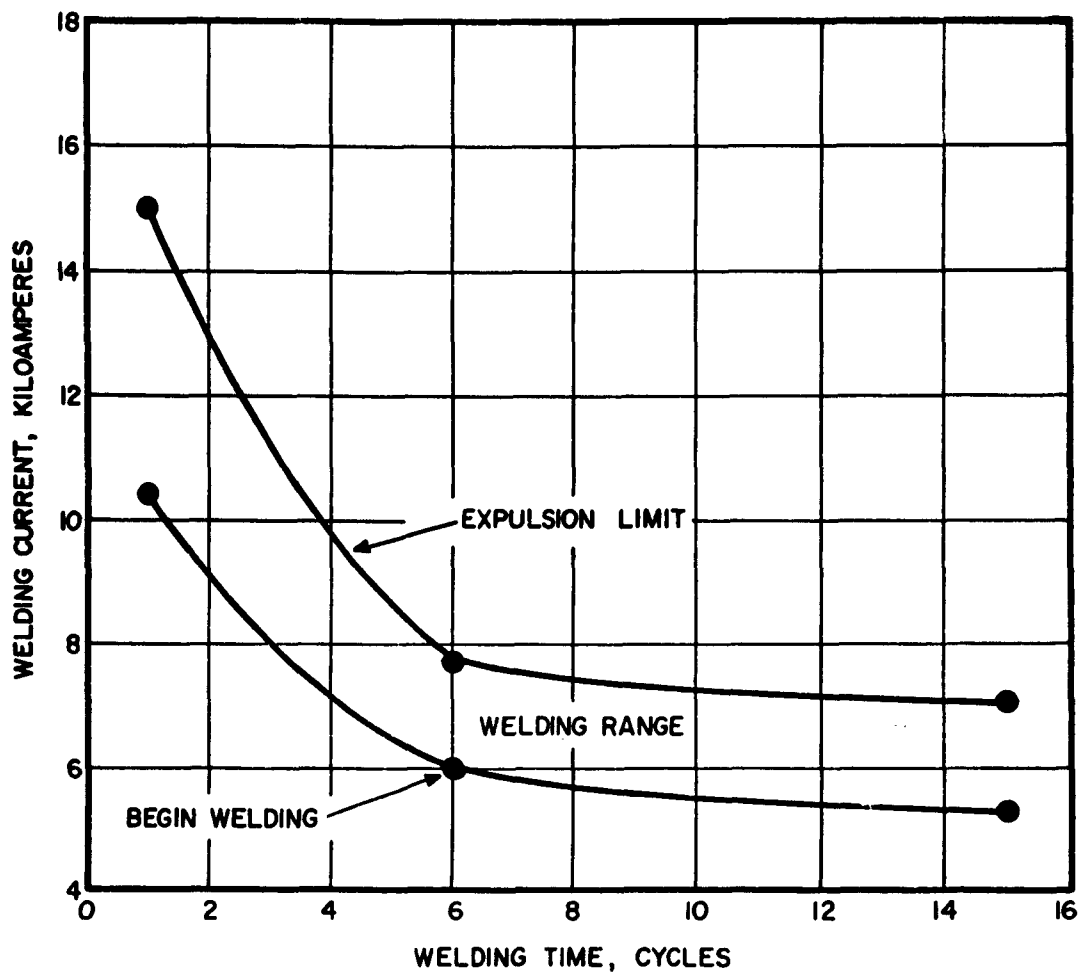


Figure 28 - Approximate welding current range as a function of welding time for 0.020-inch beryllium sheet. Electrode material: RWMA Class 2, 4-inch radius dome, 0.140-inch restricted diameter. Electrode force: 400 lbs.

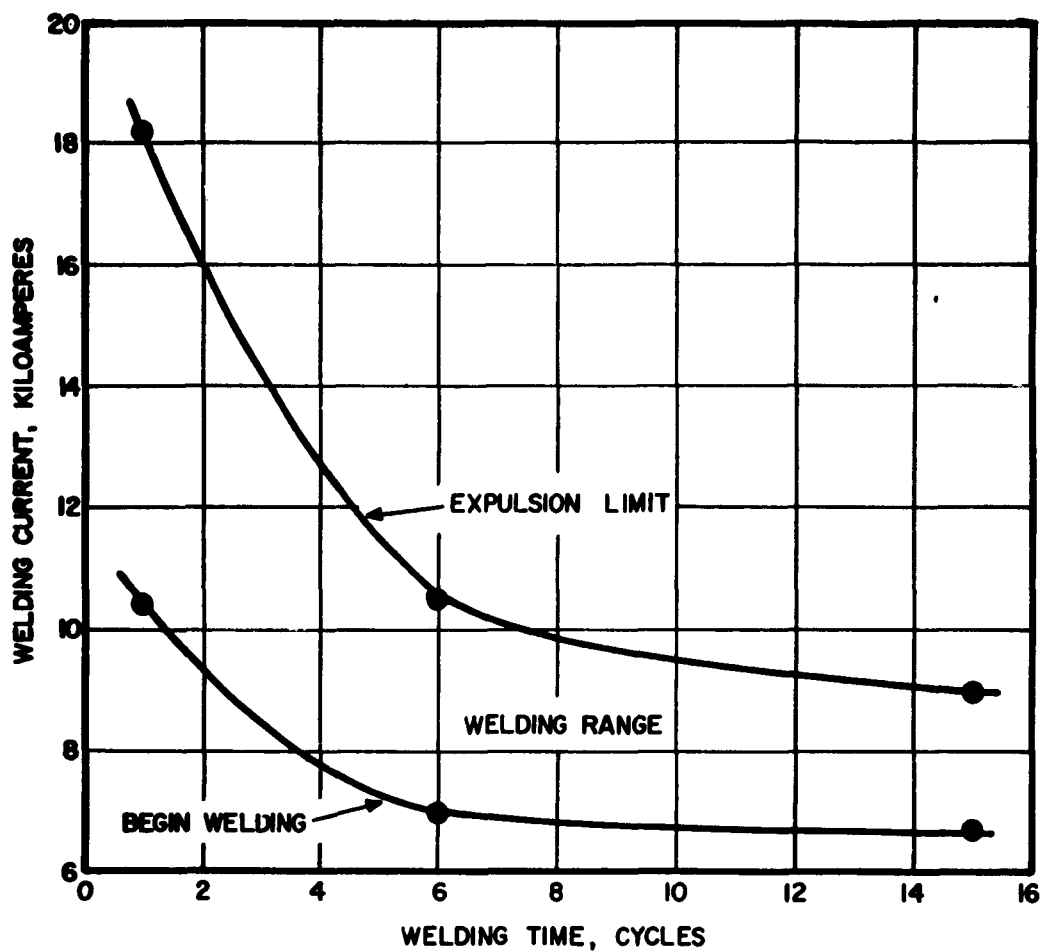


Figure 29 - Approximate welding current range as a function of welding time for 0.040-inch beryllium sheet. Electrode material: RWMA Class 2, 6-inch radius dome, 0.156-inch restricted diameter. Electrode force: 300 lbs.

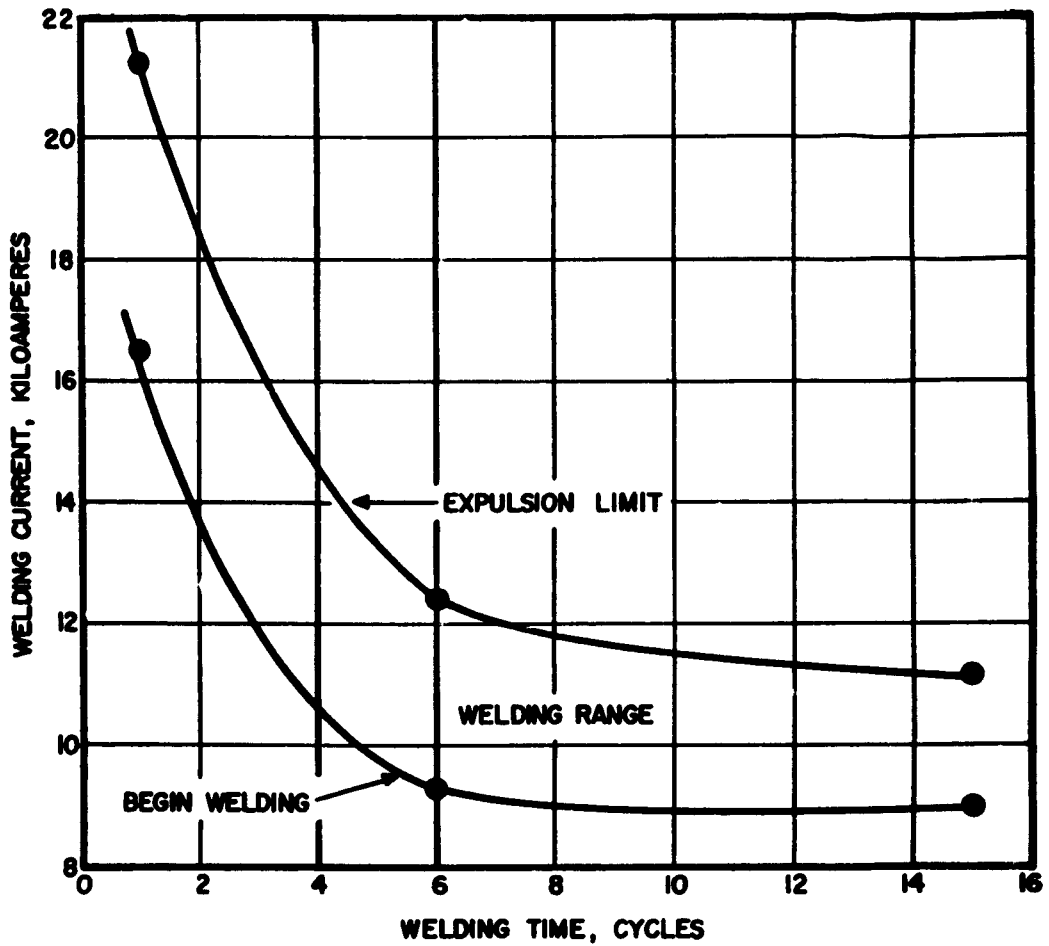


Figure 30 - Approximate welding current range as a function of welding time for 0.040-inch beryllium sheet. Electrode material: **EWMA Class 2**, 6-inch radius dome, 0.156-inch restricted diameter. Electrode force: 550 lbs.

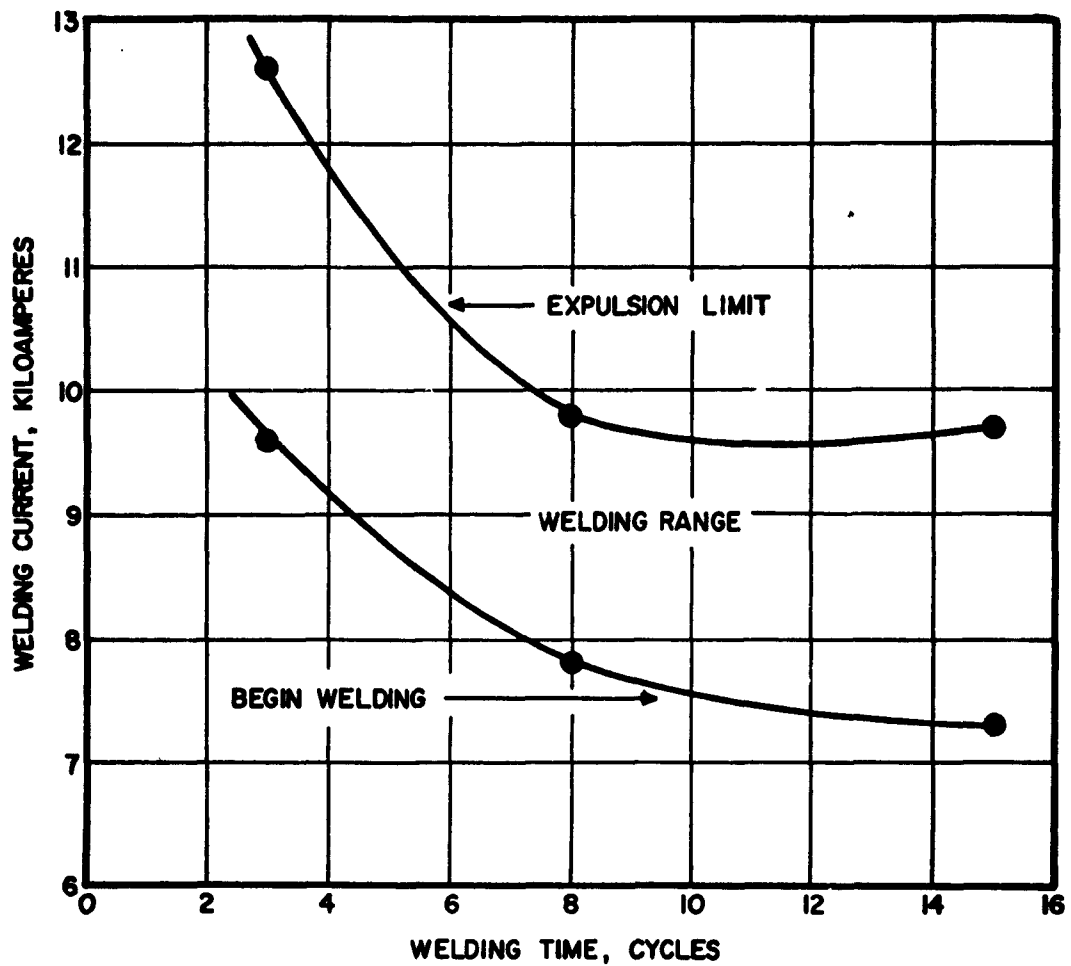


Figure 31 - Approximate welding current range as a function of welding time for 0.060-inch beryllium sheet. Electrode material: RMA Class 2, 6-inch radius dome, 0.219-inch restricted diameter. Electrode force: 500 lbs.

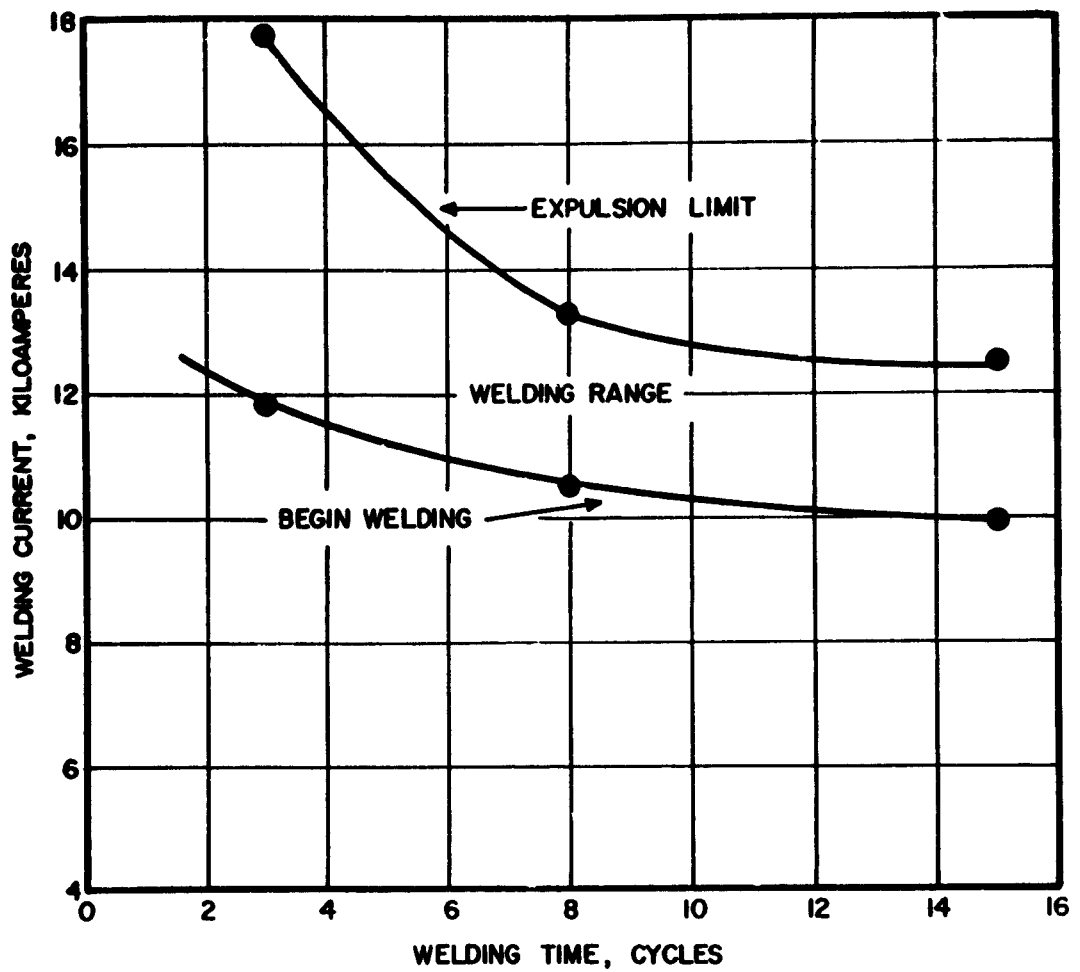


Figure 32 - Approximate welding current range as a function of welding time for 0.060-inch beryllium sheet. Electrode material: RWMA Class 2, 6-inch radius dome, 0.219-inch restricted diameter. Electrode force: 700 lbs.

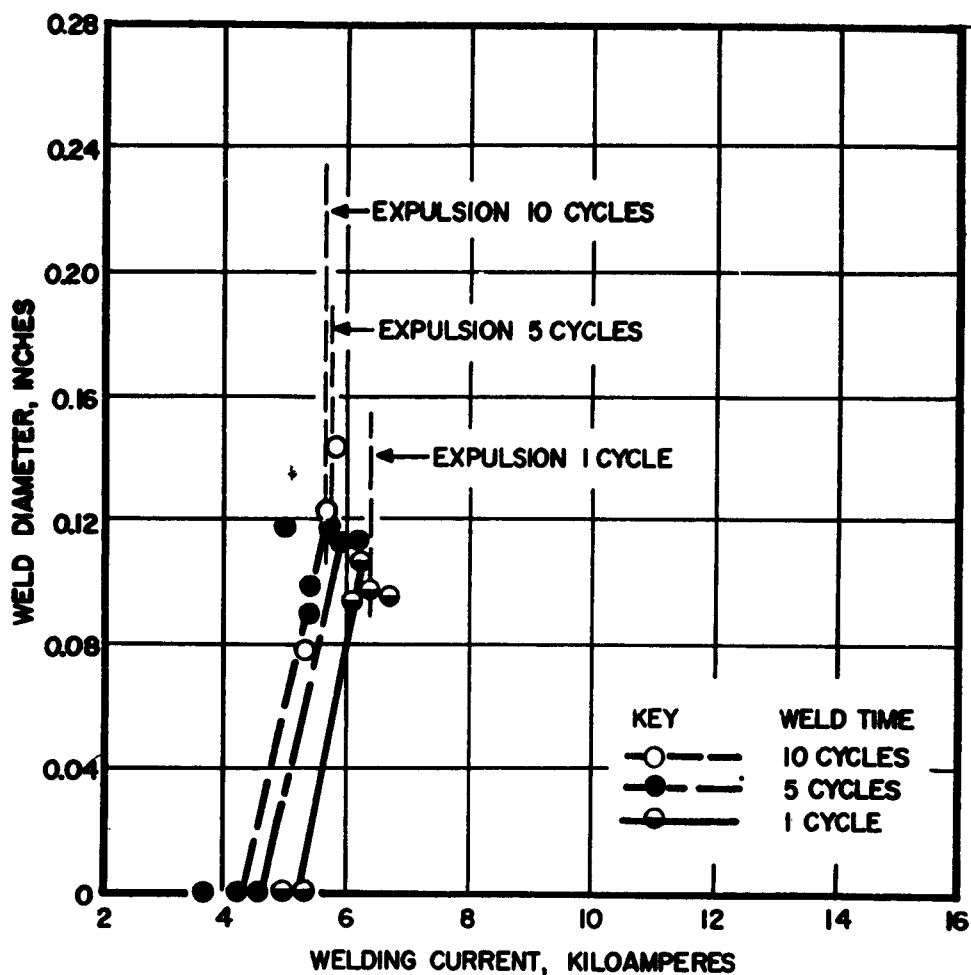


Figure 33 - Weld diameter vs. welding current, 0.020-inch beryllium sheet. Electrodes: RWMA Class 2, 4-inch radius dome, 0.140-inch restricted diameter. Electrode force: 150 lbs. Weld time: 1, 5 and 10 cycles.

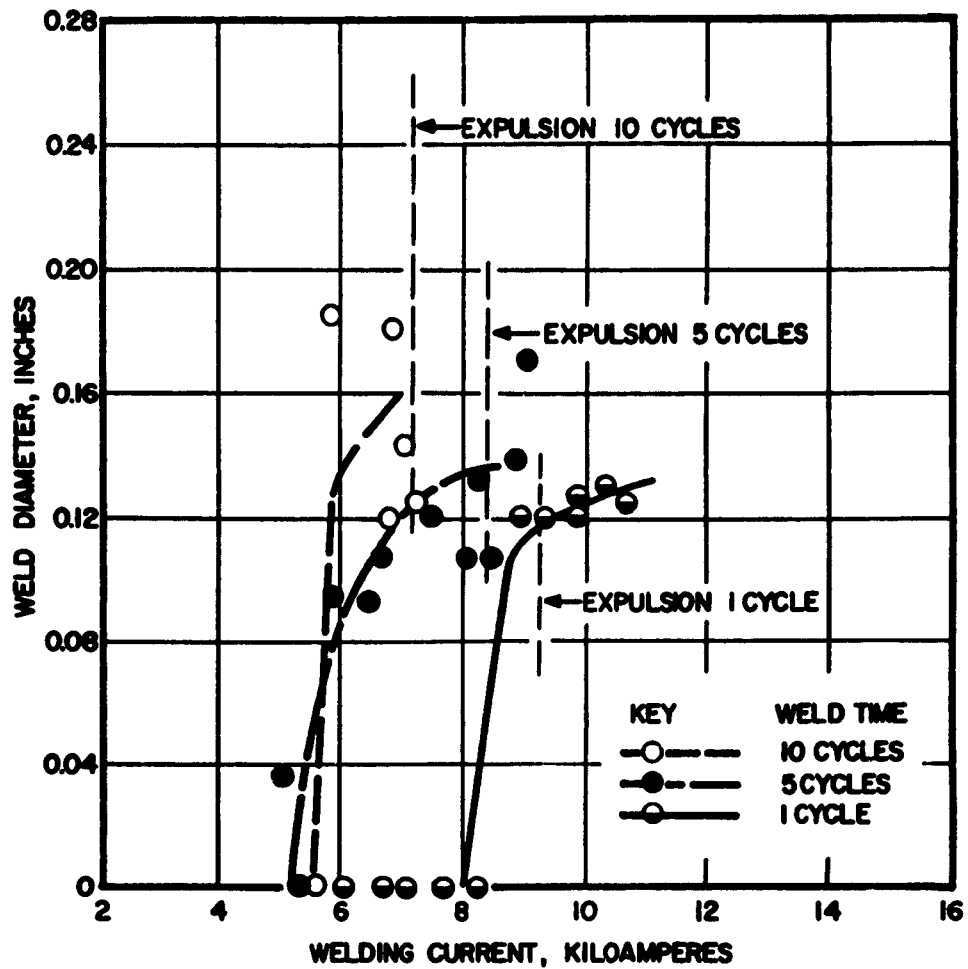


Figure 34 - Weld diameter vs. welding current, 0.020-inch beryllium sheet. Electrodes: KMA Class 2, 4-inch radius dome, 0.140-inch restricted diameter. Electrode force: 325 lbs. Weld time: 1, 5 and 10 cycles.

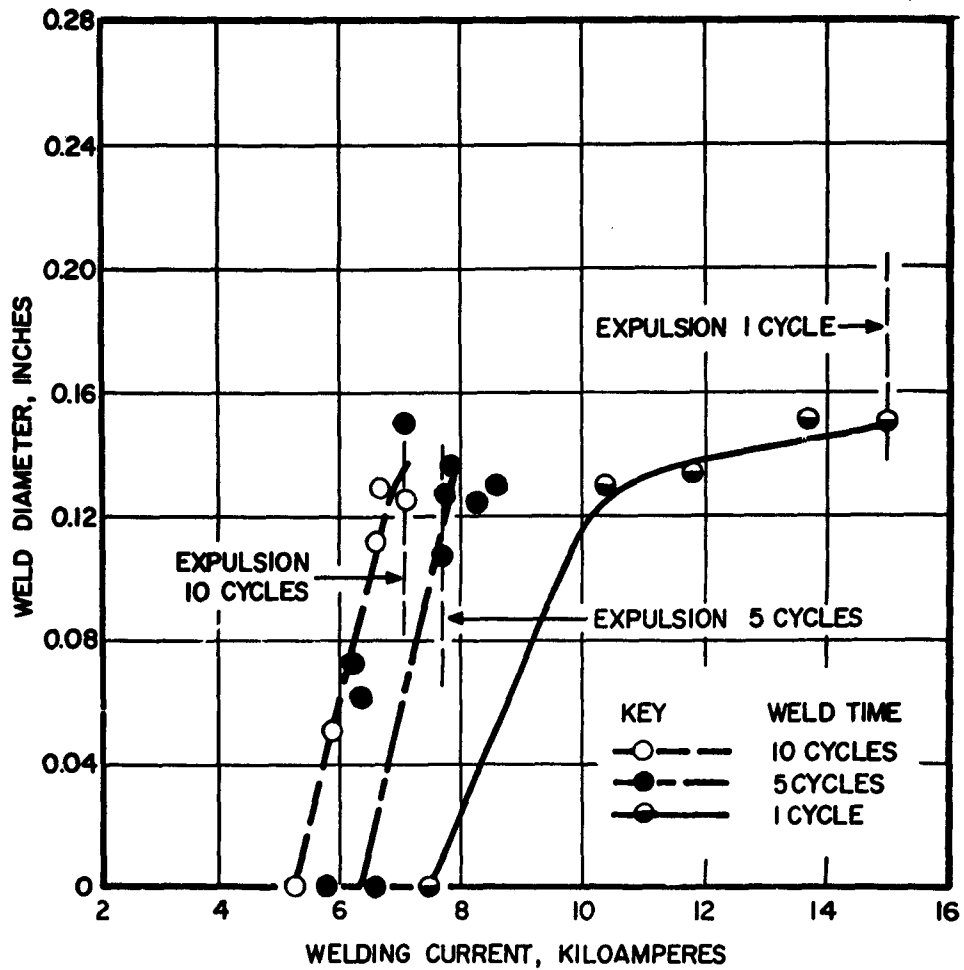


Figure 35 - Weld diameter vs. welding current, 0.020-inch beryllium sheet. Electrodes: RWMA Class 2, 4-inch radius dome, 0.140-inch restricted diameter. Electrode force: 400 lbs. Weld time: 1, 5 and 10 cycles.

requires a welding current of 7700 amperes, while a 1-cycle weld time requires a welding current of 10,200 amperes. Expulsion currents ranged from 15,000 amperes with 1-cycle to about 7100 amperes with a 10-cycle weld time when an electrode force of 400 lbs. was utilized.

Figures 36, 37, and 38 summarize the weld diameters obtained over the useful current range for 0.040-inch beryllium when using electrode forces of 300, 450 and 550 lbs., respectively. It should be noted that arcing at high currents occurred at the electrode-to-work interfaces before expulsion occurred when a weld time of 1 cycle was used with this thickness of material. The arcing was apparent at all electrode forces. This indicates that a weld time of 1 cycle would decrease the electrode life and would therefore be unsatisfactory for welding beryllium.

Figures 39 and 40 present similar data for 0.060-inch sheet with electrode forces of 500 and 700 lbs., respectively. Note that expulsion was obtained before arcing occurred when using a minimum weld time of 3 cycles. However, a weld time of 8 to 10 cycles would be considered optimum for reasons mentioned above.

The preceding curves illustrate that the current required to obtain a given weld diameter increases with decrease in weld time. The curves distinctly show that the current required to produce a given weld diameter increases markedly with decrease in weld time from 5 cycles to 1 cycle. For 0.020-inch sheet, the change in weld current is very slight from 10 cycles to 5 cycles, and for 0.040- and 0.060-inch sheet very little change in current is noted from 6 to 15 cycles. This would indicate that for all three thicknesses, times in the range 8 to 10 cycles would be considered satisfactory, since weld time exerts little influence on the current requirements to produce a given nugget diameter.

9-5.5 Tensile Tests. All tensile-shear strength tests were conducted at room temperature. The ductility of all specimens was immeasurably small, and a number made at conditions approximating the threshold of welding were so fragile they were broken in handling. An appraisal of all tensile tests made indicates that, in general, those weld specimens that failed at less than 200 lbs. in tensile-shear failed in the weld. Weld specimens that failed above 200 lbs. in tensile-shear usually exhibited base-metal failures, except for a few instances where the failure propagated through both the weld and the base metal. Base-metal failures were often the result of the propagation of a weld crack which extended into the base metal. However, welds with no apparent defects failed in the heat-affected base metal adjacent to the weld. These observations would suggest that either or both of the following contributing factors could be responsible for premature failure of the joint:

- (1) Despite the absence of external defects, unidentified internal defects which drastically reduce the load-carrying capacity of the weld may be present.
- (2) Presently available beryllium exhibits both low ductility and extreme notch sensitivity. The geometry of a spot weld provides a notch at the edge of the fusion zone between the two sheets, which can readily start a crack. Such cracks may then propagate rapidly through the base metal and cause premature failure of the welded specimen.

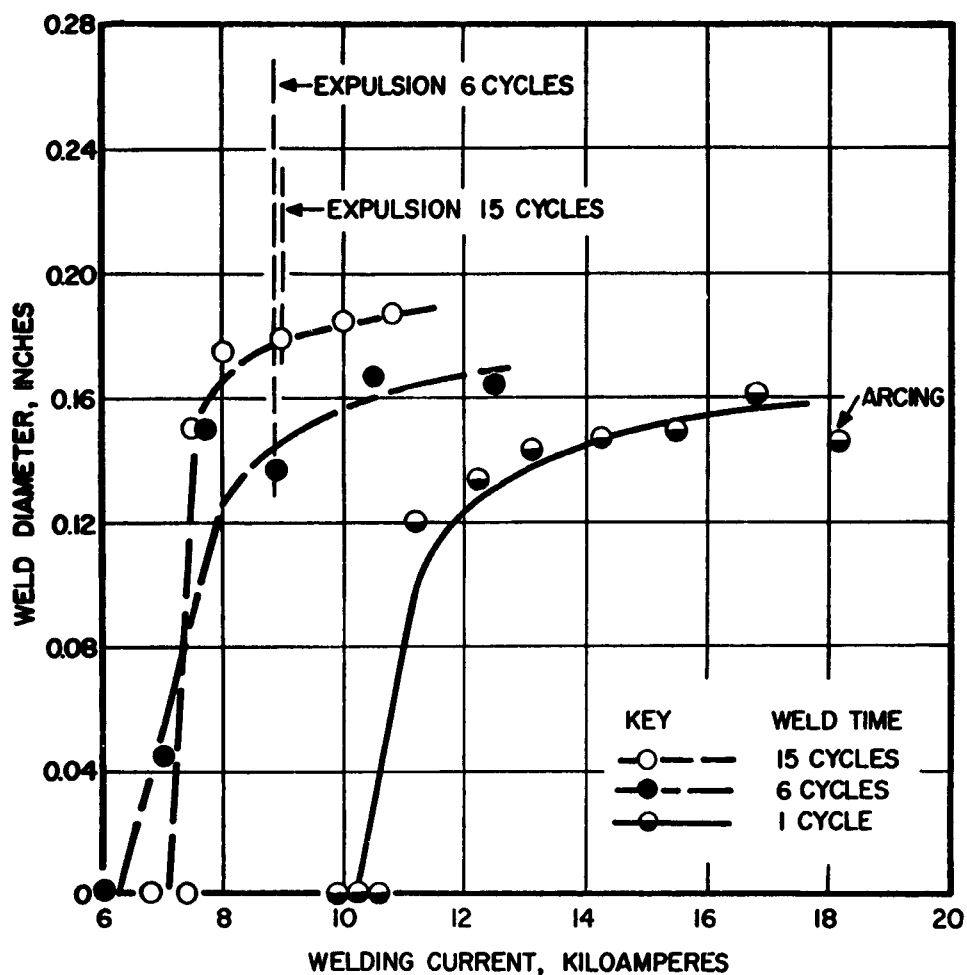


Figure 36 - Weld diameter vs. welding current, 0.040-inch beryllium sheet. Electrodes: RWMA Class 2, 6-inch radius dome, 0.156-inch restricted diameter. Electrode force: 300 lbs. Weld time: 1, 6 and 15 cycles.

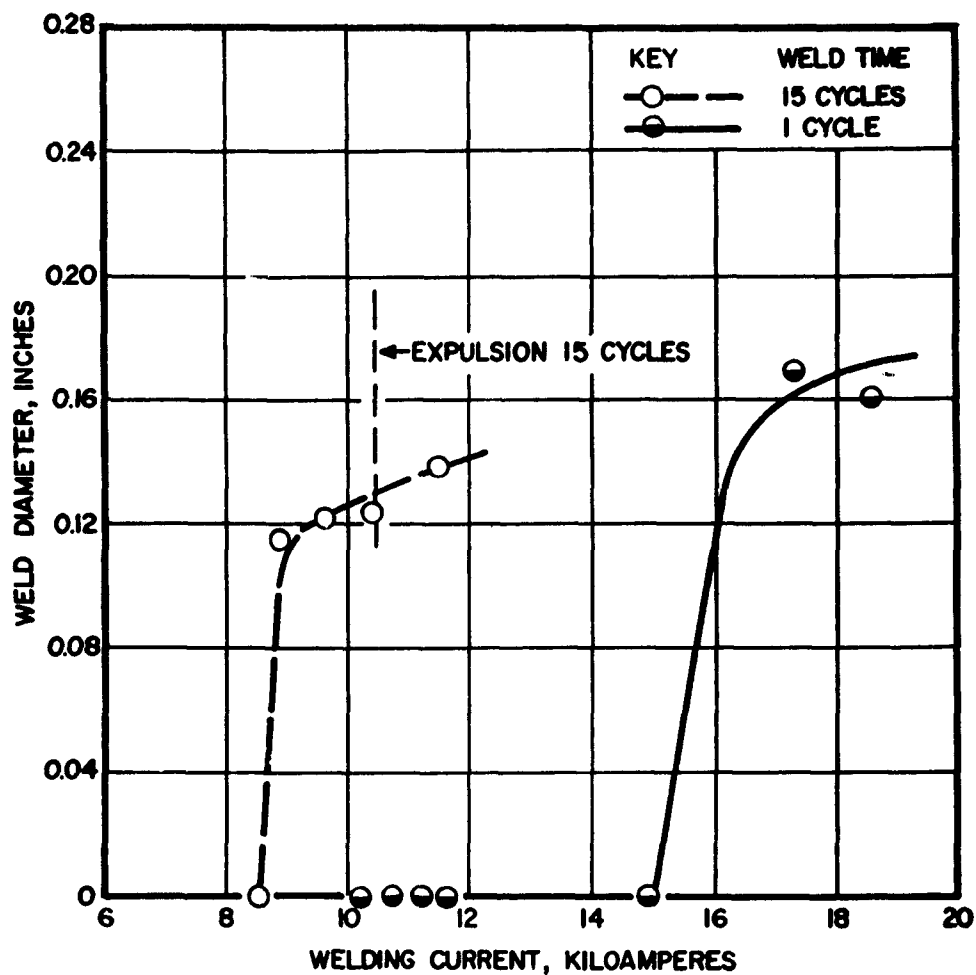


Figure 37 - Weld diameter vs. welding current, 0.040-inch beryllium sheet. Electrodes: RWMA Class 2, 6-inch radius dome, 0.156-inch restricted diameter. Electrode force: 450 lbs. Weld time: 1 and 15 cycles.

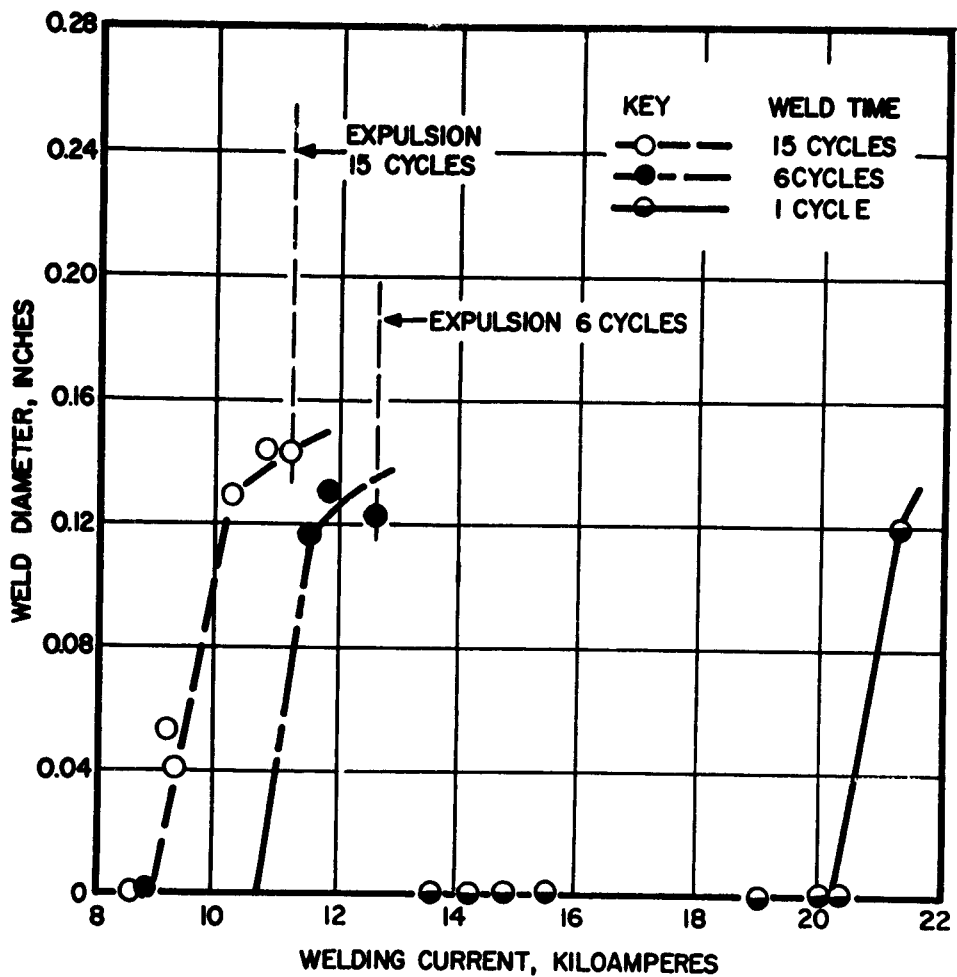


Figure 38 - Weld diameter vs. welding current, 0.040-inch beryllium sheet. Electrodes: RWMA Class 2, 6-inch radius dome, 0.156-inch restricted diameter. Electrode force: 550 lbs. Weld time: 1, 6 and 15 cycles.

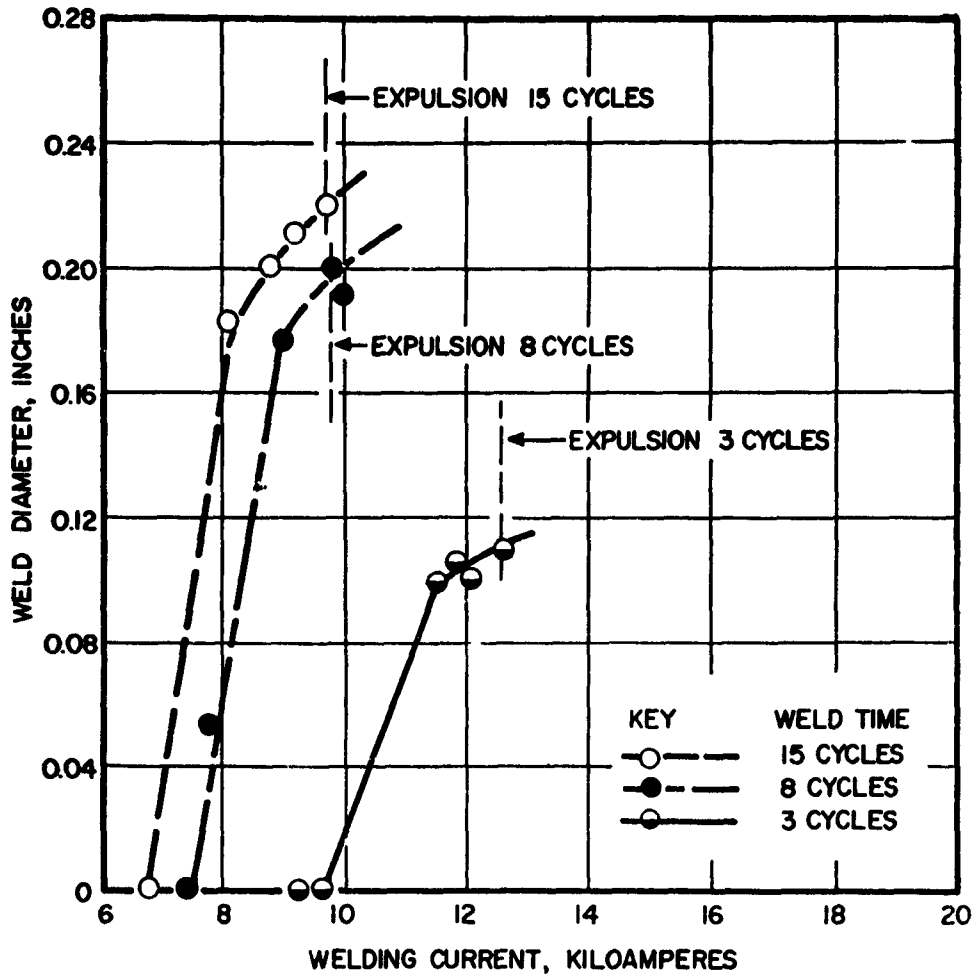


Figure 39 - Weld diameter vs. welding current, 0.060-inch beryllium sheet. Electrodes: RWMA Class 2, 6-inch radius dome, 0.219-inch restricted diameter. Electrode force: 500 lbs. Weld time: 3, 8 and 15 cycles.

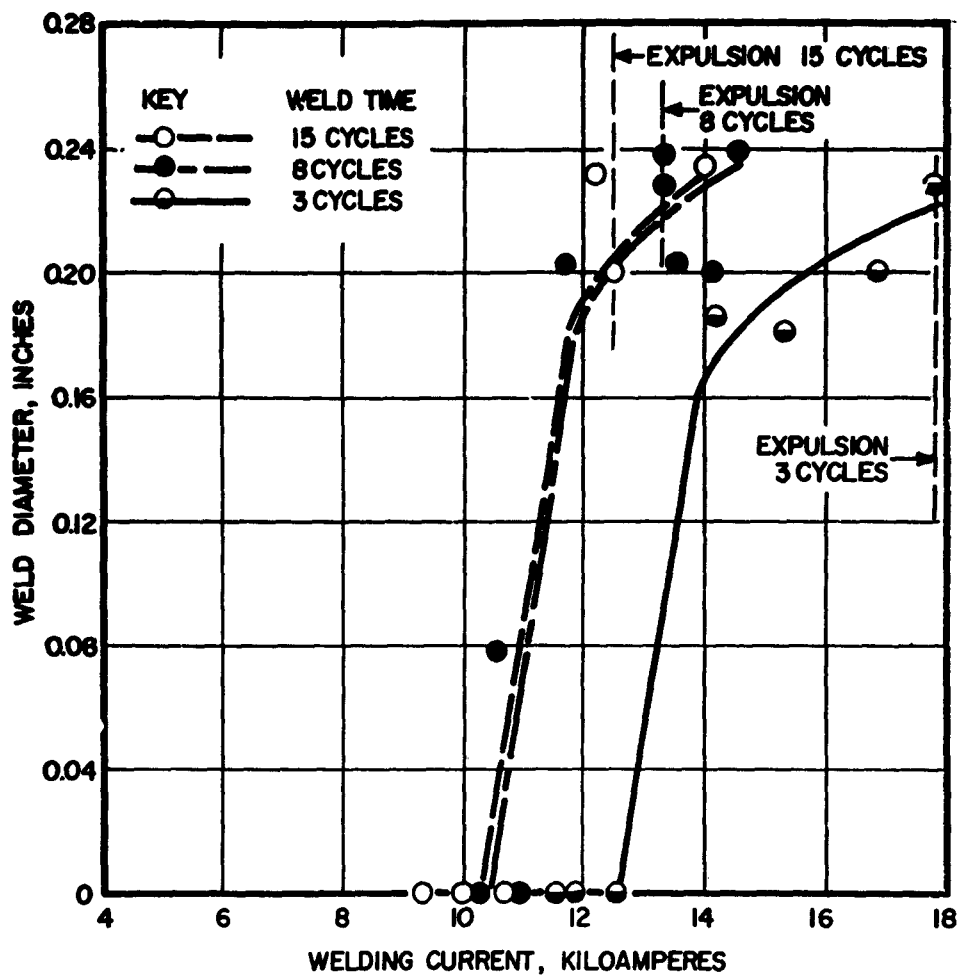


Figure 40 - Weld diameter vs. welding current, 0.060-inch beryllium sheet. Electrodes: RWMA Class 2, 6-inch radius dome, 0.219-inch restricted diameter. Electrode force: 700 lbs. Weld time: 3, 8 and 15 cycles.

Examples of typical weld fractures may be seen in Figure 41. Specimen T-16 was welded using no preheat, 8000 amperes welding current for 11 cycles, and approximately 4000 amperes postheat for 5 cycles. A forging force of 1000 lbs. was applied 1/2 cycle after the completion of the main welding current. The weld exhibited no external cracks and failed in the base metal along the edge of the weld. The tensile-shear strength was 285 lbs. at failure.

Specimen T-29 exhibited no external cracks and failed in the same manner as T-16 with a tensile-shear strength of 380 lbs. Welding conditions were: No preheat, 10,000 amperes welding current for 11 cycles, and approximately 9,500 amperes postheat for 125 cycles. A 1000 lb. forging force was applied 1/2 cycle after completion of the main welding current.

Specimen T-46 was welded using approximately 7200 amperes preheat for 200 cycles, 9000 amperes main welding current for 8 cycles, and approximately 8600 amperes postheat for 120 cycles. A 1225 lb. forging force was applied 77 cycles after the end of the main welding current. No external cracks were visible in the weld and the tensile-shear strength was 380 lbs. Note that the fracture appears to have originated at a point on the edge of the weld. This point may have been the location of an unidentified internal defect.

Specimen T-148 exhibited an external crack initially and failed in tensile-shear at 250 lbs. Close examination of the weld reveals that the fracture originated from a weld crack which had propagated into the parent metal. Welding conditions for this weld were: no preheat, 9000 amperes welding current for 11 cycles, and approximately 4500 amperes postheat for 5 cycles. A forging force of 1000 lbs. was applied 1/2 cycle after completion of the main welding current. The electrodes used in welding this specimen, and all other specimens shown in Figure 41 were RWMA Class 2 with a 5/32-inch restricted diameter and a 6-inch radius dome.

A large number of tensile-shear vs. welding current tests were conducted over a wide range of welding conditions. The results were inconclusive since the scatter of data and inconsistency of results made interpretation difficult. Thus, although it was possible to define a trend, it was impossible to arrive at any definite conclusions concerning the most desirable set of welding conditions for any particular thickness of material.

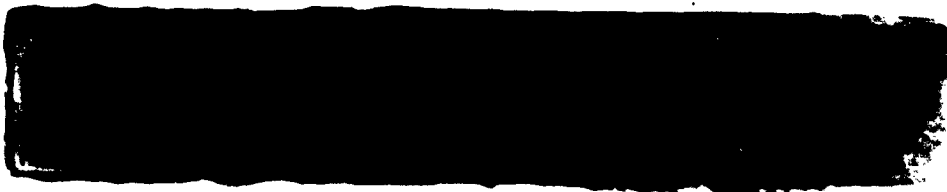
Shown in Figures 42, 43, 44, 45, 46, and 47 are tensile-shear strength data for 0.040-inch thick beryllium sheet. Figures 42 and 43 illustrate tensile-shear strength data for welds made with no preheat and a minimum of postheat. Welds shown in Figure 42 were made without the use of a forging force while those in Figure 43 were made using a forging force. Comparison of the data in Figures 42 and 43 reveals little difference in strength despite the fact that the three highest strength welds made without a forging force exhibited external cracks. Only one weld in the group made with a forging force was cracked, and that failed in the base metal at a relatively low value. Additional welds made at a welding current of approximately 9000 amperes, a current value slightly below the point of expulsion in Figure 43 were all cracked and failed at relatively low values. It should be noted that the highest strength welds were made at currents causing expulsion, a condition that is not normally acceptable.



T16



T29



T46



T148

Figure 41 - Typical examples of tensile-shear specimen failures.

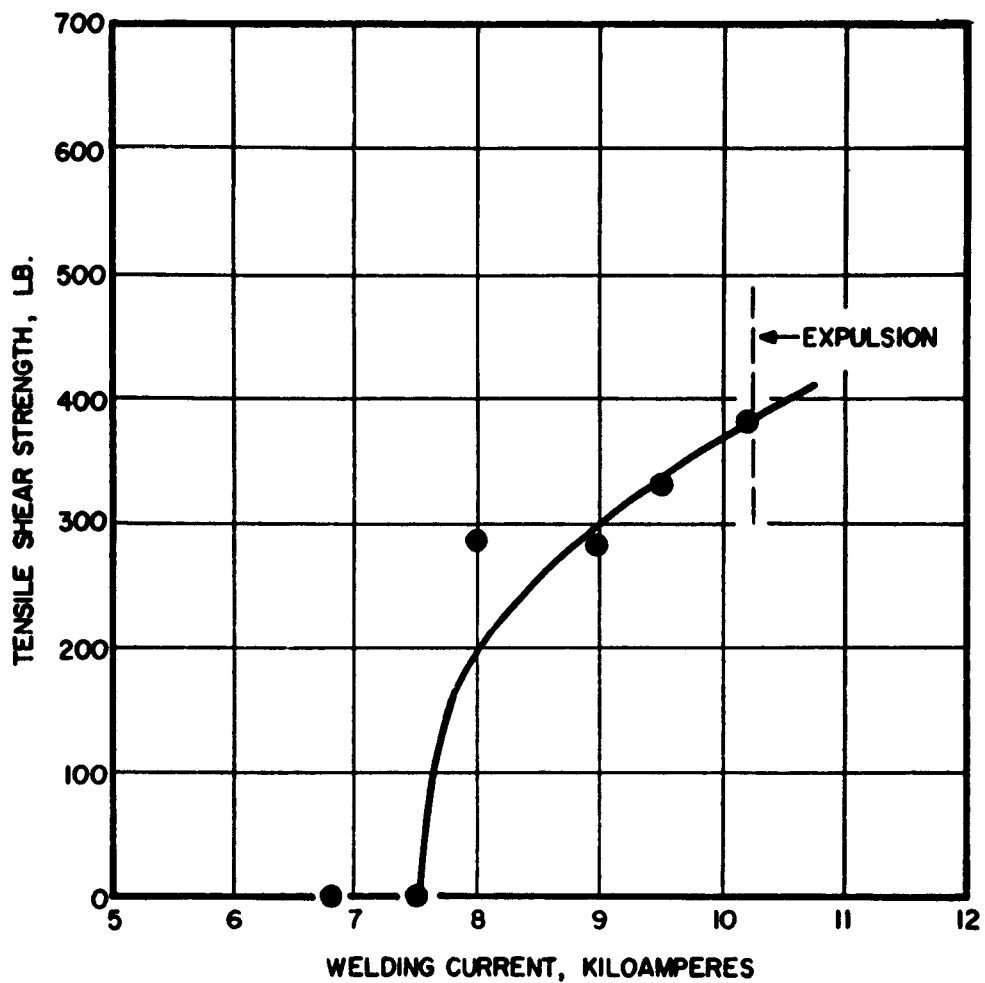


Figure 42 - Tensile shear strength vs. welding current for 0.040-inch beryllium sheet. Electrodes: RWMA Class 2, 6-inch radius dome, 0.156-inch restricted diameter. Initial force: 450 lbs. No forging force. No preheat. Postheat: 5 cycles at 50% of weld current. Welding time: 11 cycles.

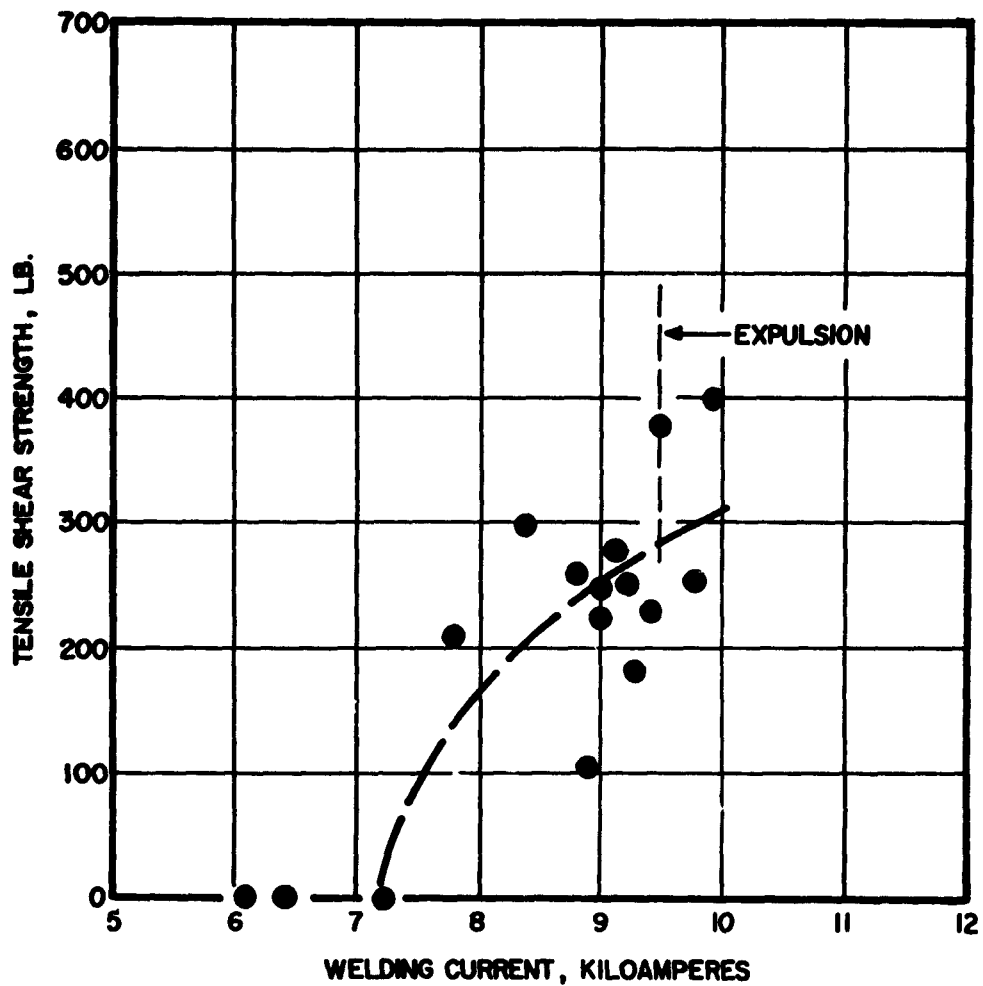


Figure 43 - Tensile shear strength vs. welding current for 0.040-inch beryllium sheet. Electrodes: RMA Class 2, 6-inch radius dome, 0.156-inch restricted diameter. Initial force: 450 lbs. Forging force: 1000 lbs. No preheat. Postheat: 5 cycles at 50% of weld current. Welding time: 11 cycles. Forging delay: 0.5 cycle after weld.

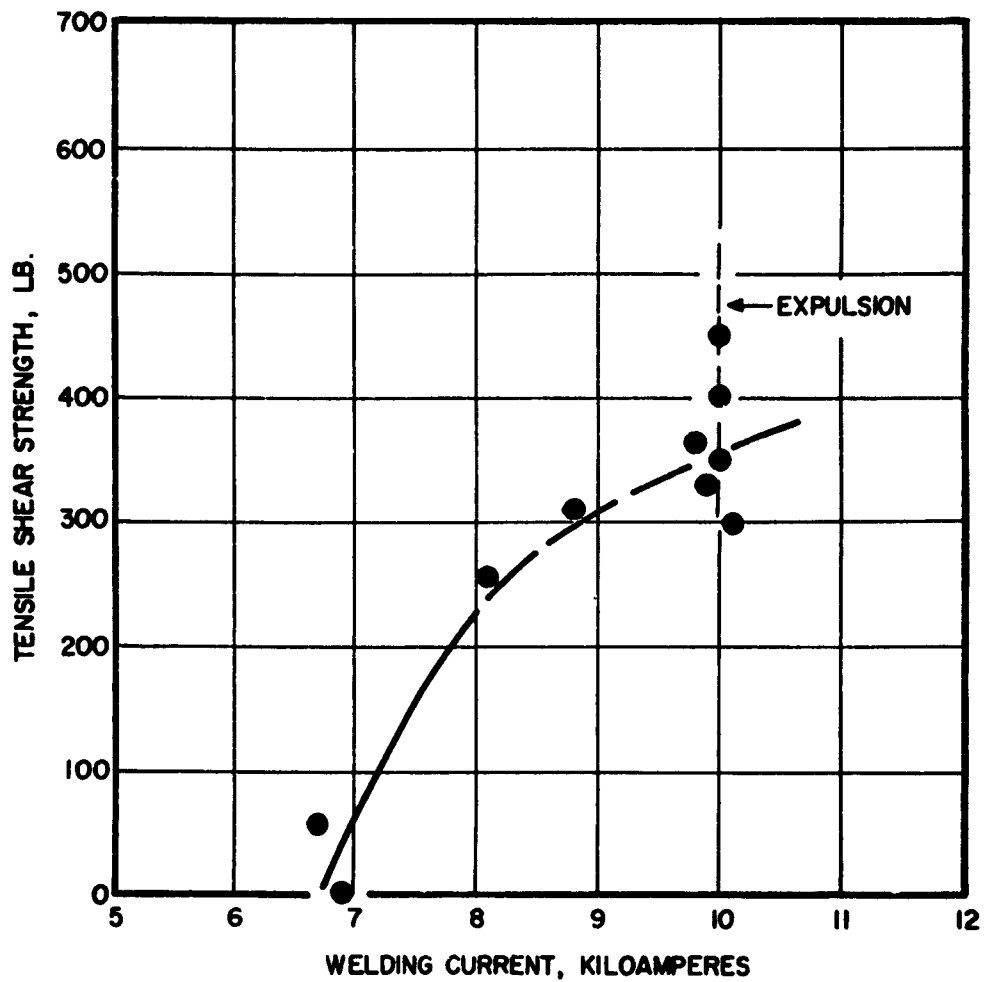


Figure 44 - Tensile shear strength vs. welding current for 0.040-inch beryllium sheet. Electrodes: RWMA Class 2, 6-inch radius dome, 0.156-inch restricted diameter. Initial force: 450 lbs. No forging force. No preheat. Postheat: 125 cycles at 95% of weld current. Welding time: 11 cycles.

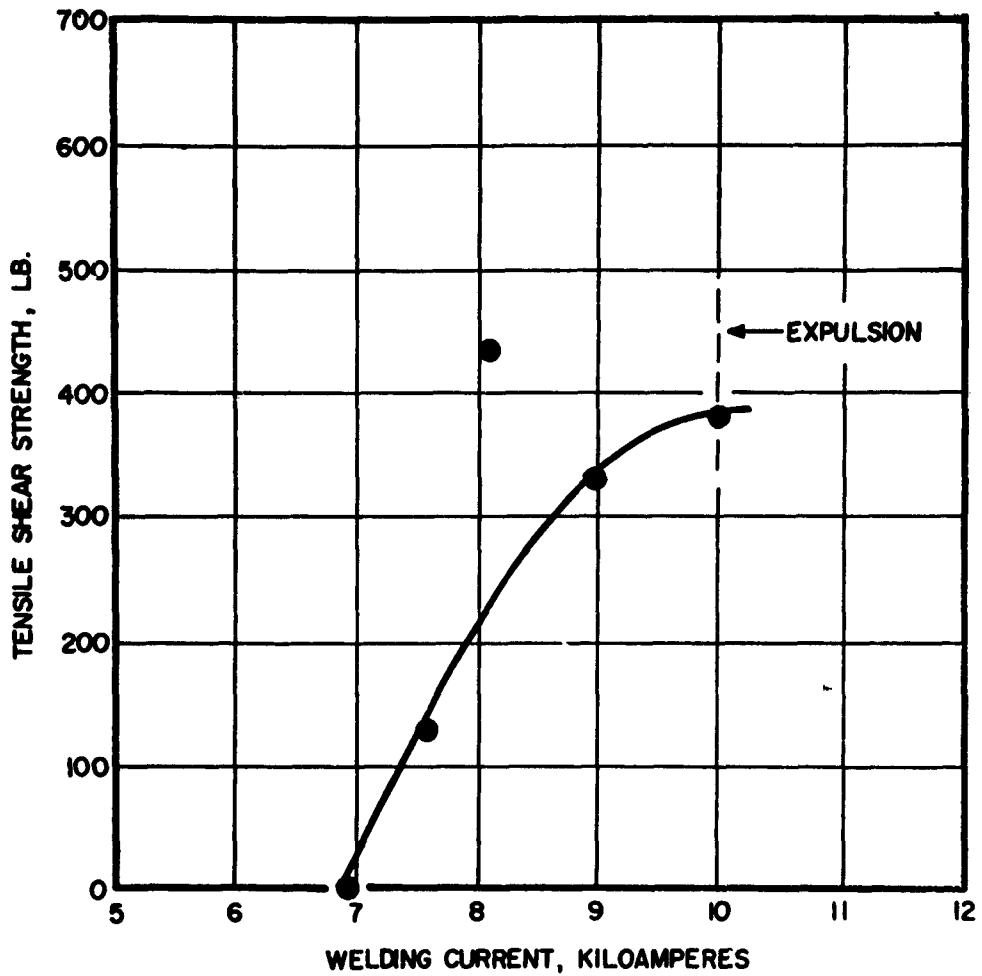


Figure 45 - Tensile shear strength vs. welding current for 0.040-inch beryllium sheet. Electrodes: RWMA Class 2, 6-inch radius dome, 0.156-inch restricted diameter. Initial force: 450 lbs. Forging force: 1000 lbs. No preheat. Postheat: 125 cycles at 95% of weld current. Welding time: 11 cycles. Forging delay: 0.5 cycle after weld.

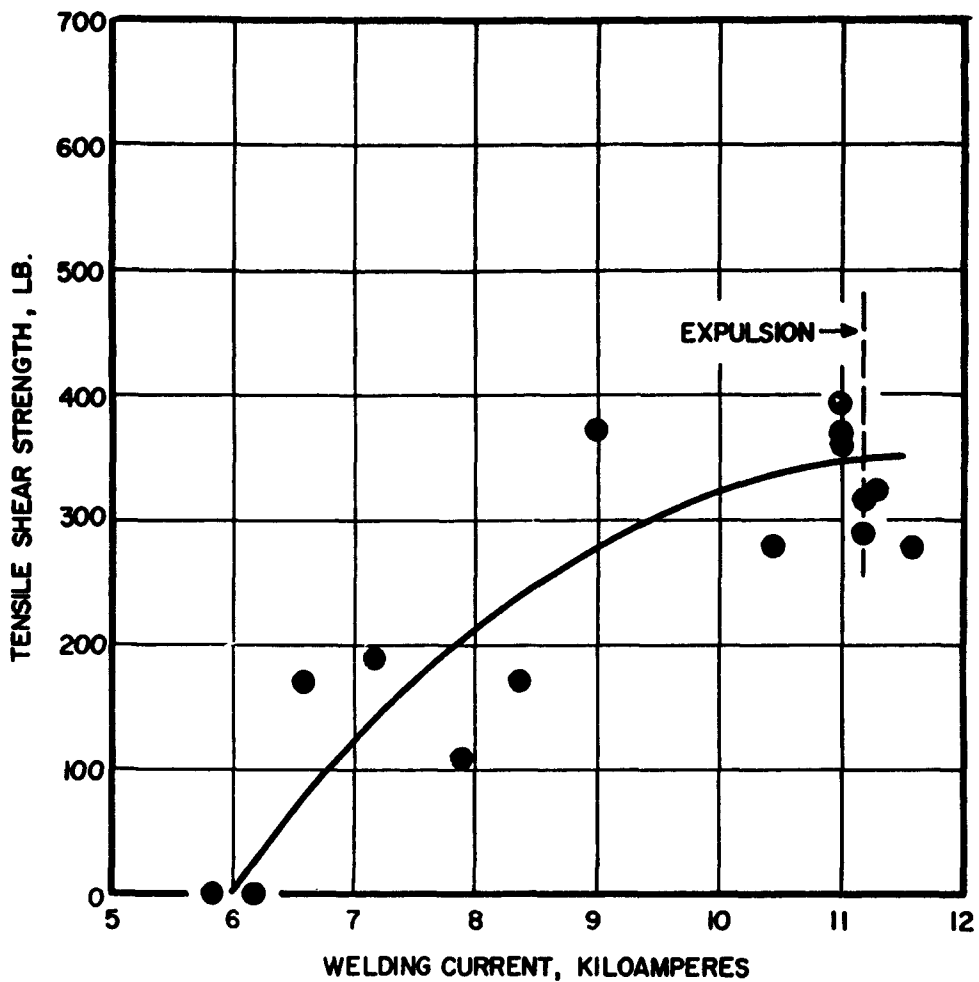


Figure 46 - Tensile shear strength vs. welding current for 0.040-inch beryllium sheet. Electrodes: RWMA Class 2, 6-inch continuous radius dome. Initial force: 550 lbs. Forging force: 1350 lbs. Preheat: 200 cycles at 80% of weld current. Postheat: 120 cycles at 95% of weld current. Welding time: 11 cycles. Forging delay: 77 cycles.

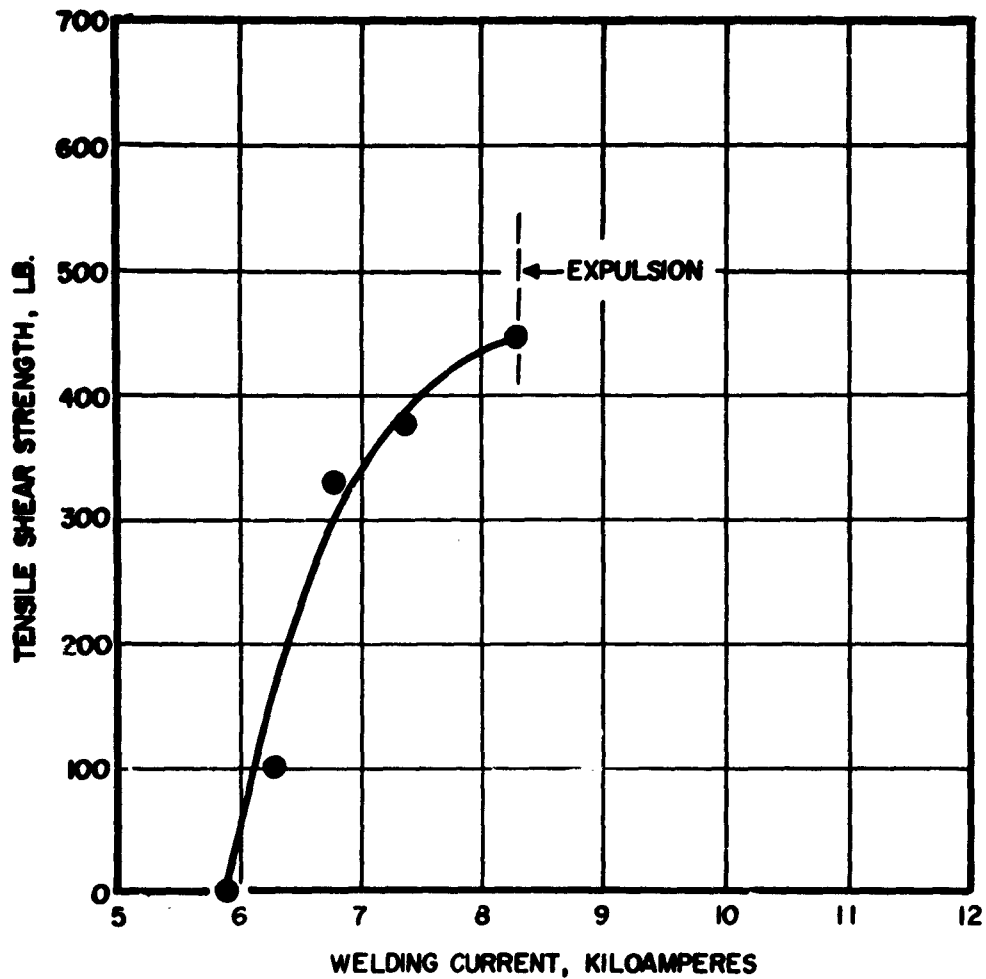


Figure 47 - Tensile shear strength vs. welding current for 0.040-inch beryllium sheet. Electrodes: RWMA Class 2, 6-inch radius dome, 0.156-inch restricted diameter. Initial force: 450 lbs. Forging force: 1225 lbs. Preheat: 200 cycles at 80% of weld current. Postheat: 120 cycles at 95% of weld current. Welding time: 11 cycles. Forging delay: 77 cycles.

Figures 44 and 45 present similar data for 0.040-inch thick beryllium sheet except that a long postheat cycle was used. Welds shown in Figure 44 some of which had external cracks, were made without a forging force, while welds shown in Figure 45 were made with a forging force and exhibited no signs of external cracking.

In Figures 46 and 47 are shown similar data obtained using a long preheat and a long postheat cycle with a forging force. Data shown in Figure 46 were obtained using a 6-inch continuous radius dome electrode, while a 5/32-inch restricted diameter, 6-inch radius electrode was used in obtaining data shown in Figure 47. Welds represented by the data in Figure 46 were well within the RWMA limits of 5 percent sheet indentation and 10 percent sheet separation, except where expulsion occurred. The welds made with a restricted diameter electrode, as in Figure 47 exceeded these limits up to 200 percent. From this evidence one would conclude that the 6-inch continuous radius electrode is more desirable for maintaining sheet separation and sheet indentation within reasonable limits. No sign of external cracking was evident in any weld in these two groups. The scatter of data in Figure 46 should be noted.

Comparison of the data presented in these curves does not show any significant difference in the tensile-shear strength regardless of the welding procedure employed. The maximum observed tensile-shear strength values fell below the theoretical strength calculated on the basis of the weld area. The use of a forging force definitely reduces the tendency to form cracks, but the tensile-shear strength is not significantly better in the absence of detectable cracks. Preheating and postheating appear to help reduce cracking, but do not improve the strength of the weld. Continuous radius electrodes are helpful in controlling sheet indentation and sheet separation.

Other tensile-shear tests were conducted in other sheet thicknesses over a wide range of conditions, but test results were equally inconclusive.

9-5.6 Metallography. Representative welds from each group of tensile-shear specimens were sectioned and examined metallographically for possible causes of failure. Welds selected were usually those which failed at the highest load.

Figure 48 shows the center section of a weld which was made with a 8800-ampere preheat for 200 cycles, a 11,000-ampere welding current for 8 cycles, and a 10,500-ampere postheat current for 120 cycles. The initial electrode force was 550 lbs. and the forging force was 1350 lbs. applied 77 cycles after the main weld interval. The electrode geometry was a 6-inch continuous radius. This weld illustrates the large columnar dendritic grains of the weld nugget, typical of resistance welds made in beryllium. This particular weld failed at 330 lbs. in tensile-shear and exhibited base-metal failure. There was no external evidence of cracks and the only defect noted in this weld is the horizontal void at the center of the nugget, far removed from the fracture.

The weld shown in Figure 49 was made using no preheat, a 9500-ampere welding current for 11 cycles, and a 9000-ampere postheat current for 125 cycles. The initial electrode force was 600 lbs. and no forging force was used. The electrode geometry was 5/32-inch restricted diameter, 6-inch radius dome. Although this



25X Pd. Lt.

Figure 48 - Section through beryllium resistance spot weld with horizontal void.



25X Bt. Lt.

Figure 49 - Beryllium resistance spot weld with
internal crack and fractures at edge
of weld.

weld initially had an external crack in the weld zone, it had a tensile-shear strength of 380 lbs. An internal crack along the columnar grain boundaries is visible in the center of the weld nugget. This crack probably extends to the surface of the weld at another location and is part of the original crack. The propagation of the crack into the base metal may have been diverted at the notch existing at the edge of the fusion zone, causing a failure in the base metal across the tensile specimen. The weld also exhibits excessive indentation, which probably was responsible for the original crack.

In Figure 50 is shown a weld that was made using no preheat, a 8900-ampere welding current for 11 cycles and a 4500-ampere postheat current for 5 cycles. The initial electrode force was 450 lbs. and a forging force of 1500 lbs. was applied 1/2 cycle after the main weld interval. The electrode had a 5/32-inch restricted diameter, 6-inch radius dome. Failure of the joint occurred in the base metal at 380 lbs. load in tensile-shear. The weld exhibits the typical large columnar dendritic grain structure at the center with some evidence of recrystallization at the outer edge. The large porosity visible in the center of the weld may have been the result of the expulsion of molten metal during welding.

A weld showing complete recrystallization of the fusion zone is shown in Figure 51. This weld was made without preheat, with a 9900-ampere welding current for 11 cycles, and a 5000-ampere postheat current for 5 cycles. Initial electrode force was 450 lbs. and a 1000-lb. forging force was applied 1/2 cycle after the main weld interval. The electrode had a 5/32-inch restricted diameter, 6-inch radius dome. Failure occurred in the base metal at 400 lbs. in tensile-shear. Among the many welds examined, this was the only one that indicated complete recrystallization. This would suggest that the timing of the application of the forging force is extremely critical or that inhomogeneities in chemistry or microstructure make the time-temperature relationship for recrystallization highly variable.

9-6 CONCLUSIONS

- (1) RWMA Class 2 electrode material was found to be satisfactory for resistance welding beryllium from the standpoint of long electrode life, reduced tip-pickup, and elimination of arcing at the electrode to work interface.
- (2) The range of welding currents required for welding 0.020-, 0.040-, and 0.060-inch beryllium have been determined for various electrode forces using weld times ranging from 1 to 15 cycles, and are summarized graphically.
- (3) The current required to produce a given weld diameter was found to increase significantly with decrease in weld time below 5 cycles.
- (4) Above 8 cycles weld time, the current required to produce a given weld diameter was found to be relatively insensitive to weld time.



33X Pd. Lt.

Figure 50 - Beryllium resistance spot weld exhibiting porosity and some recrystallization at the edges of the nugget.



25X Pd. Lt.

Figure 51 - Completely recrystallized beryllium
resistance spot weld.

- (5) Weld times of 8 to 10 cycles are believed to be satisfactory for all three gages studied.
- (6) Cracks originating in the weld zone and extending radially outward at approximately 120° intervals were almost invariable observed with single-impulse spot welds.
- (7) The incidence of cracking was reduced significantly by the utilization of a three-stage welding procedure consisting of a preheat interval, a weld interval and a postheat interval. This technique was designed to reduce the weld heating and cooling rates.
- (8) Long preheat and postheat intervals of up to 200 cycles of reduced magnitude current proved more effective in reducing cracking than did up- and down slope control of the welding current.
- (9) Temperature measurements indicated that a preheat interval that raised the temperature of the beryllium gradually to above 600°F prior to the application of the actual welding current was satisfactory.
- (10) Temperature measurements indicated that a postheat interval that provided slow cooling of the weld from the melting temperature to 600°F or below was satisfactory.
- (11) Metallographic examination revealed porosity in the weld zone in both the single-impulse welds and the three-stage welds made with a constant electrode force.
- (12) A dual pressure welding cycle utilizing a forging force of 2.5 to 3 times the welding force, applied shortly after the completion of the weld interval, was found to be the most effective means of reducing the incidence of both weld porosity and cracking.
- (13) The time of application of the forging force appears to be critical, since too short a delay in the welding force causes excessive indentation and too long a forging delay fails to eliminate weld porosity.
- (14) Recrystallization of the columnar dendritic weld metal microstructure is possible by the application of a suitable forging force at the appropriate instant following completion of the welding operation, but either the timing is too critical to permit reproducible results with existing resistance welding controls or else inhomogeneities in the sheet lead to a large variation in time-temperature conditions for recrystallization. Metallographic evidence is presented to confirm the possibility of achieving this modification of the weld microstructure.

- (15) The use of a postheat interval involving a suitable reduced magnitude current to reduce the cooling rate makes the force application time less critical and assists in eliminating cracks and porosity.
- (16) Tensile-shear tests conducted at room temperature with welds having no visible defects invariably exhibited brittle failures in the base metal.
- (17) Although failure invariably occurred in the base metal of properly made welds, the breaking loads were erratic and showed little relationship to the theoretical strength of the cross-sectional area at the failure.
- (18) No cracks or other observable defects were detected which could have contributed to the low apparent strength of the welded specimens; the cause of the premature failures is undetermined.
- (19) Although the results of this investigation did not permit determination of welding conditions for producing weld strengths approaching the theoretical strength of beryllium, the extreme notch sensitivity of currently available beryllium, and the unfavorable geometry of a spot weld when made in a relatively brittle, notch-sensitive material are believed to be the major contributing factors to the erratic tensile shear strength of spot welds in beryllium sheet. However, the possibility exists that the large-grained columnar structure of the weld contributes to the relatively low strength. Also the discontinuity between the nugget and base metal may lead to stress concentrations as a result of the anisotropy of beryllium.
- (20) A brief discussion of an exploratory resistance brazing experiment is contained in Appendix 9A.

REFERENCES

1. Development of Beryllium Sheets Rolled Flat to Gauge, AMC Technical Report No. 60-7-631, Brush Beryllium Co., Cleveland Ohio, September 1960.
2. C. O. Matthews, et al., Beryllium Crack Propagation and Effects of Surface Condition, WADD Technical Report 60-116, Lockheed Aircraft Corp., Missiles and Space Division, July 1960.
3. W. F. Hess, et al., The Surface Treatment of Alclad 24s-T Prior to Spot Welding, Welding Journal (Research Supplement) 23:402s-413s, August 1944.
4. B. MacPherson, Brush Beryllium Co., Cleveland, Ohio, private communication.

Appendix 9A

RESISTANCE BRAZING OF BERYLLIUM

9A-1 INTRODUCTION

The major portion of this program was devoted to the resistance welding of AMC beryllium sheet. It was desired, however, to investigate the possibilities of resistance brazing this material, using silver-base brazing alloys.

Beryllium has been torch brazed with qualified success. Published data (WADC TR- 59-695) show that silver-based alloys can be used successfully to achieve a brazed joint in beryllium. Because of the combined effects of brittleness, crack or notch sensitivity, and susceptibility to thermal shock, it was difficult to prevent cracks in the heat-affected zone of the joint.

Because the unusual physical properties of beryllium indicate its usefulness in the construction of space vehicles, it has become necessary to solve the problems of fabrication. This report investigates the area of joining with resistance brazing.

9A-2 OBJECT

The objects of this study are to:

- (1) Investigate the joining of beryllium sheet with resistance brazing.
- (2) Determine, in a general way, the parameters controlling the resistance brazing process.

9A-3 MATERIAL

Beryllium: AMC beryllium sheet in 1 x 3-inch samples, 0.020 inch thick from sheet 14B(1).

Braze alloy: BrBt^{*} silver-copper eutectic in 1-inch wide strip, 0.001-, 0.002-, and 0.003-inch thick.

9A-4 EQUIPMENT

Resistance brazing was performed on a 30 kva rocker arm welder shown in Figure 52. This apparatus was equipped with a ball and socket and self-aligning electrode holder mounted in a standard 500-lb, spring-loaded electrode holder. The welding control was a modified NEMA Type 5B. True RMS secondary current was measured with a commercially available secondary current meter. The 1-1/8 inch flat electrodes consisted of RWMA Class 2 bodies surfaced with RWMA Class 10 material.

- - - - -

* 72 percent Ag, 28 percent Cu eutectic alloy.



Figure 52 - 30 kva resistance welder used for resistance brazing experiments.

9A-5 PROCEDURE

Before resistance brazing, all specimens were cleaned in acetone and pickled for 3 minutes in a solution of 40% concentrated nitric acid, 4% concentrated hydrofluoric acid (48.84% HF), and 56% water.

Preliminary work was done to determine the approximate range of brazing force and current, and the best method of introducing the filler metal.

The first attempt to introduce the filler metal was made by interposing a 1-inch square of braze alloy between two samples of beryllium sheet and resistance brazing, using 6-inch continuous radius electrodes. The system was unsuccessful because the molten braze alloy was severely expelled.

The second system examined utilized flat electrodes and a 0.125-inch diameter disc of braze alloy which was placed between two specimens of beryllium and resistance brazed at a force of 350 lbs. This system was much more effective than the first, but difficulty was experienced in melting the entire disc. A 0.075-inch diameter disc was tried and proved successful. A brazing time of 20 cycles was found to be the shortest conducive to uniform melting.

Simultaneous resistance brazing of two discs was also studied. Joints were made using two 0.075-inch diameter braze discs placed side by side perpendicular to the long axis of the brazed specimen. It was necessary to place the discs so that they were nearly touching in order to melt both uniformly. Data were taken to determine the minimum current required to produce measurable strength in the joint for both a single disc and for two discs in parallel.

Strength versus current data at various forces were taken for both the single and multiple brazing systems.

Several specimens were sectioned and examined both at 25X and 500X in order to determine the nature of the joint. The etchant used was a 2% solution of FeCl_3 in water.

9A-6 DISCUSSION

9A-6.1 Cleaning. The cleaning and etching procedure used in this portion of the work is the same as that used for resistance welding. The appearance of the etched surface was observed to depend on the temperature and degree of depletion of the solution. A cold or depleted solution yielded a frosty surface, while a hot, fresh solution produced a fairly shiny surface. The rate of surface reaction was also greatly dependent on the solution condition, a hot, fresh solution causing violent reaction with the beryllium.

Surface condition affects those brazing processes that depend upon capillary flow; a rough surface impedes the flow of filler material. In resistance brazing utilizing in situ filler material, surface cleanliness should be the most important factor. Regardless of the surface appearance of the etched beryllium, uniformly low contact resistance was obtained, indicating a high degree of cleanliness.

9A-6.2 Introduction of Braze Material. Introducing the braze material as a small disc results in rather critical electrode alignment requirements. If the electrodes are not well aligned, the beryllium sheets do not contact the braze discs uniformly when the force is applied. Upon brazing, one edge of the disc tends to melt and expel, leaving most of the disc unaltered and resulting in an unsatisfactory joint.

Joints made at high current levels frequently show a small spot of slightly oxidized surface at the beryllium-electrode interface, directly in line with, and about twice the size of the braze disc. The area of best contact between the electrode and the work would be that which is in line with the braze disc, so that the braze disc effectively concentrates the current to a very restricted path. It appears that, within a wide range, the thickness of the beryllium sheet would have little effect on this mechanism.

9A-6.3 Minimum Sticking Current. Data were taken to determine the minimum sticking current under a variety of welding pressures with 0.003- and 0.002-inch BrBt alloy. It was found that this current, which showed large scatter, increased with force up to about 300 lbs., then leveled off as the force was further increased. This is as expected since the surface contact resistance reached a low value at 300 lbs. and did not decrease further at higher values of force. The current required to produce consistent joints was approximately 3000 amperes above the minimum current required to produce sticking. It can be reasoned that the current to produce sticking is dependent upon many factors. The surface condition of both the braze disc and the beryllium sheet would greatly affect the minimum sticking current. It was noted that small projections on the periphery of the braze disc would lower this minimum.

9A-6.4 Strength versus Current Data. Above certain minimum current values, the tensile specimens failed in the base material. Although no external defects were visible in many of the specimens, the maximum observed tensile-shear strength values fell below the theoretical strength based upon the braze area. Base metal failures usually propagated from a point adjacent to the resistance brazed joint. These observations would suggest that either or both of the following contributing factors were present:

- (1) The absence of external defects does not preclude the existence of internal defects which severely restrict the load-carrying capacity of the joint. Because of the great difference in X-ray absorption coefficients for beryllium and the filler alloy, it was not possible to detect defects with the X-ray technique described in the resistance welding portion of this report.
- (2) The beryllium sheet is extremely notch sensitive and thus the severe restraint imposed by the joint geometry at the edge of the braze tends to cause premature failures which propagate rapidly through the base material.

Figure 53 shows the tensile-shear strength versus current data for the joints made with a single disc of 0.003-inch BrBt alloy. A maximum strength of 260 lbs. was obtained with a current of 8500 amperes, but it was not possible to reproduce this strength. It is noted that, in general, brazing currents in excess

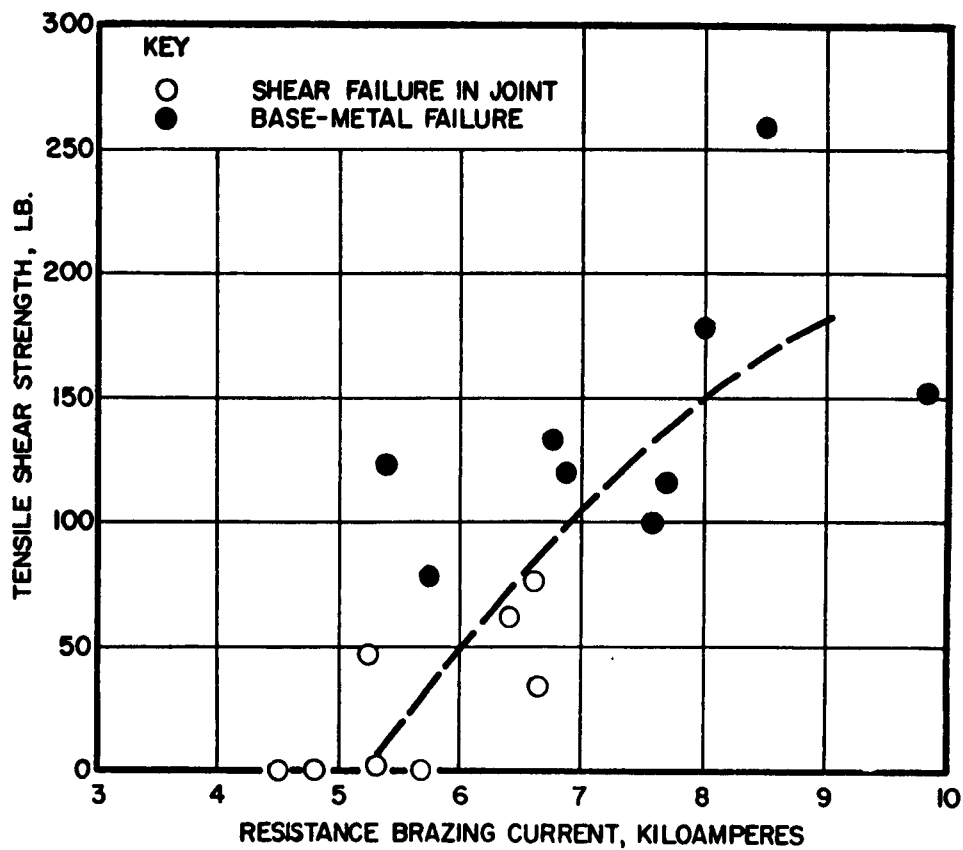


Figure 53 - Tensile shear strength as a function of resistance brazing current, 0.020-inch beryllium sheet. 9.625-inch diameter RWMA Class 10-faced electrodes. Electrode force: 350 lbs. Brazing time: 20 cycles. 0.075-inch diameter button of 0.003-inch BrBt alloy.

of approximately 6750 amperes yielded base material failures which appeared to propagate from the extremity of the joint and extend perpendicular to the tensile direction. On the other hand, shear failures through the braze alloy were observed, in most cases, at currents below 6750 amperes. In several of these failures, incomplete fusion of the braze disc was visible. The strongest joint exhibited a calculated tensile-shear strength of 33,000 psi.

The dashed line indicates a general trend. Because of insufficient data, it is not possible to specify design values.

Figure 54 summarizes the tensile-shear strength versus current data for joints made with two braze discs. The maximum strength of 250 lbs. was obtained using 11,000 amperes. Again, it was not possible to reproduce this strength. Joints made with current in excess of 6000 amperes yielded base metal failures whereas those made at current less than 6000 amperes failed in the braze alloy. Braze alloy failures were characterized by apparent incomplete fusion of the braze discs. The dashed line indicates a general trend. Because of insufficient data, it is not possible to specify design restrictions.

In order to achieve rapid follow-up of the electrode assembly, a spring-loaded electrode holder was used. Data for single-disc brazing with a 0.075-inch diameter, 0.003-inch thick disc indicate an optimum brazing force of 350 lbs. The useful limit of the spring-loaded electrode holder was 450 lbs. Consequently, the brazing force for the multiple-disc technique was less than the optimum 700 lbs.

9A-6.5 Cracking. It is difficult to avoid cracking in this material when welding. It appears that thermal shock is very deleterious and is responsible for the numerous cracks which appear. The beryllium sheet used in this investigation has a rolling texture in which the basal planes of the hexagonal-close packed beryllium are essentially parallel to the sheet surfaces. Cracks may be induced by stresses resulting from the differences in expansion coefficients of the braze and highly oriented sheet. It is suspected that the brazed joints may contain defects which are confined to the material immediately adjacent to the joint, and do not extend to the external surfaces. The material immediately adjacent to the joint is subjected to extremely high thermal gradients which might lead to thermal shock.

It is probable, therefore, that the electrode force in conjunction with thermal shock causes cracking in the brazed joints and base material.

9A-6.6 Photomicrography. Figure 55 shows a photomicrograph of a brazed joint taken at 500X after etching in a 2% aqueous solution of FeCl_3 . There appears to be a sound metallurgical bond between the filler metal and the base metal. Evidence of diffusion is not visible up to 2000X magnification. This would be as expected considering the very short time at elevated temperature.

Because this portion of the beryllium joining program was de-emphasized, it was not possible to complete a thorough examination of resistance brazing. Among the several areas warranting further work are:

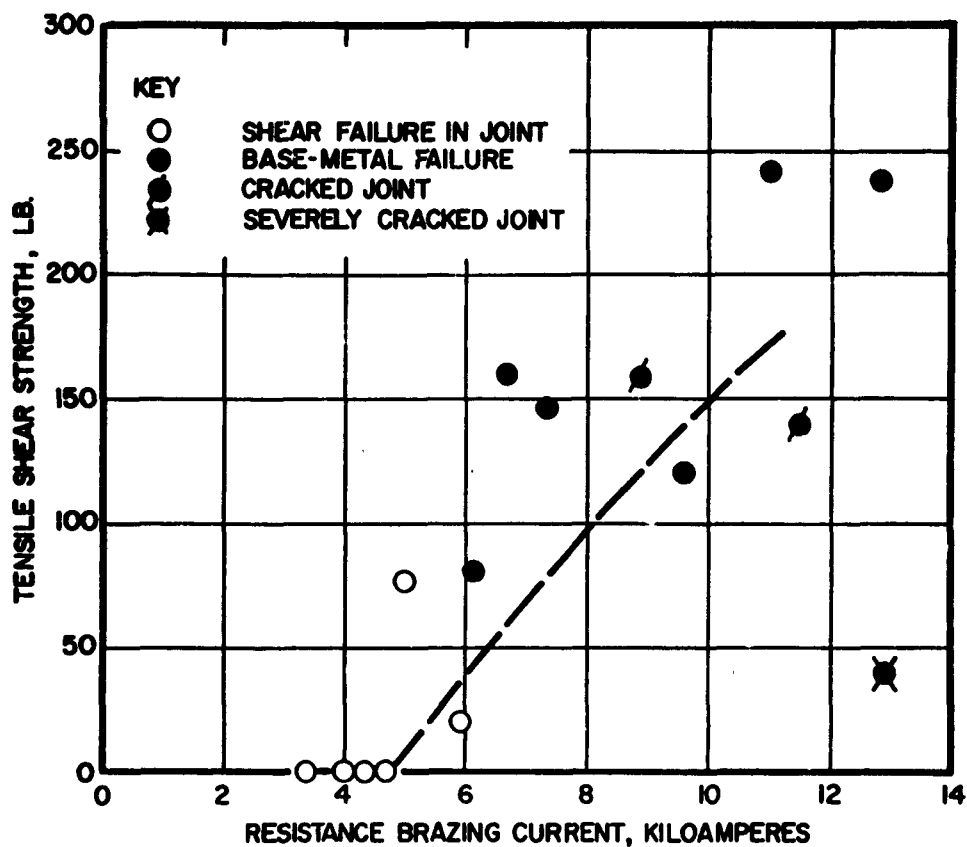
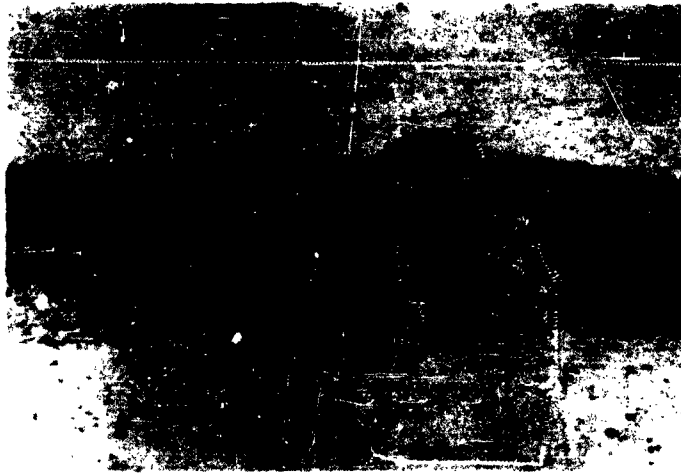


Figure 54 - Tensile shear strength as a function of resistance brazing current, 0.020-inch beryllium sheet. 0.625-inch diameter RWMA Class 10-faced electrodes. Electrode force: 450 lbs. Brazing time: 20 cycles. Two 0.075-inch diameter buttons of 0.003-inch BrBt alloy located 0.090-inch on centers transverse to axis of loading.



500X Unetched.

Figure 55 - Resistance braze in beryllium sheet.

- (1) Determination of optimum electrode forces in multiple resistance brazing operations.
- (2) Investigation of the effect of various resistance brazing cycles including pre- and postheats.
- (3) Investigation of fine silver and other filler metals.

9A-7 SUMMARY AND CONCLUSIONS

- (1) The filler metal was introduced as a 0.075-inch diameter disc which also served as current concentrator. Electrode alignment was critical with this system. Brazing force of 350 lbs was used.
- (2) Multiple brazing was performed using two 0.075-inch diameter discs placed on centers 0.090-inch apart on a line perpendicular with long axis of brazed specimen. A brazing force of 450 lbs. was used.
- (3) Data were taken to determine minimum bonding current for the single disc technique, using a range of resistance brazing forces. The bonding current was of the order of 5000 amperes.
- (4) Strength-versus-current data were taken for both single and multiple brazing techniques. Both sets of data indicated transition current values at which the mode of failure changed from shear in the braze alloy to tensile failure of the base material. It was not possible with either technique to reproduce joints exhibiting high strength.
- (5) Multiple brazing showed no strength advantage over single brazing, as fractures occurred in the base metal at comparable tensile-shear load values. It was proposed that this effect is due to internal defects in the joints.
- (6) Photomicrographs indicate the achievement of a sound metallurgical bond with no observable diffusion.

9A-8 LITERATURE CITED

- (1) Development of Beryllium Sheets Rolled Flat to Gauge, Brush Beryllium Company, Cleveland, Ohio, AMC Technical Report No. 60-7-631, September, 1960.

SECTION 10

THE PURIFICATION OF BERYLLIUM BY DISTILLATION

J. P. Pensler, S. H. Gelles,
E. D. Levine and A. R. Kaufmann

(Nuclear Metals, Inc., Concord, Massachusetts)

ABSTRACT

Distillation has been used to produce beryllium of very high purity in order to determine the relation between purity and the mechanical properties of the metal.

Purification was achieved by distillation from the melt in a beryllia crucible heated to 1375°C . The distillate was condensed on a tantalum collector heated by radiation from the crucible to approximately 1090°C at the collector top and 1160°C at the bottom.

Results indicate that metal impurities can be substantially removed in a single distillation. Iron, nickel, and chromium contents were reduced to the 1 - 5 ppm range.

Mechanical property measurements indicate that singly distilled beryllium has limited ductility. The properties appear to be affected by the presence of precipitate particles containing silicon, iron, sulfur and aluminum. The source of these impurities has not been determined at this time.

10-1 INTRODUCTION

When this work was initiated, the question of whether impurities adversely affect the mechanical properties of beryllium was unresolved. There were many indications⁽¹⁾ that impurities play an important role in the brittleness of this metal, but positive proof that elimination of impurities would produce ductile metal was lacking.

Evidence has been given in the literature^(2,3) that purification of beryllium produces a softer metal which can be deformed at somewhat lower stress levels and can sustain somewhat more deformation before fracture than commercially pure beryllium. The recent work of Herman and Spangler⁽⁴⁾ is the strongest evidence presented thus far. Beryllium single crystals produced by zone refining showed substantial improvements in ductility compared with impure single crystals. A large reduction in the critical resolved shear stress for slip upon the basal plane was also noted.

The conclusive demonstration of the adverse effect of impurities on the ductility of single crystals has added incentive to obtaining high purity polycrystalline beryllium in order to determine whether the polycrystalline material shows a similar improvement and to explore the relationship of impurities to other properties. Furthermore, impetus is provided to develop an alternative and perhaps more economical source of high purity beryllium.

10-2 THEORY

The factors affecting the purity of distilled beryllium have been discussed by Martin⁽⁵⁾ and by Sinelnikov.⁽²⁾ As a first approximation, the impurities in beryllium distill at rates dependent upon their relative vapor pressures, molecular weights, and concentrations according to the relation:

$$R = \frac{5.833 \times 10^{-2} PC}{\sqrt{MT}}$$

where R = molar rate of evaporation in moles/cm²-sec.

P = vapor pressure in mm of Hg

C = concentration in mole fraction

M = molecular weight

T = temperature in °K.

Thus, the more-volatile impurities such as sodium, magnesium and the chlorides would be expected to concentrate in the initial material distilled from the molten beryllium. Low vapor pressure impurities such as iron, chromium, nickel and beryllium oxide would be expected to accumulate in the melt. If the distillate is collected on a heated surface such as described by Sinelnikov,⁽²⁾ the highly volatile impurities will be unable to condense. If an exit for the vapors exists

at the top of the condenser, the highly volatile impurities will be eliminated from the system and will not contaminate the distillate. Further, the possibility exists that elements such as manganese, which have vapor pressures slightly higher than beryllium, will migrate in the thermal gradient of the collector due to repeated re-evaporation and condensation, and thereby preferentially collect on the coolest portion of the heated collector surface.

Other factors affecting the purity of the product include the rate of efflux, rate of condensation, temperature of distillation, temperature of collector, area of collector, and percentage of the total charge distilled.(2,5)

10-3 PREVIOUS DISTILLATION RESULTS

Pearsall⁽⁶⁾ distilled a small quantity of beryllium in an ultra-high vacuum in order to eliminate oxygen from the distillate. Calculations indicated that the oxygen content of the distilled material was appreciably less than one part per million. Since the entire mass of beryllium was evaporated, no attempt at purification from other impurities was made, and the condensate was less pure than the charged material. Crude bend tests were performed on the distillate, and no evidence of improved ductility was found.

Martin⁽⁵⁾ discussed the theory and experimental approach to the distillation of beryllium in some detail. However, no results were reported on the purity of distillate actually obtained.

Sinelnikov and co-workers⁽²⁾ succeeded in producing significant quantities of distilled beryllium using a heated collector surface. Analytical determinations of the purity of their distillate are reproduced below.

	Element, ppm										
	Fe	Si	Al	Mn	Ni	Cu	Cr	N	Pb	Ti	Co
Starting Material	6500	3000	1000	500	300	250	200	100	50	13	10
After first distillation	60	100	20	20	10	5	40	10	10	10	0.5
After second distillation	12	30	10	10	10	5	-	10	10	10	0.5

The starting material was quite impure, and considerable improvement was obtained during a first distillation. Redistillation further improved the purity, but the extent of improvement was not as great as was obtained in the first distillation. No information regarding the analytical techniques was reported, nor was there any mention of the oxygen content of the distilled material.

No reports of mechanical tests were given in the paper by Sinelnikov and co-workers. However, Garber et al, working with distilled material presumably obtained from Sinelnikov's work, reported⁽³⁾ that basal slip can be observed in single crystals of distilled material at temperatures as low as 20°K, whereas in commercially pure beryllium basal slip could not be observed below 78°K. In addition, the critical resolved shear stress was found to be less in the purer material, and the amount of compressive strain before fracture was greater.

Amonenko et al⁽⁷⁾ give evidence for the existence of Be₂O, an oxide more volatile than BeO. The oxygen content of beryllium distilled from BeO crucibles is ascribed to the volatility of Be₂O.

Hooper and Keen⁽⁸⁾ distilled small quantities of beryllium from BeO and tantalum crucibles onto a vertical condenser closed at the top. Some impurities were found to fractionate anomalously (e.g., iron, aluminum and silicon behaved as relatively volatile substances). The purest material collected was only about as pure as that obtained by Sinelnikov et al⁽²⁾ after one distillation, although the starting material, Pechiney flake, was considerably purer than that used by the aforementioned investigators.

10-4 EXPERIMENTAL WORK

The distillations were performed in the bell jar vacuum system shown in Figure 56. The charge, ranging from 250 - 450 grams of beryllium, was contained in a beryllia crucible 2-3/4 inches in diameter by 4-3/4 inches deep. This in turn was contained within a furnace which consisted of tantalum wire wound around a beryllia crucible, nested in a second beryllia crucible. A slurry of beryllium oxide that had been poured between the crucibles served as an insulator for the tantalum wire. The furnace was mounted on a beryllia plate, which in turn was seated on a succession of tantalum or molybdenum radiation shields. The distilled beryllium was collected on a tantalum cone seated on the distillation crucible. A hole in the top of the cone enabled highly volatile material to escape from the system. Thermocouples monitored the temperature of the crucible containing the melt; during the first seven runs, the temperature of the tantalum collector was similarly monitored. A series of concentric radiation shields of tantalum or molybdenum were placed around the crucible. A copper plate with attached copper coils was positioned between the diffusion pump and the bell jar vacuum system. Trichloroethylene in contact with solid CO₂ (-78°C) was circulated through the coils during each run. This was found to greatly reduce contamination of the system by silicone diffusion pump oil. Pressure was measured with an ion tube contained within the vacuum system. The vacuum maintained during distillation was of the order of $2 - 5 \times 10^{-6}$ millimeters of mercury. The crucible containing the molten beryllium charge was heated to about 1375°C, and the metal was distilled for six to nine hours. The tantalum collector was heated primarily by radiation from the crucible and attained temperatures of about 1160°C at the bottom of the condenser and 1090°C at the top.

Fifteen single distillations were performed using vacuum-melted "CR" grade Pechiney flake as the starting material; in addition, single distillations using vacuum melted super purity Pechiney material and vacuum melted Brush QMV powder were made. Charges of about 250 - 450 grams were used, and the distillates ranged in weight from about 60 - 440 grams. The deposits obtained were shiny and substantially dense. A brittle layer was present between the tantalum collector and the beryllium deposit. This layer crumbled upon rolling the collector on a hard surface, thus allowing the beryllium deposit to be readily extracted. Details of the distillations are given in Table 12. A photograph of the distilled metal is shown in Figure 57.

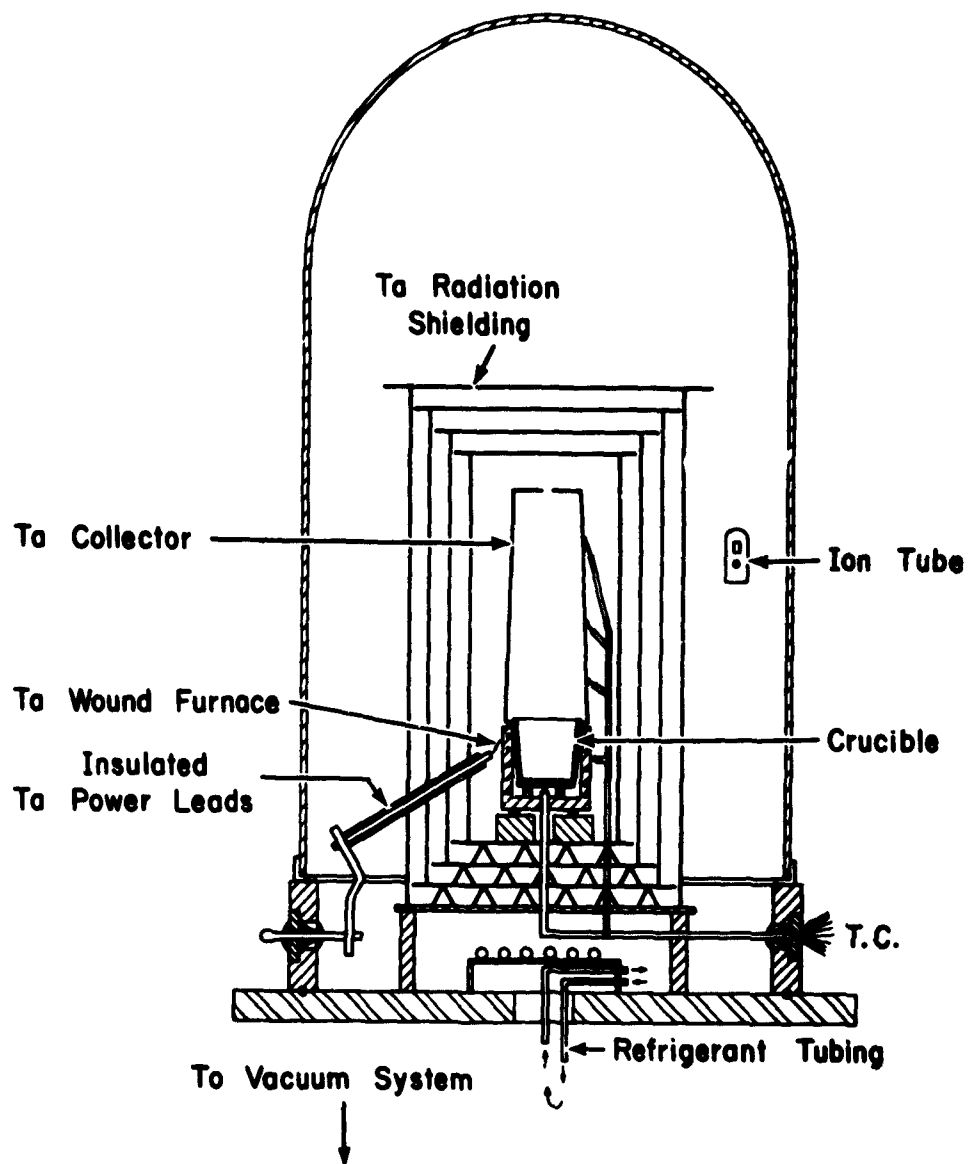


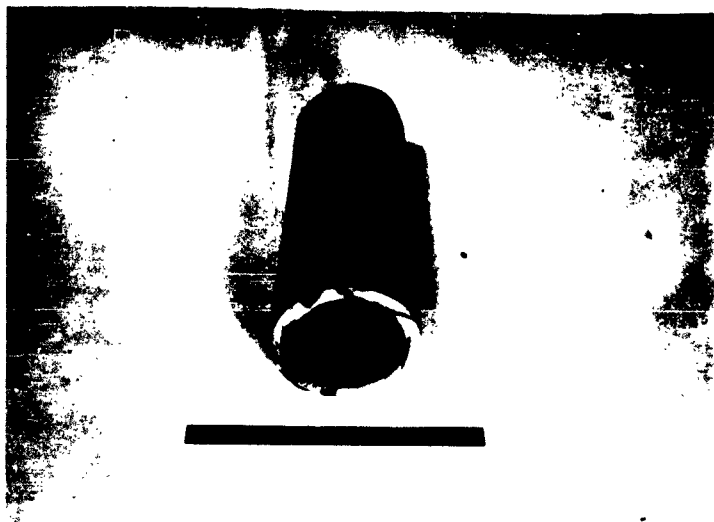
Figure 56 - Diagram of distillation apparatus.

Table 12. DESCRIPTION OF DISTILLATION EXPERIMENTS

Distillation No.	Weight of Charge (grams)	Weight of Product (grams)	% Distilled	Temperature of Collector (°C)			Time at Temp. (hrs.)	Comments (b)
				Bottom	Middle	Top		
1	430	100	23	1100	1100	950	6	Portion of the material bridged over the melt. Cone heated by second furnace.
2	300	67	22	1090	1040	1000	5	
3	247	147	60	1130	1130	1090	6	
4	296	154	52	1200	1140	1100	6	Cone heated by second furnace.
5	301	117	39	1175	1145	1120	6	Pronounced oxide film on residue causing low yield.
6	297	102	34	1140	1105	1070	7	
7	462	306	66	1155	1130	1090	9	Starting material was vacuum melted super pure Pechiney.
8	288	104	36				6	
9	357	232	65				9	Starting material was vacuum melted Brush QMV powder.
10	344	205	60				9	Crucible broke during run Distilled virtually all material.
11	423	not obtained	~65 est				13	
12	400	200	50				11	
13	435	not obtained	~65 est				14	
14	412	0	0				-	
15	438	~438	~100				17	
16	446	306	68				12	Crucible broke during run Distilled virtually all material.
17	412	313	76				12	

(a) Temperature of collector not determined for runs 8 - 17.

(b) Starting material was vacuum-melted CR grade Pechiney flake beryllium unless otherwise specified.



RF-7896

Figure 57 - Cone of distilled beryllium.

10-5 CHEMICAL EVALUATION OF DISTILLED BERYLLIUM

The high purity of distilled beryllium precludes the use of techniques commonly employed for the chemical analysis of commercial beryllium. A review of the procedures for the determination of specific impurities in beryllium indicated that very few of these, in their usual form, are reliable for impurity contents of a few parts per million. It was therefore necessary to modify the commonly employed techniques. Since it would be a task of considerable magnitude to develop procedures for all conceivable impurities, work in the present investigation was restricted to a few impurities suspected to be important with respect to their effect on mechanical properties. The specific impurities investigated were iron, nickel, chromium, manganese, aluminum, silicon, copper, carbon, nitrogen and oxygen. In the following discussion, the techniques employed for each of the above impurities are briefly described.

10-5.1 Techniques for Specific Elements.

(1) Iron. Iron is complexed as ferrous bathophenanthrolate and extracted into nitrobenzene. The iron concentration is determined spectrophotometrically. The minimum detection limit is 1 ppm.

(2) Nickel. In the initial experiments, nickel was oxidized to Ni^{+++} with bromine and then complexed with dimethylglyoxime. It was found possible to lower the minimum detection limit from 8 ppm to 4 ppm by performing the complexing operation in 50 milliliter volumes instead of the 100 milliliter volumes previously used. In later work, a new method was evolved in which Ni^{++} is complexed with dimethylglyoxime and extracted into chloroform. Ni^{++} is back-extracted into dilute hydrochloric acid. Bromine is used to oxidize Ni^{++} to Ni^{+++} which is then complexed with dimethylglyoxime. The nickel concentration is determined spectrophotometrically. This procedure reduces the minimum detection limit to 1 ppm.

(3) Chromium. Chromium is oxidized with potassium permanganate. The excess oxidant is destroyed with potassium bromide, and the chromate ion is complexed by s-diphenylcarbazide. The color is stable for 1 hour. The chromium concentration is determined spectrophotometrically. The minimum detection limit is 1 ppm.

(4) Manganese. Manganese is oxidized with silver persulphate. The permanganate concentration is determined spectrophotometrically. The minimum detection limit is 15 ppm.

(5) Aluminum. Aluminum is complexed as the 8-hydroxyquinolate at a pH of 5.0, and interferences are complexed as the orthophenanthrolates. A buffer of sodium hydroxide and sodium acetate is used to complex the beryllium. Aluminum 8-hydroxyquinolate is extracted into chloroform and the traces of water are removed by sodium sulfate. The blanks are low and reproducible. The aluminum concentration is determined spectrophotometrically. The minimum detection limit is 5 ppm.

(6) Silicon. Hydrochloric acid is used to dissolve the sample, and hydrofluoric acid is used to convert silicon to a reactive form. The sample stock solution is adjusted to a pH of 1.0. Molybdic acid, hydrochloric acid (pH = 1.5),

1
tartaric acid and a mixed reductant including sodium bisulfate, sodium hydroxide and 1 amino-2 naphthol-4 sulfonic acid are used as special reagents. The silicon concentration is determined spectrophotometrically. The minimum detection limit is 5 ppm.

(7) Copper. Copper is reduced to Cu^+ with hydroxylamine hydrochloride. Cu^+ is complexed by neocuprine and extracted into chloroform. The copper concentration is determined spectrophotometrically. The minimum detection limit is 4 ppm.

(8) Carbon. Carbon is burned in oxygen in an induction furnace. The evolved carbon dioxide is determined in a barium hydroxide conductometric cell. The minimum detection limit is 25 ppm.

(9) Nitrogen. The sample is dissolved in hydrofluoric acid. The nitrogen is distilled as ammonia by micro-Kjeldahl distillation. The ammonia in the distillate is absorbed by boric acid solution. The nitrogen concentration is determined by titration with hydrochloric acid solution. The minimum detection limit is 5 ppm.

(10) Oxygen. The technique used for oxygen determination was a modification of the chloride volatilization method. In this technique, a stream of hydrogen chloride gas is passed over a beryllium sample at 650°C, converting the beryllium to beryllium chloride which volatilizes and later condenses in a cooled chamber in the reaction vessel. The unreacted beryllium oxide is left as a residue in the volatilization chamber and is analyzed for beryllium spectrophotometrically, using p-nitrobenzeneazoorcinol as a colorimetric reagent.

In the present investigation this method was modified to remove possible sources of oxygen contamination. These and other modifications consisted of the following: (1) a vacuum system was provided to evacuate the reaction chamber prior to the introduction of hydrogen chloride gas; (2) a dry ice-acetone cold trap was provided to remove moisture from the hydrogen chloride gas; (3) a long platinum tube was placed in the hot zone to minimize reaction of hot hydrogen chloride or beryllium chloride with the glass reaction container; (4) the condensation chamber was enlarged to permit use of samples as large as 2.5 grams; (5) X-ray diffraction and emission spectroscopy were performed on the volatilization residue to determine if volatilization was complete.

These modifications resulted in a reduction in the values obtained from approximately 1000 ppm to approximately 300 ppm for vacuum melted beryllium. It is believed that the values are still too high because of oxygen pickup from the reaction of SiO_2 with HCl .

10-5.2 Analytical Results. Results of chemical analyses are presented in Tables 13 to 15. Table 13 gives typical analyses of the various starting materials employed in the program. In the early stages of the investigation, beryllium flake was compacted in a steel die prior to vacuum melting. This resulted in some iron contamination of the flake. Later in the program a beryllium die was used for compacting and, as shown in Table 13 the iron content of the vacuum melted material was reduced appreciably.

Table 13. CHEMICAL ANALYSES OF BERYLLIUM STARTING MATERIAL

Material	Impurity Content, ppm by weight						
	Fe	Ni	Cr	Mn	Al	Cu	C
Vacuum melted Pechiney flake, regular grade; flake compacted in steel die prior to melting.	275	99	9	20	55	9	<25
Vacuum melted Pechiney flake, regular grade; flake compacted in beryllium die prior to melting.	161	128	19	15			
Vacuum melted Pechiney flake, super-pure grade.	43	8			20	4	
Vacuum melted Brush QMV powder.	1180		176		585	40	

Table 14. CHEMICAL ANALYSES OF BERYLLIUM PRODUCED BY VACUUM DISTILLATION

Distillation No.	Impurity Content, ppm by weight								
	Fe	Ni	Cr	Mn	Al	Si	Cu	C	N
2 (bottom)	5	1	2	25					
2 (middle)	25	3							
3 (middle and top)	<1	1	1	15					
4 (middle)	<1	<1	<1	<15					
4 (top)	5	1	<1	25					
5 (bottom)	<1	<1	<1	<15				30	
5 (middle)	2.5								
6 (bottom)	4	1	3	<15				35	
6 (bottom and middle)	3	2	2	<15					
6 (middle)	2.5	2	2	<15				<25	7
6 (middle and top)	3.5	3	1	<15					
6 (top)	3.5	5	<1	<15					
7 (bottom)	1.5	1	<1	<15					
7 (middle)	3	1	1	<15					7
7 (top)	3	4		15					
8 (bottom)	2.5	1		<15	5		<4		
8 (middle)	2	1		<15					
9 (bottom)	4.5	2	1						
9 (middle)	6	2	1		120				
9 (top)	3	1							
10 (bottom)			1						
10 (middle)	4								
11 (bottom)	1	1		<15					
11 (middle)	1.5	1		<15					
11 (top)	2	1		<15					
15 (bottom)	13	1	5	<15		13			
15 (top)	4	1	2	15		11			
16 (bottom)	2	1	1	<15	30-65		7		
Sheet produced by rolling distilled Be in steel sheath	6.5								
Vacuum melted distillate	4	1		<15	25				
Vacuum melted distillate after extrusion in steel sheath	9.5	2	<1	<15	35				

Table 15. CHEMICAL ANALYSES OF DISTILLATION RESIDUES

Distillation No.	Impurity Content, ppm by weight					
	Fe	Ni	Cr	Mn	Al	Cu
4	570	230	18	20		
8	80					
9					1080	
12	785			36	100	29
16					70	19

Table 14 lists analyses of beryllium produced by vacuum distillation. Samples were taken from various portions of the cones in order to observe gradients due to different condensation temperatures. As mentioned previously, temperature was highest at the bottom of the cone. Also listed in Table 14 are analyses of distilled beryllium after various fabrication procedures were performed.

On the basis of the results obtained, it is possible to make the following statements concerning beryllium produced by vacuum distillation:

- (1) Iron, nickel and chromium are reduced to contents below 5 ppm by vacuum distillation.
- (2) Manganese and silicon are reduced to contents below 15 ppm by vacuum distillation.
- (3) For distillation yields up to approximately 65%, final content of the above impurities appears to be insensitive to the starting material employed except for possibly the aluminum content (distillations 8 and 9, Tables 12 and 14).
- (4) The aluminum appears to be distributed inhomogeneously (see distillation 16, Table 14).
- (5) The only effect of collector temperature appears to be an increase tendency for manganese to deposit at the lower temperatures.
- (6) Further processing of distilled beryllium, including vacuum melting, warm rolling in steel sheaths, or hot extrusion in steel sheaths, does not appear to produce significant contamination, at least by any of the elements for which further analyses were made. The apparent increase in iron content observed in the distillate that was vacuum melted and then hot extruded is probably due to small amounts of sheath material not removed by pickling.
- (7) Not enough information is available to comment on the removal of carbon and oxygen by distillation; this is primarily due to limitations of the analytical techniques for these elements.

Analyses of distillation residues are presented in Table 15. From these data it is possible to calculate mass balances for non-volatile impurities such as iron, nickel and chromium. In each case, mass balances between starting material, condensate and residue indicate, within experimental error, that these impurities distill in agreement with the equation given in Section 10-2.

10-6 MECHANICAL EVALUATION OF DISTILLED BERYLLIUM

10-6.1 Characteristics of Distilled Beryllium. In order to evaluate properly the mechanical properties of distilled beryllium, it was necessary to consider the following characteristics of the distilled product:

(1) Geometry. As previously indicated, the beryllium deposits were in the shape of a hollow truncated cone approximately 3-1/4 inches in diameter at the bottom, 2-1/4 inches in diameter at the top, and 7 inches in height. The thickness of the deposit varied along the height of the cone, the thickest portion being at the bottom, near the crucible. The thickness of the deposit at the bottom of the cone was a function of distillation time, and varied from 1/8 - 3/8 inches. The thickness at the top of the cone was usually less than 1/16 inch.

(2) Grain Size. Grain size also varied along the height of the cone, apparently being determined by the temperature of condensation. Accordingly, the largest grains, approximately 1/8 inch in diameter, were at the bottom of the cone. At the top of the cone, the grain diameter was less than 1/16 inch. All grains were fairly equiaxed, and there was no observed variation in grain size across the thickness of the deposit.

(3) Soundness. The deposits were coherent, but considerable micro-porosity was generally evident.

In view of the above characteristics, it was necessary to consolidate the distilled material, the object being to produce dense, reasonably fine grained material suitable for mechanical evaluation. Since the brittle behavior of beryllium is emphasized in sheet subjected to tri-axial stressing, consolidation procedures aimed at production of sheet specimens were employed. The following consolidation methods were attempted: (1) warm rolling and annealing; (2) hot up-setting, warm rolling and annealing; (3) vacuum melting, extrusion, warm rolling and annealing; (4) attritioning to powder and hot pressing. Vacuum melted Pechiney flake was employed as a control material for each of the above procedures. In addition to the above attempts to obtain fine grained material, an experiment was performed to obtain a single crystal of distilled beryllium for evaluation.

10-6.2 Fabrication and Mechanical Properties of Beryllium.

(1) Specimens Warm Rolled and Annealed. Initial fabrication experiments were performed on specimens from distillate No. 5, which had a maximum thickness of 1/8 inch. The degree of porosity appeared to be somewhat less than that characteristic of most other distillates.

One and one-half inch by 3/4 inch sections, taken from near the bottom of the cone, were sheathed in vacuum de-gassed mild steel and rolled at 760°C to a thickness of 0.050 inch, giving a reduction in thickness of 2.5:1. This temperature was expected to be sufficiently high to eliminate porosity, and sufficiently low to impart a small amount of cold work to the material. The specimens were then annealed for 2 hours at 750°C.

The as-rolled beryllium exhibited an extremely rough surface. This appeared to be caused by non-uniform deformation, certain grains undergoing extensive plastic flow while others remained essentially undeformed. Despite the high microscopic stresses this non-uniform deformation would be expected to produce, no cracking or rupturing of grain boundaries was observed. Figure 58 is a photomicrograph of the as-rolled structure, showing that deformation was sufficient to cause the formation of fairly fine grains (approximately 60 microns in diameter). Deformation of



B-405-2

Figure 58 - Longitudinal section of distillate No. 5 after rolling at 760°C through a 2.5:1 reduction (polarized light; 50X).

unfavorably oriented grains, however, was evidently insufficient for grain refinement, resulting in the mixed grain structure shown. Upon annealing, the fine grains produced by deformation were observed to grow to about 200 microns, as shown in Figure 59. The large grains remained unchanged.

The extreme surface roughness of the rolled beryllium prevented the machining of finished specimens for mechanical testing. Crude bend tests were performed, however. A specimen bent about an axis perpendicular to the rolling direction exhibited a radius of curvature at fracture of approximately 1/8 inch and a bend angle of 65°. This corresponds to a tensile strain in the outer fibers of approximately 20%. Vacuum melted Pechiney flake material of about twice the grain size of the distilled material, when fabricated and tested under similar conditions, exhibited zero fiber strain at fracture. Extruded and cross rolled QMV material of the same width: thickness ratio (15:1), would commonly exhibit⁽⁹⁾ a bend angle of approximately 10 to 25°.

Experiments similar to the above were performed on specimens from distillate No. 7, which has an initial maximum thickness of 3/8 inch. Although a greater amount of porosity was observed in this distillate than in distillate No. 5, the greater thickness afforded the opportunity to employ greater reductions during rolling so as to obtain finer grain sizes and still maintain sufficient thickness to permit finish machining. Rolling reductions up to 4:1 were performed at 760°C. The annealing procedures that were previously used were again followed.

Bend specimens 1-1/2 by 3/4 by .060 inches were machined from the rolled and annealed samples. After etching in 10% sulphuric acid to remove the cold worked layer, numerous voids and cracks were observed in the specimens. Unlike the specimens from distillation No. 5, bend tests on specimens from distillate No. 7 resulted in radii of curvature at fracture of at least 3/8 inch and bend angles of less than 25°. The corresponding tensile strain in the outer fibers at fracture was less than 7%.

(2) Specimens Hot Upset, Warm Rolled and Annealed. An additional experiment performed on specimens from distillate No. 7 was to hot upset the material at 1065°C prior to warm rolling. This was undertaken to eliminate porosity and to produce flat specimens for further working. Hot upsetting was performed on specimens jacketed in outgassed low carbon steel. Reductions in thickness were limited to 1.2:1, so that sufficient thickness would remain to allow further working at lower temperature.

After hot upsetting, rolling and annealing procedures similar to those described in the previous section were employed. Again, little or no ductility was observed in bend tests on sheet fabricated under these conditions.

(3) Specimens Vacuum Melted, Extruded, Warm Rolled and Annealed. In order to obtain void-free specimens of larger size for mechanical working experiments, material from several distillates was vacuum melted in a BeO crucible in the distillation apparatus and allowed to solidify in place. A 2-5/8 inch diameter by 2 inch long ingot was obtained.



B-405-1

Figure 59 - Longitudinal section of distillate No. 5 after rolling at 760°C through a 2.5:1 reduction and subsequently annealing for 2 hours at 750°C (polarized light; 50X).

The ingot was canned in an outgassed mild steel container which was then evacuated and sealed. The assembly was extruded into a flat at 1065°C and a reduction in area of 8:1. Pressure was recorded during the extrusion, permitting calculation of an extrusion constant for canned distilled beryllium. The value obtained was 35,500 psi. Although this figure can be regarded as only tentative, since only one measurement was made, it is interesting to note that corresponding values for the extrusion constant of steel-canned commercial beryllium generally run above 40,000 psi.

The steel can was pickled off, yielding a rectangular beryllium bar 12 by 1-5/8 by 1/2 inch. The bar was sectioned into square billets for further fabrication by bi-directional rolling. Specimens were rolled through a 3:1 reduction at temperatures of 705, 760, and 815°C and annealed 1 hour at 750°C.

Since the total reduction for this material was 24:1, a much more uniform grain size was obtained than for the warm rolled specimens described previously. The grain size of extruded and warm rolled material was approximately 50 microns. A few large elongated grains were also found.

Bend tests were performed on 0.050 inch thick as-extruded material and on extruded, rolled and annealed specimens. Width:thickness ratios of 10:1 to 20:1 were employed. As was the case with warm rolled specimens from distillate No. 7, no appreciable transverse ductility was observed in any of these specimens.

(4) Powder Preparation. Approximately 15 grams of powder were prepared by crushing distillate No. 9 in a beryllium mortar and pestle. The mortar and pestle were made from vacuum melted Pechiney beryllium, since it was found that a similar apparatus made from extruded QMV beryllium increased the iron content of powder made from distilled beryllium from less than 5 ppm to 14 ppm.

It was not found possible to classify the powders so produced either by sieving or by air elutriation without contamination. Sieving steel screens increased the iron content to 100 ppm. Air elutriation caused significant copper and zinc contamination from brass parts of the apparatus.

Because of the severe contamination produced by these experiments, no further work with powder material was performed.

(5) Single Crystal Experiment. A rod from the vacuum melted and extruded distillate, approximately 8-inches long by 1/4-inch diameter, was subjected to a single molten zone pass in a vertical floating zone refining apparatus at the Franklin Institute. At the start of the pass, the rod was joined to a single crystal seed having {0001} <1120> 45° to the rod axis, thus converting the polycrystalline rod to a single crystal favorably oriented for basal slip. The molten zone was traversed 1-1/2 inches per hour, a speed considered fast enough to prevent further purification with respect to all elements except silicon and aluminum.

A portion of the single crystal, including the first region to solidify, was machined into a tensile specimen using the spark discharge method commonly employed by Spangler and Herman,⁽⁴⁾ and was stressed in tension to fracture at room temperature. The critical resolved shear stress for basal slip was observed to be

approximately 900 psi. Since Pechiney beryllium subjected to a single molten zone pass has been observed to have a critical resolved shear stress of approximately 1100 psi, it appeared that distilled beryllium represents a somewhat higher level of purity. Approximately 65% glide strain took place prior to fracture, which occurred near the grip ends, thus indicating premature failure.

10-6.3 Evidence of Impurities in Distilled Beryllium. In an attempt to discover the reasons for the poor mechanical properties of beryllium fabricated from vacuum distilled material, a metallographic study was performed of the fracture surfaces of several specimens, both in the as-distilled condition and after fabrication. The specimens were fractured at 77°K in order to obtain as smooth a fracture as possible, and the fracture surfaces were examined metallographically at magnifications up to 1000X.

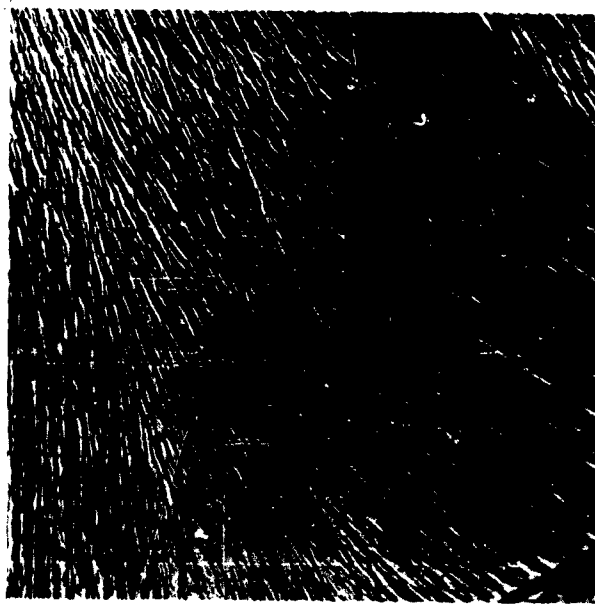
Spherical precipitate particles less than 2 microns in diameter were observed on all the fracture surfaces so examined. One distillate, No. 5, contained only a slight trace of precipitate, but all other materials examined, including distillates 6, 7, 8, 9, 15 and 16 and the extruded material, appeared to contain relatively increased amounts of the precipitate. Typical appearances of fracture surfaces are shown in Figures 60 and 61.

The small amount of precipitate observed in distillate No. 5 strongly suggests that the precipitate particles seriously affect the mechanical properties of distilled beryllium. As mentioned previously, fairly ductile behavior was exhibited by material fabricated from distillate No. 5, but specimens fabricated in an identical manner from distillate No. 7 exhibited little or no ductility. The amount of precipitate observed in distillate No. 7 was much greater than in distillate No. 5.

Further evidence of the harmful effect of impurity precipitation on ductility was obtained by examination of the fracture surfaces of beryllium single crystals purified by zone refining by Spangler and Herman.⁽⁴⁾ Essentially no evidence of precipitation was observed on the fracture surface of a crystal that had been purified by 8 molten zone passes and had shown considerable basal plane ductility. A small amount of precipitate was observed on the fracture surface of a crystal that had been subjected to only 2 passes and had exhibited very little ductility.

Attempts were made to identify the precipitate particles by means of X-ray diffraction and electron microbeam probe analysis. Debye-Scherrer patterns and diffractometer traces of the as-distilled material contained up to 4 extra lines which as yet have not been identified. It is certain, however, that they do not correspond to any of the compounds usually found in impure beryllium; i.e., BeO, Be₂C, Be₃N₂ or any of the intermetallic beryllides whose structure is known. Possible evidence of BeO peaks was contained in diffractometer traces of vacuum melted and extruded distillate.

Electron microbeam probe studies were performed at Advanced Metals Research Corporation on fracture surfaces of both as-deposited and vacuum melted and extruded distillate. These studies revealed that the precipitate particles contain silicon, iron and sulphur in the approximate proportions by weight of 3:3:1.



B-435

Figure 60 - Precipitate particles on fracture surface
of distillate No. 16 (bright light; 515X).



B-429a

Figure 61 - Precipitate particles on fracture surface of vacuum melted and extruded distillate (bright light; 500X).

Aluminum was found to be a constituent of a relatively small number of particles. In the particles containing aluminum, the aluminum concentration was roughly 10 - 20% of the silicon concentration. Occasional indications of a small amount of copper were also obtained. In addition, two particles were observed to contain zinc, with no indication of the above elements. These particles fluoresced strongly, indicating they were very probably zinc oxide. The only difference noted between as-distilled and fabricated material was that particles containing aluminum appeared to be more abundant in fabricated material, suggesting the possibility of aluminum pickup from the BeO crucible during melting.

In contrast to the observations on precipitate particles, no impurities were observed in the matrix of either specimen.

In order to test the possibility that the impurity phase precipitates during slow cooling from the distillation temperature, a specimen of distillate No. 16 was solution treated in vacuum at 1000°C for one hour, quenched in water, and then fractured. No change in the microstructure of the fracture surface was observed. Evidently the precipitate is still insoluble at 1000°C.

Although the above experiments have not resulted in a positive identification of the precipitate phase, they have indicated that it is probably a very complex compound containing iron and silicon.

10-7 SUMMARY

- (1) Vacuum distillation was employed to produce beryllium metal of high purity.
- (2) Distillation resulted in the reduction of iron, nickel and chromium to contents below 5 ppm, and of manganese and silicon to contents below 15 ppm.
- (3) Limited ductility was observed in distilled beryllium. Precipitate particles containing silicon, iron, sulfur and aluminum were observed on fracture surfaces. These particles appear to have an adverse effect on ductility.
- (4) The source of the precipitate particles has not been determined at this time.

ACKNOWLEDGEMENT

The authors wish to thank Mr. E. N. Pollock for developing the analytical techniques used to determine the purity of the beryllium.

REFERENCES

1. S. H. Gelles, J. J. Pickett and A. K. Wolff, "Recent Advances in Beryllium Metallurgy", J. of Metals, 12:789 (1960).
2. K. D. Sinelnikov, V. E. Ivanov, V. M. Amonenko and V. D. Burlakov, Refining Beryllium and Other Metals by Condensation on Heated Surfaces, A/Conf. 15/P/2051, Second United Nations International Conference on the Peaceful Uses of Atomic Energy, September, 1958.
3. R. I. Garber, I. A. Gindin and Yu V. Shubin, "Slip in Single Crystals of Beryllium at Low Temperatures", Part III, J. of Experimental and Theoretical Physics (Russian), 36:376 (1959).
4. G. E. Spangler and M. Herman, Preparation and Evaluation of High Purity Beryllium, Bi-Monthly Progress Report to Bureau of Naval Weapons, P-A2476-2, Franklin Institute, January 2 - March 1, 1961.
5. A. J. Martin, "The Purification of Beryllium by Distillation", Vacuum, 1957-58, 7 and 8, 38.
6. C. S. Pearsall, Effect of Oxygen on the Ductility of Beryllium Prepared by High-Vacuum Distillation, USAEC Report NMI-1104, Nuclear Metals, Inc., December 4, 1952.
7. V. M. Amonenko, L. N. Reabchickov, G. F. Tikhinskii and V. A. Finkel, "Mechanism of the Evaporation of Beryllium in High Vacuum", Doklady Akad. Nauk SSSR, 128:977 (1959).
8. E. W. Hooper and N. J. Keen, The Purification of Beryllium Metal by a Distillation Process, UKAEA Report AERE-R-3321, November, 1960.
9. J. Greenspan, G. A. Henrikson and A. R. Kaufmann, Beryllium Research and Development in the Area of Composite Materials, WADD Technical Report 60-32 (NMI-9410), Nuclear Metals, Inc., April 1960.

SECTION 11

AGING AND STRAIN AGING IN BERYLLIUM

A. K. Wolff, L. R. Aronin and S. H. Gelles

(Nuclear Metals, Inc., Concord, Massachusetts)

ABSTRACT

An investigation has been carried out to determine the effect of aging and strain aging in commercially pure beryllium and to relate the role of impurities to the observed changes in tensile properties.

Pronounced changes in ultimate tensile strength and ductility were obtained by aging of solution-treated beryllium rod between 200 and 800°C. No significant changes were obtained, however, in yield strength. A yield point, although absent in the as-solution-treated material, was observed after certain aging treatments at 400°C. The yield point appeared to be sensitive to minor variations introduced in processing, presumably differences in grain size.

X-ray diffractometer studies revealed that precipitation occurred during aging. It is concluded that the precipitation process, by removing a detrimental impurity or impurities from solid solution, results in the improvements observed in ductility and ultimate strength.

The impurity diffraction peaks correspond in location to an fcc structure having a lattice parameter of 6.07 Å, and indicate a preferred orientation of the precipitate with respect to the beryllium matrix.

Strain aging of beryllium was found to occur between 300 and 400°C. The activation energy for return of the yield point was determined to be 48,000 calories per gram-mole.

11-1 INTRODUCTION

11-1.1 Objective. This program was designed to study the quench-aging and strain-aging behavior of commercially pure polycrystalline beryllium extruded from powder. The objective was to obtain increased understanding of the mechanical behavior of beryllium by developing a systematic relationship between aging treatments and the resulting tensile properties and by attempting to identify the impurity elements responsible for the observed changes in tensile properties.

11-1.2 General Background.

(1) **The Brittleness Problem.** The principal deterrent to the widespread use of beryllium in structural applications has been its lack of ductility. The reason or reasons for this lack of ductility have not been fully explained. Yans, Donaldson and Kaufmann⁽¹⁾ have shown, however, that dilute solutions of some of the transition elements, particularly iron, have a detrimental effect on the ductility of beryllium. Gelles, Pickett and Wolff⁽²⁾ showed for extruded material that was solution treated and quenched that aging for increasing times at 600°C produced marked improvements in ultimate strength and ductility relative to as-solution treated metal. These changes in properties were not associated with either changes in texture or microstructure due to recrystallization or grain growth. Mash⁽³⁾ has also pointed out that the strength and ductility of beryllium undergo marked changes during aging heat treatments.

(2) **Precipitation During Aging.** Gelles et al.⁽²⁾ observed considerable decreases in resistivity with increasing aging times between 400 and 800°C, indicating precipitation occurred during heat treatment. X-ray diffraction studies confirmed the presence of unidentified impurity peaks and the growth of a representative impurity peak with increased aging. An excellent qualitative correlation was obtained between decreasing resistivity and increasing amount of precipitate. Pointu et al.⁽⁴⁾ reported for commercial beryllium the presence of X-ray lines which appear to be characteristic of an MBe₅ structure having a lattice constant of 6.07 Å. In a recent study, Moore⁽⁵⁾ confirmed the occurrence of a fcc precipitate developed by an aging treatment and having a lattice constant of 6.07 Å. Brown et al.⁽¹¹⁾ have proposed that improvements in high temperature ductility after specific aging treatments are due to either precipitation at the grain boundaries or the redistribution of impurity elements(s) to the grain boundary. Sawkill, Meredith and Parsons,⁽⁶⁾ employing special etching techniques, were able to observe the growth and distribution of particles precipitated during aging. Iron-rich particles as identified by an electron microbeam probe were found to form during aging.^(2,6)

(3) **Presence of a Yield Point.** Mash⁽³⁾ has reported the presence of a yield point at room temperature in commercially pure beryllium after certain heat treatments. Gelles et al.⁽²⁾ also observed that a yield point absent in as-quenched material was present after certain aging treatments for a sample tensile tested at room temperature.

11-2 EXPERIMENTAL PROCEDURE AND RESULTS

11-2.1 Materials. In order to ensure consistent chemical composition, a single lot of Brush -200 mesh QMV beryllium powder was employed for all studies. The analysis of this material is presented in Table 16.

11-2.2 Fabrication Techniques. Billets of beryllium weighing approximately 2-3/4 pounds each were cold compacted from powder under a pressure of approximately 42 tsi. The resulting cylinders were 2.760 inches in diameter and approximately 75 percent of theoretical density. All compacting was performed in mild steel cans. The cans were subsequently evacuated to 10^{-4} mm Hg and sealed off preparatory to extrusion. The billets were heated to 1950°F (1066°C), then extruded in a 1000-ton extrusion press at a reduction in area of 30:1. The die diameter was 0.550 inch. The resulting rods were approximately 200 inches long.

11-2.3 Preparation of Sample Blanks. The rods were pickled in nitric acid to remove the mild steel cladding. They were then cut into 3-1/2 inch-long sections, yielding approximately 50 tensile blanks per rod. Each sample was given a light etch in a dilute sulfuric acid solution and identified according to its prior location in the extruded rod.

11-2.4 Quench-Aging Studies.

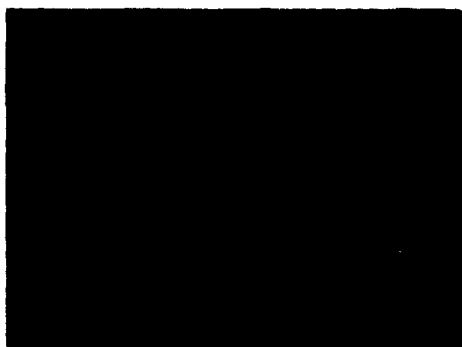
(1) Solution Treatment. Gelles et al.⁽²⁾ demonstrated that solutionizing in beryllium occurred at temperatures above 1000°C. To obtain solution-treated specimens, they employed a treatment of 1100°C for one hour. The only concern about this treatment for the current program was that it might result in excessive grain size. Accordingly, a study was made to determine the extent to which grain growth occurs.

Four discs approximately 1/4 inch thick were cut from the central area (with respect to length) of one rod. Two of the discs were etched in dilute sulfuric acid and sealed in quartz tubing which was evacuated to a pressure of 10^{-5} mm Hg. They were then heat treated in a platinum-wound furnace at 1100°C for a total time of one hour. Following this treatment the quartz tubing was broken and the specimens were water quenched. The heat-treated samples, along with those that had been left in the as-extruded state, were prepared for metallographic observation of the grain size both transverse and parallel to the extrusion direction. The solution-treated samples displayed severe grain growth to a depth of 0.005 inch from all surfaces, but little grain growth occurred at greater depths (Figure 62). Since the metal near the surface was to be removed in subsequent machining of tensile samples, the solution treatment was considered satisfactory for the purposes of the program.

The tensile blanks, in lots of four, were sealed in quartz tubing for heat treatment. One-sixth atmosphere of argon was introduced into the evacuated tubes before they were sealed to prevent their collapse during heat treatment. Each tube contained samples from divergent positions along the length of a given rod or from similar positions in different rods. In this way any variations in microstructure which were introduced during the fabrication processes and which might affect the reproducibility of subsequent tests could be studied. The samples were

Table 16 ANALYSIS OF BRUSH BERYLLIUM COMPANY
 -200 MESH QMV BERYLLIUM POWDER
 (Lot No. V-5051)

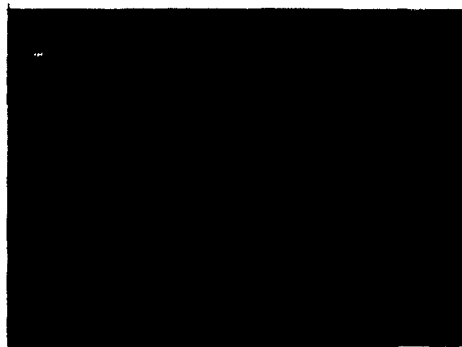
Constituent	Amount Present (w/o)
Be (assay)	99.0
BeO	1.01
Al	0.060
Ag	0.0002
B	0.00007
Cd	<0.00001
Ca	<0.010
C	0.10
Cr	0.05
Co	0.0001
Cu	0.007
Fe	0.073
Pb	<0.002
Li	0.0001
Mg	0.020
Mn	0.007
Mo	<0.002
Ni	0.013
N	0.017
Si	0.030
Zn	<0.010



150X - Pd. Lt.

B380-4T

(a) As extruded.



150X - Pd. Lt.

B380-1T

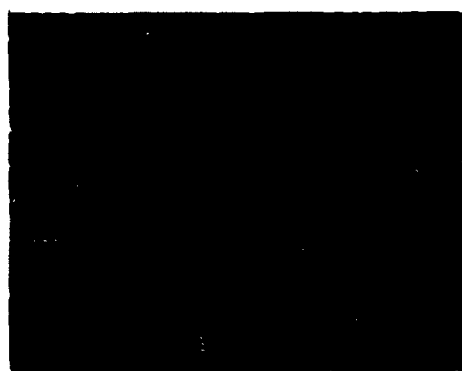
(b) After solution treatment-
surface of rod.



150X - Pd. Lt.

B380-2T

(c) After solution treatment-
approximately 0.005-inch
removed from surface.



150X - Pd. Lt.

B380-1Tb

(d) After solution treatment-
approximately 0.010-inch
removed from surface.

Figure 62 - Effect of solution treatment at 1100°C for 1 hour on grain size of hot-extruded beryllium (all photos transverse to extrusion direction).

heat treated in a platinum-wound furnace at $1100 \pm 5^{\circ}\text{C}$ for one hour and, in most cases, water quenched. Other samples were air cooled and still others were furnace cooled from the solution-treating temperature. The samples that were quenched were resealed in evacuated quartz tubing and aged at various temperatures and for various times.

(2) Aging Treatment. The solution-treated-and-quenched tensile blanks were given a light etch in dilute sulfuric acid to remove possible surface contamination and were resealed in lots of four in evacuated quartz tubing under one-sixth atmosphere argon. They were then aged at various temperatures from 200 to 800°C and for times from 15 minutes to 8 days. All aging treatments were carried out in a Nichrome-wound furnace controlled to a maximum temperature variation of $\pm 3^{\circ}\text{C}$. These treatments were followed by a water quench. No grain growth was noted after any of the aging treatments.

(3) Preparation of Tensile Samples. All blanks were machined into cylindrical tensile samples having a 1-inch gauge length and 0.200-inch gauge diameter. The design of the machined tensile samples is shown in Figure 63. Very light finishing cuts on the order of 0.0005-inch per pass were employed to minimize surface damage, and the small remaining surface damage was removed by etching about 0.005 inch off the sample diameter with dilute sulfuric acid. The final gauge diameter was approximately 0.195 inch.

(4) Tensile Testing Facilities. All tensile tests were made at room temperature on a Tinius-Olsen Electromatic universal testing machine having a 60,000-pound capacity and attachments for maintaining a constant strain rate and for automatic recording of the stress-strain curve. A Tinius-Olsen S-3 extensometer was employed to record the early portion of the stress-strain curve, but was usually disconnected prior to fracture of the specimen in order to protect the extensometer. The balance of the stress-strain curve was determined by means of a dial gauge mounted between the tensile sample grips. A special subpress, which was designed at Nuclear Metals, was used to ensure accurate alignment of the tensile sample, since the ductility of beryllium is very sensitive to the introduction of any biaxial strains. The elastic region and initial portions of the plastic region were obtained at a strain rate of 0.0025 min^{-1} . At approximately 60,000 psi, the strain rate was increased to 0.01 min^{-1} and maintained until fracture.

(5) Effect on Tensile Properties of Cooling Rate From the Solutionizing Temperature. In order to determine the effect of cooling rate on the tensile properties of solution-treated extruded beryllium, tensile tests were made on these samples in the furnace-cooled, air-cooled, and water-quenched conditions. The ultimate tensile strengths and elongations for solutionized material with each cooling rate and for as-extruded material are shown in Figures 64 and 64. The as-extruded material shows the highest strength, while the solution-treated materials invariably exhibit lower strengths, the values decreasing with increasing cooling rate. The percent elongation (Figure 65) decreases as the ultimate strength decreases, ranging from approximately 17 percent for as-extruded samples to about 3 percent for water-quenched samples.

(6) Effect of Solution Treatment on Texture. In order to determine whether the decreases in tensile properties observed after solution treatment of the extruded rod were associated with changes in texture, Norton rod analyses were

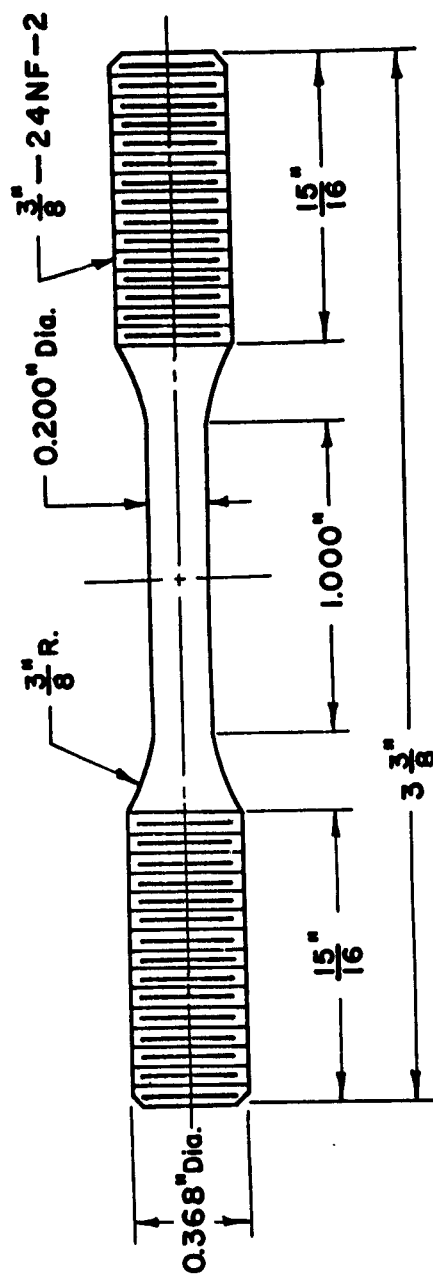


Figure 63 - Design of cylindrical sample employed in tensile testing of beryllium rod.
(As machined) (Drawing No. RA-185)

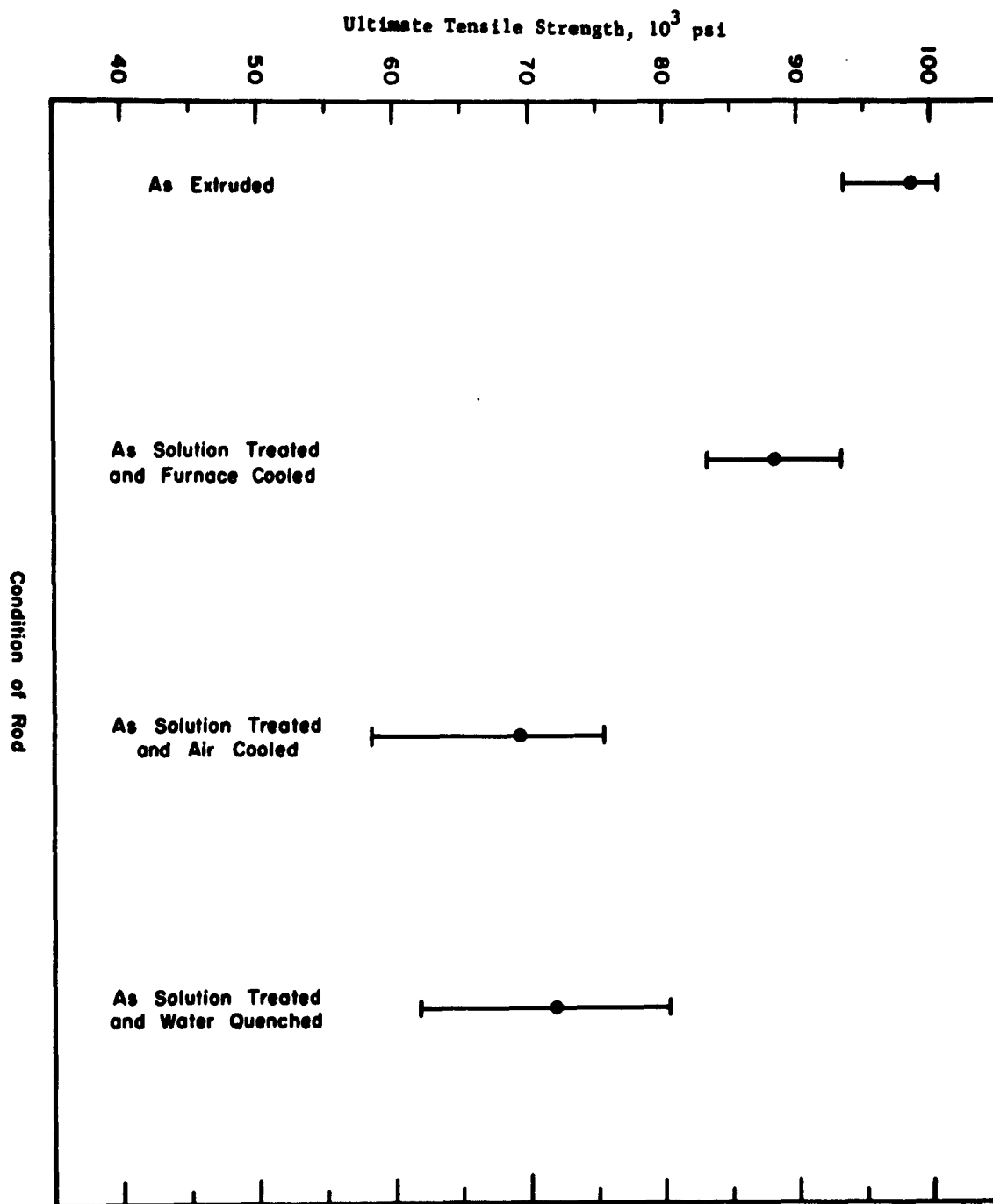


Figure 64 - Effect of various cooling rates from the solutionizing temperature on ultimate tensile strength of polycrystalline beryllium rod. (Solution treatment: 1100°C; 1 hr) (Drawing No. RA-2205)

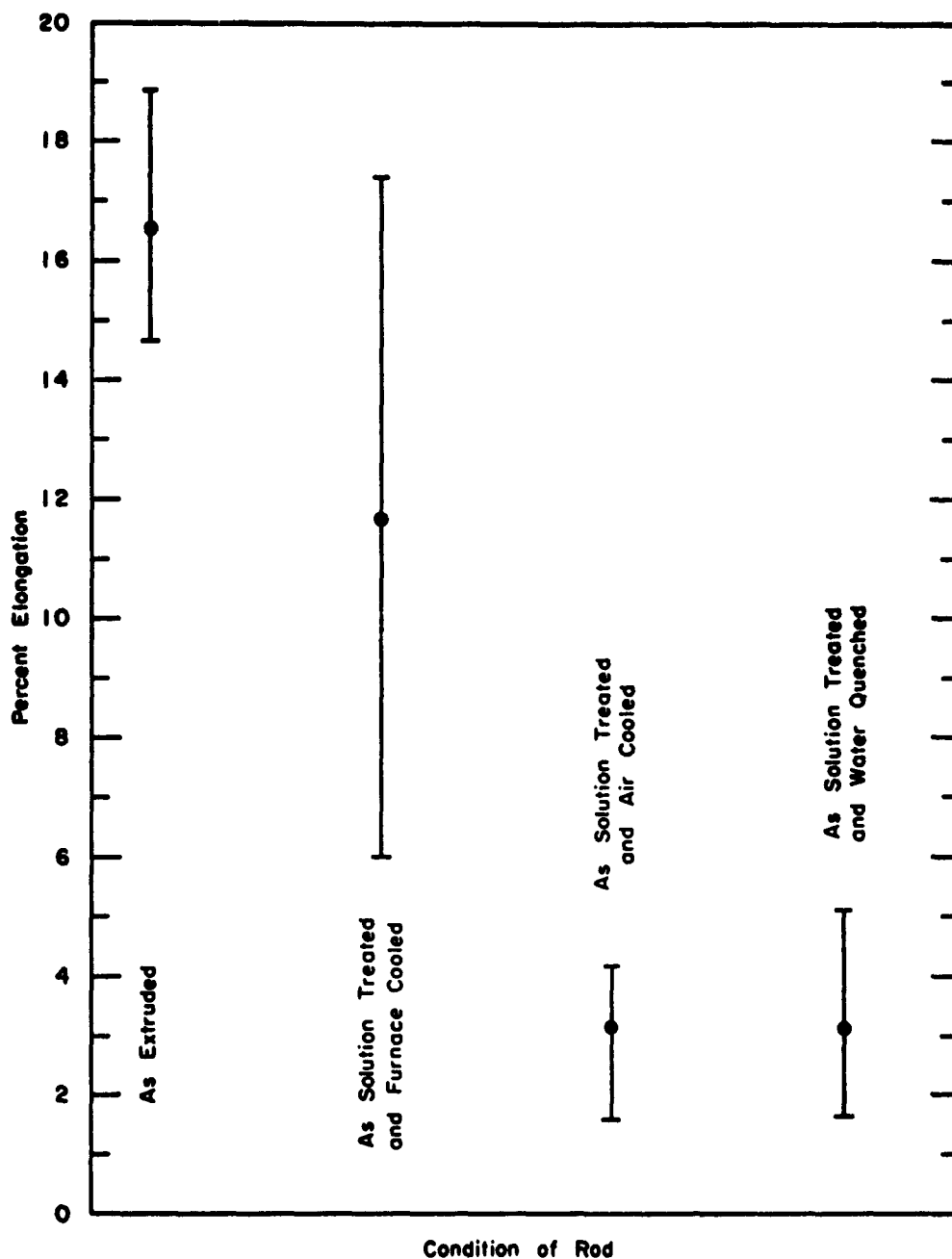


Figure 65 - Effect of various cooling rates from the solutionizing temperature on the percent elongation of polycrystalline beryllium rod. (Solution treatment: 1100°C; 1 hr) (Drawing No. RA-2338)

made for samples in the solution-treated-and-quenched state and in the as-extruded state. The Norton rod is a small cylindrical sample cut in such a way that its axis coincides with a diameter of the original rod. A rotation of the Norton rod around its own axis in an X-ray spectrometer is sufficient to completely determine the orientation of a given plane (since in an extruded rod it may be assumed that there is complete symmetry about the extrusion axis). In this case, a study of the basal (0002) and prism pole {1010} distributions was carried out using a Norelco diffractometer with filtered $\text{CuK}\alpha$ radiation. Results of this study indicate that the solution treatment does not affect the texture. In both as-extruded and solution-treated samples, the basal planes lay parallel to the extrusion axis with the $\langle 1010 \rangle$ crystallographic direction parallel to the extrusion direction.

(7) Investigation of Fracture Surfaces. The fractures observed during testing of the samples were invariably of the brittle type. The failure could be traced in every case by means of "river" markings on the fracture surface leading to a single point of origin. These points of origin appeared to be randomly located with respect to the cross section and, in some instances, appeared to occur at or near the surface. A large majority were subsurface, however, indicating that the specimen preparation was adequate to eliminate detrimental surface damage. In most cases, the failure propagated in more than one plane, sometimes resulting in fracture into three sections instead of the usual two. Some typical fractures are shown in Figure 66. The directions of propagation are symmetrical around a plane perpendicular to the tensile axis and make a constant angle with this plane. Careful measurement of these angles confirmed this observation. Wherever the configuration of the fracture surface permitted measurement, the angle was found to be $20 \pm 2^\circ$. This angle of fracture may be explained in terms of fracture along {11 $\bar{2}$ 0} planes. Previous investigators⁽⁷⁾ have found that the $\langle 1010 \rangle$ fiber texture associated with extruded beryllium rod has a spread of approximately 15° around the extrusion direction. This would result in the {11 $\bar{2}$ 0} planes lying at an angle of $30 \pm 8^\circ$ to the transverse plane. Those planes oriented at the smallest angle to the transverse plane would have the highest resolved tensile stress acting upon them and would thus be expected to fracture before those oriented at larger angles. Therefore, the predicted angle of failure of approximately 22° to the transverse plane agrees very well with the observed angles.

(8) Effect of Aging on Tensile Properties. The parameters investigated to determine the effect of aging treatment on room-temperature tensile properties were ultimate tensile strength, 0.2 percent offset yield strength, percent elongation and modulus of elasticity. The data obtained are summarized in Table 17, which presents the average values obtained for each of these parameters (a minimum of four samples were tested under each condition). The values obtained for individual samples are tabulated in Appendix 11-A.

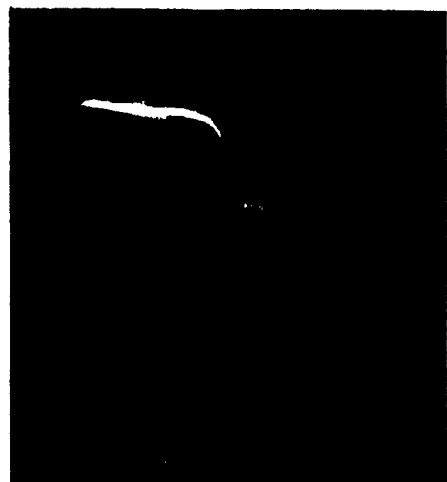
The ultimate strengths are plotted as a function of aging time for various temperatures in Figure 67. In general, the ultimate tensile strength initially decreases from the strength (about 70,000 psi) of the solution-treated-and-quenched material. With increasing aging time, this value goes through a minimum at approximately 60,000 psi and then begins to rise, approaching a maximum value on the order of 95,000 psi. These stages occur at successively shorter times with increasing aging temperature. It should be noted that the initial drop in strength shown for samples aged at 700 and 800°C is not based on actual data points (the minimum aging time was 0.25 hour), but rather on a logical extrapolation of data obtained for



2.5X

RF-8352

Two-piece fracture, originating at or near surface.



2.5X

RF-8349

Two-piece fracture, originating below the surface.



2.5X

RF-8350

Three-piece fracture, originating at or near surface.



2.5X

RF-8351

Three-piece fracture, originating subsurface. Middle section tilted to show concave surface and hole at point of origin.

Figure 66 - Typical fractures of aged beryllium rod showing characteristic angle of fracture propagation ($\sim 70^\circ$ to tensile direction).

Table 17. ROOM TEMPERATURE TENSILE PROPERTIES AS A FUNCTION OF AGING TREATMENT
FOR BERYLLIUM ROD EXTRUDED FROM BRUSH QMW POWDER

Heat Treatment*	Yield Strength, 0.2% Offset (10 ³ psi)			Ultimate Tensile Strength (10 ³ psi)			Percent Elongation			Modulus of Elasticity (10 ⁶ psi)			Curve Type and Number of Samples**
	High	Avg	Low	High	Avg	Low	High	Avg	Low	High	Avg	Low	
As Extruded	50	49	46	100	99	94	19	17	15	43	40	37	c(3), a(1)
Furnace cooled	46	44	43	93	88	83	17	12	6	49	40	35	a(2), b(2)
Air cooled	42	41	40	75	69	58	4	3	2	40	38	36	a(3), b(1)
As quenched	47	44	42	80	72	62	5	3	2	41	37	34	a(5), b(7)
200°C, 24 hrs	45	44	44	71	69	66	3	3	2	41	36	33	a(4)
200°C, 1 week	51	50	48	74	70	61	3	2	1	45	40	38	a(4)
300°C, 24 hrs	47	45	42	72	70	66	3	3	2	40	38	36	a(1), c(3)
300°C, 1 week	52	48	45	70	66	60	2	2	1	51	43	36	a(4)
400°C, 15 min	46	45	43	67	64	59	2	2	1	42	38	36	b(4)
400°C, 2 hrs	47	46	44	73	64	53	4	2	1	40	40	40	c(4)
400°C, 7 hrs	48	45	41	86	70	56	6	3	1	47	42	34	a(4), b(2), d(2)
400°C, 16 hrs	47	46	43	76	66	57	4	2	1	45	42	40	b(1), c(1), d(2)
400°C, 24 hrs	47	46	44	72	62	48	3	2	0	45	42	40	a(4), b(7), d(1)
400°C, 30 hrs	46	44	43	69	60	50	3	2	1	45	44	42	b(2), d(2)
400°C, 42 hrs	45	44	43	65	56	44	2	1	0	44	43	41	b(4)
400°C, 60 hrs	48	47	45	70	66	60	2	2	1	51	43	36	b(1), c(2), d(1)
400°C, 1 week	45	45	44	71	62	55	3	2	1	41	38	35	a(4)
400°C, 8 days	44	43	42	67	52	48	3	1	0	46	43	40	a(4)
500°C, 15 min	48	47	46	67	62	56	2	2	1	43	39	35	a(4)
500°C, 2 hrs	48	47	45	73	63	54	3	2	1	45	41	38	a(4)
500°C, 24 hrs	48	45	43	70	64	51	3	2	1	42	37	33	a(4)
500°C, 1 week	49	47	45	87	82	79	8	6	4	43	40	38	a(4)

Table 17. (Continued)

Heat Treatment*	Yield Strength, 0.2% Offset (10 ³ psi)			Ultimate Tensile Strength (10 ³ psi)			Percent Elongation			Modulus of Elasticity (10 ⁶ psi)			Curve Type and Number of Samples**
	High	Avg	Low	High	Avg	Low	High	Avg	Low	High	Avg	Low	
600°C, 15 min	44	43	42	74	64	58	3	2	1	38	37	36	a(4)
600°C, 2 hrs	47	46	45	75	71	64	4	3	2	40	38	35	a(4)
600°C, 24 hrs	49	48	47	92	80	63	4	3	2	40	38	35	a(4)
600°C, 1 week	44	44	43	94	86	79	18	10	5	40	39	37	a(4)
700°C, 15 min	46	44	43	76	67	57	4	2	1	44	39	36	a(4)
700°C, 2 hrs	47	46	46	85	81	79	6	5	4	38	37	35	a(4)
700°C, 24 hrs	46	45	45	92	82	74	16	8	4	45	38	32	a(4)
700°C, 1 week	49	48	48	96	95	92	17	14	9	40	37	33	a(4)
800°C, 15 min	46	43	42	76	70	57	4	3	1	45	40	37	a(3), d(1)
800°C, 2 hrs	44	44	43	86	80	75	9	6	4	45	40	36	a(4)
800°C, 24 hrs	46	45	45	92	91	90	16	14	12	45	38	35	a(4)
800°C, 1 week	49	47	44	96	94	90	17	14	8	37	36	35	a(4)

* All specimens, except those that were as extruded, were given a solution treatment at 1100°C for 1 hr preceding the treatments listed. Except where furnace or air cooling is noted, the solution treatment was concluded with a water quench.

** Letters correspond to curve designations in Figure 70. Numbers in parentheses indicate number of samples in group showing designated curve type.

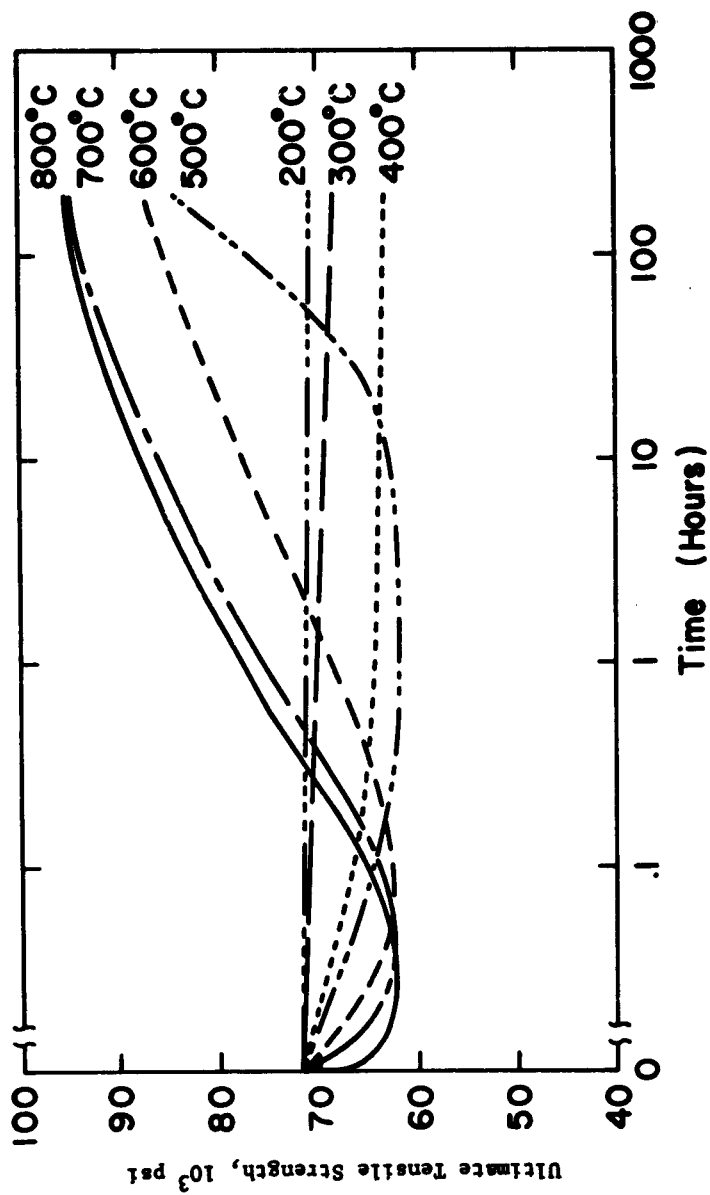


Figure 67 - Ultimate tensile strength vs aging time for solution-treated beryllium rod aged at various temperatures.
(Drawing No. RB-1092)

lower temperatures. The maximum value of 95,000 psi is somewhat lower than the ultimate tensile strength of the as-extruded rod (100,000 psi), probably because the grain size increases slightly during the solution treatment.

Percent elongation increases with increasing ultimate tensile strength, varying from about one percent for samples aged at 400°C for eight days to about 14-1/2 percent for samples aged at 700 and 800°C for one week.

No appreciable changes in yield stress with aging treatment were observed during the course of testing, with values ranging from 42,000 to 50,000 psi.

The results obtained for the modulus of elasticity showed considerable scatter and did not appear to be affected by aging treatment.

(9) Observations on the Aging Mechanism. It is apparent on the basis of these studies that aging of solution-treated beryllium results in pronounced improvements in both ultimate tensile strength and percent elongation. However, in view of the fact that no significant changes in yield strength were observed, it appears that the mechanism involved is not one of dispersion-hardening. Rather, the higher strengths and ductilities appear to be associated with the removal of a premature failure mechanism (possibly by the precipitation of a detrimental impurity from solution and the resulting purification of the matrix.*) When all the ultimate tensile strength-percent elongation data are plotted as in Figure 68, the points fall within narrow limits on a single "master" tensile curve, which shows that the plastic properties of the material which determine the shape of the tensile curve are not significantly altered by aging treatment. However, aging does affect the position on the master curve at which failure occurs.

Still another fact which tends to support the theory of a premature failure mechanism is that the scatter in the data points generally decreases with increasing strength and ductility. This is shown in Figure 69, where ultimate tensile strength is shown as a function of aging time at 800°C. It can be seen that the scatter band is considerably decreased for increased strengths. This direct relationship between strength and reproducibility was generally observed throughout the entire aging schedule and is presumed to be due to the statistical nature of the premature failure mechanism.

(10) Effect of Aging on Yield Point Phenomena. During tensile testing, yield points were observed after certain of the aging treatments. The effect of aging treatment on the occurrence of a yield point is summarized in the final column of Table 17. The letter in this column refers to the corresponding curve

- - - - -

* It is difficult to explain, in terms of this mechanism, why both the ductility and ultimate strength are highest in the as-extruded material. Limited X-ray analysis has indicated that precipitation is not as extensive as tensile properties would imply. It may be that the dispersion or orientation of the precipitate induced during extrusion is different from that occurring during subsequent solution treatment, thereby complicating diffractometer studies. The state of precipitation existing in the as-extruded material should be given further, more extensive investigation.

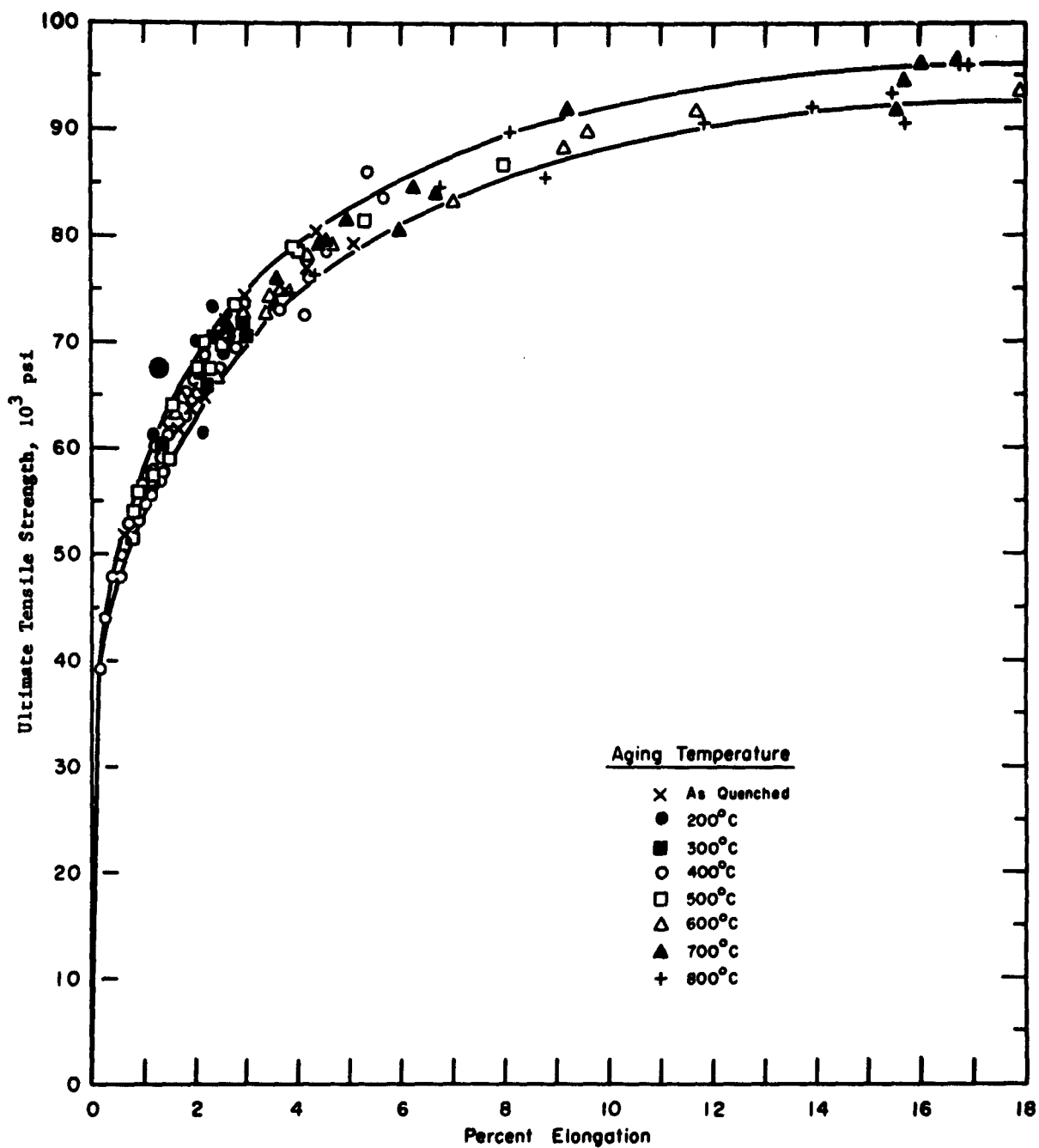


Figure 68 - Ultimate tensile strength vs percent elongation for solution treated beryllium rod after various aging treatments.
(Drawing No. RA-2210)

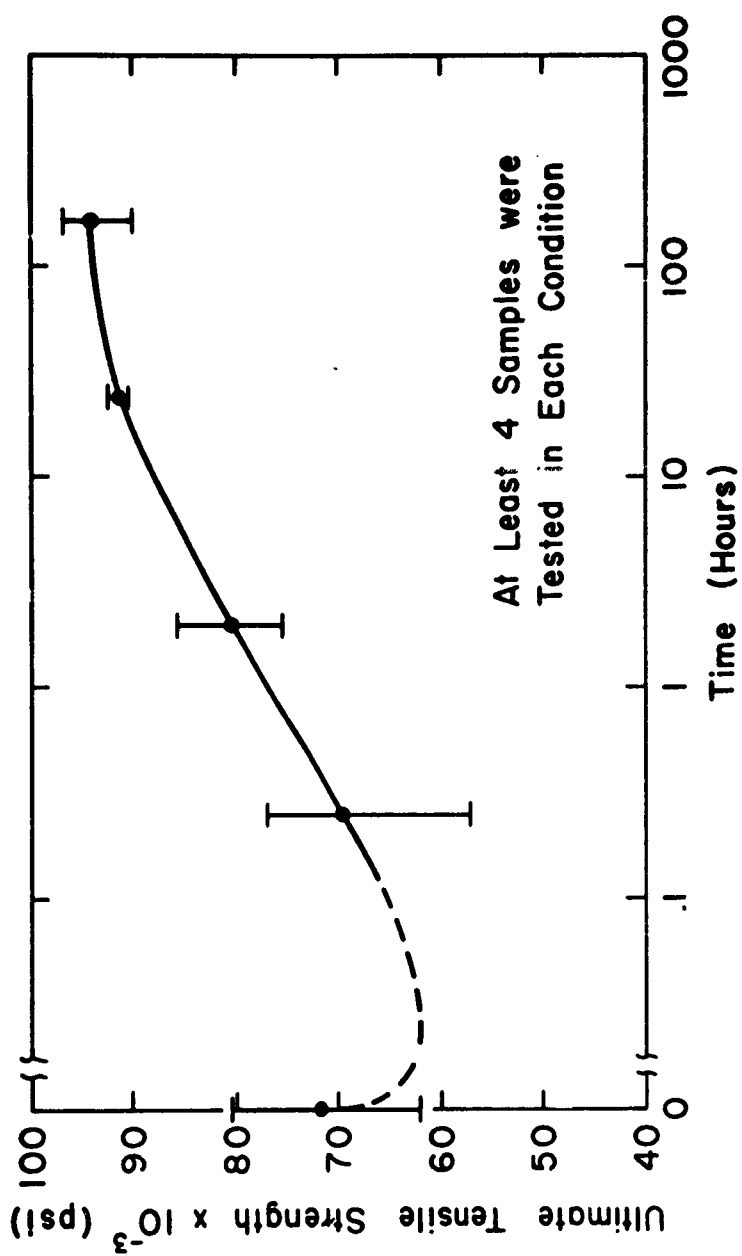


Figure 69 - Ultimate tensile strength vs aging time for solution-treated beryllium rod aged at 800°C, with vertical lines showing the scatter in the data. (Drawing No. RB-1091)

in Figure 70, wherein are shown the various types of tensile curves encountered. It may be seen from Table 17 that yield points for the aged specimens generally occurred only after aging at 400°C. A region of easy glide was observed during tensile testing of the as-extruded material. No yield points were observed in any of the as-solution-treated materials, although some inflections occurred.

Even within a single heat-treatment lot aged at 400°C, the occurrence of a yield point was not consistent. A careful check of sample sources indicated that of the three rods comprising the bulk of the material for the aging studies; samples from two of the rods almost invariably showed a yield point response after aging at 400°C, while samples from the third rod never exhibited a yield point. Since the Cottrell mechanism for occurrence of the yield point⁽⁸⁾ proposes the interaction of mobile impurity elements with dislocations, it was felt that compositional differences might be the cause of the variations in yield phenomena. An extensive study was therefore made using spectrographic and chemical analyses to determine the impurity content of the various rods, but no correlation could be obtained between impurity content and yield point response. (For a complete tabulation of chemical and spectrographic results, see Appendix 11-B.) A metallographic study of the three rods revealed, however, that the grain size of the rod exhibiting no yield points (designated rod "C") was somewhat larger than that of the remaining two rods (rods "A" and "D"), as may be seen in Figure 71. It has been shown⁽⁹⁾ for some materials that the grain size is significant in determining the degree of yield response, and that a critical upper limit exists beyond which no yield point occurs. The fact that as-extruded material exhibited a yield point, whereas solution-treated-and-aged samples of comparable strength did not, may also be related to the finer grain size of the as-extruded stock. A detailed study of the yield point response as a function of grain size would, however, be necessary for verification.

11-2.5 X-Ray Diffraction Studies.

(1) Precipitate Growth. Gelles and Wolff⁽¹⁰⁾, using X-ray diffractometer scans on various aged samples, showed that precipitation occurred during aging of extruded and solution treated beryllium, and that the growth of the precipitate could be qualitatively studied by the growth of a representative impurity peak. In order to establish whether the same phenomenon occurred during aging in the present program, and to learn more about the characteristics of the precipitate, a similar study was performed on samples in various aged conditions. Scans made on a Norelco diffractometer for planes parallel to the extrusion direction revealed the growth of an impurity peak identical to that noted in the previous work. ($2\theta = 25.4^\circ$ for $\text{CuK}\alpha$ radiation). Diffractometer scans were also made for planes perpendicular to the extrusion direction. These scans showed the growth, during aging, of an extremely strong impurity peak at approximately 42.2° , 2θ . The two peaks paralleled one another in occurrence and growth, indicating that they represent different lines of the same phase and that this phase has a marked preferred orientation with respect to the extruded rod and the beryllium matrix.

(2) Identification of the Precipitate.

Diffractometer Studies. In an effort to locate additional peaks of the oriented precipitate, diffractometer scans were made on planes lying at various angles to the extrusion axis. Norton rods (Section 11-2.4(6)) were

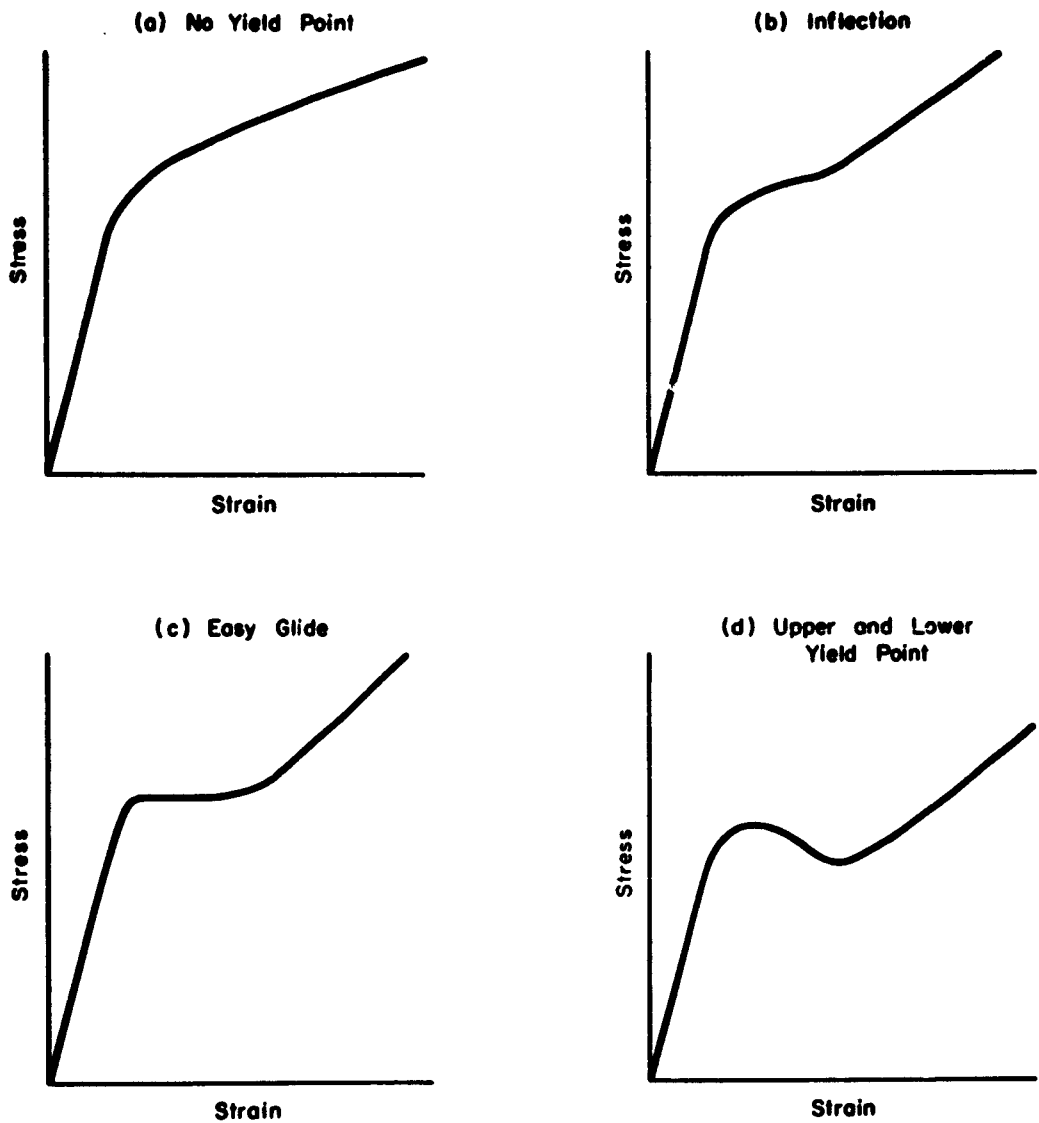
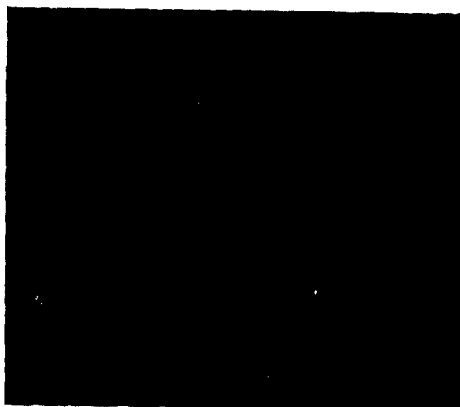


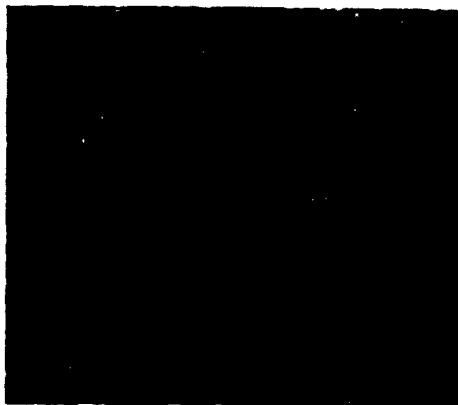
Figure 70 - Typical tensile curve shapes obtained after aging of solution treated and quenched beryllium rod. (Drawing No. RA-2209)



Sharp upper and lower yield point.
Rod A.

150X

B407-5



Sharp upper and lower yield point.
Rod D.

150X

B407-4



No yield point observed.
Rod C.

150X

B407-3

Figure 71 - Variation in grain size among three beryllium rods extruded at 1050°C and a 30:1 reduction and subsequently aged at 400°C for 7 hours. (All photos transverse to extrusion direction.)

employed for this purpose. Diffractometer scans were made between 20° and 120° , 2θ for planes lying at 10° intervals with respect to the extrusion direction. In addition, scans were made for planes lying at 45° to the extrusion direction. A sample in the solution-treated-and-quenched state and a sample that had been similarly treated and aged at 600°C for one week were used for this analysis. Several additional impurity peaks were observed, as summarized in Table 18. The impurity peaks correspond to a precipitate having an fcc structure with a lattice spacing of 6.07 \AA , which is in agreement with the findings of Pointu⁽⁴⁾ and Moore⁽⁵⁾. The characteristic 2θ angles for this structure are given in Table 11-3. It should be noted that some of the traces predicted for this structure were not observed during the present study. However, this is to be expected in view of the highly oriented nature of the precipitate and the fact that only 10° intervals were investigated. Also, since the observed impurity diffraction peaks were of low intensity, it is probable that some of the inherently weaker reflections for this structure cannot be detected by the technique used.

In an attempt to detect other diffraction peaks, the Norton rod was rotated rapidly (60 rpm) while being scanned slowly ($1/2^\circ/\text{min}$). This allows diffraction from crystallographic planes oriented at a wide range of angles to the extrusion direction. A 2θ scan might therefore be expected to show all reflections. However, intensities were so greatly reduced by this procedure that no impurity peaks could be observed.

Debye-Scherrer Studies. In a further attempt to detect other precipitate lines, Debye-Scherrer powder patterns were prepared from several beryllium tensile samples having various aging treatments. The impurity traces observed by this technique were extremely faint and inconclusive. No significant differences could be observed between traces obtained for samples in the solution-treated-and-quenched state and samples aged at 800°C for one week.

(3) Texture of the Precipitate. The preferred orientation of the precipitate was determined by rotation of the Norton rod with the diffractometer at specific 2θ angles associated with the observed impurity peaks. The basal and prism pole distributions of the beryllium were also obtained for the aged specimens. A comparison of these results shows that the texture is consistent with the $\{110\}$ planes of the precipitate (based on the assumption of an fcc structure, $a_0 = 6.07 \text{ \AA}$) lying parallel to the $\{10\bar{1}0\}$ planes of the beryllium and the $\{111\}$ planes of the precipitate parallel to the (0002) planes of the beryllium. This agrees with the orientation relation based on single crystal rotation patterns obtained by Pointu et al.⁽⁴⁾

11-2.6 Strain-Aging Studies. Strain-aging studies were conducted to determine the kinetics of the yield point return and to define the impurity or impurities causing the yield point in beryllium.*

- - - - -

* Strain-aging is interpreted by Cottrell⁽⁸⁾ as the migration of impurity atoms to free dislocations during aging, the dislocations having been broken away from solute atmospheres by prior straining.

Table 18. POSITION AND ORIENTATION RELATION
OF OBSERVED PEAKS OCCURRING DURING AGING

Predicted Reflections for fcc Structure, $a_0 = 6.07 \text{ \AA}$		Observed Impurity Peaks		
(hkl)	2 θ Angle($^\circ$)	2 θ Angle ($^\circ$)	Orientation ($^\circ$)*	Relative Intensity**
111	25.4	25.4	90	Strong
111	25.4	25.4	32	Medium
002	29.4	29.0	0	Medium
022	42.2	42.2	0	Very strong
022	42.2	42.2	60	Medium
113	50.1			
222	52.5			
004	61.3	61.8	45	Weak
133	67.3			
420	69.0			
422	76.7	77.4	45	Weak
333	82.2			
440	92.1	92.3	0	Medium
513	99.0			

* Given as α , the angle between the pole of the diffracting plane and the extrusion direction.

** Relative to strongest peak ($2\theta = 42.2$, $\alpha = 0^\circ$).

(1) Initial Heat Treatment. Pronounced and reproducible yield points for strain-aging studies were obtained by heat treatment of as-extruded tensile blanks at 400°C for 24 hours followed by a water quench. The heat-treated blanks were then machined into tensile samples and etched in sulfuric acid to remove surface damage. The techniques employed for the 24-hour aging treatment and the preparation of tensile samples were identical to those employed in the quench-aging portion of this program (Section 11-2.4(2) and (3)).

(2) Strain-Aging Cycles. Figure 72 shows a typical strain-aging cycle. All straining was carried out with the same tensile subpress and testing machine used for the quench-aging portion of this program (Section 11-2.4(4)). All tensile data were automatically recorded with a Tinius-Olsen S-3 extensometer. The samples were strained at a rate of 0.025 min⁻¹, which was experimentally determined to be rapid enough to effect a sharp yield point yet slow enough to control the degree of strain applied. The samples were strained to 1/2 percent total elongation and the load removed. An upper and lower yield point and subsequent strain hardening were invariably observed over this interval. The samples were immediately reloaded to an additional 0.2 percent plastic elongation and the load removed. In all cases, upon reloading, the yield point was absent and the plastic portion of the curve followed along an extrapolation of the original tensile curve.

The strained samples were then sealed in evacuated Vycor tubing and given various aging treatments at temperatures between 300 and 400°C for times ranging from 10 minutes to 72 hours. All treatments were concluded with a water quench. The samples were then lightly etched in sulfuric acid to remove any possible surface contamination introduced during heat treatment. The samples were again strained as before to one-half percent elongation to determine which of the aging treatments used would cause a return of the yield point.

Strain-aging data are given in Table 19. With increasing aging time and/or temperature, the following phenomena were observed. After the initial straining but prior to subsequent heat treatment, the samples showed no indication of a yield point, with the tensile curve assuming the form shown in Figure 70 (a). After a short-time and/or low-temperature heat treatment, an inflection was observed at the beginning of the plastic region (Figure 70 (b)). This inflection became more pronounced with increasing severity of heat treatment, progressing to a stage of easy glide (Figure 70 (c)). With further increases in aging temperature and/or time, an upper and lower yield point appeared (Figure 70 (d)), and the sharpness and magnitude of the yield point generally became gradually greater. (In this report, the magnitude of the yield point refers to the difference in stress between the upper and lower yield points.) Although recovery of the yield point was extremely rapid at 400°C, it should be noted that the magnitude of the yield point was generally smaller than that observed after aging at lower temperatures. This is presumably due to the increase with temperature in atomic mobility and the consequent decrease in impurity-dislocation locking.

The initiation of the yield point was arbitrarily defined for purposes of this study to be the point at which easy glide is first observed (i.e., the magnitude of the yield point equals zero). At 300°C the yield point was initiated by aging for 12 hours. With increasing temperature, the time of initiation became

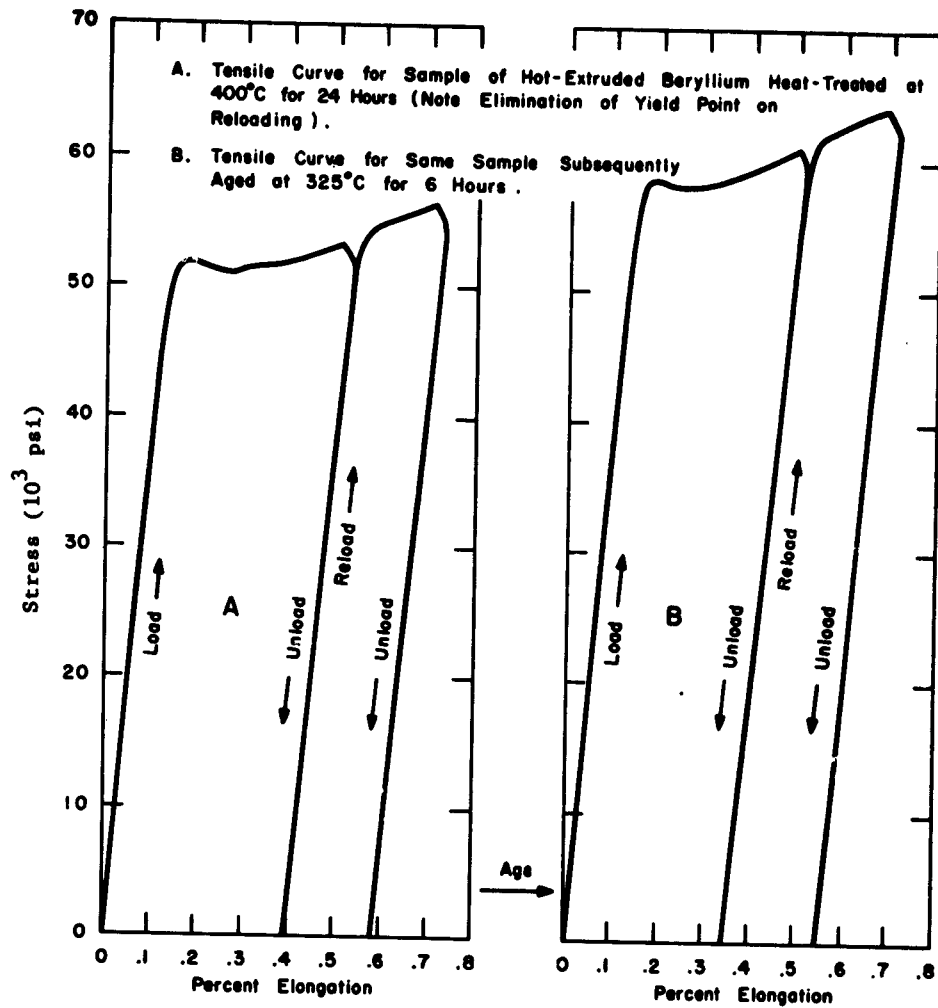


Figure 72 - Recovery of the yield point in beryllium by strain aging. (Drawing No. RB-1124)

Table 19 - SUMMARY OF STRAIN AGING DATA

Aging Temp. (°C)	Aging Time (hrs)	Yield Point	Magnitude of the Yield Point (psi)	No. of Prior Cycles
300	2.00	No	---	0
	7.50	No	---	1
	12.00	Easy glide	0	1
	16.00	Easy glide	0	0
	20.00	Easy glide	0	2
	21.00	Yes	70	4
	27.00	Yes	643	0
	72.00	Yes	104	3
325	2.00	No	---	1
	2.25	Easy glide	0	1
	2.50	Yes	136	1
	3.00	Yes	135	1
	6.00	Yes	402	1
	19.00	Yes	292	2
	20.00	Yes	135	1
350	0.25	No	---	0
	0.50	Easy glide	0	0
	0.75	Easy glide	0	2
	1.00	Yes	134	0
	2.00	Yes	303	0
	7.50	Yes	605	0
375	0.17	Easy glide	0	3
400	0.25	Yes	106	1
	2.00	Yes	100	0
	4.00	Yes	130	0
	8.00	Yes	102	1

shorter until at 400°C a yield point was observed for all aging times studied (i.e., down to 15 minutes). Yield points had not been observed after heat treatment of solution-treated-and-quenched material at 400°C for 15 minutes or at 300°C for one week. It therefore seems that the smaller grain size or the state of precipitation in the unsolutionized samples is more readily conducive to the initiation of a yield point.

(3) Determination of the Activation Energy for Yield Point Recovery. According to the Cottrell theory,⁽⁸⁾ the activation energy for return of the yield point should be equal to that for diffusion in beryllium of the impurity causing the yield point. The line in Figure 73 shows the conditions under which yield point recovery is first observed. By calculation from the slope of this line, the activation energy for yield point recovery is found to be approximately 48,000 cal/gm-mole, which compares closely with the activation energies for diffusion of iron and nickel in beryllium. This is consistent with the observations of Sawkill⁽⁶⁾, who pointed out that the strain aging noted in beryllium can be best interpreted in terms of the movement of substitutional impurity atoms.

11-2.7 Hot Tensile Properties of Aged and Slow-Cooled Powder Material. Brown et al.⁽¹¹⁾ showed that the high-temperature ductility of ingot beryllium after extrusion can be much improved by an aging heat treatment. In their work the beryllium was held at 780°C for 120 hours and then slowly cooled to room temperature over a period of 120 hours. This resulted in an improvement in ductility which increased with increasing tensile testing temperature, whereas beryllium normally exhibits a maximum in ductility at some temperature in the range of 300 to 400°C. The improvement was attributed to precipitation at or solute redistribution to the grain boundaries which inhibited the onset of intergranular failure normally found at temperatures above 400°C.

A similar study was made in the current program to determine if the same heat treatment is effective in improving the high-temperature ductility of extruded powder material. Four tensile blanks in the as-extruded condition were etched in a dilute solution of sulfuric acid, wrapped in tantalum, and sealed in evacuated quartz tubing. They were then held at 780°C in a Nichrome-wound tube furnace for 120 hours and slow cooled in the furnace for 120 hours at a rate of approximately 6°C per hour. The blanks were then machined into cylindrical tensile samples of the same design and dimensions as were used throughout the quench-aging and strain-aging portions of this program. Following machining, the samples were etched in dilute sulfuric acid to remove any surface defects. Two of the samples were tensile tested at 700°C, and two were tested at 600°C, all under argon atmosphere using a Tinius-Olsen mechanical drive tensile unit. Temperature was recorded by means of a thermocouple attached to the gauge length of the samples. The data obtained from these tests are presented in Table 20 and therein compared with results reported by Brown, Morrow and Martin⁽¹¹⁾. The NMI data show no significant change in either ductility or strength over values generally reported for unaged samples. It is concluded that either the treatment is not applicable to powder metallurgy material or that the aging schedule is extremely sensitive to compositional differences.

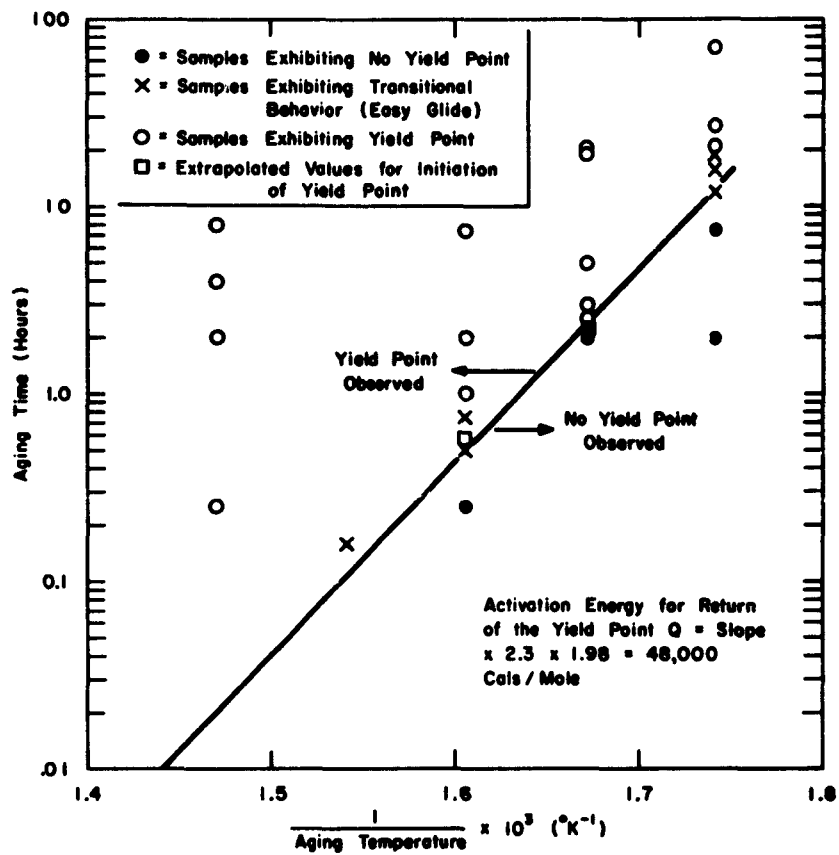


Figure 73 - - Effect of aging time and temperature on yield point recovery in strained beryllium. (Drawing No. RB-1123a)

Table 20 - ELEVATED TEMPERATURE TENSILE PROPERTIES OF BERYLLIUM

Data Source	Material and Condition	Test Temperature (°C)	UTS (psi)	Elongation (%)
NMI	QMV powder; extruded at 1950°F, 30:1 reduction; aged 780°C for 120 hours, slow cooled over 120-hour period.	600	18,100	11.6
		600	19,400	11.3
		700	5,000	16.9
		700	4,600	13.1
Brown, Morrow and Martin (Ref. 11)	Vacuum-cast pebble; extruded 1050°C (1922°F), 44:1 reduction.	600	20,000	12
		700	10,000*	10*
	Vacuum-cast pebble; extruded 1050°C (1922°F), 44:1 reduction; aged 780°C for 120 hours, slow cooled over 120-hour period.	600	14,000	65
		700	10,000	75

*Extrapolated from curves given by Brown, Morrow and Martin in Ref. 11.

11-3 CONCLUSIONS

The following observations and conclusions are made on the basis of the previously described studies on hot-extruded commercially pure powder beryllium.

(1) Solution treatment at 1100°C for one hour followed by aging at temperatures between 200 and 800°C has verified the fact that commercially pure beryllium is essentially a dilute alloy and undergoes changes in tensile properties during aging. Solution treatment of as-extruded material results in a loss in both ductility and ultimate tensile strength. However, these properties may be largely recovered by suitable heat treatment, particularly aging at $700 - 800^{\circ}\text{C}$ for one week. It is expected that a similar degree of recovery of properties would be obtained at lower aging temperatures if sufficient aging time were used.

(2) The aging mechanism in this material does not seem to be associated with the dispersion-hardening effect of a precipitate, but rather with the removal of a premature failure mechanism, presumably by precipitation of a detrimental impurity from solution and by the consequent purification of the matrix. This conclusion is based on the fact that the ductility increases with increasing ultimate strength and that there is no significant change in yield strength with changes in aging treatment.

(3) Neither changes in texture nor substantial grain growth accompany the observed changes in tensile properties.

(4) The faster the cooling rate from the solutionizing temperature, the lower the strength and ductility. However, the cooling rate seems to be important only for a wide divergence in the severity of quench (i.e., water quench versus furnace cool).

(5) Precipitation occurs during the aging of beryllium, as evidenced by the appearance and growth of impurity peaks detected by X-ray diffractometer scans of aged samples. Not all reflections for the precipitate could be observed, due to its high degree of orientation with respect to the beryllium matrix; however, the peaks noted correspond to an fcc structure having a lattice constant of 6.07 \AA .

(6) Assuming the structure noted above, the texture of the precipitate is consistent with the $\{110\}$ planes of the precipitate lying parallel to the $\{1010\}$ planes of the beryllium and the $\{111\}$ planes of the precipitate parallel to the (0002) plane of the beryllium.

(7) A region of easy glide was observed in the tensile curve of as-extruded material. Yield points were also observed in several instances after aging of solution-treated material at 400°C . A yield point was detected in only one of the samples aged at higher temperatures. Some inconsistencies in the 400°C yield point behavior were probably due to variations in grain size, the yield point being reduced or eliminated as the grain size increased.

(8) A study of fracture surfaces in the tensile specimens indicated that fracture originated at a single point, which was randomly located within the cross section of the piece, and then propagated along $\{1120\}$ planes.

(9) Strain-aging studies demonstrated that the yield point in beryllium can be eliminated by room-temperature plastic strain and recovered by subsequent aging between 300 and 400°C. The aging time required for recovery decreases with increasing temperature, but the yield point phenomena is less pronounced at 400°C than at lower temperatures. Strain-aging observations were consistent with the Cottrell mechanism of yield point occurrence.

(10) The activation energy for return of the yield point in strained material was found to be 48,000 cal/gm-mole, which compares closely with reported activation energies for diffusion of iron and nickel in beryllium.

(11) The high-temperature ductility of extruded powder material was not improved by an aging treatment reported to significantly improve the high-temperature ductility of extruded ingot material.

REFERENCES

1. F. M. Yans, A. D. Donaldson and A. R. Kaufmann, The Effects of Iron, Copper, Nickel and Chromium on the Tensile Properties of Preferentially Oriented Beryllium Sheet, USAEC Report NMI-1192, Nuclear Metals, Inc., February 1958.
2. S. H. Gelles, J. J. Pickett and A. K. Wolff, Recent Advances in Beryllium Metallurgy, J. of Metals, **12**:189 (1960).
3. D. R. Mash, Aging Effects in Commercially Pure Beryllium, J. of Metals, **7**:1235 (1955).
4. P. Pointu et al., Study of the Precipitation of Trace Impurities in Beryllium, Compte rendus, **250**:2365 (1960).
5. A. Moore, Improved Mechanical Properties and Associated Constitution Changes in Commercially Pure Ingot Beryllium as Affected by Heat Treatment Above 700°C, J. of Nuclear Materials, **3**:113 (1961).
6. J. Sawkill, J. E. Meredith and A. E. Parsons, A Precipitation Reaction in Commercially Pure Beryllium, Report No. 127, Tube Investments Research Laboratories, January 1961.
7. J. L. Klein, V. Macres, D. Woodard and J. Greenspan, Ductility of Beryllium as Related to Preferred Orientation and Grain Structure, in The Metal Beryllium (D. W. White, Jr. and J. E. Burke, Eds.), pp. 425-465, Amer. Soc. Metals, Cleveland, 1955.
8. A. H. Cottrell and B. A. Bilby, Dislocation Theory of Yielding and Strain Aging of Iron, Proc. Phys. Soc., **A62**:49 (1949).
9. R. B. Jones and V. A. Phillips, Yield Point Phenomena in a Number of Commercial Copper Alloys and One Nickel Base Alloy, 42nd Annual Convention of ASM, Philadelphia, October 17-21, 1960, ASM Preprint No. 219.
10. S. H. Gelles and A. K. Wolff, Impurity Effects in Commercially Pure Beryllium, USAEC Report NMI-1238, Nuclear Metals, Inc., February 1961.
11. A. B. Brown, F. Morrow and A. J. Martin, The Effect of Strain Rate, and Heat Treatment, on the Tensile Properties of Extruded Beryllium Rods Between 25 and 600°C, J. of Less Common Metals, **3**:62 (1961).

Appendix 11-A

COMPLETE QUENCH-AGING TENSILE DATA

Heat Treatment	Specimen Identification*	0.2% Offset Yield Stress (psi)	Ultimate Tensile Stress (psi)	Percent Elongation	Elastic Modulus (10 ⁶ psi)	Yield Point
As extruded	A-41-XXVIII	49,500	99,400	14.6	43	Easy Glide
"	A-42 "	49,700	100,200	17.0	42	Easy Glide
"	C-41 "	46,100	93,600	18.9	37	No
"	D-41 "	49,600	100,400	15.7	40	Easy Glide
Furnace cooled	C-51-XXXV	43,400	83,400	6.0	35	No
"	C-52 "	43,500	93,500	17.4	49	No
"	D-51 " **	45,300	78,700	4.0	40	Inflection
"	D-52 " **	46,000	73,600	2.8	37	Inflection
Air cooled	A-23-I	42,100	75,500	3.9	40	Inflection
"	C-22-"	40,900	58,300	1.6	39	No
"	C-23 "	40,100	72,600	4.1	36	No
"	D-22 "	40,000	70,000	2.9	-	No
As quenched	A-24-II	43,100	79,500	5.1	37	Inflection
"	C-24 "	42,300	64,700	2.2	35	No
"	D-23 "	43,000	61,900	1.6	36	Inflection
"	D-24 "	43,500	63,800	1.9	37	No
As quenched	D-8-XVIII	43,700	77,000	4.1	36	Inflection
"	D-18 "	44,100	70,600	2.6	37	Inflection
"	D-28 "	43,100	74,800	3.7	37	Inflection
"	D-38 " **	44,800	50,800	-	34	Inflection

Appendix 11-A Continued

Heat Treatment	Specimen Identification*	0.2% Offset Yield Stress (psi)	Ultimate Tensile Stress (psi)	Percent Elongation	Elastic Modulus (10 ⁶ psi)	Yield Point
As quenched	A-45-XXXI	47,100	72,300	2.6	41	No
"	A-46 "	46,000	74,500	3.0	40	Inflection
"	C-45 " **	44,300	51,900	0.8	38	No
"	D-45 "	46,000	80,500	4.4	41	No
200°C, 24 hr.	D-6-XVI	44,800	66,500	2.1	41	No
"	D-16 "	44,700	71,400	2.8	33	No
"	D-26 "	44,200	70,300	2.6	37	No
"	D-36 "	44,000	69,400	2.6	33	No
200°C, 1 wk.	D-9-XIX	49,300	61,400	1.2	38	No
"	D-19 "	50,200	70,100	2.0	38	No
"	D-29 "	48,200	73,600	3.0	38	No
"	D-39 "	51,200	73,300	2.4	45	No
300°C, 24 hr.	D-7-XVII	46,200	71,700	2.9	36	Easy glide
"	D-17 "	46,300	66,000	2.3	39	Easy glide
"	D-27 "	42,200	70,600	3.0	38	No
"	D-37 "	46,600	70,000	2.7	40	Easy glide
300°C, 1 wk.	D-10-XX	51,600	70,200	2.4	42	No
"	D-20 "	45,200	67,200	2.1	51	No
"	D-30 "	48,100	67,500	1.3	44	No
"	D-40 "	47,200	60,500	1.3	36	No
400°C, 15 min.	A-5-III	46,000	65,100	2.0	38	Inflection
"	A-15 "	44,600	58,700	1.3	37	Inflection
"	A-25 "	42,600	64,700	2.2	36	Inflection
"	A-35 "	45,200	67,300	2.4	42	Inflection

Appendix 11-A (Continued)

Heat Treatment	Specimen Identification*	0.2% Offset Yield Stress (psi)	Ultimate Tensile Stress (psi)	Percent Elongation	Elastic Modulus (10^6 psi)	Yield Point
400°C, 2 hr.	A-11-XXI	46,100	55,600	1.2	40	Easy glide
"	A-12 "	47,100	53,400	0.9	40	Easy glide
"	C-11 "	43,900	73,100	3.6	40	Easy glide
"	D-11 "	46,300	72,500	4.1	39	Easy glide
400°C, 7 hr.	A-43-XXIX	48,300	86,000	5.4	44	Yes
"	C-42 "	45,500	78,900	4.6	47	Infection
"	C-43 "	45,300	83,700	5.7	39	Infection
"	D-42 " **	47,200	67,200	1.9	41	Yes
400°C, 7 hr.	F-24-ZII	42,100	52,900	0.7	34	No
"	G-24 "	44,400	58,900	1.3	45	No
"	H-23 "	42,300	55,600	1.2	44	No
"	H-24 "	40,600	57,000	1.1	42	No
400°C, 16 hr.	A-48-XXXIII	46,800	56,700	1.0	40	Easy glide
"	C-48 "	43,500	76,200	4.2	40	Infection
"	D-47 "	46,800	68,900	2.1	45	Yes
"	D-48 "	45,800	64,100	1.7	43	Yes
400°C, 24 hr.	C-2-XXXVIII	44,100	71,100	3.0	41	No
"	D-2 " **	46,400	62,400	1.5	40	Infection
"	D-3 " **	45,900	65,100	1.8	40	Infection
"	F-2 "	45,900	53,400	0.8	41	No

Appendix 11-A (Continued)

Heat Treatment	Specimen Identification*	0.2% Offset Yield Stress (psi)	Ultimate Tensile Stress (psi)	Percent Elongation	Elastic Modulus (10 ⁶ psi)	Yield Point
400°C, 24 hr.	A-49-XXXVI	46,900	47,900	0.4	45	No
"	C-53 "	44,900	60,900	1.5	44	No
"	D-53 "	45,700	66,500	2.0	44	Yes
"	G-56 "	45,700	73,000	2.9	43	Inflection
400°C, 24 hr.	F-43-ZXXIX	44,600	66,000	2.1	40	Inflection
"	G-42 "	43,800	65,800	2.1	40	Inflection
"	G-43 "	44,600	58,100	1.2	43	Inflection
"	H-42 "	44,300	57,000	1.2	40	Inflection
400°C, 30 hr.	A-47-XXXII	45,100	61,200	1.5	45	Yes
"	C-46 "	42,600	69,400	2.8	42	Inflection
"	C-47 "	44,300	59,500	1.4	45	Inflection
"	D-46 "	46,000	49,900	0.6	45	Yes
400°C, 42 hr.	F-23-ZI	44,000	64,600	1.9	43	Inflection
"	G-22 "	43,200	57,900	1.4	44	Inflection
"	G-23 "	44,200	58,600	1.3	43	Inflection
"	H-22 "	44,600	44,900	0.3	41	Inflection
400°C, 60 hr.	A-44-XXX	46,600	70,200	2.4	42	Easy glide
"	C-44 "	45,200	67,200	2.1	51	Inflection
"	D-43 "	48,100	67,500	1.3	44	Easy glide
"	D-44 "	47,200	60,500	1.3	36	Yes
400°C, 1 wk.	C-9-XIII	44,900	58,300	1.3	41	No
"	C-19 "	44,300	70,900	3.0	38	No
"	C-29 "	44,600	63,400	1.8	37	No
"	C-39 "	44,800	54,700	1.0	35	No

Appendix 11-A (Continued)

Heat Treatment	Specimen Identification*	0.2% Offset Yield Stress (psi)	Ultimate Tensile Stress (psi)	Percent Elongation	Elastic Modulus (10^6 psi)	Yield Point
400°C, 8 days	F-46-ZXXIII	42,100	67,500	2.5	40	No
"	G-14 "	-	39,300	0.1	46	No
"	H-13 "	43,900	47,800	0.5	46	No
"	H-14 "	44,400	54,400	1.0	41	No
500°C, 15 min.	A-13-XXII	46,800	67,300	2.1	36	No
"	C-12 "	45,800	67,300	2.3	35	No
"	C-13 "	45,800	57,500	1.2	43	No
"	D-12 "	47,700	56,000	0.9	41	No
500°C, 2 hr.	A-8-VI	47,400	64,200	1.6	38	No
"	A-18 "	46,300	53,900	0.8	38	No
"	A-28 "	45,200	59,300	1.4	45	No
"	A-38 "	48,000	73,400	2.8	43	No
500°C, 24 hr.	C-5-IX	48,100	69,800	2.2	42	No
"	C-15 "	44,700	69,700	2.6	36	No
"	C-25 "	44,500	51,300	0.7	37	No
"	C-35 "	43,500	67,100	2.4	33	No
500°C, 1 wk.	A-34-XXVII	45,400	81,500	5.3	43	No
"	C-34 "	47,600	86,700	8.0	40	No
"	D-33 "	49,000	79,000	3.9	38	No
"	D-34 "	47,900	78,600	4.0	38	No
600°C, 15 min.	A-6-IV	43,700	74,200	3.5	36	No
"	A-16 "	42,400	66,400	2.4	38	No
"	A-26 "	44,200	57,700	1.3	36	No
"	A-36 "	43,500	58,000	1.4	37	No

Appendix 11-A (Continued)

Heat Treatment	Specimen Identification*	0.2% Offset Yield Stress (psi)	Ultimate Tensile Stress (psi)	Percent Elongation	Elastic Modulus (10 ⁶ psi)	Yield Point
600°C, 2 hr.	A-21-XXIV	46,600	64,300	1.7	39	No
"	A-22 "	46,200	75,000	3.6	35	No
"	C-21 "	45,100	72,700	3.4	40	No
"	D-21 "	46,900	72,700	2.9	38	No
600°C, 24 hr.	C-6-X	48,600	91,800	11.8	40	No
"	C-16"	47,600	78,200	4.2	38	No
"	C-26"	47,100	63,200	1.6	32	No
"	C-36"	47,000	88,200	9.1	33	No
600°C, 1 wk.	C-10-XIV	44,400	93,600	17.8	39	No
"	C-20 "	42,800	83,200	7.0	37	No
"	C-30 "	44,400	89,800	9.6	40	No
"	C-40 "	44,000	79,200	4.7	39	No
700°C, 15 min.	A-33-XXVI	44,600	76,000	3.6	40	No
"	C-32 "	43,500	64,200	2.0	37	No
"	C-33 "	42,900	57,400	1.3	44	No
"	C-32 "	45,900	71,700	2.6	36	No
700°C, 2 hr.	A-9-VII	46,500	81,500	4.9	38	No
"	A-19 "	45,500	79,100	4.4	37	No
"	A-29 "	45,700	79,600	4.6	38	No
"	A-39 "	46,400	84,600	6.2	35	No
700°C, 24 hr.	C-7-XI	45,800	83,800	6.7	45	No
"	C-17 "	45,500	73,600	3.6	41	No
"	C-27 "	45,100	80,400	6.0	32	No
"	C-37 "	44,800	91,700	15.6	34	No

Appendix 11-A (Continued)

Heat Treatment	Specimen Identification*	0.2% Offset Yield Stress (psi)	Ultimate Tensile Stress (psi)	Percent Elongation	Elastic Modulus (10 ⁶ psi)	Yield Point
700°C, 1 wk.	A-14-XXIII	49,300	95,900	16.0	33	No
"	C-14 "	47,900	94,300	15.7	39	No
"	D-13 "	48,300	96,400	16.7	40	No
"	D-14 "	48,200	91,800	9.2	37	No
800°C, 15 min.	A-7-V	42,500	74,600	3.9	45	No
"	A-17"	42,000	70,900	3.0	42	No
"	A-27"	45,700	56,800	1.3	37	Yes
"	A-37"	41,700	76,400	4.3	37	No
800°C, 2 hr.	A-31-XXV	44,300	84,700	6.8	45	No
"	A-32 "	44,200	75,300	3.6	40	No
"	C-31 "	42,800	85,500	8.8	36	No
"	D-31 "	44,200	75,600	3.6	38	No
800°C, 24 hr.	C-8-XII	45,400	92,200	13.9	45	No
"	C-18 "	45,300	90,600	11.8	35	No
"	C-28 "	44,600	90,500	15.7	36	No
"	C-38 " **	45,500	64,000	1.9	38	No
800°C, 1 wk.	D-5-XV	44,300	93,400	15.4	37	No
"	D-15 "	47,600	89,800	8.1	36	No
"	D-25 "	48,100	95,900	16.9	36	No
"	D-35 "	48,900	96,100	16.8	35	No

* The letter refers to the extruded rod, the number refers to the sample location in the rod, and the Roman numeral designates the lot number.

** Sample failed in threads, (ultimate stress and percent elongation not included in average).

Appendix 11-B

RESULTS OF CHEMICAL AND SPECTROGRAPHIC ANALYSES

Specimen No.	400° C Heat Treatment (hr)	Impurities									
		C (ppm)	N (ppm)	BeO (w/o)	Fe (ppm)	Ni (ppm)	Cr (ppm)	Si (ppm)	Mg (ppm)	Al (ppm)	Mn (ppm)
A-43-XXIX	7	350 ^a	203	1.40	>750	130	40	115	135	260	50
C-42-XXIX	7	660 ^b	199	1.28	>750	120	50	85	200	290	80
C-43-XXIX	7	630	-	-	-	-	-	-	-	-	-
C-46-XXXII	30	630	-	-	>750	165	60	85	180	265	50
D-42-XXIX	7	660 ^b	188	1.35	~1000	160	90	105	235	325	50
D-46-XXXII	30	660	-	-	~1000	>500	150	130	245	290	45
F-43-ZXXIX	24	470 ^b	175	1.37	~1000	>250	125	160	215	265	50
G-43-ZXXIX	24	320 ^c	-	-	-	-	-	-	-	-	-
H-42-ZXXIX	24	300 ^c	-	-	-	-	-	-	-	-	-

a, average of six values.

b, average of three values.

c, average of two values.

SECTION 12

RAISING THE YIELD STRENGTH OF BERYLLIUM

E. D. Levine and L. R. Aronin

(Nuclear Metals, Inc., Concord, Massachusetts)

ABSTRACT

The effects of rolling temperature, rolling reduction and small additions of copper on the mechanical properties of bi-directionally rolled beryllium sheet were investigated. Sheet rolled to reductions of 6:1 at 1400°F exhibits considerably higher transverse ductility than high-reduction sheet, with somewhat lower yield and tensile strengths. The addition of 1 - ^w/o copper results in strengths approaching those characteristic of high-reduction sheet, with little sacrifice in transverse ductility.

An electroless plating process was developed for the preparation of homogeneous alloys of beryllium and copper.

12-1 INTRODUCTION

The use of beryllium sheet as a structural material has been limited by the inability to develop suitable combinations of yield strength and ductility in the finished material. Considerable effort has been expended in the utilization of fabrication procedures aimed at maximizing either strength or ductility, but, in general, improvements in one of these properties have been accompanied by decreases in the other. For example, the use of high-reduction fabrication techniques was employed by Wickle, Armstrong and Perrin⁽¹⁾ resulted in the attainment of yield strengths as high as 70,000 psi in sheet cross-rolled 36:1 at 1400°F. Transverse ductility, however, as measured by bending of specimens of varying width-to-thickness ratios, was considerably lower than that obtainable in ordinary hot-pressed material. On the other hand, the use of low-reduction techniques, such as hot-upsetting⁽²⁾ or hot bi-directional rolling⁽³⁾, while improving transverse ductility characteristics, has resulted in lower yield strengths, in the range 30,000 to 35,000 psi.

Extensive studies of low-reduction fabrication techniques have been carried out only at high fabrication temperatures (1850 to 1950°F). The use of lower fabrication temperatures would be expected to produce increases in yield strength due to changes in grain size and texture and to the introduction of cold work into the material. Consideration of the factors involved suggests that it may be possible to accomplish such strengthening without loss in transverse ductility.

Another possible means of increasing the yield strength in beryllium sheet is by solid solution strengthening. Yans, Donaldson and Kaufmann⁽⁴⁾ have demonstrated that small additions of copper, iron and chromium have a strengthening effect in extruded and cross-rolled beryllium sheet; in the case of copper, the strengthening was obtained at no sacrifice of uniaxial ductility. However, no measurements were made in these experiments of transverse ductility.

The purpose of this program was to determine what combinations of strength and ductility can be obtained by extending a low-reduction process to lower fabrication temperatures, both in unalloyed beryllium and in beryllium containing small copper additions. Bi-directional rolling was selected as the fabrication technique, since previous experience had shown that the production yield for this procedure is normally higher than that for hot upsetting. Rolling reductions up to 6:1 at temperatures from 1400 to 1800°F were studied. In addition, the effect of light finish passes at still lower temperatures was investigated.

12-2 EXPERIMENTAL PROCEDURE

12-2.1 Unalloyed Beryllium

(1) Material. Two lots of AEC nuclear grade Brush QMV -200 mesh powder were used as the starting material for sheet fabrication. The first lot, V-5051, was used in the fabrication of unalloyed beryllium sheet and for preliminary experiments with beryllium-copper alloys; the second, V-5846, was used for the preparation of beryllium-copper alloys that were ultimately fabricated into sheet. Chemical analyses of both lots are presented in Table 21, along with AEC nuclear grade specification NP-100-A.

Table 21. CHEMICAL ANALYSES OF BRUSH QMV -200 MESH POWDER STARTING MATERIAL

Element	Lot V-5051	Lot V-5846	AEC Nuclear Grade Specification NP-100-A
Be (assy)	99.0	98.7	98.5*
BeO	1.01	0.79	1.2
Al	0.060	0.04	0.14
Ag	0.0002		0.0005
B	0.00007		0.0002
Cd	<0.00001		0.0002
Ca	<0.010		0.02
C	0.10	0.09	0.12
Cr	0.05		0.03
Co	0.0001		0.0005
Cu	0.007		0.015
Fe	0.073	0.10	0.16
Pb	<0.002		0.002
Li	0.0001		0.0003
Mg	0.020	0.01	0.06
Mn	0.007		0.015
Mo	<0.002		0.002
Ni	0.013		0.04
N	0.017		0.05
Si	0.030	0.03	0.10
Zn	<0.010		0.02

* Minimum specification. All other specifications maximum.

** All values are wt. percent.

(2) Fabrication. Six billets were cold compacted to 70 percent density in 3-1/2 inch ID by 4-inch OD mild steel cans. Compacting pressure was 250 tons. The billets were outgassed at 1000°F to less than 0.1 microns, sealed off, heated 4 hours at 1950°F while covered with graphite, and hot compacted to 100 percent density in a 1000-ton horizontal press. After hot compacting, each billet was 3-1/2 inches in diameter by approximately 4-1/2 inches long.

The cans were stripped off by pickling in 50 percent HNO₃ and each billet was sectioned into individual rolling billets 0.150 to 0.600 inches thick. Different thicknesses were used so that billets rolled to various reductions would have a final thickness of 0.100 inches. The individual billets were then re-canned in 3-1/2 inch ID by 4-inch OD mild steel tubing with 1/4-inch thick mild steel plates welded on, and were then annealed 1 hour at 1950°F.

Billets were bi-directionally rolled 1.5:1, 3:1 and 6:1 at temperatures of 1800, 1600 and 1400°F. Each pass was 10 percent of the existing thickness, and in a direction 90° to the preceding pass. An equal number of passes was made in each direction. Specimens were reheated between passes. After the last pass, each sheet was reheated to the rolling temperature and press-flattened. After air cooling to room temperature, the cans were stripped, and specimens were cut from the sheets for determination of mechanical properties. As far as possible, specimens were cut in several orientations with respect to the orthogonal rolling directions.

The effect of finish passes at lower temperatures on the mechanical properties of beryllium sheet was studied. In one part of this study, billets were rolled according to schedules identical to those given above, except that the final 10 percent reduction was performed at 1000°F. In a second portion of the study, billets were rolled approximately 3:1 at 1950°F and then finish rolled 5 and 10 percent at temperatures between 800 and 1400°F. All finish reductions were accomplished in one pass, thus producing a slight departure from strict bi-directional rolling conditions.

(3) Evaluation of Mechanical Properties. Specimens fabricated under the above conditions were evaluated by means of tensile and bend tests. Tensile specimens were machined to the dimensions shown in Figure 12-1. After machining, specimens were etched in 25% H₂SO₄ to remove possible surface cracks and twinning. Final thickness of the specimens ranged between 0.049 and 0.071 inches.

Tensile testing was performed in a 60,000 pound capacity Tinius-Olsen mechanical drive tensile machine, employing a strain rate of 0.01 per minute. A 1-inch gage length S-3 extensometer, attached to the narrow face of the specimen, was employed to measure and record strain.

Rectangular bend specimens, 0.050 ± 0.004 inches thick, with width-to-thickness ratios ranging from 4.5:1 to 29.9:1, were prepared in a similar manner. They were tested in simple beam, single point bending. A 0.200-inch radius ram pushed the specimen between 2.400-inch diameter steel rollers with centers 3.00 inches apart. The angle of bend at fracture was taken as the index of bend ductility. Bend deflection and radius of curvature at fracture were also measured.

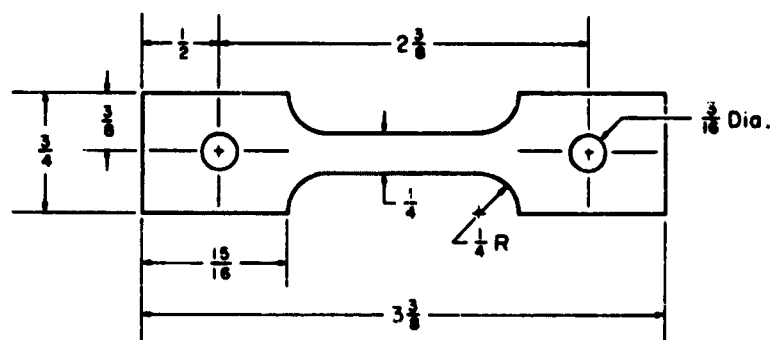


Figure 74 - Geometry of tensile specimens.

12-2.2 Beryllium-Copper Alloys

(1) Alloy Preparation. The preparation of alloys of beryllium with moderately heavy metals such as copper by the usual techniques of powder blending, consolidation and annealing generally results in inhomogeneous material, owing to the density differences between the components. In the present investigation, a technique was developed for preparing homogeneous alloys containing up to 6 w/o copper by producing a uniform deposit of copper on individual beryllium powder particles. This was done by means of an electroless plating technique, in which cupric ions were reduced by metallic beryllium in the presence of small amounts of H_2SO_4 . Alloy content was controlled to close limits by limiting the amount of cupric ion in a $\text{Cu}(\text{NO}_3)_2$ solution and depositing all the copper in solution on the beryllium. This was possible provided there was an appropriate concentration of H_2SO_4 present.

The optimum concentration of H_2SO_4 was determined by plating copper onto 1 gm samples of beryllium from 0.25M $\text{Cu}(\text{NO}_3)_2$ solutions containing 800 milligrams copper and various concentrations of H_2SO_4 . Table 22 shows that for a 0.5 volume percent H_2SO_4 concentration practically all the copper was plated out.

Using this technique, alloy powder containing 1 and 6 w/o copper was prepared in 400-gram batches. The beryllium was added to the $\text{Cu}(\text{NO}_3)_2$ solution containing the calculated amount of copper. Solution and powder were then mechanically stirred until the powder appeared homogeneously distributed. The predetermined amount of diluted H_2SO_4 was then added and stirring was continued for 15 minutes. The copper-plated powder was filtered out with a kochner funnel and then dried in an oven at 200 F. Approximately 5 pounds of powder of each composition were produced. The close control of composition possible by this technique is shown in Table 23, which gives the copper content of random samples of powder of each batch.

(2) Homogenization of Alloys. The copper-plated powders were cold compacted and hot pressed in a manner identical to that employed for unalloyed beryllium. The hot-pressed billets were then annealed at 2025 F for 1 hour to produce a homogeneous solid solution of copper in beryllium. This particular treatment was chosen on the basis of an X-ray diffraction study of beryllium - 6 w/o copper alloys after various treatments. Debye-Scherrer photographs of as-plated powders revealed the patterns of elemental beryllium and copper. After hot pressing, the elemental copper lines had disappeared, and no intermetallic compound lines were observed, indicating that the copper had gone completely into solution in the beryllium. Observations of the spacings between {1014} planes, however, indicated that complete homogeneity had not yet been obtained. The {1014} spacing continued to increase after subsequent annealing for various times at 1950 F. At 2100 F, the spacing appeared to reach an equilibrium value after a very short time, indicating that diffusion was complete at this temperature. Since some grain growth was observed at this temperature, 2025 F was chosen as the temperature at which a fairly homogeneous solid solution would be obtained with a minimum of grain growth. Billets annealed at this temperature exhibited a grain size of approximately 40 microns, which was the same as that observed for the unalloyed beryllium annealed at 1950 F.

Table 22. EFFECT OF H_2SO_4 CONTENT ON DEPOSITION OF
COPPER ON BERYLLIUM FROM $\text{Cu}(\text{NO}_3)_2$ SOLUTION

Percent H_2SO_4 by Volume	Percent Cu Plated From Solution
0.0	1
0.1	0
0.2	67
0.5	99

**Table 23. UNIFORMITY OF COPPER CONTENT IN BERYLLIUM
POWDER PROCESSED TO OBTAIN COPPER CONTENTS OF
1 AND 6 WEIGHT PERCENTS**

Group 1 1 w/o Cu Nominal		Group 2 6 w/o Cu Nominal	
Sample No.	Percent Cu	Sample No.	Percent Cu
1	0.988	8	6.00
2	1.015	9	6.07
3	1.012	10	6.03
4	0.997	11	5.97
5	1.005	12	6.00
6	1.000	13	6.08
7	0.988	14	5.96

The above X-ray diffraction study also revealed that small amounts of CuO and Cu_2O were formed during oven drying of the powder. During subsequent exposure to high temperature, during hot pressing and annealing, the copper oxides were reduced by beryllium, resulting in a somewhat higher BeO content in the beryllium-copper alloys than in the corresponding unalloyed material. It is possible to avoid this situation by drying the powders at room temperature or in a vacuum at elevated temperatures. No CuO or Cu_2O lines were observed in Debye-Scherrer patterns from powders that had been dried at room temperature.

(3) Fabrication. It was originally intended to study the effects of fabrication variables on both 1 and 6 w/o copper alloys. However, because of limited funds and because preliminary experiments indicated that the fabricability of beryllium - 6 w/o copper alloys is probably marginal, only beryllium - 1 w/o copper alloys were fabricated. Fabrication procedures were similar to those employed for unalloyed beryllium. In one phase of the fabrication program billets were bi-directionally rolled 1.5:1, 3:1 and 6:1 at 1800 and 1600°F, 3.5:1 and 4.4:1 at 1500°F and 1.5:1 at 1400°F. The effect of finish passes was studied by rolling billets 3:1 at 1950°F and finish rolling 5, 10 and 15 percent at 1400°F.

(4) Evaluation of Mechanical Properties. Procedures for the evaluation of mechanical properties were identical to those employed for unalloyed beryllium.

12-3 RESULTS

12-3.1 Fabricability of Sheet

(1) Unalloyed Beryllium. Very little difficulty was experienced in obtaining 0.100-inch sheet of unalloyed beryllium by means of fabrication procedures described in the preceding sections. Minor edge cracking was observed in some cases, but in general, sheet prepared by bi-directional rolling was sound, reasonably flat, and of apparently uniform quality.

The only problems encountered were in the finish rolling at 1000°F of sheets initially rolled at 1800°F, 1600°F, and 1400°F. When the prior reduction at these temperatures was 1.5:1, no cracking occurred, but prior reduction of 3:1 and 6:1 led to considerable cracking during finish rolling at 1000°F.

(2) Beryllium - 1 w/o Copper Alloys. Beryllium - 1 w/o copper alloys were somewhat more difficult to fabricate than unalloyed beryllium. At 1400°F, the maximum reduction that could be employed without cracking was 1.5:1. At 1600°F and 1800°F, however, reductions of 6:1 were successfully employed. Because of the marginal fabricability at 1400°F, some specimens were rolled at an intermediate temperature, 1500°F, where reductions as high as 4.4:1 were successful.

Studies of the effect of low-temperature finish passes were restricted, because of the above effects, to 5, 10 and 15 percent passes at 1400°F after prior rolling at 1950°F.

12-3.2 Tensile Properties of Bi-Directionally Rolled Sheet.

(1) Unalloyed Beryllium. Tensile data on unalloyed beryllium bi-directionally rolled 1.5:1, 3:1 and 6:1 at 1800°F, 1600°F and 1400°F are presented in Table 24. Average values represent the results of at least three tests for each condition. Minimum and maximum values are also reported.

The data are presented graphically in Figures 75, 76, and 77. The values of yield strength, ultimate strength and percent elongation for zero reduction in thickness in rolling correspond to those for hot pressed beryllium reported by Beaver and Wickle⁽⁵⁾. It is evident that fairly large increases in yield and tensile strengths and in uniaxial ductility can be obtained by rolling at lower temperatures to greater reduction. For example, rolling 6:1 at 1400°F, the most severe condition employed in this program, increased yield and tensile strengths to 57,800 and 77,800 psi, respectively, and elongation to 15.2 percent.

The effect of a 10 percent finish pass at 1000°F after various reductions at higher temperatures is presented in Table 25 and Figures 78, 79, and 80. Yield strengths as high as 73,600 psi were obtained by this procedure, but uniaxial ductility was sacrificed, the highest value observed being 6.3 percent.

The effect of finish rolling at temperatures between 800°F and 1400°F after prior rolling 3:1 at 1950°F is shown in Table 26 and Figures 28, 29, and 30. Reductions up to 10 percent at temperatures between 1000°F and 1400°F appear not to have any strengthening effect; in fact, a slight reduction in yield and tensile strengths was observed. Not until the finish rolling temperature was reduced to 800°F were increases in yield strength obtained, and these were minor. As shown in Figure 83, no systematic effect on tensile elongation could be observed.

(2) Beryllium - 1 W/o Copper Alloys. Tensile data for beryllium - 1 W/o copper alloys rolled at various temperatures are presented in Table 27 and Figures 84, 85, and 86. Significant strengthening due to the addition of copper was observed. For example, in the hot-pressed condition, the yield strength was increased to 41,800 psi and the tensile strength to 56,100 psi. By rolling 4.4:1 at 1500°F, further increases to 65,100 psi yield strength and 82,500 psi tensile strength were obtained. The strengthening was achieved with no apparent sacrifice in tensile elongation.

Data on the effect of light finish passes on alloy sheet initially rolled 3:1 at 1950°F are presented in Table 28 and Figure 87. Slight increases in yield strength were observed, accompanied by small decreases in tensile elongation.

12-3.3 Transverse Ductility of Bi-Directionally Rolled Sheet. Transverse ductility data for unalloyed beryllium and beryllium - 1 W/o copper alloys are presented in Tables 29 and 30. Because of the higher strengths observed in material rolled to reductions of 6:1, only sheet given this reduction was tested in bending.

The variation of bend angle at fracture with width-to-thickness ratio for both materials is shown in Figure 88. Since no effect of fabrication temperatures on transverse ductility was observed, data for different temperatures are plotted as one curve for each material. Figure 88 shows that unalloyed beryllium exhibits slightly more transverse ductility than the beryllium - 1 W/o copper alloy at equivalent width-to-thickness ratios.

Table 24. TENSILE PROPERTIES OF UNALLOYED BERYLLIUM SHEET
BI-DIRECTIONALLY ROLLED AT TEMPERATURES BETWEEN
1400 AND 1800°F TO REDUCTIONS BETWEEN 1.5:1 AND 6:1

Rolling Temp. (°F)	Reduction Ratio	0.2% Offset Yield Strength (psi)			Ultimate Tensile Strength (psi)			Percent Elongation in 1 inch	
		Min.	Max.	Avg.	Min.	Max.	Avg.	Min.	Avg.
1800	1.5:1	29,100	30,800	30,200	36,200	62,000	49,100	0.8	3.6
1800	3:1	32,100	37,700	35,100	57,700	64,100	61,600	10.2	10.9
1800	6:1	39,700	47,000	42,000	62,500	70,300	67,300	4.6	8.0
1600	1.5:1	38,000	39,300	38,600	58,100	61,500	59,800	5.2	5.8
1600	3:1	39,900	42,300	41,000	70,800	73,100	71,600	14.4	16.1
1600	6:1	36,100	39,100	37,700	64,500	66,000	65,300	12.8	16.6
1400	1.5:1	39,700	45,300	42,800	61,700	65,100	63,600	5.7	6.3
1400	3:1	58,300	59,700	59,100	70,300	77,400	74,000	4.2	6.6
1400	6:1	57,100	58,400	57,800	74,600	79,600	77,800	7.5	15.2

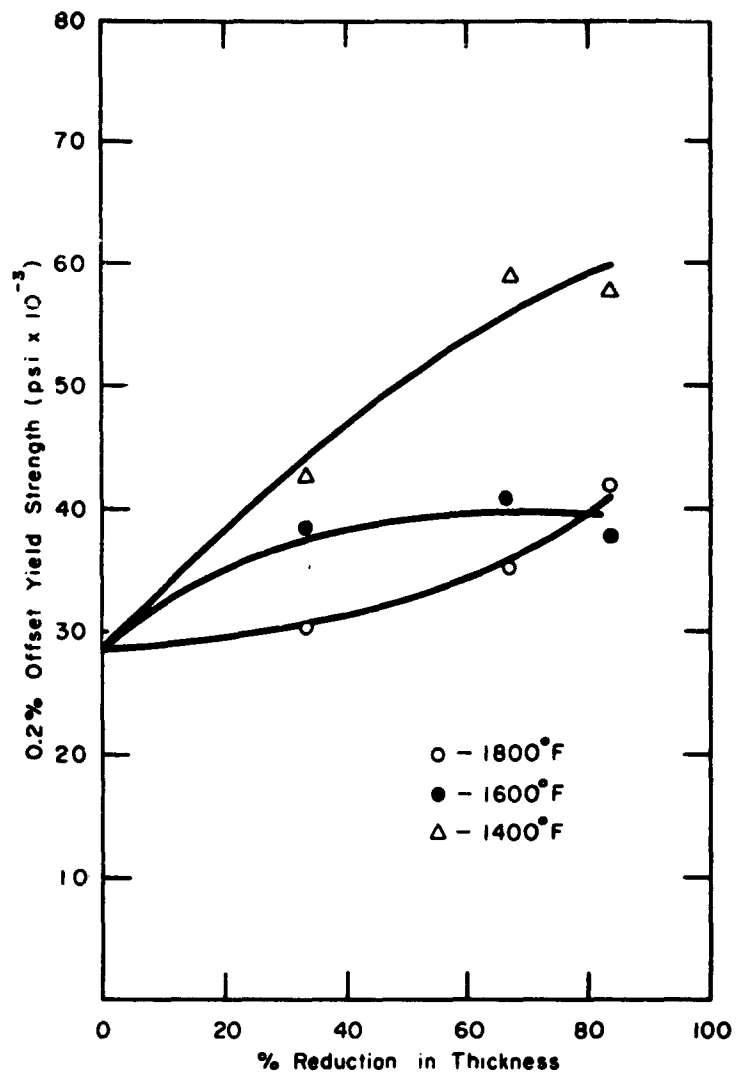


Figure 75 - Variation in 0.2% offset yield strength with reduction in thickness of unalloyed beryllium sheet bi-directionally rolled at various temperatures.

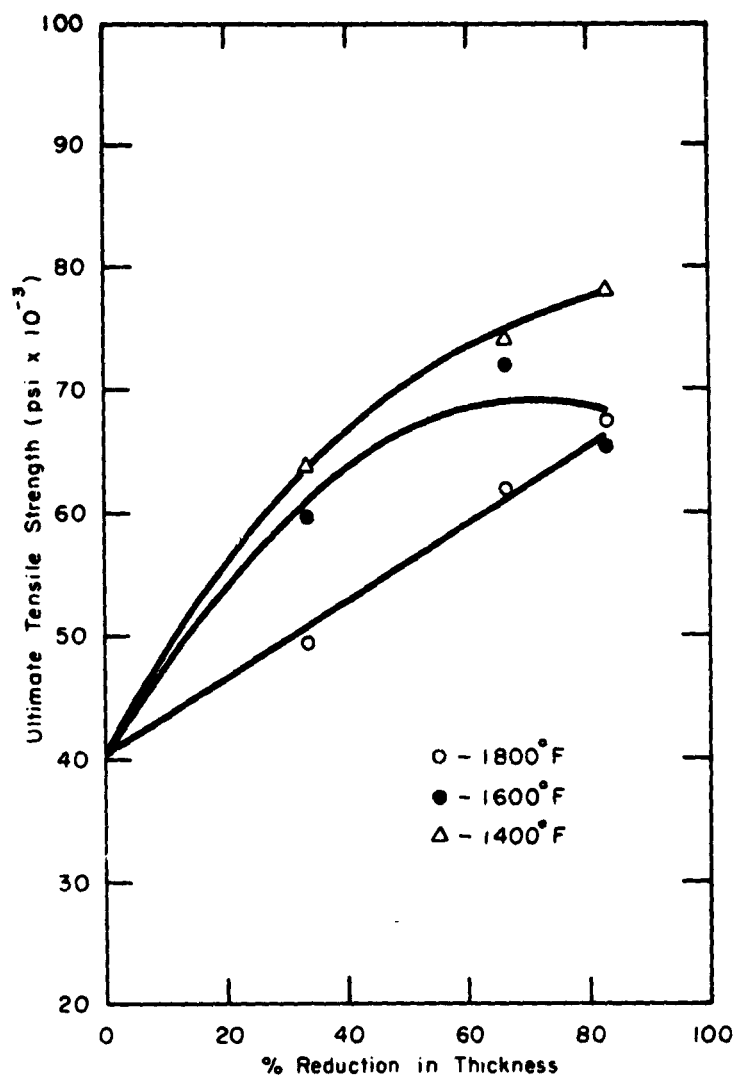


Figure 76 - Variation in ultimate tensile strength with reduction in thickness of unalloyed beryllium sheet bi-directionally rolled at various temperatures.

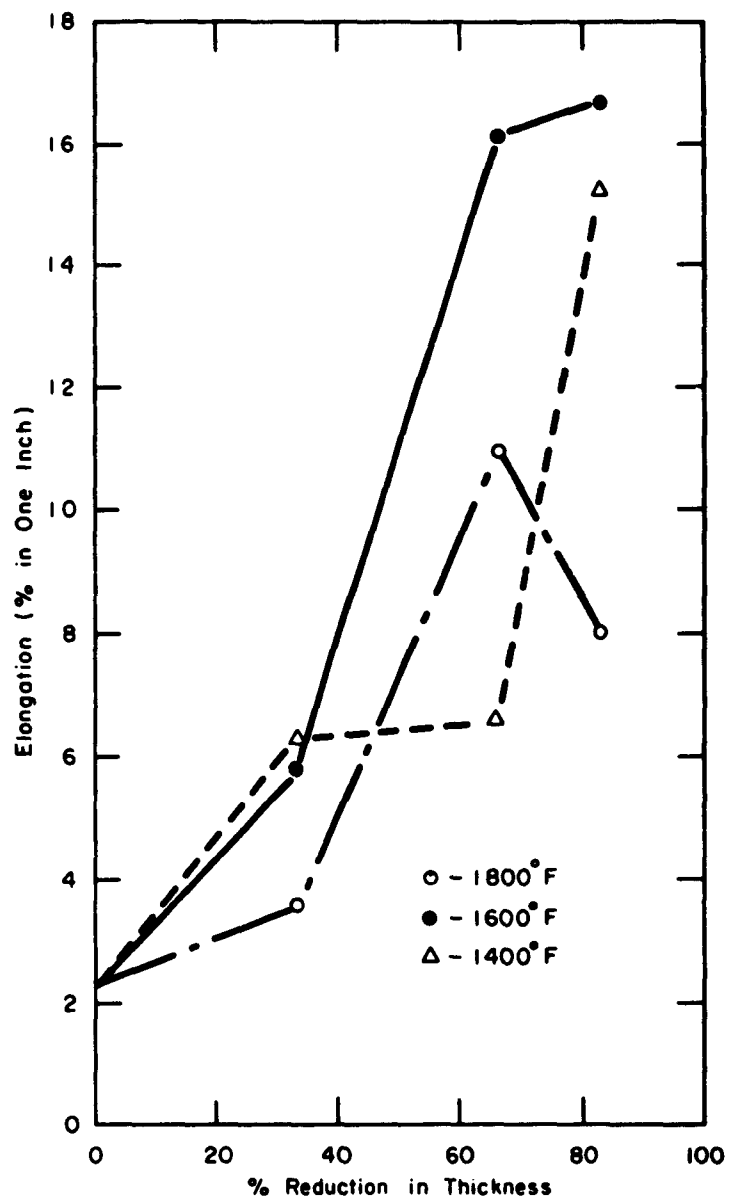


Figure 77 - Variation in tensile elongation with reduction in thickness of unalloyed beryllium sheet bi-directionally rolled at various temperatures.

Table 25. EFFECT OF A 10% FINISH PASS AT 1000°F ON THE TENSILE PROPERTIES
OF UNALLOYED BERYLLIUM SHEET BI-DIRECTIONALLY ROLLED AT TEMPERATURES
BETWEEN 1400 AND 1800°F TO REDUCTIONS OF 1.5:1 AND 3:1

Initial Rolling Temp. (°F)	Initial Reduction Ratio	0.2% Offset Yield Strength (psi)			Ultimate Tensile Strength (psi)			Percent Elongation in 1 inch		
		Max.	Min.	Avg.	Max.	Min.	Avg.	Max.	Min.	Avg.
1800	1.5:1	58,300	57,500	57,800	67,400	64,600	66,000	2.6	1.7	2.0
1800	3:1	53,100	49,300	51,600	60,100	53,900	57,800	2.2	1.2	1.7
1600	1.5:1	63,900	47,100	57,400	72,200	67,800	69,900	3.5	1.8	2.7
1400	1.5:1	58,300	51,500	55,800	70,400	67,200	68,800	4.8	2.9	3.7
1400	3:1	74,900	72,400	73,600	85,700	81,400	84,200	8.4	3.1	6.3

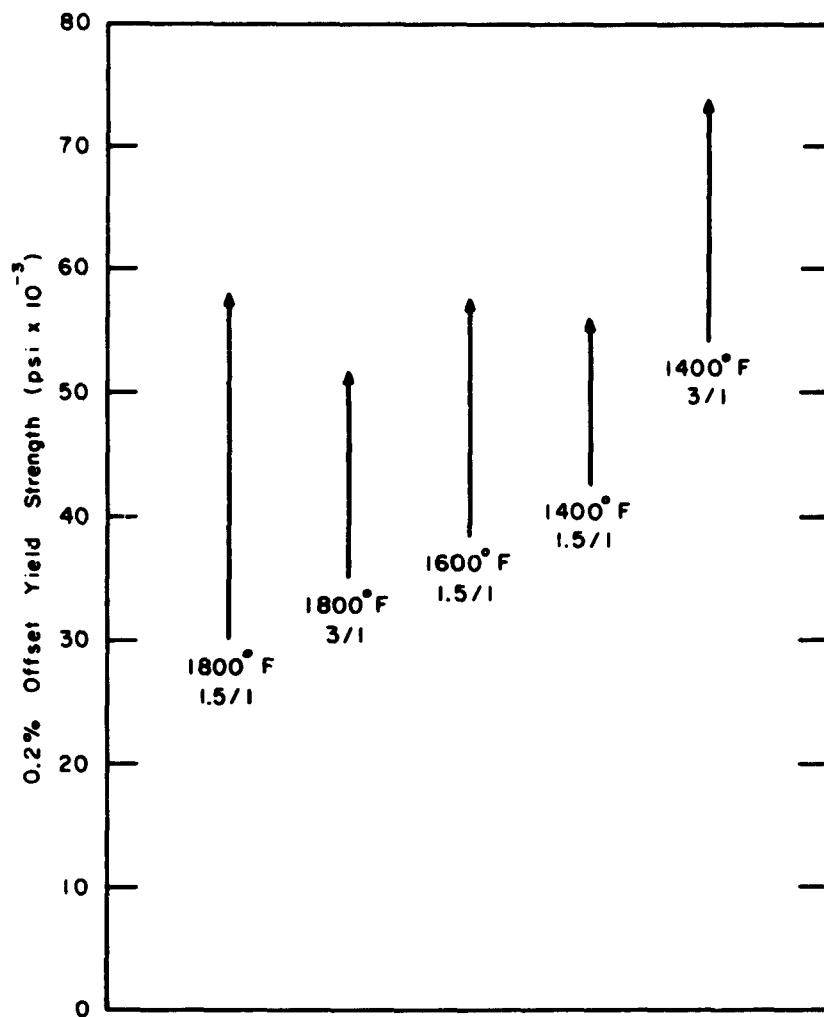


Figure 78 - Effect of a 10% finish pass on 0.2% offset yield strength of unalloyed beryllium sheet after various prior rolling procedures.

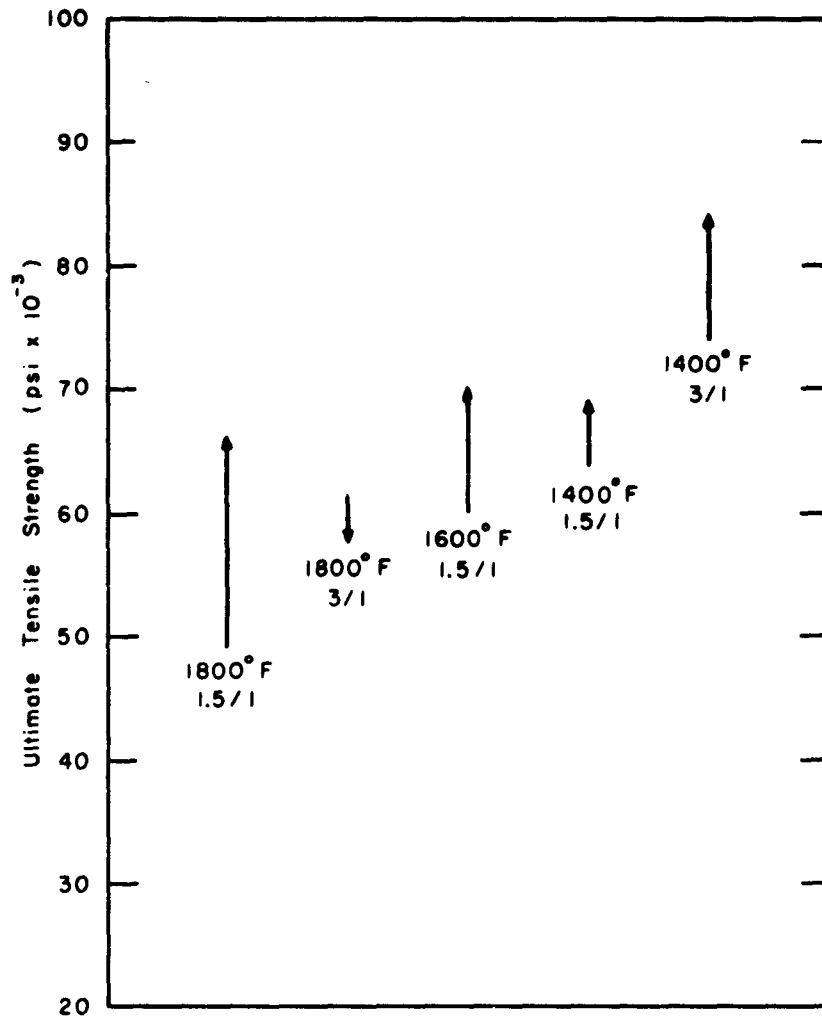


Figure 79 - Effect of a 10% finish pass on ultimate tensile strength of unalloyed beryllium sheet after various prior rolling procedures.

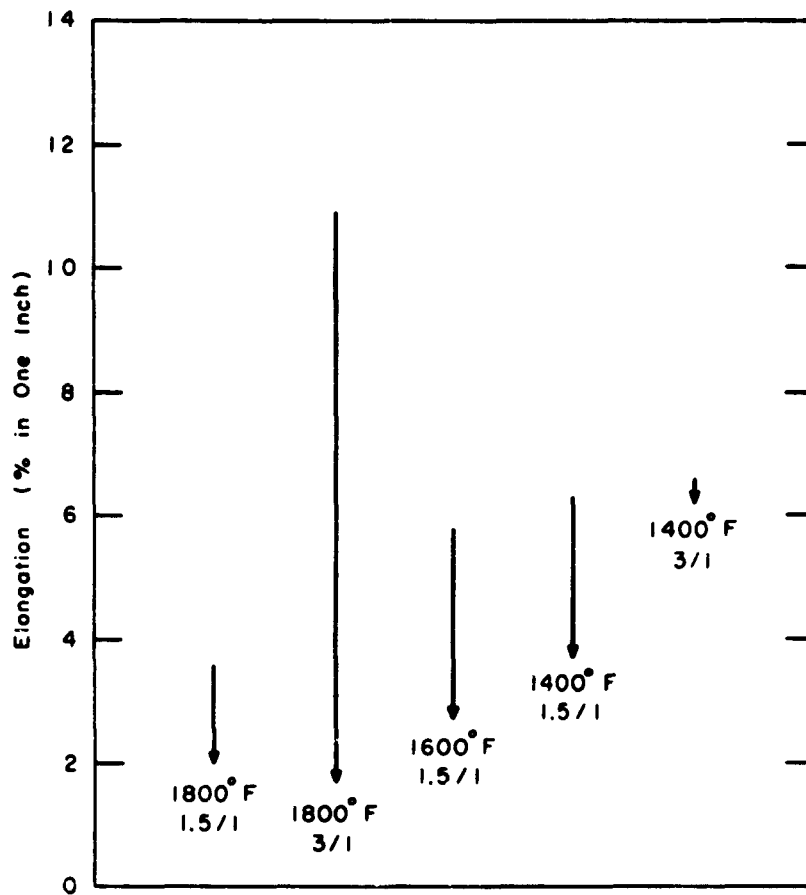


Figure 80 - Effect of a 10% finish pass on tensile elongation of unalloyed beryllium sheet after various prior rolling procedures.

Table 26. EFFECT OF LOW-TEMPERATURE FINISH PASSES ON THE TENSILE PROPERTIES
OF UNALLOYED BERYLLIUM SHEET BI-DIRECTIONALLY ROLLED 3:1 AT 1950°F

Finish Pass Temp. (°F)	Percent Finish Reduction	0.2% Offset Yield Strength (psi)			Ultimate Tensile Strength (psi)			Percent Elongation in 1 inch		
		Max.	Min.	Avg.	Max.	Min.	Avg.	Max.	Min.	Avg.
No finish passes		32,900	32,100	32,300	64,000	59,600	61,800	13.2	9.7	11.3
1400	5	30,700	30,100	30,400	58,500	52,100	55,300	8.8	4.9	6.9
1400	10	35,300	29,300	31,500	63,300	60,600	61,500	15.0	11.7	13.5
1200	5	31,500	30,600	31,100	59,700	56,300	57,700	11.2	8.2	9.1
1200	10	32,000	28,500	29,900	61,100	54,400	57,600	12.3	8.9	10.8
1000	5	32,000	30,400	30,900	60,600	58,300	59,700	14.1	11.3	12.9
1000	10	25,200	24,500	24,900	46,200	46,200	46,200	7.5	6.7	7.1
800	5	35,800	33,200	34,400	62,500	61,900	62,300	15.2	13.5	14.4
800	10	43,500	42,200	42,800	62,900	61,100	62,000	11.0	9.5	10.3

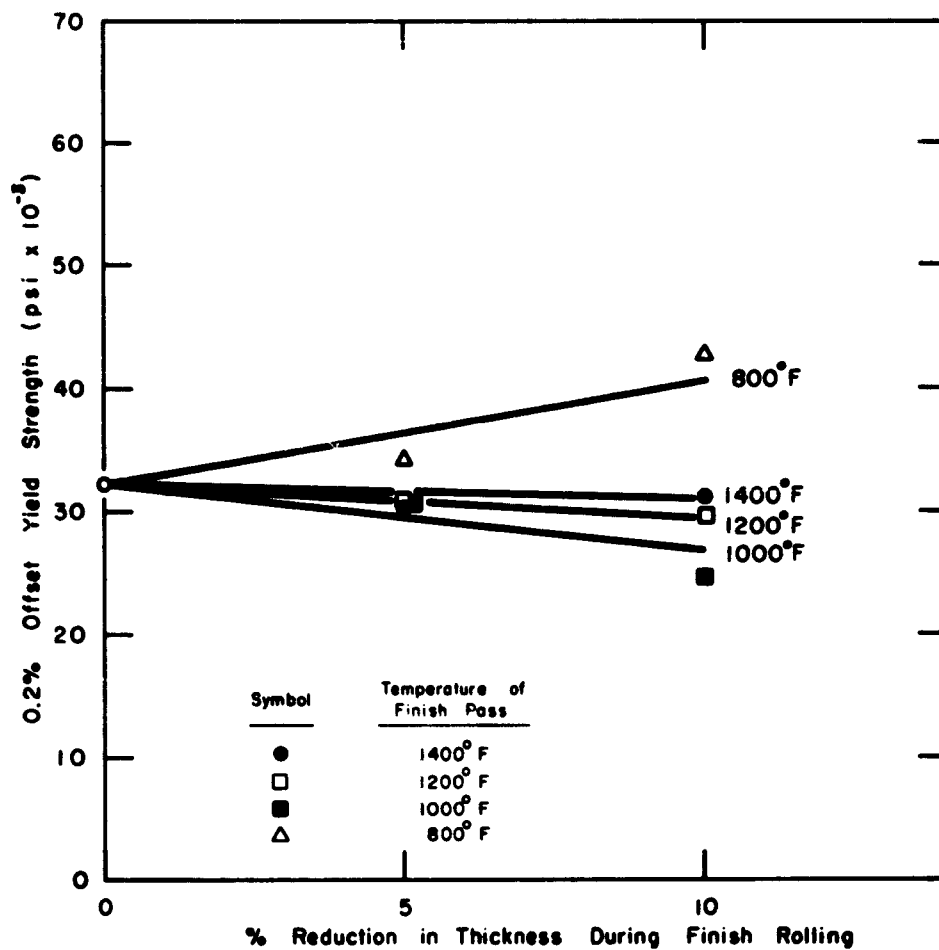


Figure 81 - Effect of finish rolling at various temperatures on the 0.2% offset yield strength of unalloyed beryllium sheet after prior reduction at 1950°F.

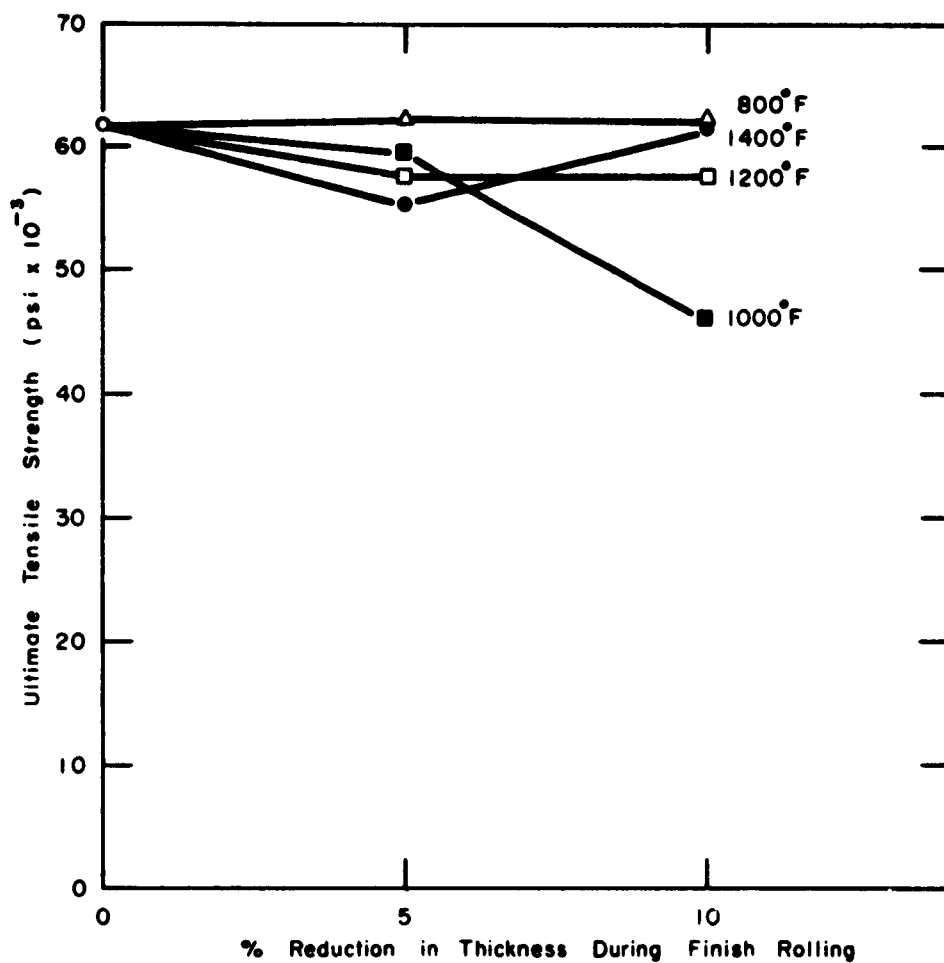


Figure 82 - Effect of finish rolling on the ultimate tensile strength of unalloyed beryllium sheet after prior reduction at 1950°F.

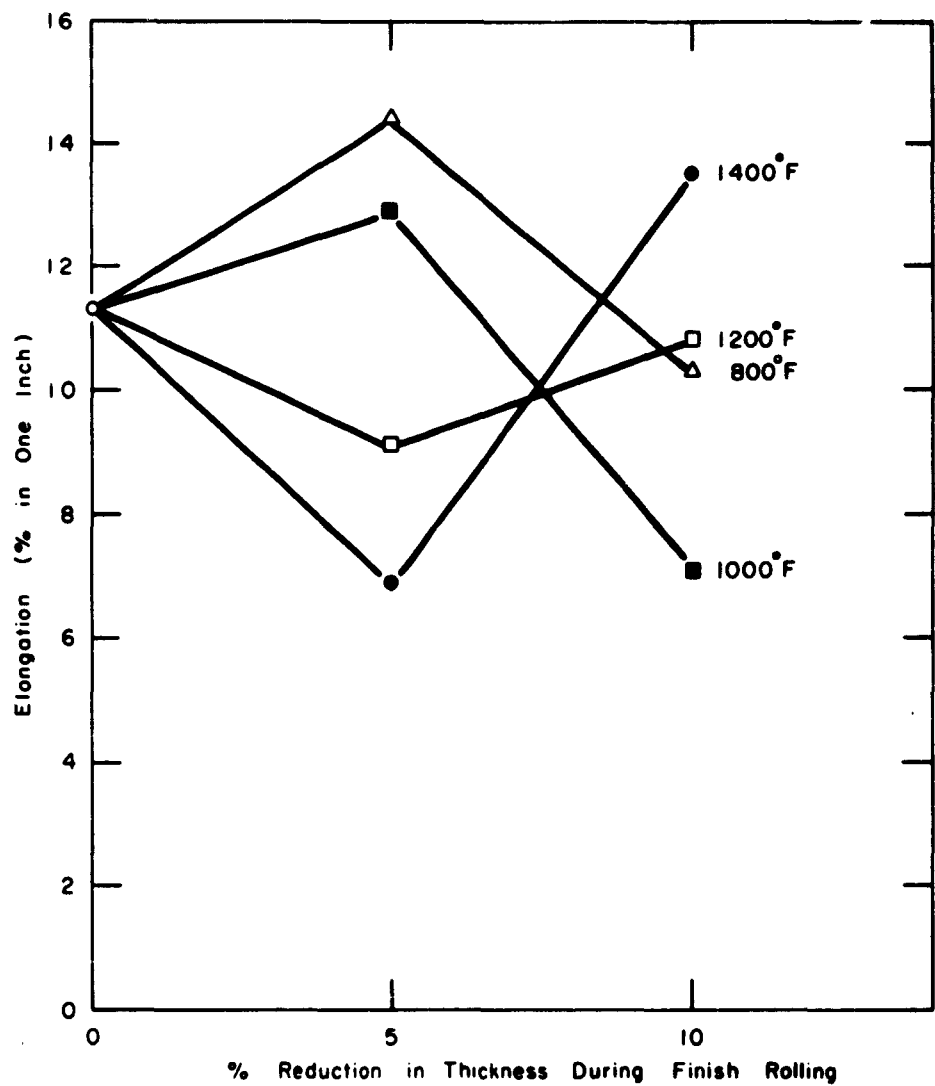


Figure 83 - Effect of finish rolling on the tensile elongation of unalloyed beryllium sheet after prior reduction at 1950°F.

Table 27. TENSILE PROPERTIES OF BERYLLIUM - 1^W/O COPPER ALLOY SHEET
BI-DIRECTIONALLY ROLLED AT TEMPERATURES BETWEEN 1400 and
1800° F TO REDUCTIONS BETWEEN 1.5:1 AND 6:1

Rolling Temp. (° F)	Reduction Ratio	0.2% Offset Yield Strength (psi)			Ultimate Tensile Strength (psi)			Percent Elongation in 1 inch		
		Max.	Min.	Avg.	Max.	Min.	Avg.	Max.	Min.	Avg.
Hot pressed		42,100	41,400	41,800	57,300	54,300	56,100	4.3	3.0	3.7
1800	1.5:1	44,000	44,000	44,000	63,100	54,900	59,000	4.9	4.2	4.6
1800	3:1	42,900	41,200	42,300	69,700	62,300	66,400	9.0	7.4	8.2
1800	6:1	52,700	49,900	51,300	79,700	64,600	72,200	18.4	4.4	10.2
1600	1.5:1	54,600	54,400	54,500	68,200	59,700	63,000	3.9	1.2	2.5
1600	3:1	52,900	52,200	52,500	76,900	76,100	76,600	10.5	9.8	10.1
1600	6:1	57,900	56,100	57,000	81,400	81,200	81,300	18.6	15.8	17.2
1500	3.5:1	64,200	62,800	63,500	81,200	80,700	80,900	9.5	7.8	8.6
1500	4.4:1	66,200	64,100	65,100	62,500	82,500	82,500	11.3	11.3	11.3
1400	1.5:1	60,300	59,500	59,800	71,400	67,500	69,700	3.4	1.9	2.9

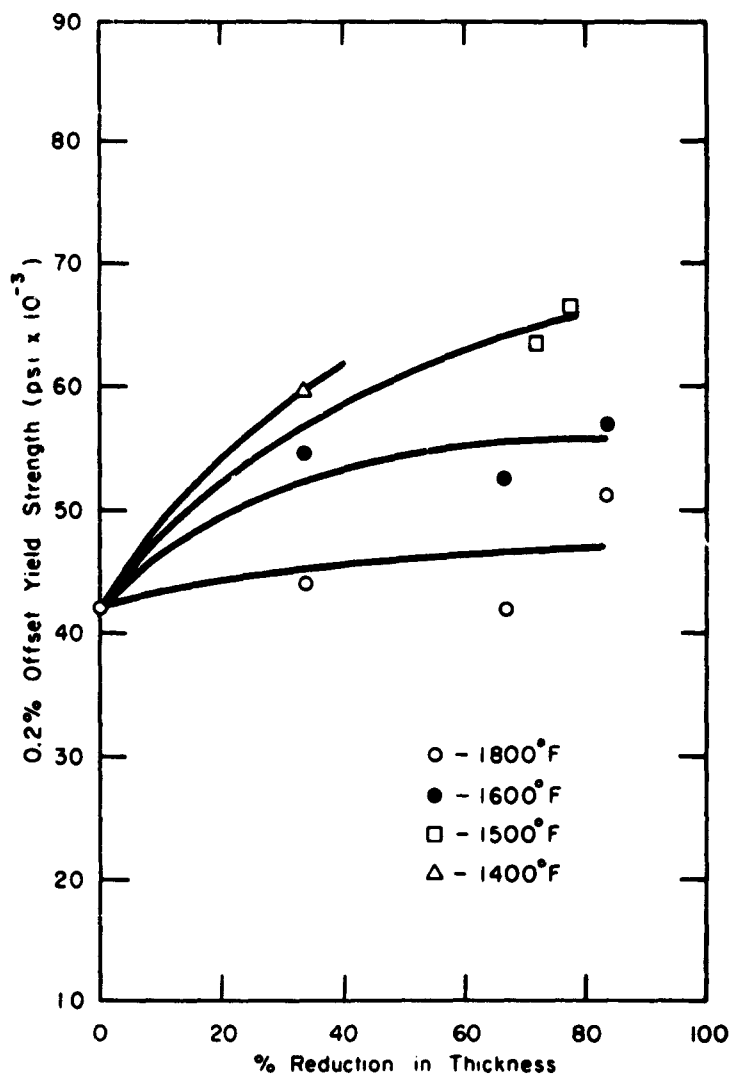


Figure 84 - Variation in 0.2% offset yield strength with reduction in thickness of beryllium - 1 w/o copper alloys bi-directionally rolled at various temperatures.

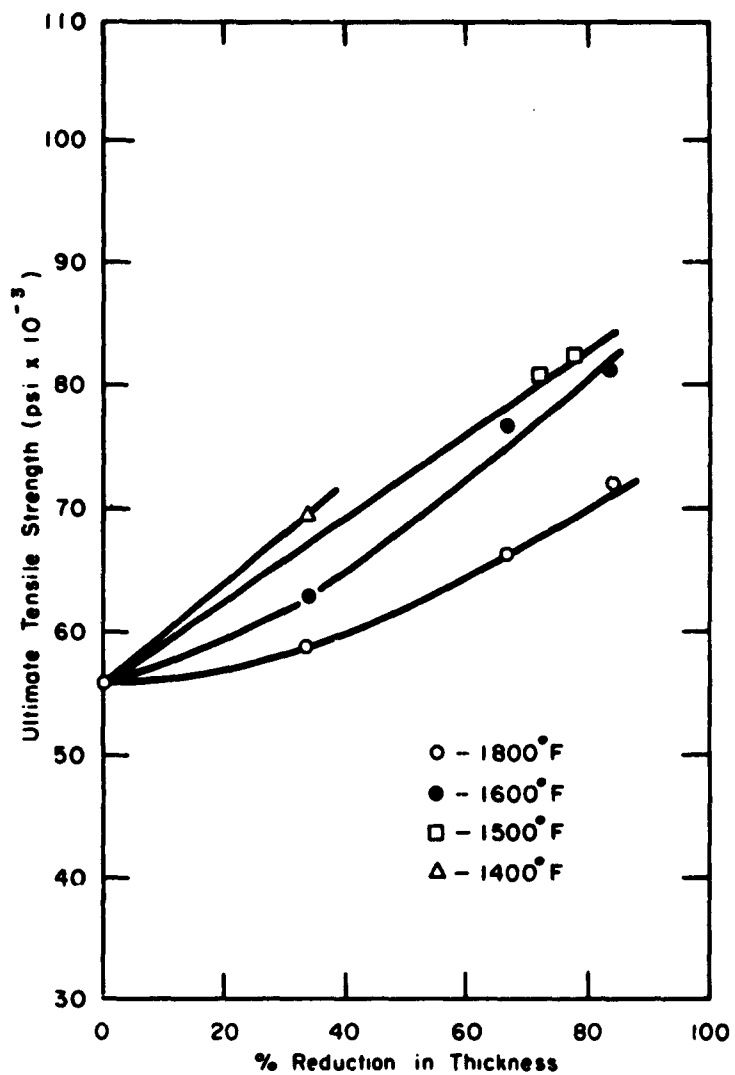


Figure 85 - Variation in ultimate tensile strength with reduction in thickness of beryllium - 1 w/o copper alloys bi-directionally rolled at various temperatures.

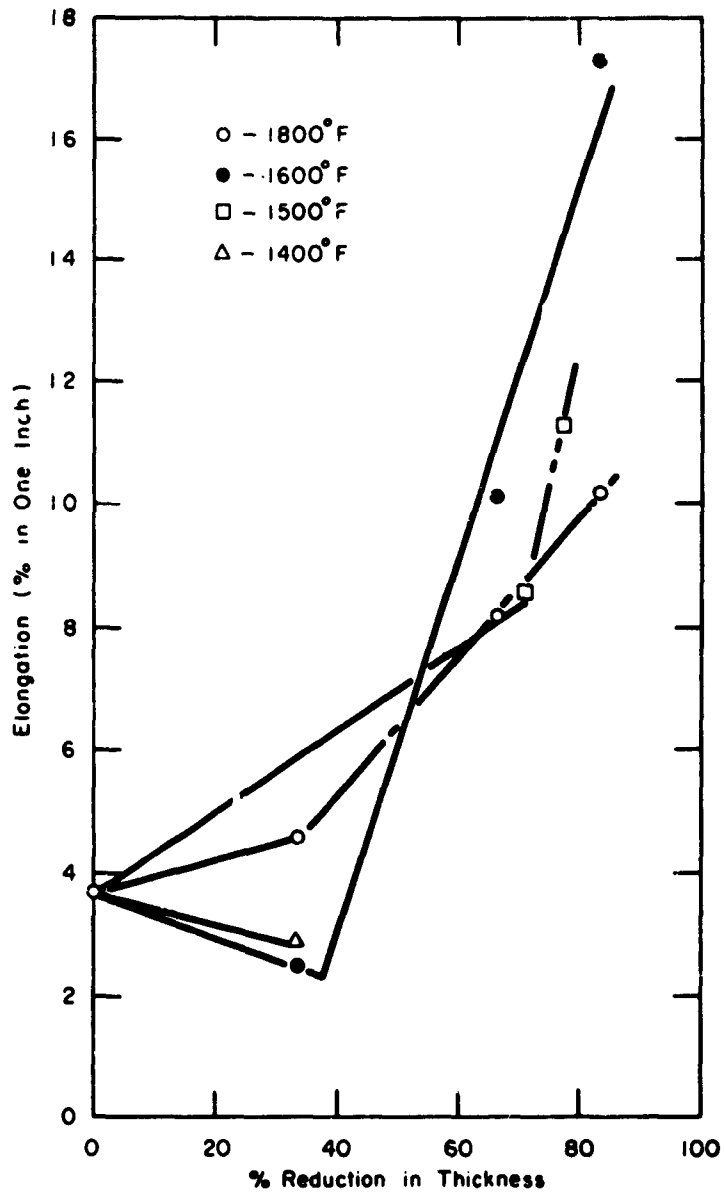


Figure 86 - Variation in tensile elongation with reduction in thickness of beryllium - 1 % copper alloys bi-directionally rolled at various temperatures.

Table 28. EFFECT OF FINISH PASSES AT 1400°F ON THE TENSILE PROPERTIES
OF BERYLLIUM - 1 W/O COPPER ALLOY SHEET INITIALLY ROLLED
BI-DIRECTIONALLY 3:1 AT 1950°F

Percent Finish Reduction	0.2% Offset Yield Strength (psi)			Ultimate Tensile Strength (psi)			Percent Elongation in 1 inch		
	Max.	Min.	Avg.	Max.	Min.	Avg.	Max.	Min.	Avg.
0	42,800	41,000	41,900	72,500	69,300	70,900	12.5	10.1	11.2
5	44,500	42,500	43,600	72,000	69,200	70,600	11.2	9.2	10.2
10	53,400	53,400	53,400	75,700	71,700	73,700	11.1	7.9	9.5
15	51,700	50,500	51,000	74,200	71,100	72,900	10.1	6.7	8.3

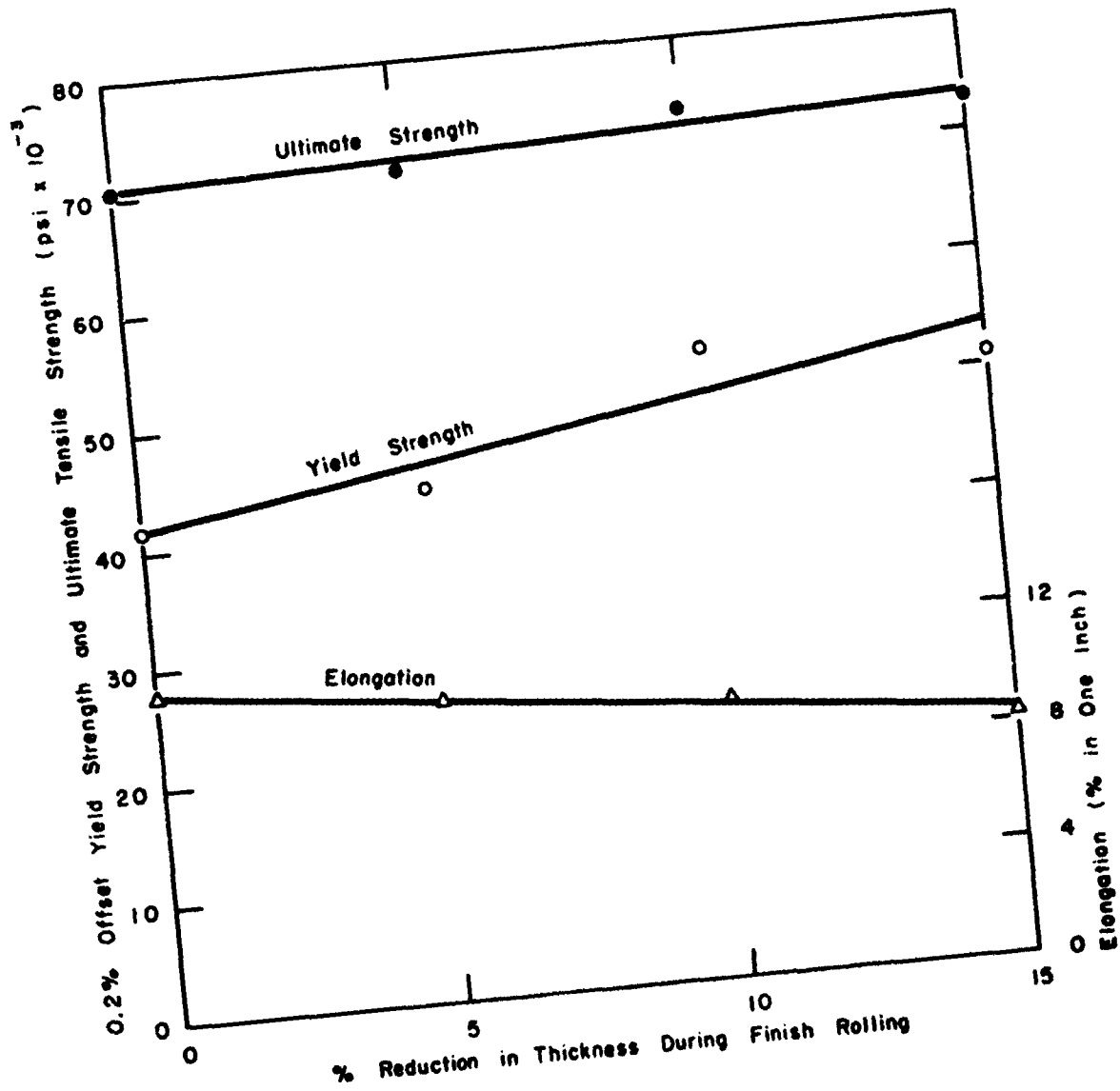


Figure 87 - Effect of finish rolling at 1400°F on the tensile properties of beryllium - 1 w/o copper alloys after prior rolling at 1950°F.

Table 29. BEND PROPERTIES OF BI-DIRECTIONALLY ROLLED BERYLLIUM SHEET

Fabrication Condition	Width Thickness	Bend Angle at Fracture (degrees)	Radius of Curvature at Fracture (inches)	Ram Deflection at Fracture (inches)
6:1 at 1800°F	4.5	>180	<0.2	--
	5.4	85	5/16	0.852
	10.0	39	3/4	0.447
	10.1	35	3/4	0.399
	15.0	30	1	0.339
6:1 at 1600°F	4.7	75	3/8	0.797
	5.0	98	3/8	0.938
	8.4	40	11/16	0.469
	9.0	31	13/16	0.373
	15.1	21	1-1/8	0.253
	15.2	27	15/16	0.285
6:1 at 1400°F	5.1	82	5/16	0.850
	10.1	30	13/16	0.373
	15.0	24	1	0.282
	25.0	14	1-3/8	0.206
	29.9	16	1-7/16	0.200

Table 30. BEND PROPERTIES OF BI-DIRECTIONALLY ROLLED
BERYLLIUM - 1 ^W/o COPPER ALLOY SHEET

Fabrication Condition	<u>Width</u> <u>Thickness</u>	Bend Angle at Fracture (degrees)	Radius of Curvature at Fracture (inches)	Ram Deflection at Fracture (inches)
6:1 at 1800°F	14.8 14.9	16 18	1-5/16 1-1/8	0.211 0.238
6:1 at 1600°F	14.1 15.1	18 15	1 1-3/16	0.245 0.218

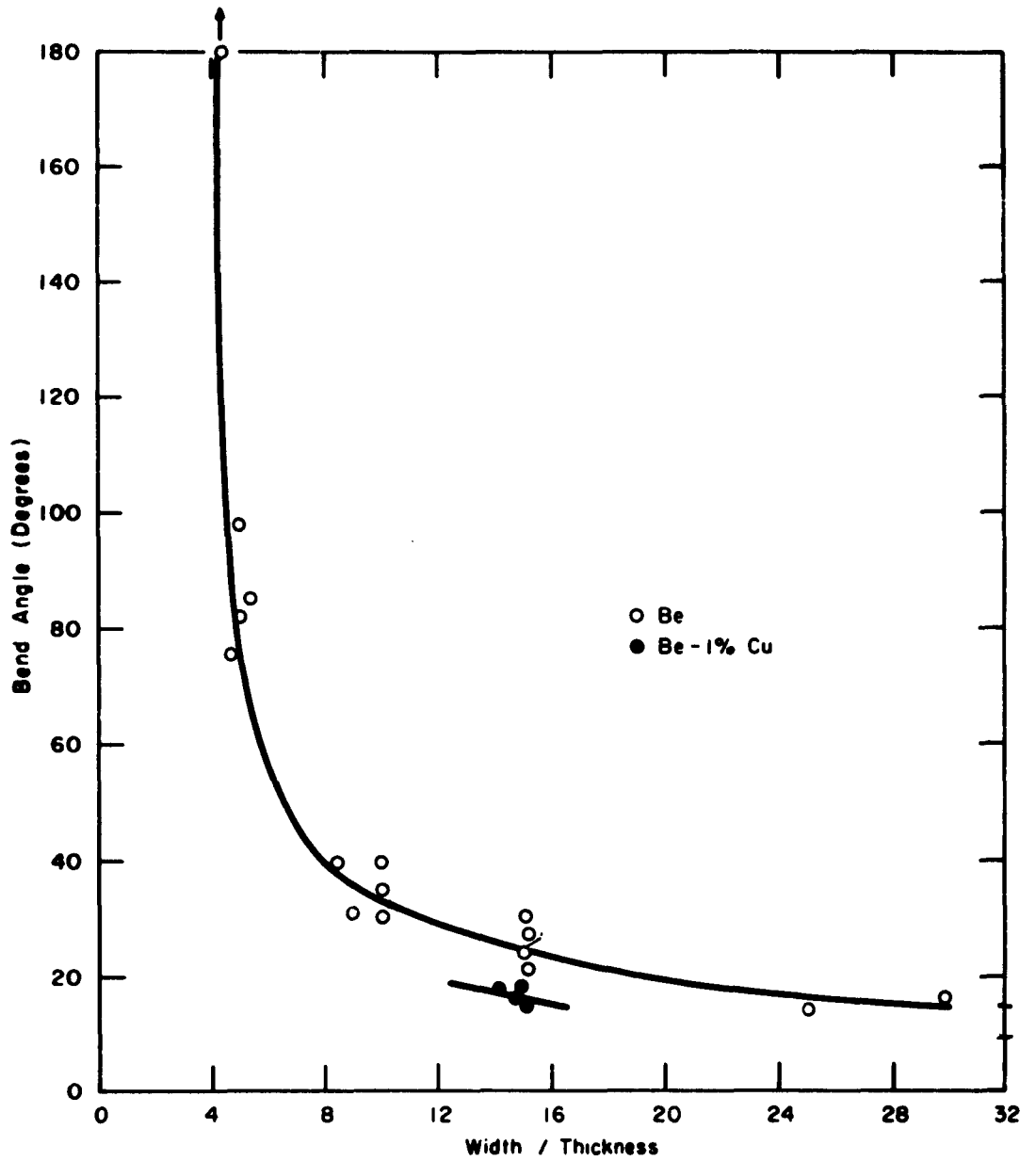


Figure 88 - Transverse ductility of beryllium and beryllium - 1 ^w/o copper alloy sheet bi-directionally rolled to reductions of 6:1.

12-4 DISCUSSION

It is of interest to compare the mechanical properties of sheet prepared in this program with sheet fabricated by other techniques. Differences in mechanical properties produced by varying fabrication temperature and amount of reduction can generally be explained by considering the effect of these variables on important metallurgical parameters such as grain size and preferred orientation.

Some measure of the effects of the fabrication variables on grain size, texture and mechanical properties can be obtained from an examination of the data of Wickle, Armstrong and Perrin⁽¹⁾. In experiments aimed at the determination of useful fabrication temperatures and reductions for rolling beryllium sheet, they achieved increases in yield and tensile strength, both by increasing the amount of reduction at a given temperature, and by decreasing the rolling temperature to achieve a given reduction. These experiments separated, to some extent, the effects of grain size and preferred orientation. At constant temperature, grain size was essentially independent of amount of reduction, but increasing the reduction rapidly increased the development of a (0001) texture. Strengthening was thus achieved by work hardening and by the progressive favoring of prismatic slip, which requires higher stresses for activation than basal slip.

Conversely, reducing the fabrication temperature to achieve a given reduction resulted in sharp reductions in grain size, while having only a minor effect on the development of a (0001) preferred orientation. The observed strengthening in this case was therefore primarily produced by grain refinement.

Transverse ductility would also be expected to improve with grain refinement. However, as Greenspan⁽³⁾ has shown, the development of a (0001) texture eliminates modes of deformation transverse to the plane of the sheet, thus reducing transverse ductility.

Because of the above factors, sheet produced by high-reduction techniques has high strength and low transverse ductility, while sheet produced by low-reduction, high temperature techniques retains some measure of transverse ductility, but has low strength.

Low-reduction, bi-directional rolling at temperatures down to 1400°F, takes advantage of the favorable effects of grain refinement, and at the same time prevents the development of too strong a (0001) texture, thus resulting in sheet of fairly high strength with retention of transverse ductility. By taking advantage of an additional strengthening mechanism, i.e., alloying, strengths approaching those typical of high-reduction processes can be obtained.

To illustrate the above tendencies, some graphic comparisons of bi-directionally rolled sheet with sheet produced by other techniques are presented in Figures 89 through 92. The upper and lower shaded regions in Figures 89 and 90 represent the range of yield and tensile strengths observed in this program for bi-directionally rolled beryllium - 1 w/o copper and unalloyed beryllium respectively. These values are compared to strengths of sheet produced by hot upsetting at 1850°F to 1950°F⁽²⁾, a typical low-reduction process performed at high fabrication temperatures, and to sheet prepared by high-reduction cross-rolling at 1400°F in the ANC sheet rolling program⁽¹⁾. Two ranges of data are presented for the high-reduction sheet, representing material prepared in two different phases of the program.

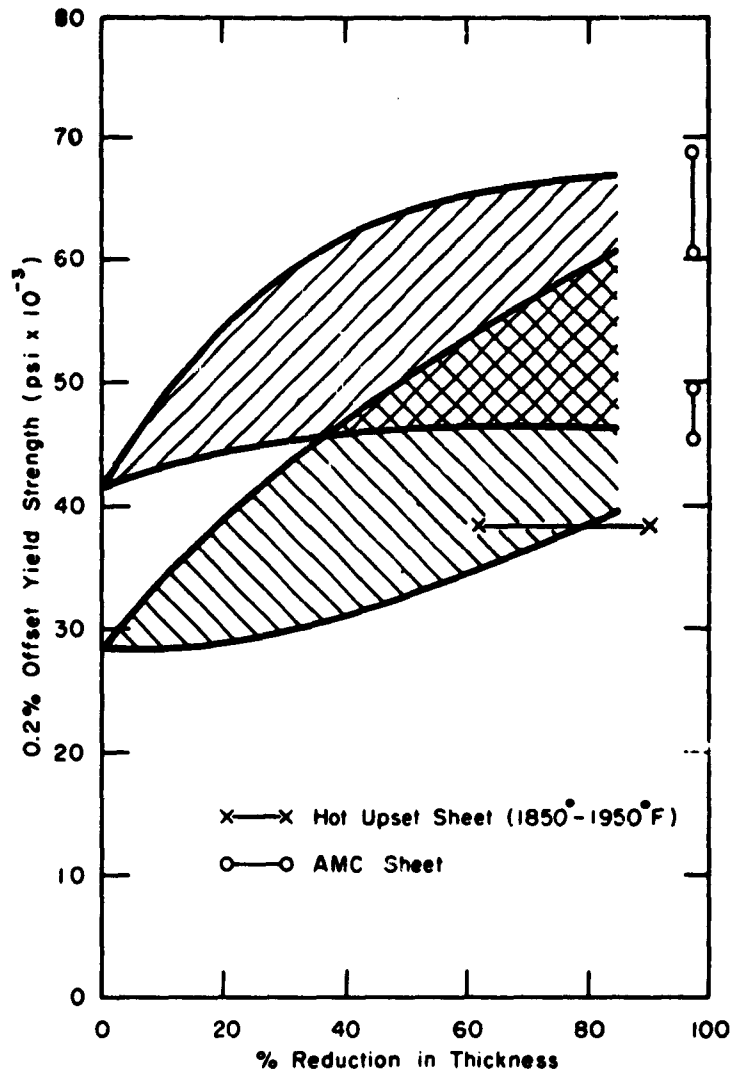


Figure 89 - Comparison of 0.2% offset yield strengths of sheet produced by various techniques.

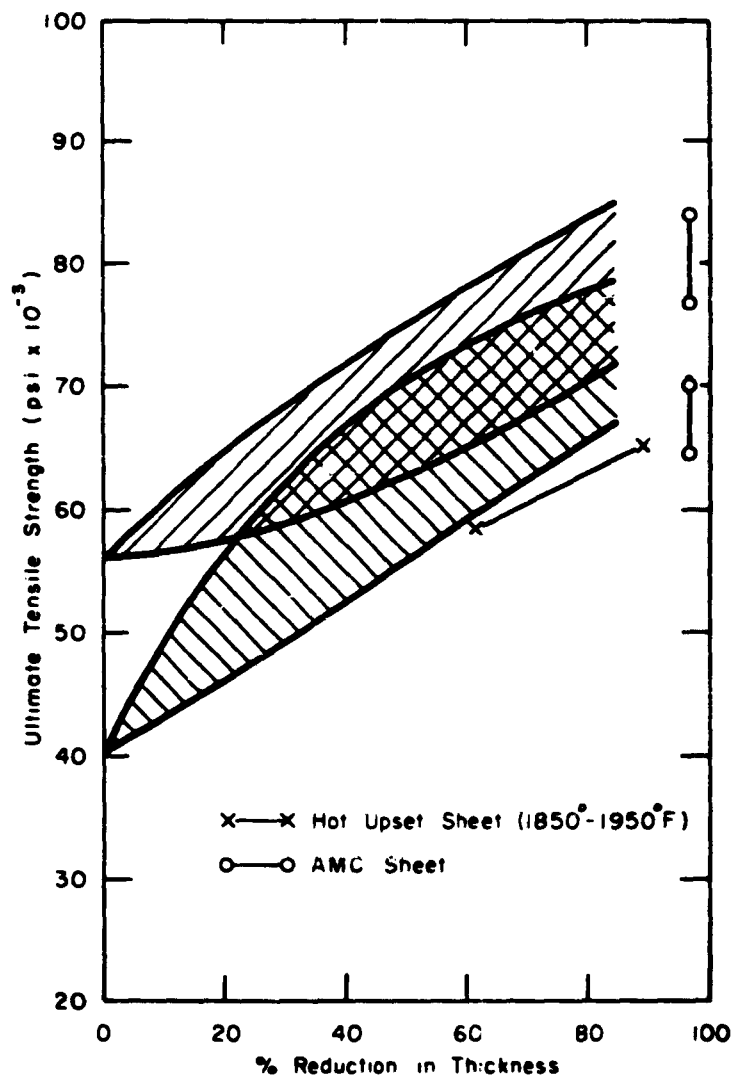


Figure 90 - Comparison of ultimate tensile strengths of sheet produced by various techniques.

Tensile elongations are compared in Figure 91. The cross-hatched area represents both unalloyed beryllium and beryllium - 1 w/o copper, since alloying produced little change in tensile elongation. For reductions near 6:1, bi-directional sheet appears to be equivalent to high-reduction sheet and to the best hot-upset sheet.

The transverse ductility of bi-directional sheet is compared to sheet produced by several processes in Figure 92. At high width-to-thickness ratios, the transverse ductility of unalloyed beryllium sheet bi-directionally rolled at 1800°F and below is about equivalent to that of hot bi-directionally rolled, hot pressed and hot upset sheet⁽³⁾. Although these materials have about the same ability to deform under triaxial stress conditions, the stress level at which the deformation takes place is highest for material produced by the warm low-reduction rolling procedure. The relatively high strengthened beryllium - 1 w/o copper sheet has somewhat lower ductility. All of the above materials have greater bend ductility than high-reduction sheet.⁽¹⁾.

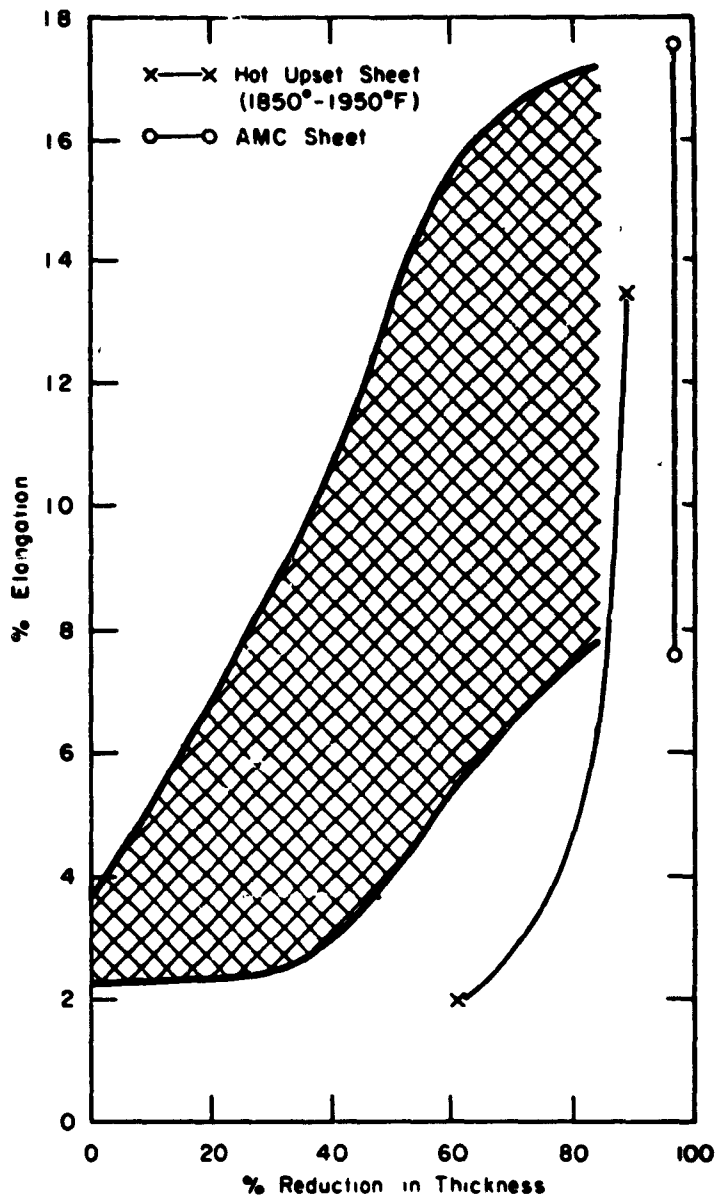


Figure 91 - Comparison of tensile elongations of sheet produced by various techniques.

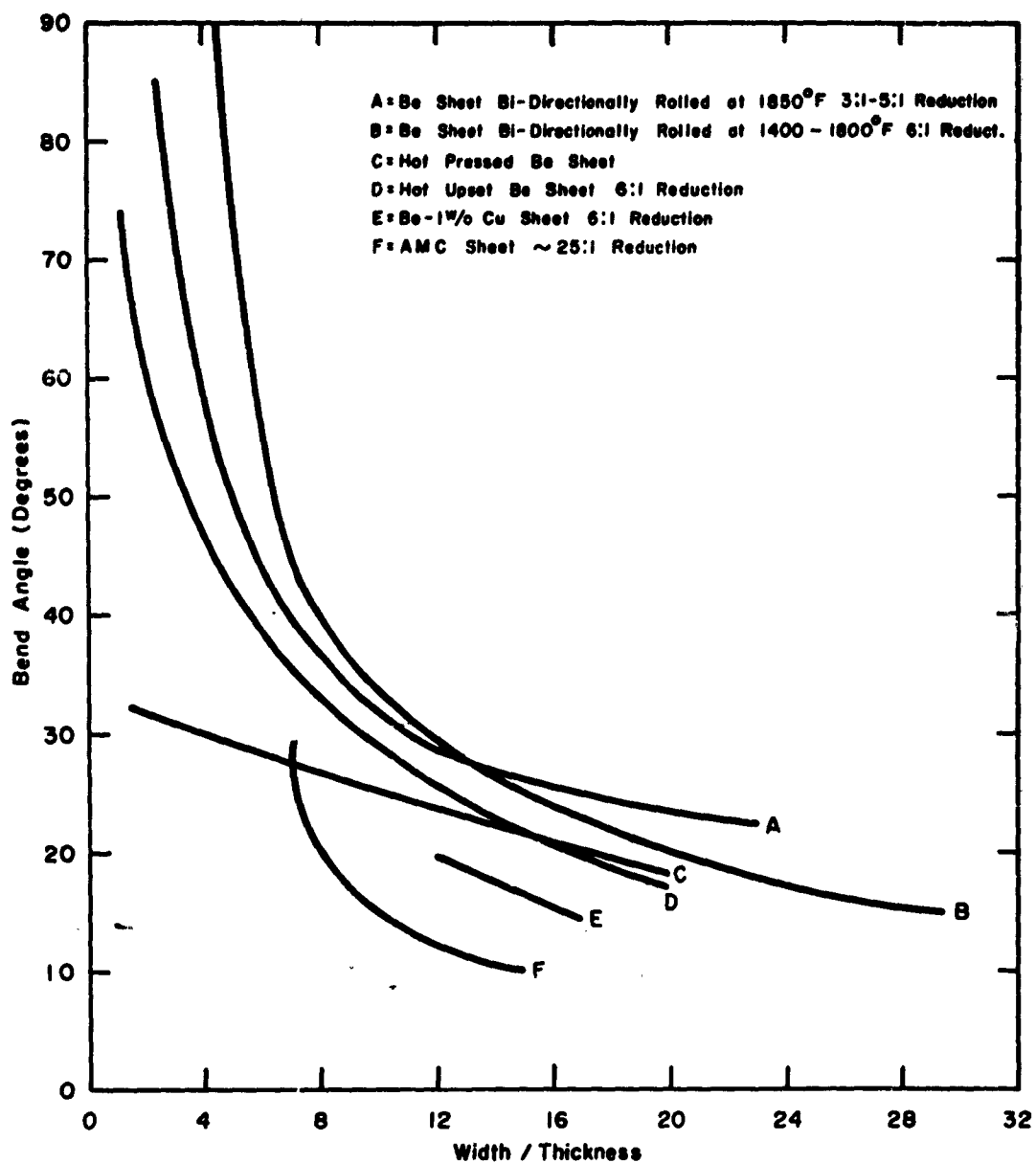


Figure 92 - Comparison of transverse ductility of sheet produced by various techniques.
 Drawing No. RA-2325

REFERENCES

1. K. G. Wikle, J. W. Armstrong and H. N. Perrin, Production of Beryllium Sheets Finished Flat to Gauge, Final Report to Air Materiel Command, Contract No. AF33(600)-35829, Brush Beryllium Company, March 1960.
2. F. M. Yans, Third-Dimensional Ductility and Crack Propagation in Beryllium Sheet, NMI-1212, March 18, 1959.
3. J. Greenspan, G. A. Henrikson and A. R. Kaufmann, Beryllium Research and Development in the Area of Composite Materials, WADD Technical Report 60-32 (NMI-9410), April 1960.
4. F. M. Yans, A. D. Donaldson and A. R. Kaufmann, The Effect of Copper, Nickel, Iron and Chromium on the Tensile Properties of Preferentially Oriented Beryllium Sheet, NMI-1192, February 14, 1958.
5. W. W. Beaver and K. G. Wikle, Mechanical Properties of Beryllium Fabricated by Powder Metallurgy, AIME Trans., 200:559-573 (1954).

SECTION 13

FUTURE PROGRAM

Work during the continuing program will still have as its objective to make beryllium more useful as an Air Force structural material. Two major areas will be investigated: (1) the effect of impurities and purification on the mechanical properties and (2) the effect of grain size on these properties.

In the first group of studies, efforts will continue to produce high purity polycrystalline beryllium and to evaluate its mechanical properties. Other studies in this category include an electron microscope study to determine the effect of impurities on dislocation structure of beryllium, and an optical and electron microscope study on impurities and on the identification of impurities and precipitates in beryllium.

In the second group of studies, on the evaluation of fine-grained beryllium, two subcontractors will be preparing ultra-fine powder (less than or equal to one micron) which will be consolidated by powder metallurgy techniques into bodies whose mechanical properties will be evaluated.

Other studies which are not directly connected with the above two groups, will include: recrystallization and grain growth in beryllium as a function of impurity level and oxide distribution, and the factors affecting the ductile-to-brittle type of transition which occurs in beryllium from approximately room temperature to 300° to 400°C.

The following is a list of the projects to be conducted and the sites at which they will be carried out:

A Study of the Brittle Behavior of Beryllium by Means of Transmission Electron Microscopy	Franklin Institute	F. Wilhelm H. G. F. Wilsdorf
Metallurgical Factors Affecting the Ductile-Brittle Transition in Beryllium	Lockheed Missiles and Space Co.	M. I. Jacobson E. C. Burke
Preparation of Ultra-Fine Beryllium Powders	National Research Corporation	P. L. Raymond P. J. Clough
Preparation and Evaluation of Fine-Grained Beryllium	New England Materials Laboratory	A. S. Bufferd R. Widmer N. J. Grant
Recrystallization and Grain Growth in Beryllium	Pechiney	A. Saulnier R. Syre P. Vachet

Identification of Impurities
and Precipitates in Beryllium

Pechiney

A. Saulnier
R. Syre
P. Vachat

Preparation and Evaluation
of High-Purity Beryllium

Nuclear Metals, Inc.

E. Levine
J. P. Pensler

Fabrication and Evaluation of
Fine-Grained Beryllium Produced
from Ultra-Fine Powders

Nuclear Metals, Inc.

A. K. Wolff

SECTION 14

REPORTS AND PUBLICATIONS GENERATED ON THIS CONTRACT

The following progress reports were generated on this program:

Monthly Progress Letters

NMI-9500	NMI-9507
NMI-9501	NMI-9510
NMI-9503	NMI-9511
NMI-9504	NMI-9513
NMI-9506	NMI-9514

Quarterly Progress Reports

NMI-9502
NMI-9505
NMI-9509
NMI-9512
NMI-9515

The following is a list of publications generated as a result of this contract:

H. G. F. Wilsdorf and F. Wilhelm, "The Behavior of Dislocations in Beryllium", Paper No. 41, International Conference on the Metallurgy of Beryllium, London, England, October 16-18, 1961.

M. I. Jacobson, F. M. Almeter and E. C. Burke, "Surface Damage in Beryllium", Trans. Am. Soc. of Metals, 55, (1962) 492.

J. P. Pemsler, S. H. Gelles, E. D. Levine and A. R. Kaufmann, "The Purification of Beryllium by Distillation", Paper No. 12, International Conference on the Metallurgy of Beryllium", London, England, October 16-18, 1961.

A. K. Wolff, S. H. Gelles, L. R. Aronin, "Impurity Effects in Commercially Pure Beryllium", Paper No. 66, International Conference on the Metallurgy of Beryllium, London, England, October 16-18, 1961.

Aeronautical Systems Division, Dir/Materials and Processes, Metals and Ceramics Lab, Wright-Patterson AFB, Ohio.
Rpt No. ASD-TTR-62-509, Vol. II. BERYLLIUM RESEARCH AND DEVELOPMENT PROGRAM. Interim report, Apr 63, 207p. incl illus, tables, refs.

Unclassified Report

The report summarizes the work conducted on the Beryllium Research and Development Program for the period April 1, 1960 through September 30, 1961. The aim of this program is to make beryllium more useful as an Air Force structural material.

(over)

The program was divided into eleven major efforts, eight of which were subcontracted and three carried out at the site of the prime contractor, Nuclear Metals, Inc. Detailed abstracts of each program are presented in their respective sections. In addition, work contemplated for a future program is described in a separate section.

1. Beryllium
2. Metallurgy
3. Welding
- I. AFSC Project 7351, Task 735104
- II. Contract AF 33 (616)-7065
- III. Nuclear Metals, Inc., Concord, Massachusetts
- IV. S. H. Gelles
- V. Aval fr OTS
- VI. In ASTIA collection

Aeronautical Systems Division, Dir/Materials and Processes, Metals and Ceramics Lab, Wright-Patterson AFB, Ohio.
Rpt No. ASD-TTR-62-509, Vol. II. BERYLLIUM RESEARCH AND DEVELOPMENT PROGRAM. Interim report, Apr 63, 207p. incl illus, tables, refs.

Unclassified Report

The report summarizes the work conducted on the Beryllium Research and Development Program for the period April 1, 1960 through September 30, 1961. The aim of this program is to make beryllium more useful as an Air Force structural material.

(over)

The program was divided into eleven major efforts, eight of which were subcontracted and three carried out at the site of the prime contractor, Nuclear Metals, Inc. Detailed abstracts of each program are presented in their respective sections. In addition, work contemplated for a future program is described in a separate section.

1. Beryllium
2. Metallurgy
3. Welding
- I. AFSC Project 7351, Task 735104
- II. Contract AF 33 (616)-7065
- III. Nuclear Metals, Inc., Concord, Massachusetts
- IV. S. H. Gelles
- V. Aval fr OTS
- VI. In ASTIA collection